

IL NUOVO CIMENTO

ORGANO DELLA SOCIETÀ ITALIANA DI FISICA
SOTTO GLI AUSPICI DEL CONSIGLIO NAZIONALE DELLE RICERCHE

VOL. XI, N. 3

Serie decima

1° Febbraio 1959

On the Thinning Down of Tracks of Heavy Nuclei in Nuclear Emulsions.

P. G. BIZZETI and M. DELLA CORTE

Istituto Nazionale di Fisica Nucleare - Sottosezione di Firenze
Istituto di Fisica dell'Università - Arcetri (Firenze)

(ricevuto il 29 Luglio 1958)

Summary. — Photometric measurements of track widths have been carried out in the thin-down region on ^{12}C and ^{16}O tracks and also on tracks of α and singly charged particles stopping in the emulsion. An appropriate model for the process of track formation in the thin-down region is proposed, and successfully tested on the experimental material.

Introduction.

The thinning down of heavy nuclei tracks was first observed in 1948 by the Minnesota and Rochester groups ⁽¹⁾ on nuclear emulsions exposed to cosmic rays at balloon altitude. An interpretation of this phenomenon was given by FREJER *et al.* ⁽²⁾ as an effect of the decreasing electric charge of the ions due to the electron pick-up in the last part of their range.

However, the first experimental data ⁽³⁾ on the thin-down length are in marked disagreement with the values calculated on the assumption that the tapering of tracks is due only to electron pick-up ^(2,4).

⁽¹⁾ P. FREJER, E. J. LOFGREN, E. P. NEY, F. OPPENHEIMER, H. L. BRADT and B. PETERS: *Phys. Rev.*, **74**, 213 (1948).

⁽²⁾ P. FREJER, E. J. LOFGREN, E. P. NEY and F. OPPENHEIMER: *Phys. Rev.*, **74**, 1818 (1948).

⁽³⁾ T. F. HOANG and D. MORELLET: *Compt. Rend.*, **231**, 695 (1950).

⁽⁴⁾ J. P. LONCHAMP: *Ann. de Phys.*, **10**, 201 (1955).

A possible effect of low energy secondary electrons on the tapering of tracks was suggested by PERKINS in 1950 ⁽⁵⁾. An evaluation of the width of the track as a function of the residual range based on this hypothesis was made by CRUSSARD ⁽⁶⁾ and independently by LONCHAMP ⁽⁴⁾. Using a very simplified model, LONCHAMP has given an order of magnitude estimate for the track width and the thin-down length. LONCHAMP compared his results with the data of HOANG and MORELLET ⁽³⁾, obtained by visual measurement of the tracks.

However, the micrometric measurement of the width and of the thin-down length are very difficult on account of the irregular contour of the tracks ^(*). Moreover, measurements of thin-down length are affected by a non-negligible subjective factor, as pointed out by CÜER, LONCHAMP and GEGAUFF ⁽⁷⁾.

It appeared therefore interesting to carry out a number of photometric measurements of the width of heavy ion tracks in Ilford G-5 emulsions and to attempt to give a theoretical model for the thinning-down effect.

1. - Experimental results on the photometrical width.

In three previous papers ⁽⁸⁻¹⁰⁾ we have defined the «photometric width» of a track, and described a method employed in determining it. This method is very simple and objective; the possibility of correcting the results so as to take into account the dipping of the tracks and the eventual different degree of development of the plates makes this method very suitable for the present work.

Photometric measurement techniques very different from ours are used in some laboratories ^(11,12).

We have measured the photometric width of tracks of artificially accelerated ions (¹⁶O, ¹²C, ⁴He), and of ⁴He and singly charged particles from cosmic-rays stars.

⁽⁵⁾ D. H. PERKINS: *Proc. Roy. Soc.*, A **203**, 399 (1950).

⁽⁶⁾ J. CRUSSARD: *Thèse* (Paris, 1952).

^(*) An important improvement in micrometric measurement technique has been introduced in the Nuclear Emulsion Laboratory of the University of Milan ⁽¹⁶⁾ through the use of a Clausen micrometer.

⁽⁷⁾ P. CÜER, J. P. LONCHAMP and M. C. GEGAUFF: *Compt. Rend.*, **240**, 856 (1955).

⁽⁸⁾ M. DELLA CORTE: *Nuovo Cimento*, **4**, 1565 (1956).

⁽⁹⁾ P. G. BIZZETI and M. DELLA CORTE: *Nuovo Cimento*, **7**, 231 (1958).

⁽¹⁰⁾ P. G. BIZZETI, M. G. DAGLIANA, M. DELLA CORTE and L. TOCCI: *Nuovo Cimento*, **10**, 388 (1958).

⁽¹¹⁾ T. JOHANSSON: *Ark. f. Phys.*, **13**, 129 (1958).

⁽¹²⁾ O. V. LOZHKIN: *Sov. Phys. Journ. Exp. Phys. Theor.*, **5**, 293 (1957).

Successive non-overlapping cells of 12.7 μm length have been used and the data have been elaborated according to the procedure explained in paper ⁽⁹⁾. Tracks were studied on three different Ilford G-5 plates.

In plate B there is a large number of tracks of ^{12}C and ^{16}O of the same HQ ; the discrimination between these two types of ion tracks could be obtained with great certainty by measuring their residual range, *i.e.* independently from photometric measurements.

Plate L contains ^{12}C and ^4He tracks of the same HQ , whose discrimination can obviously be made visually.

Plate S was exposed to cosmic rays (Sardinia expedition). A certain number of tracks of singly and doubly charged particles have been found in it as secondaries from large stars. Their photometric width λ was measured in the last 200 μm of range, and the mean values are reported in Fig. 1. The two groups among which the values are distributed have been interpreted as belonging to particles of $Z = 1$ and 2. Measurements of scattering by the constant sagitta method were made whenever the length of the track allowed it; they confirmed in every case the value of Z attributed on the basis of the photometric method. The two thicker tracks are surely ^6Li tracks because they show the characteristic hammer at the end of their range.

Number and type of the tracks measured in the various plates are summarized in Table I.

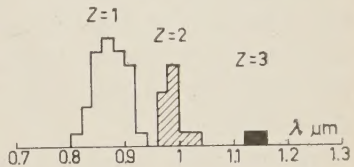


Fig. 1. — Distribution of the mean track width in the first 200 μm of range for particle widths $z = 1, 2, 3$ in plate S.

TABLE I.

Plate	Z	No. tracks	λ (12–140 μm)
B (50 μm thick)	8	50	—
	6	50	1.722 ± 0.007
L (200 μm thick)	6	25	1.619 ± 0.020
	2	20	1.110 ± 0.010
S (600 μm thick)	2	12	0.971 ± 0.006
	1	33	—

(*) The wider dispersion of the data in plate L is due to a heavy background fog in this plate.

Owing to the difference in the degree of development of the three plates, the photometric widths have been reduced to the same degree of development, assuming as a standard that of the plate S.

As previously shown in (10) for Ilford G-5 emulsions, it is justified to write

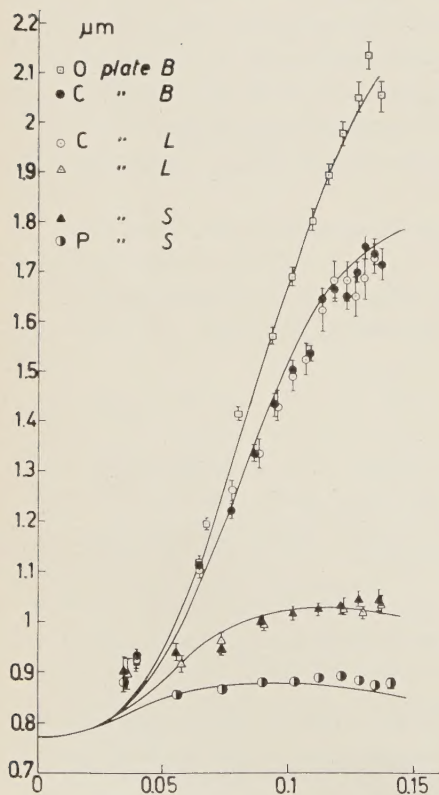
$$(1) \quad \lambda = \lambda_0 + \lambda_1(\beta, Z),$$

where the effect of the development is contained in the term λ_0 which, on the other hand, is independent of Z and β . The correction for taking into account the difference of development between plates is therefore a constant term to be added to λ . Hence it can be evaluated, once and for all, as it is given by the difference of the track-width of particles of the same kind in the same range interval.

In the present case, for plates L and S the correction term has been calculated from the average width of α -particle tracks, in the first 12 cells starting from a residual range of $12.7 \mu\text{m}$. (The last $12.7 \mu\text{m}$ were discarded because the scattering of the particle would produce too large a dispersion.)

We have obtained:

$$(2) \quad \lambda_0^L - \lambda_0^S = (0.139 \pm 0.012) \mu\text{m}.$$



Likewise by comparing ^{12}C -ion tracks in plates L and B and taking into account result 2) we get

$$(3) \quad \lambda_0^B - \lambda_0^L = (0.103 \pm 0.021) \mu\text{m},$$

$$(4) \quad \lambda_0^B - \lambda_0^S = (0.242 \pm 0.025) \mu\text{m}.$$

The corrected values of λ , for different kinds of particles, are plotted in Fig. 2 as a function of β .

The usefulness and effectiveness of the development correction is confirmed by the good agreement between the points representing the same kind of particles in different plates.

Fig. 2. - Photometric width of tracks corresponding to different particles in different plates, as a function of β . Correction for the different degree of development between plates has been taken into account. The full lines represent theoretical values of $\lambda(\beta, Z)$ calculated in Sect. 4.

TABLE II.

¹⁶ O			¹² C			⁴ He			¹ H		
β	Z_{eff}	$\lambda \pm \Delta\lambda$ (μm)	β	Z_{eff}	$\lambda \pm \Delta\lambda$ (μm)	β	Z_{eff}	$\lambda \pm \Delta\lambda$ (μm)	β	Z_{eff}	$\lambda \pm \Delta\lambda$ (μm)
0.0385	5.67; 5.70	0.920 ± 0.012	0.0389	4.68; 4.68	0.931 ± 0.012	0.0373	1.99	0.899 ± 0.019	0.0351	1	0.881 ± 0.017
0.0672	6.97; 7.10	1.194 ± 0.011	0.0651	5.45; 5.56	1.111 ± 0.012	0.0569	2	0.929 ± 0.010	0.0569	1	0.855 ± 0.008
0.0835	7.30; 7.50	1.414 ± 0.013	0.0788	5.56; 5.78	1.236 ± 0.011	0.0743	2	0.952 ± 0.009	0.0743	1	0.865 ± 0.008
0.0950	7.38; 7.67	1.569 ± 0.016	0.0893	5.64; 5.89	1.334 ± 0.012	0.0901	2	0.999 ± 0.007	0.0901	1	0.879 ± 0.007
0.103	7.45; 7.80	1.689 ± 0.018	0.0975	5.69; 5.96	1.432 ± 0.015	0.103	2	1.016 ± 0.010	0.103	1	0.880 ± 0.006
0.111	7.51; 7.86	1.802 ± 0.021	0.104	5.72; 6.00	1.500 ± 0.014	0.114	2	1.023 ± 0.010	0.114	1	0.889 ± 0.004
0.118	7.55; 7.96	1.895 ± 0.021	0.110	5.75; 6.00	1.533 ± 0.014	0.122	2	1.032 ± 0.012	0.122	1	0.892 ± 0.007
0.124	7.58; 8.00	1.977 ± 0.026	0.116	5.77; 6.00	1.638 ± 0.019	0.130	2	1.031 ± 0.010	0.130	1	0.882 ± 0.008
0.129	7.61; 8.00	2.050 ± 0.029	0.121	5.78; 6.00	1.668 ± 0.018	0.136	2	1.036 ± 0.011	0.136	1	0.874 ± 0.008
0.134	7.64; 8.00	2.135 ± 0.026	0.125	5.80; 6.00	1.658 ± 0.020	—	—	—	0.1415	1	0.876 ± 0.011
0.138	7.67; 8.00	2.052 ± 0.028	0.129	5.81; 6.00	1.689 ± 0.018	—	—	—	—	—	—
—	—	—	0.133	5.82; 6.00	1.732 ± 0.022	—	—	—	—	—	—
—	—	—	0.136	5.83; 6.00	1.733 ± 0.018	—	—	—	—	—	—
—	—	—	0.139	5.84; 6.00	1.714 ± 0.027	—	—	—	—	—	—

In Table II we give the values of λ as a function of β obtained by a weighted mean of the experimental data from plates B, L and S. Values of the effective charge Z_{eff} which have been calculated by PAPINEAU ⁽¹³⁾ are also reported in Table II (*).

2. - Comparison with the existing theories.

The thin-down length for ions of $Z=6$ and 8 evaluated according to the electron pick-up hypothesis ⁽²⁾ should be 25 and 45 μm , respectively. Both these values are in very marked disagreement with our experimental results, which indicate a thin-down length of far more than 100 μm . This discrepancy shows that the tapering cannot be entirely ascribed to electron pick-up.

A quantitative evaluation of the δ -ray effect has been given by LONCHAMP ⁽⁴⁾, who makes the basic assumption that δ -rays are no longer distinguishable singularly and practically form a continuous core, when their density exceeds a prescribed value n_0 ($n_0=400$ in 100 μm , in the numerical computations).

By making the auxiliary and simplifying assumptions that δ -rays are emitted at right angles and are not affected by scattering, the A. proceeds to evaluate the width of the track and the thin-down length. For this purpose he starts from the well known Rutherford's formula in its integral form:

$$(5) \quad n = 5.34 \cdot 10^{-3} \frac{Z_{\text{eff}}^2}{\beta^2} \left(\frac{510}{W_0} - \frac{1}{2\beta^2} \right)$$

giving the average number of δ -rays of energy $\geq w_0$ (keV), in 100 μm of length, and introduces a suitable range energy relation for very slow electrons.

A direct comparison of Lonchamp's model with our experimental data is clearly impossible, not only for the lack of knowledge of the range-energy relation of slow electrons, but also because it is impossible to give an *a priori* numerical value to the constant λ_0 of equation (1).

A test of Lonchamp's basic assumption, however, can be carried out as follows:

From the experimental data of Table II it is possible to evaluate, for a given value of λ , the corresponding β and Z_{eff} for Oxygen and Carbon ion tracks. Since in the formula (5), W_0 is a function of λ only, and n is assumed

⁽¹³⁾ A. PAPINEAU: *Compt. Rend.*, **242**, 2933 (1956) and private communication.

(*) The two values given for ^{12}C and ^{16}O in Table II are extreme values given by Papineau; the mean of these two values was used in our calculation.

to be a constant, if we substitute in (5) our values of β and Z_{eff} , it is possible to calculate both $W_0(\lambda)$ and n , for any value of λ , and to verify whether n turns out to be a constant or not.

In this comparison, no assumption has been made as to the numerical value of λ_0 , and on the range-energy relation of slow electrons.

The results of the calculation are shown in Table III.

TABLE III.

λ (μm)	0.95	1	1.1	1.2	1.3	1.4	1.5	1.6	1.7
$W_0(\lambda)$ (keV)	1.65	2.10	3.04	3.77	4.60	5.68	6.69	7.98	8.88
n for 100 μm	3 960	2 950	1 470	1 375	982	663	489	351	300

It is evident that n is by no means a constant. Therefore Lonchamp's hypothesis does not seem able to account for the experimental data.

In the next section, a different model for the track formation will be proposed and developed. Comparison with experiment will be carried out in Section 4.

3. - Model for the process of formation of heavy ion tracks.

The main difficulties of a quantitative theory of the thinning down, based on the δ -ray hypothesis, are, as we already pointed out, the existing uncertainty on the behaviour of very slow electrons and the difficulty of taking into proper account the effect of the development.

The model we propose has the following advantages: *a*) it relies on very simple assumptions, completely consistent with what is known from other pieces of evidence on the mechanism of track formation; *b*) it can be easily and most directly compared with the various available experimental material, by using a minimum number of adjusted parameters (one or two) as we shall see later.

Let us ignore for the moment the presence of δ -rays, and consider only the primary ionization of the heavy ions. In the range of energy of interest we can reasonably assume that this ionization is so high that all crystals touched by the particle path should be activated. As is currently admitted, the crystals grow during the development and the developed grains will increase their diameter by a factor g .

The width of the track after the development will therefore be determined by the outer surface of the developed grains. Namely, if g is sufficiently large, the track will appear as a solid cylinder of diameter:

$$(6) \quad \lambda_0 = (g + 1)d.$$

Now, to take into account the effect of secondary electrons on the track-width, a reasonable starting point could be to assume that a minimum amount of ionization is necessary to activate a grain.

The ionization density however, falls off quite rapidly, even within a grain diameter, with increasing distance from the particle path, as can be easily anticipated on theoretical grounds and is confirmed by the fact that the track contour appears well defined. Therefore the above condition can be reasonably substituted by the more simple assumption that the grains which will be activated are only those which lie, at least partially, within a distance x from the path of the particle: the distance x is such that the energy flux per unit

Fig. 3. - Section of a track normal to the path (trace 0). Every grain which lies even in part within the cylinder surface of radius x (continuous line) is developable. A represents a grain which is just developable being at the farthest point. The small broken circle centered at A and with radius $g(d/2)$ represents the dimensions of the grain A after development. The outside circle of radius $\lambda/2$ is the section across the developed track.

surface out of the cylinder having radius x and the particle path as axis, exceeds a given constant value E^* . As a matter of fact, when this flux is near to the minimum value E^* we can be quite sure that the total energy flowing out of the cylinder will be dissipated within a Δx smaller than a grain diameter d .

Once the distance x , for a given particle and energy, is evaluated, the track width after development will be obviously (see Fig. 3)

$$(7) \quad \lambda = (g + 1)d + 2x = \lambda_0 + \lambda_1,$$

where according to (1) and (6) we get

$$(8) \quad \lambda_0 = (g + 1)d, \quad \lambda_1 = 2x,$$

so that the problem reduces to the evaluation of $x(\beta, Z)$. The hypothesis just

illustrated, can be expressed by

$$(9) \quad \frac{E(x)}{2\pi x} = E^* = \text{const.}$$

Now the energy $E(x)$ transferred by secondary electrons, per unit length of primary path, outside the cylinder of radius x , can be, in principle, evaluated from Rutherford's formula:

$$(10) \quad dn = K \frac{Z_{\text{eff}}^2}{\beta^2} \frac{dW}{W^2},$$

with

$$K = \frac{2\pi N e^4}{m_0 c^2}.$$

We have namely

$$(11) \quad E(x) = K \frac{Z_{\text{eff}}^2}{\beta^2} \int_{W(x)}^{W_{\text{max}}} \frac{W(x, w)}{w} \frac{dw}{w},$$

where $W_{\text{max}} = 2m_0 c^2 \beta^2$ is the maximum energy of δ -rays; $\overline{W}(x, w)$ is the average value of the energy transferred out of the cylinder by a δ -ray of energy w .

Let us assume a range-energy relation for δ -rays expressed by

$$(12) \quad r = k w^\alpha,$$

then

$$(13) \quad E(x) = \frac{K}{\alpha} \frac{Z_{\text{eff}}^2}{\beta^2} \int_x^R \frac{\overline{W}(x, r)}{W(r)} \frac{dr}{r},$$

$R = k(2m_0 c^2 \beta^2)^\alpha$ being the maximum range of δ -rays for a given β . The ratio $\overline{W}(x, r)/W(r)$ can be shown (see details in the Appendix) to be a function of the ratio x/r only. It is then clear that $E(x)$ will be a function of x through x/R only:

$$(14) \quad E(x) = \frac{K}{\alpha} \frac{Z_{\text{eff}}^2}{\beta^2} I\left(\frac{x}{R}\right).$$

In deriving this result, we have made some simplifying assumptions not unusual in this kind of problems, such as the possibility of considering the δ -rays as following rectilinear paths and having an angular distribution independent of their energy. Surely, this is far from being an acceptable assumption for a single δ -ray; however, it may be expected to supply a fairly correct picture for the average behaviour of many δ rays, particularly when a suitable angular distribution is chosen. Fluctuations, of course, are also neglected.

From the relation (9) and (14) and remembering that $x = (\lambda - \lambda_0)/2$ ((7), (8)) we obtain

$$(15) \quad \frac{Z_{\text{eff}}}{\beta\sqrt{R}} = \varphi\left(\frac{\lambda - \lambda_0}{2R}\right),$$

so that, the ratio $(\lambda - \lambda_0)/2R$ should be a function of $Z_{\text{eff}}/\beta\sqrt{R}$ only. This result can be tested experimentally, provided we specify the range-energy relation and give a numerical value to the constant λ_0 . For the range-energy relation we have assumed

$$(16) \quad r \text{ (}\mu\text{m)} = 2.1 \cdot 10^{-2} w^{1.72} \text{ (keV)}.$$

The exponent 1.72 has been suggested by GLOCKER ⁽¹⁴⁾ for energies between 1 and 100 keV and the constant $2.1 \cdot 10^{-2}$ has been calculated to fit the existing experimental data reported by SACTON at the energy of 30 keV, as shown in Fig. 4.

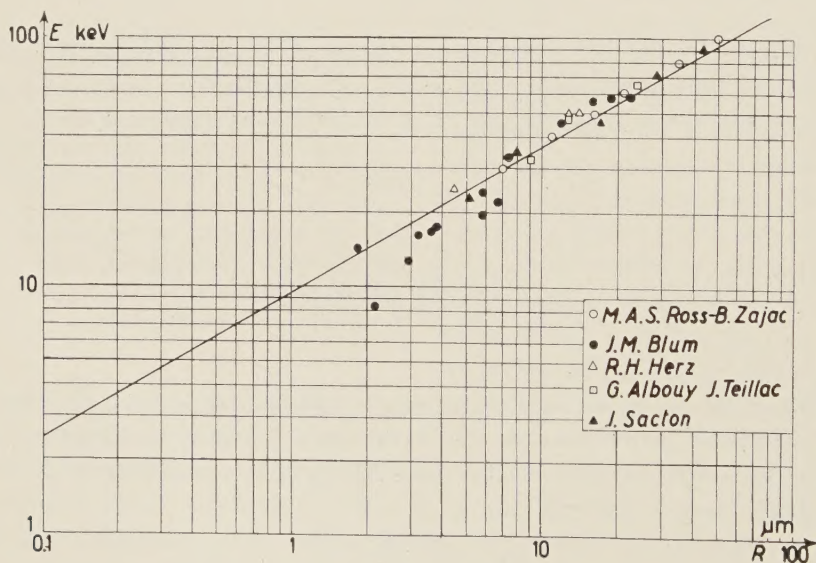


Fig. 4. - Range-energy relations for very slow electrons.

The constant λ_0 has been determined by trial and error to fit our experimental data, but the value thus found $\lambda_0 = 0.77$ can be accounted for by some independent considerations as will be shown later on.

(14) L. KATZ and A. S. PENFOLD: *Rev. Mod. Phys.*, **24**, 28 (1952).

The results are shown in Fig. 5. We see that, within the limits of error, the experimental points corresponding to ions with $Z = 1, 2, 6$ and 8 with values of β falling within the range $0.05 \leq \beta \leq 0.15$ all lie on the same curve.

For $\beta \leq 0.05$, corresponding to a range less than about $13 \mu\text{m}$, no reliable photometric data are obtainable, owing to the distortion introduced by the scattering.

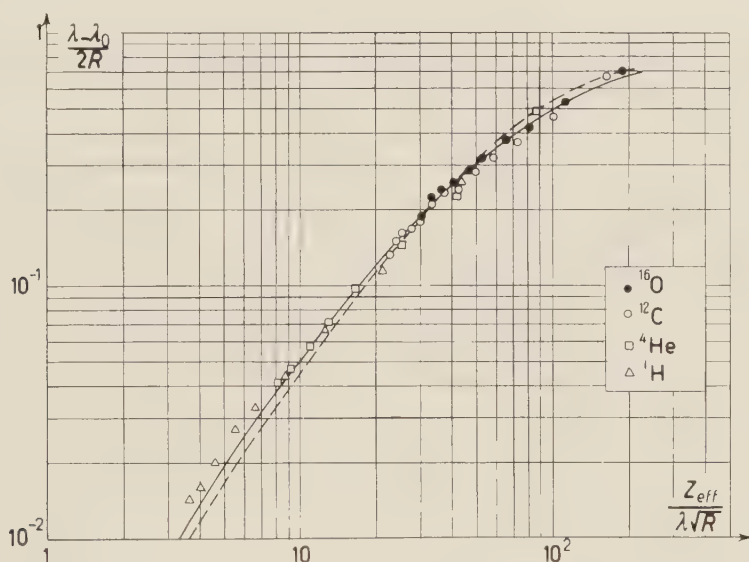


Fig. 5. — Experimental values of $(\lambda - \lambda_0)/2R$ as a function of $Z_{\text{eff}} \beta \sqrt{R}$ for $0.05 \leq \beta \leq 0.15$ and different Z . Theoretical curve calculated in our hypothesis (full line) and assuming δ -rays to be emitted perpendicularly to the track (broken line).

It is worth-while to emphasize that this result has been obtained with λ_0 as the only adjusted parameter. It is also independent of the value of constant factor in the range-energy relation (16), while a variation of the exponent of about 20% does not affect the agreement.

If we assume according to DODD and WALLER⁽¹⁵⁾ $d = 0.27$ for the average diameter of grains, from the value of λ_0 we obtain for the developing factor (eq. (6)) the value $g = 1.85$.

An independent estimate of this factor can be obtained from the dependence of the mean photometrical width λ of Po α -particle tracks from the time of development, as it is shown in Fig. 1 of paper⁽⁸⁾.

⁽¹⁵⁾ E. C. DODD and C. WALLER: *Fundamental Mechanism of Photographic Sensitivity* (London, 1951), p. 266.

The extrapolation to the time 0 of this curve gives a value ($g=1$)

$$(17) \quad \bar{\lambda} = 2d + \bar{\lambda}_1 = 0.69 \mu\text{m}$$

for α -particles near the end of their range. From this relation we have

$$(18) \quad \bar{\lambda}_1 = 0.69 - 0.54 = 0.15 \mu\text{m}.$$

On the other hand, from values of the width of tracks of the same kind and of the same range in the plate S we have

$$(19) \quad \bar{\lambda}_1 = 0.924 - 0.77 = 0.154 \mu\text{m},$$

in very good agreement with the value just found (18).

This can be considered also a test of the proportionality of g to the time of development.

There is therefore an experimental evidence that our model of track formation is a good representation of the real process.

4. - Evaluation of the function $\lambda(\beta, Z)$.

As we have just pointed out, the relation (15)

$$\frac{Z_{\text{eff}}}{\beta\sqrt{R}} = \varphi\left(\frac{\lambda - \lambda_0}{2R}\right),$$

(where φ is for the moment an unknown function) is well confirmed by the experimental material.

Now an attempt can be made to evaluate an explicit form for the function φ and thus derive the photometric width as a function of β and Z .

Let us assume that δ -rays are isotropically emitted around the track (*). As a matter of fact, a randomization of the direction of the δ -ray paths can be expected as a scattering effect.

(*) The assumption $f(\theta)=\text{const}$ is really too restrictive (see Appendix). In fact, the same result is obtained under the assumption of an angular distribution of the form

$$f(\theta) = a + b \cos \theta,$$

or, even more generally, by setting

$$f(\theta) + f(\pi - \theta) = \text{const}.$$

Under these assumptions (see Appendix) we find:

$$(20) \quad I\left(\frac{x}{R}\right) = \int_1^{R/\sigma} \left(1 - \frac{1}{y}\right)^{1/\alpha} \sqrt{1 + \left(\frac{xy}{R}\right)^2} \frac{dy}{y},$$

$$(12) \quad \varphi\left(\frac{x}{R}\right) = \left[\frac{2\pi\alpha E^*}{K} \frac{x}{R} \frac{1}{I(x/R)} \right]^{\frac{1}{2}}.$$

The integral $I(x/R)$ has been evaluated by numerical computation, and the function $\varphi[(\lambda - \lambda_0)/2R]$ is plotted as a continuous line in Fig. 5.

The agreement with experimental behaviour can be considered sufficiently good having in mind the crudeness of our assumptions. From the last relation (21) it is possible to evaluate numerically the function $\lambda(\beta, Z)$. The calculated values of this function are plotted in Fig. 2 and show a satisfactory agreement with the experimental points.

It is interesting to observe that the calculated widths for singly and doubly charged particles show a maximum in the neighbourhood of $\beta = 0.085$ and 0.1 , respectively. For larger values of β , the calculated widths show a more pronounced decrement than the experimental ones. Indeed, a maximum in the width for proton tracks was observed by ALVIAL *et al.* ⁽¹⁶⁾ at $\lambda = 0.09$, in the course of very accurate measurements with a Clausen Micrometer.

The value of the constant E^* giving the best fit with experimental data is $4.9 \text{ keV } \mu\text{m}^{-2}$. This value represents the flow of energy per unit surface of the cylinder with radius $(\lambda - \lambda_0)/2$.

As a by-product of this investigation an order of magnitude estimate of the threshold energy ε can be made by multiplying E^* by the mean cross-section of the crystals.

We have

$$\varepsilon = 0.057 \cdot 4.9 \text{ keV} = 280 \text{ eV}.$$

This estimate, though uncertain, (as is clear from the whole procedure) is of the correct order of magnitude and compares satisfactorily with other estimates ⁽¹⁷⁾.

⁽¹⁶⁾ G. ALVIAL, A. BONETTI, C. DILWORTH, M. LADU, J. MORGAN and G. OCCHIALINI: *Suppl. Nuovo Cimento*, **4**, 244 (1956).

⁽¹⁷⁾ K. C. BOGOMOLOV: *Compt. Rend. Coll. Intern. Photographie Corpusculaire* (Strasbourg, 1957, in press).

5. - Conclusions.

In conclusion, the interpretation of the thinning down effect on the basis of electron pick-up, as first suggested by FREJER ⁽²⁾, although still used in some Laboratories for the identification of tracks, is clearly ruled out by our data.

The hypothesis of a δ -ray effect, as proposed by CRUSSARD and by LONCHAMP, seems to offer the only alternative.

A quantitative evaluation of the effect requires some specific hypotheses and is subject to considerable uncertainties regarding auxiliary data. Nevertheless, we believe that the particular specification of the δ -ray hypothesis given by LONCHAMP, is also inconsistent with our experimental results.

We have therefore proposed another detailed interpretation which still assumes a δ -ray effect but looks in a different way to the mechanism of track-formation and δ -ray contribution to it.

The general lines of the approach appear to be quite resonable and consistent both with current views on latent image formation and with our experimental results. The fact that the experimental points of Fig. 5, which refer to different particles (^{16}O , ^{12}C , ^4He , ^1H), and to values of β extending from 0.05 to 0.15, fall in a quite regular line by adjusting a single parameter, strongly supports our approach. It is also worth-while to point out that the value of the adjusted parameter λ_0 can be tested by an independent method (see eq. (18) and (19)).

The quantitative comparison of a detailed theory based on the above mentioned approach is subject, however, to greater uncertainty in the auxiliary data. Nevertheless it is comforting to see, that by adjustment of a second parameter only (E^*) and by using currently accepted values, however uncertain, for the auxiliary parameter, the agreement between calculated values (full lines of Fig. 2 and 5) and experimental points is pretty good.

As this work was just ended a paper of SKJEGGESTAD on the same subject appeared on the *Nuovo Cimento* ⁽¹⁸⁾.

The experimental data of the author do not seem to agree completely with ours. The reason for the discrepancy is not clear, though the different experimental method for the evaluation of the track width may partly account for it. Skjeggstad's interpretation is also based on the δ -ray hypothesis but is developed along different lines.

* * *

We wish to express our thanks to Professor S. FRANCHETTI, for his continuous interest in this work and to Professor M. MANDÒ for many helpful discussions.

(¹⁸) O. SKJEGGESTAD: *Nuovo Cimento*, **8**, 927 (1958).

We thank most heartily Dr. M. DAGLIANA and Dr. L. TOCCI for their valuable work in collecting experimental data.

We are also indebted to Professor G. OCCHIALINI of the University of Milan, who kindly supplied plate «B».

APPENDIX

The evaluation of the average energy W was made using the following scheme:

- a) δ -electron paths are assumed rectilinear;
- b) the angular distribution of same is supposed energy-independent

The energy transferred out of the cylinder of radius x by a «rectilinear» δ -ray will be

$$(A.1) \quad w(r, x, \theta) = k^{-1/\alpha} \left(r - \frac{x}{\sin \theta} \right)^{1/\alpha},$$

with

$$(A.2) \quad \theta_0 \leq \theta \leq \pi - \theta_0; \quad \theta_0 = \sin^{-1} \frac{x}{r},$$

so that

$$(A.3) \quad \begin{aligned} W(r, x) &= \frac{1}{k^{1/\alpha}} \int_{\theta_0}^{\pi - \theta_0} \left(r - \frac{x}{\sin \theta} \right)^{1/\alpha} f(\theta) 2\pi \sin \theta d\theta, \\ \frac{W(r, x)}{W(r)} &= \int_{\theta_0}^{\pi - \theta_0} \left(1 - \frac{x}{r \sin \theta} \right)^{1/\alpha} f(\theta) 2\pi \sin \theta d\theta = \\ &= \int_{\theta_0}^{\pi/2} \left(1 - \frac{x}{r \sin \theta} \right)^{1/\alpha} \{f(\theta) + f(\pi - \theta)\} 2\pi \sin \theta d\theta. \end{aligned}$$

Now $f(\theta) d\Omega$ represents the probability of δ -ray emission within a cone $d\Omega$ at an angle θ to the ion path, and is assumed to be independent of the energy of secondary electrons, namely from their range r .

Therefore, the integral (A.3) will depend only on the ratio x/r so that the integral

$$(A.4) \quad I = \int_x^R \frac{W(x, r)}{W(r)} \frac{dr}{r},$$

will be a function of the ratio x/R only.

Now if we require a quantitative evaluation of the integral $I(x/R)$ we must somewhat specify the form of the probability distribution $f(\theta)$. The simplest assumption will be to choose

$$(A.5) \quad f(\theta) + f(\pi - \theta) = \frac{1}{2\pi} = \text{const},$$

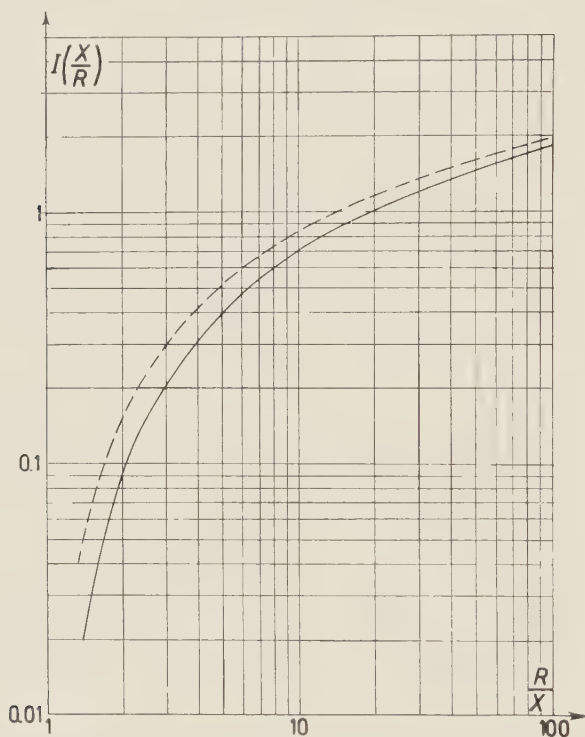


Fig. 6. - Numerical values of $I(x/R)$ calculated in our hypothesis (full line) and assuming δ -rays to be emitted perpendicularly to the track (dotted line).

the numerical value of the constant being $1/2\pi$, in order to obtain

$$\int_0^\pi f(\theta) 2\pi \sin \theta d\theta = 1.$$

From (A.3) and (A.5) we obtain

$$(A.6) \quad \frac{\bar{W}(x, r)}{W(r)} = \int_{\theta_0}^{\pi/2} \left(1 - \frac{x}{r \sin \theta}\right)^{1/\alpha} \sin \theta d\theta = \frac{1}{z} \int_1^z \left(1 - \frac{1}{y}\right)^{1/\alpha} \frac{y dy}{\sqrt{z^2 - y^2}},$$

where we have set

$$z = \frac{r}{x}, \quad y = \frac{r \sin \theta}{x}.$$

From (A.4) and (A.6) it is possible to calculate the integral $I(x/R)$

$$I\left(\frac{x}{R}\right) = \int_x^R \frac{W(x, r)}{W(r)} \frac{dr}{r} = \int_1^{R/x} \frac{dz}{z} \cdot \frac{1}{z} \int_1^z \left(1 - \frac{1}{y}\right)^{1/\alpha} \frac{y dy}{\sqrt{z^2 - y^2}} =$$

$$= \int_1^{R/x} \left(1 - \frac{1}{y}\right)^{1/\alpha} y dy \int_y^{R/x} \frac{1}{\sqrt{z^2 - y^2}} \frac{dz}{z^2},$$

namely

$$(A.7) \quad I\left(\frac{x}{R}\right) = \int_1^{R/x} \left(1 - \frac{1}{y}\right)^{1/\alpha} \sqrt{1 - \left(\frac{xy}{R}\right)^2} \frac{dy}{y}.$$

The integral $I(x/R)$ has been evaluated by numerical computation and is given in Fig. 6 as a function of x/R (continuous line). For comparison the same calculation has been made under the assumption that all δ -rays are perpendicular to the particle path; the result is also reported as a dotted line in Fig. 6.

RIASSUNTO

È stata misurata la larghezza fotometrica di tracce di ioni pesanti (^{16}O e ^{12}C), di particelle α e di particelle di carica 1, terminanti nell'emulsione, allo scopo di studiare il fenomeno dell'assottigliamento delle tracce di ioni pesanti e più in generale il meccanismo di formazione della traccia in fine percorso. Il modello di formazione della traccia che proponiamo è basato su semplici ipotesi e sembra in accordo sia con le idee correntemente accettate sull'effetto dello sviluppo, sia coi nostri risultati sperimentali. Un controllo delle nostre ipotesi è possibile indipendentemente dalla conoscenza dettagliata del comportamento degli elettroni di bassissima energia; con l'uso di una relazione range-energia estrapolata dai dati sperimentali, è possibile valutare quantitativamente l'andamento della larghezza della traccia in funzione della velocità della particella, e i risultati di questo calcolo sono in soddisfacente accordo con i nostri dati sperimentali.

Double Elastic Scattering of Deuterons in a Magnetic Field.

O. D. CHEISHVILI and G. R. KHUTSISHVILI

Physical Institute of the Georgian Academy of Sciences - Tbilissi

(ricevuto il 4 Ottobre 1958)

Summary. — In this work we consider the double elastic scattering of a deuteron beam in a magnetic field. The expression for the angular distribution of the double elastic scattering is obtained. The discussion is given of possible experiments on deuteron double elastic scattering with and without a magnetic field. It is shown that the double elastic scattering in a magnetic field can give some additional information about the scattering amplitude and the polarization in comparison with the double scattering without a magnetic field.

1. — The theoretical study of double elastic scattering of an electron beam in this paper ⁽¹⁾ is made for the case when a constant homogeneous magnetic field affects the beam. An electron has an anomalous magnetic moment which causes an additional scattering, the measurement of the latter allows one to determine experimentally the anomalous moment.

This work deals with the theoretical study of the double elastic scattering of a beam of particles with spin 1 in a magnetic field. It is found in this case (contrary to the case of a particle with spin $\frac{1}{2}$) that the measurement of the double elastic scattering in a magnetic field gives some additional information about the scattering amplitude.

⁽¹⁾ H. MENDLOWITZ and K. CASE: *Phys. Rev.*, **97**, 33 (1955).

2. - The scattering amplitude of a deuteron on a nucleus with spin 0 is given by (2)

$$(1) \quad F(\vartheta, \varphi) = A(\vartheta) + B(\vartheta)(\mathbf{S}\mathbf{n}) + C(\vartheta)(\mathbf{S}\mathbf{n})^2 + \\ + \frac{1}{2}D(\vartheta)\{(\mathbf{S}\mathbf{k}_0)(\mathbf{S}\mathbf{k}) + (\mathbf{S}\mathbf{k})(\mathbf{S}\mathbf{k}_0)\},$$

where \mathbf{k}_0 and \mathbf{k} are unit vectors along the momentum of the deuteron before and after the scattering respectively, $\mathbf{n} = [\mathbf{k}_0 \times \mathbf{k}] / \sin \vartheta$ is the unit vector perpendicular to the plane of scattering, \mathbf{S} is the deuteron spin operator, A , B , C and D are functions of the scattering angle and of the deuteron energy. The cross-section of the polarized beam is calculated from the formula

$$(2) \quad I(\vartheta, \varphi) = \text{Tr} \{ F(\vartheta, \varphi) \varrho F^+(\vartheta, \varphi) \},$$

where ϱ is the spin density matrix of the deuteron beam

$$(3) \quad \varrho = \frac{1}{3} \sum_{jM} \langle T_{jM} \rangle T_{jM}^+,$$

the following operators are used

$$(4) \quad \left\{ \begin{array}{l} T_{1\pm 1} = \mp \frac{\sqrt{3}}{2} (S_x \pm iS_y), \quad T_{10} = \sqrt{\frac{3}{2}} S_z, \\ T_{2\pm 2} = \frac{\sqrt{3}}{2} (S_x \pm iS_y)^2, \quad T_{2\pm 1} = \mp \frac{\sqrt{3}}{2} \{ (S_x \pm iS_y) S_z + S_z (S_x \pm iS_y) \}, \\ T_{20} = \frac{1}{\sqrt{2}} (3S_z^2 - 2), \end{array} \right.$$

$\langle T_{jM} \rangle$ is the mean value of T_{jM} .

Substituting the value of the polarization after the first scattering for T_{jM}

$$(5) \quad \langle T_{jM} \rangle I_0(\vartheta) = \frac{1}{3} \text{Tr} \{ F(\vartheta, \varphi) F^+(\vartheta, \varphi) T_{jM} \}$$

and using the co-ordinate system in which the plane of the first scattering coincides with the plane XOZ , and the plane of the second scattering passes through the Z axis (in other words, the Z direction is along the direction of the deuteron momentum after the first scattering), we get the differential cross-section of the double elastic scattering in the following form

$$(6) \quad I(\vartheta_1, \vartheta, \varphi) = I_0(\vartheta) \{ 1 + \langle T_{20}(\vartheta_1) \rangle \langle T_{20}(\vartheta) \rangle + 2 [\langle T_{11}(\vartheta_1) \rangle \langle T_{11}(\vartheta) \rangle^* + \\ + \langle T_{21}(\vartheta_1) \rangle \langle T_{21}(\vartheta) \rangle] \cos \varphi + 2 \langle T_{22}(\vartheta_1) \rangle \langle T_{22}(\vartheta) \rangle \cos 2\varphi \},$$

(2) O. CHEISHVILI: *Journ. Exp. Theor. Phys. USSR*, **30**, 1147 (1956).

where ϑ_1 and ϑ are the angles of the first and the second scattering respectively, φ is the angle between the two planes of scattering, $I_0(\vartheta)$ is the differential cross-section of the unpolarized beam

$$(7) \quad I_0(\vartheta) = |A|^2 + \frac{2}{3}|B|^2 + \frac{2}{3}|C|^2 + \frac{1}{2}(\cos^2 \vartheta + \frac{1}{3})|D|^2 + \\ + \frac{4}{3} \operatorname{Re}[A^*(C + \cos \vartheta D)] + \frac{2}{3} \cos \vartheta \operatorname{Re}(C^* D),$$

$\langle T_{11} \rangle$, $\langle T_{20} \rangle$, $\langle T_{21} \rangle$ and $\langle T_{22} \rangle$ are given by

$$(5') \quad \langle T_{11} \rangle I_0(\vartheta) = -i \frac{2}{\sqrt{3}} \operatorname{Re} \left[\left(A + C + \frac{1}{2} \cos \vartheta D \right) B^* \right],$$

$$(5'') \quad \langle T_{20} \rangle I_0(\vartheta) = -\frac{\sqrt{2}}{6} (|B|^2 + |C|^2) + \frac{\sqrt{2}}{8} \left(\cos^2 \vartheta - \frac{1}{3} \right) |D|^2 - \\ - \frac{\sqrt{2}}{3} \operatorname{Re}[(A - \cos \vartheta D) C^*] + \frac{2\sqrt{2}}{3} \cos \vartheta \operatorname{Re}(A^* D) + \frac{\sqrt{2}}{2} \sin \vartheta \operatorname{Im}(B^* D),$$

$$(5''') \quad \langle T_{21} \rangle I_0(\vartheta) = -\frac{\sqrt{3}}{6} \sin \vartheta \cos \vartheta |D|^2 - \frac{\sqrt{3}}{3} \sin \vartheta \operatorname{Re}[(A + C) D^*] + \\ + \frac{\sqrt{3}}{3} \cos \vartheta \operatorname{Im}(B^* D),$$

$$(5''') \quad \langle T_{22} \rangle I_0(\vartheta) = -\frac{\sqrt{3}}{6} \left\{ |B|^2 + |C|^2 + \frac{\sin^2 \vartheta}{4} |D|^2 + 2 \operatorname{Re}[(A + \cos \vartheta D) C^*] + \right. \\ \left. + \sin \vartheta \operatorname{Im}(B^* D) \right\}.$$

We recall the following relations for the $T_{1,M}$

$$(8) \quad \langle T_{1,-M} \rangle = (-1)^{M+1} \langle T_{1,M} \rangle, \quad \langle T_{2,-M} \rangle = (-1)^M \langle T_{2M} \rangle.$$

3. — It is known that due to the anomalous magnetic moment of the electron the precession of the electron spin in a magnetic field takes place somewhat quicker than the precession of the orbital angular momentum, therefore when the polarized electron beam is in a magnetic field, generally speaking, the polarization will change (we mean the direction of the polarization relative to the direction of the beam) ^(1,3). For the particle with spin $\frac{1}{2}$ the initial polarization will be changed only if the particle has an anomalous magnetic moment (*i.e.* the Lande factor is not two). In the case of a particle with spin 1 the initial polarization will be changed even if there is no anomalous magnetic moment (*i.e.* even if the Lande factor g is one).

(3) K. CASE: *Phys. Rev.*, **106**, 173 (1957).

According to paper ⁽¹⁾, the density matrix when there is a magnetic field is given by

$$\varrho(t) = \exp[i(\omega_L \mathbf{L} + \omega_s \mathbf{S})\mathbf{h}t] \varrho(0) \exp[-i(\omega_L \mathbf{L} + \omega_s \mathbf{S})\mathbf{h}t],$$

where $\varrho(0)$ is the density matrix when there is no magnetic field, $\varrho(t)$ is the density matrix at time t after the magnetic field had been applied, \mathbf{h} is the unit vector along the field and

$$(9) \quad \omega_L = \frac{eH}{mc}, \quad \omega_s = \frac{geH}{2mc}.$$

Writing

$$(10) \quad \xi = (\omega_s - \omega_L)t, \quad \eta = \omega_L t,$$

we get

$$\varrho(t) = \exp[i\mathbf{J}\mathbf{h}\eta] \exp[i\mathbf{S}\mathbf{h}\xi] \varrho(0) \exp[-i\mathbf{S}\mathbf{h}\xi] \exp[-i\mathbf{J}\mathbf{h}\eta]$$

(where $\mathbf{J} = \mathbf{L} + \mathbf{S}$ is the total moment).

It is easy to show that the differential cross-section of the double-elastic scattering is

$$(11) \quad I(\vartheta, \varphi) = Q(t) \operatorname{Tr} \{F(\vartheta, \varphi) \varrho'(t) F^\dagger(\vartheta, \varphi)\} Q^{-1}(t),$$

where

$$(12) \quad \varrho'(t) = \exp[i\mathbf{S}\mathbf{h}\xi] \varrho(0) \exp[-i\mathbf{S}\mathbf{h}\xi],$$

$$(13) \quad Q(t) = \exp[i\mathbf{L}\mathbf{h}\eta].$$

The calculations give

$$(14) \quad \varrho'(t) = \frac{1}{3} + \frac{1}{2} P_i(t) S_i + T_{ik}(t) S_i S_k,$$

where

$$(15) \quad P_i(t) = \cos \xi P_i + (1 - \cos \xi) h_i h_k P_k + \sin \xi \varepsilon_{ikn} h_n P_k,$$

$$(16) \quad \begin{aligned} T_{ik}(t) = & \cos 2\xi T_{ik} + (\cos \xi - \cos 2\xi) h_i (h_k T_{ke} + h_k T_{ie}) - \\ & - \sin \xi (\cos \xi - 1) h_n h_m (h_i \varepsilon_{ken} + h_k \varepsilon_{ien}) T_{em} + \sin \xi \cos \xi h_n (\varepsilon_{ien} T_{ke} + \varepsilon_{ken} T_{ie}) + \\ & + (\cos \xi - 1)^2 h_i h_k h_e h_m T_{em} - \sin^2 \xi \delta_{ik} h_e h_m T_{em}, \end{aligned}$$

$$P_i = \operatorname{Tr} [S_i \varrho(0)] = P_i(0),$$

$$T_{ik} = \operatorname{Tr} \left\{ \left[\frac{1}{2} (S_i S_k + S_k S_i) - \frac{2}{3} \delta_{ik} \right] \varrho(0) \right\} = T_{ik}(0).$$

It is easy to prove that $T_{ik}(t) = T_{ki}(t)$, $T_{ii}(t) = 0$.

For the further calculations it is convenient to use the irreducible spin tensors of Racah (4), the mean values of which are

$$(17) \quad \begin{cases} \langle T_{1\pm 1}(t) \rangle = \mp \frac{\sqrt{3}}{2} \{P_x(t) \pm iP_y(t)\}, & \langle T_{10}(t) \rangle = \sqrt{\frac{3}{2}} P_z(t), \\ \langle T_{2\pm 2}(t) \rangle = \frac{\sqrt{3}}{2} \{T_{xx}(t) - T_{yy}(t) \pm 2iT_{xy}(t)\}, & \langle T_{2\pm 1}(t) \rangle = \mp \sqrt{3} \{T_{xz}(t) \pm iT_{yz}(t)\}, \\ \langle T_{20}(t) \rangle = \frac{3}{\sqrt{2}} T_{zz}(t). \end{cases}$$

So using (15), (16) and (17) we can express $\langle T_{jM}(t) \rangle$ by means of $\langle T_{jM}(0) \rangle$.

It is easy to get the following expression for $Q'(t)$

$$(18) \quad Q'(t) = \frac{1}{3} \sum_{jM} \langle T_{jM}(t) \rangle T_{jM}^+.$$

Let us consider the cases of longitudinal and transverse magnetic fields.

In the case of a longitudinal magnetic field (*i.e.* \mathbf{h} is parallel to z), equations (16), (17) and (8) give

$$\begin{aligned} \langle T_{1\pm 1}(t) \rangle &= \exp[\mp i\xi] \langle T_{1\pm 1} \rangle, & \langle T_{10}(t) \rangle &= 0, \\ \langle T_{2\pm 2}(t) \rangle &= \exp[\mp 2i\xi] \langle T_{2\pm 2} \rangle, & \langle T_{2\pm 1}(t) \rangle &= \exp[\mp i\xi] \langle T_{2\pm 1} \rangle, & \langle T_{20}(t) \rangle &= \langle T_{20} \rangle \end{aligned}$$

In the case of a transverse magnetic field (\mathbf{h} is parallel to y) we get

$$\begin{aligned} \langle T_{1\pm 1}(t) \rangle &= \langle T_{1\pm 1} \rangle, & \langle T_{10}(t) \rangle &= 0, \\ \langle T_{2\pm 2}(t) \rangle &= \frac{1}{2} (1 + \cos^2 \xi) \langle T_{2\pm 2} \rangle \pm \frac{1}{2} \sin 2\xi \langle T_{2\pm 1} \rangle + \frac{1}{2} \sqrt{\frac{3}{2}} \sin^2 \xi \langle T_{20} \rangle, \\ \langle T_{2\pm 1}(t) \rangle &= \cos 2\xi \langle T_{2\pm 1} \rangle \mp \frac{1}{2} \sin 2\xi \langle T_{2\pm 2} \rangle \pm \frac{1}{2} \sqrt{\frac{3}{2}} \sin 2\xi \langle T_{20} \rangle, \\ \langle T_{20}(t) \rangle &= \frac{1}{2} (\cos 2\xi + \cos^2 \xi) \langle T_{20} \rangle + \sqrt{\frac{3}{2}} \sin^2 \xi \langle T_{22} \rangle - \sqrt{\frac{3}{2}} \sin 2\xi \langle T_{21} \rangle. \end{aligned}$$

In the case of a longitudinal field the operator $Q(t)$ is

$$Q(t) = \exp \left[\eta \frac{\partial}{\partial \varphi} \right],$$

and the differential cross-section of the double elastic scattering is

$$(19) \quad I_{\parallel}(\vartheta_1, \vartheta, \varphi) = I_0(\vartheta) \{ 1 + \langle T_{20}(\vartheta_1) \rangle \langle T_{20}(\vartheta) \rangle + 2[\langle T_{11}(\vartheta_1) \rangle \langle T_{11}(\vartheta) \rangle^* + \langle T_{21}(\vartheta_1) \rangle \langle T_{21}(\vartheta) \rangle] \cos(\varphi + \eta + \xi) + 2\langle T_{22}(\vartheta_1) \rangle \langle T_{22}(\vartheta) \rangle \cos 2(\varphi + \eta + \xi) \}.$$

In the case of a transverse magnetic field

$$Q(t) = \exp \left[\eta \cos \varphi \frac{\partial}{\partial \vartheta} - \eta \sin \varphi \operatorname{ctg} \vartheta \frac{\partial}{\partial \varphi} \right],$$

and the differential cross-section of the double elastic scattering is

$$(20) \quad I_{\perp}(\vartheta_1, \vartheta, \varphi) = I_0(\vartheta) \{ 1 + a(\vartheta_1 + \eta \cos \varphi, \vartheta) + b(\vartheta_1 + \eta \cos \varphi, \vartheta) \cdot \\ \cdot \cos(\varphi - \eta \sin \varphi \operatorname{ctg} \vartheta_1) + c(\vartheta_1 + \eta \cos \varphi, \vartheta) \cos 2(\varphi - \eta \sin \varphi \operatorname{ctg} \vartheta_1) \},$$

where

$$(21') \quad a(\vartheta_1, \vartheta) = \langle T_{20}(\vartheta) \rangle \left\{ \frac{1}{2} (\cos 2\xi + \cos^2 \xi) \langle T_{20}(\vartheta_1) \rangle + \right. \\ \left. + \sqrt{\frac{3}{2}} \sin^2 \xi \langle T_{22}(\vartheta_1) \rangle - \sqrt{\frac{3}{2}} \sin 2\xi \langle T_{21}(\vartheta_1) \rangle \right\},$$

$$(21'') \quad b(\vartheta_1, \vartheta) = 2 \left[\langle T_{21}(\vartheta) \rangle \left\{ \cos 2\xi \langle T_{21}(\vartheta_1) \rangle - \frac{1}{2} \sin 2\xi \langle T_{22}(\vartheta_1) \rangle + \right. \right. \\ \left. \left. + \frac{1}{2} \sqrt{\frac{3}{2}} \sin 2\xi \langle T_{20}(\vartheta_1) \rangle \right\} + \langle T_{11}(\vartheta) \rangle^* \langle T_{11}(\vartheta_1) \rangle \right],$$

$$(21''') \quad c(\vartheta_1, \vartheta) = 2 \langle T_{22}(\vartheta) \rangle \left\{ \frac{1}{2} (1 + \cos^2 \xi) \langle T_{22}(\vartheta_1) \rangle + \right. \\ \left. + \frac{1}{2} \sin 2\xi \langle T_{21}(\vartheta_1) \rangle + \frac{1}{2} \sqrt{\frac{3}{2}} \sin 2\xi \langle T_{20}(\vartheta_1) \rangle \right\}.$$

4. — The problem of the multiple scattering is to determine the scattering amplitude from experimental data. We need seven independent relations (to determine four moduli and three phase differences) to determine the coefficients of the scattering amplitude (1). We can get one relation among the coefficients A , B , C and D by measuring the scattering intensity of the unpolarized beam of deuterons (see (7)).

We shall consider now the experiments on simple double scattering (*i.e.* when there is no magnetic field), and we shall treat only the case when both scatterings take place almost under the same conditions (*i.e.* $\vartheta_1 \approx \vartheta$, and the energies are also approximately equal). It is seen from expression (6) that experiments on the simple double scattering give three relations for the coefficients of the scattering amplitude. In fact

$$(22') \quad \frac{\frac{1}{2\pi} \int_0^\infty I d\varphi - I_0}{I_0} = \langle T_{20}(\vartheta) \rangle^2,$$

$$(22'') \quad \frac{I(\varphi=0) - I(\varphi=\pi)}{2I_0} = 2[|\langle T_{11}(\vartheta) \rangle|^2 + \langle T_{21}(\vartheta) \rangle^2],$$

$$(22''') \quad \frac{\frac{1}{2}I(\varphi=0) + \frac{1}{2}I(\varphi=\pi) - I(\varphi=\pi/2)}{2I_0} = 2\langle T_{22}(\vartheta) \rangle^2.$$

Thus the experiments on simple double scattering cannot determine (contrary to the case of spin $\frac{1}{2}$) $\langle T_{11} \rangle$, *i.e.* the degree of polarization of the beam after the first scattering.

Finally we shall consider the experiments on double scattering in a transverse magnetic field (the case of a longitudinal magnetic field does not give anything new in comparison with the simple double scattering). From expression (20) we can show

$$\begin{aligned} \frac{I_1(\varphi=0) - I_1(\varphi=\pi)}{2I_0} &= \frac{1}{2} \{ a(\vartheta + \eta, \vartheta) - a(\vartheta - \eta, \vartheta) + \\ &+ b(\vartheta + \eta, \vartheta) + b(\vartheta - \eta, \vartheta) + c(\vartheta + \eta, \vartheta) - c(\vartheta - \eta, \vartheta) \}. \end{aligned}$$

We shall choose the value of the magnetic intensity and the time spent by the deuteron in the field (*i.e.* the time between the scatterings) in such a way that (n is an integer)

$$(23) \quad \eta = 2\pi n, \quad \text{i.e.} \quad Ht = 2\pi n \frac{mc}{e}.$$

Then

$$(24') \quad \frac{I_{\perp}(\varphi=0) - I_{\perp}(\varphi=\pi)}{2I_0} = 2 \left[|\langle T_{11}(\vartheta) \rangle|^2 + \langle T_{21}(\vartheta) \rangle \left\{ \cos 2\xi \langle T_{21}(\vartheta) \rangle - \right. \right. \\ \left. \left. - \frac{1}{2} \sin 2\xi \langle T_{22}(\vartheta) \rangle + \frac{1}{2} \sqrt{\frac{3}{2}} \sin 2\xi \langle T_{20}(\vartheta) \rangle \right\} \right].$$

Similarly we get

$$(24'') \quad \frac{I_{\perp}(\varphi=0) + I_{\perp}(\varphi=\pi)}{2I_0} = 1 + \langle T_{20}(\vartheta) \rangle \left\{ \frac{1}{2} (\cos 2\xi + \cos^2 \xi) \langle T_{20}(\vartheta) \rangle + \right. \\ \left. + \sqrt{\frac{3}{2}} \sin^2 \xi \langle T_{22}(\vartheta) \rangle - \sqrt{\frac{3}{2}} \sin 2\xi \langle T_{21}(\vartheta) \rangle \right\} + \\ + 2 \langle T_{22}(\vartheta) \rangle \left\{ \frac{1}{2} (1 + \cos^2 \xi) \langle T_{22}(\vartheta) \rangle + \frac{1}{2} \sin 2\xi \langle T_{21}(\vartheta) \rangle + \frac{1}{2} \sqrt{\frac{3}{2}} \sin^2 \xi \langle T_{20}(\vartheta) \rangle \right\},$$

$$(24''') \quad \frac{\frac{1}{2}I_{\perp}(\varphi=0) + \frac{1}{2}I_{\perp}(\varphi=\pi) - I_{\perp}(\varphi=\pi/2)}{I_0} = \\ = - \frac{I_{\perp}(\varphi=0) - I_{\perp}(\varphi=\pi)}{2I_0} \sin(2\pi n \operatorname{ctg} \vartheta) + 2(1 + \cos(4\pi n \operatorname{ctg} \vartheta)) \cdot \\ \cdot \langle T_{22}(\vartheta) \rangle \left\{ \frac{1}{2} (1 + \cos \xi) \langle T_{22}(\vartheta) \rangle + \frac{1}{2} \sin 2\xi \langle T_{21}(\vartheta) \rangle + \frac{1}{2} \sqrt{\frac{3}{2}} \sin^2 \xi \langle T_{20}(\vartheta) \rangle \right\}.$$

Let us note that for the above mentioned value of Ht we have

$$(25) \quad \xi = 2\pi n \left(\frac{g}{2} - 1 \right).$$

Thus we have six relations (22) and (24). Of course not all of them are independent of each other but they are sufficient for the determination of $\langle T_{11} \rangle$, $\langle T_{20} \rangle$, $\langle T_{21} \rangle$ and $\langle T_{22} \rangle$. Having found these quantities and obtained the expression of $I_0(\theta)$, we have five equations for seven unknown quantities of the scattering amplitude.

We have considered the case of a field along y in detail. If the field is along x , *i.e.* parallel to the plane of the first scattering and perpendicular to the deuteron momentum after the first scattering we do not get any additional data about the scattering amplitude (no more than those which are obtained in the case of the field along y). We can say the same about the case of an arbitrary direction of the field.

Thus though the measurements of the double elastic scattering in a magnetic field give some additional data about the scattering amplitude they are not enough for its complete definition.

So we see that the double elastic scattering in a magnetic field gives less data about the scattering amplitude than simple triple scattering (the latter gives all the data about the scattering amplitude). That is because the magnetic field does not change the absolute value of the polarization vector as well as the sum of the squares of the components of the tensor $\langle T_{2M} \rangle$.

RIASSUNTO (*)

Nel presente lavoro si considera lo scattering elastico doppio di un fascio di deutoni in un campo magnetico. Si ottiene l'espressione per la distribuzione angolare per lo scattering elastico doppio. Si discutono i possibili esperimenti sullo scattering elastico doppio dei deutoni in presenza e in assenza di campo magnetico. Si dimostra che lo scattering elastico doppio in presenza di campo magnetico può fornire qualche maggior dato sull'ampiezza di scattering e la polarizzazione in confronto con lo scattering doppio in assenza di campo magnetico.

(*) Traduzione a cura della Redazione.

Irreducibility Constraints and Field Equations for the Elementary Particles.

I. - Bosons.

C. G. BOLLINI

Comisión Nacional de la Energía Atómica - Buenos Aires ()*

(ricevuto il 21 Ottobre 1958)

Summary. — The conditions needed to describe an elementary particle by an irreducible quantity in the Lorentz group, are here taken as constraint equations to be imposed on the field entity. The independent components are extracted in a covariant way. The field equations are deduced from a Lagrangian in which only the free components are permitted to be varied. The commutation relations, compatible with the constraints, are also given. In Sect. 1 the field entity is a tensor, in a forthcoming paper we will consider spin-tensors and simple Dirac spinors for which second order wave equations will be proposed.

1. - Introduction.

The field of an elementary particle with integer spin, is represented by means of a tensor A . Irreducibility under the Lorentz group and uniqueness of spin is assured if the following conditions are imposed ⁽¹⁾. A must be *a)* completely symmetric, *b)* traceless, *c)* divergenceless. These three conditions reduce the number of independent components to $2s+1$ which is the right number of possible orientations of a particle with spin s .

Condition *c* for example, implies the spacial character of the spin in the rest system. Nevertheless this condition is usually deduced, whenever possible ($m \neq 0$), from a suitable Lagrangian, being then dependent on the equations of motion.

(*) Now on leave of absence.

(¹) H. UMEZAWA: *Quantum field theory* (1956), pp. 64-66.

Our viewpoint is different. We are going to take $a)$, $b)$ and $c)$ as constraint conditions to be imposed on the field tensor independently of the equation of motion. It will be shown that no difference with the usual procedure will result in the free field case. But new possibilities arise in the presence of interactions.

Something similar happens when the particle is a fermion. The representing field may be chosen to be a spin-tensor ⁽²⁾ which must be: $a')$ completely symmetric, $b')$ «perpendicular» to γ_μ , and $c')$ divergenceless. The traceless character can be deduced from $a')$ and $b')$. Here too, complicated Lagrangians must be written down in order to be able to deduce $b')$ and $c')$ as equations of motion ^(2,3). We have now two ways opened. We can take either a first or a second order wave equation ⁽⁴⁾. With our point of view the second possibility seems more logical because a Dirac spinor in itself has two redundant components ⁽⁴⁾. Also, the connection between spin and statistics is indeed independent of the equation of motion ⁽⁵⁾. In order to eliminate the redundant components we are going to change $c')$ in favour of a natural and more stringent condition which will be mentioned in Part II.

Summarizing. — Our aim is: 1) The statement of the constraint equations. 2) The extraction, in a covariant way, of the independent components of the field entity representing any particle with spin greater than zero (the $S = 0$ case being trivial). 3) The deduction of the field equations for the independent components and the field entity. 4) The quantization of the field in a way compatible with the constraints.

For the sake of clearness we only treat in this paper the integer spin case. In a forthcoming second part we are going to treat the fermion fields.

2. — Basic tensors.

We first arbitrarily choose three space-like unit vector operators which are perpendicular to the impulse vector $p_\mu = -i\partial_\mu$

$$(2.1) \quad \begin{cases} a_\mu a_\mu = b_\mu b_\mu = c_\mu c_\mu = 1, \\ a_\mu b_\mu = b_\mu c_\mu = c_\mu a_\mu = 0, \\ a_\mu p_\mu = b_\mu p_\mu = c_\mu p_\mu = 0. \end{cases}$$

⁽²⁾ W. RARITA and J. SCHWINGER: *Phys. Rev.*, **60**, 61 (1941).

⁽³⁾ H. UMEZAWA: *Quantum field theory* (1956), p. 120.

⁽⁴⁾ R. P. FEYNMAN and M. GELL-MANN: *Phys. Rev.*, **409**, 193 (1958).

⁽⁵⁾ N. BURGOYNE: *Nuovo Cimento*, **8**, 607 (1958).

These three operators, together with the properly normalized impulse vector ⁽⁶⁾ d_μ

$$(2.2) \quad d_\mu = p^{-1} p_\mu, \quad d_\mu d_\mu = -1$$

form a basic system of vectors. We have

$$(2.3) \quad \delta_{\mu\nu} = a_\mu a_\nu + b_\mu b_\nu + c_\mu c_\nu - d_\mu d_\nu.$$

Any field tensor $A_{\mu_1 \dots \mu_s}$ satisfying conditions a , b and c , can be expressed in terms of a basic system of tensors satisfying also the same constraints. Such a basis may be formed with the following tensor operators

$$(2.4) \quad \begin{cases} N^{(r)} p_{\mu_1 \dots \mu_s}^{(2r-1)} = p_{\mu_1 \dots \mu_{s+1}}^{(2r-2)} a_{\mu_{s+1}} + p_{\mu_1 \dots \mu_{s+1}}^{(2r-3)} b_{\mu_{s+1}} \\ N^{(r)} p_{\mu_1 \dots \mu_s}^{(2r)} = p_{\mu_1 \dots \mu_{s+1}}^{(2r-2)} b_{\mu_{s+1}} - p_{\mu_1 \dots \mu_{s+1}}^{(2r-3)} a_{\mu_{s+1}} \end{cases} \quad r = 1, 2, \dots, s.$$

This is a recurrence chain which allows any tensor to be written in terms of $p_{\mu_1 \dots \mu_{s+1}}^{(0)}$ ⁽⁷⁾. A formula for the latter is given in the appendix. $N^{(r)}$ are normalization constants. We have

$$(2.5) \quad p_{\mu_1 \dots \mu_s}^{(\varrho)} p_{\mu_1 \dots \mu_s}^{(\sigma)} = \delta^{\varrho\sigma} \quad \varrho, \sigma = 0, 1, \dots, 2s.$$

Any one of the tensors $p_{\mu_1 \dots \mu_s}^{(\varrho)}$ is symmetric, traceless and perpendicular to d_μ (i.e., ∂_μ). They may be called « polarization tensors » for the fields $A_{\mu_1 \dots \mu_s}$ satisfying the constraints a , b and c .

3. - Projection operators.

As is always the case when we have a base for a given subspace, the corresponding projection operator may be formed by means of

$$(3.1) \quad P_{\mu_1 \dots \mu_s; \nu_1 \dots \nu_s} = \sum_{\varrho=0}^{2s} p_{\mu_1 \dots \mu_s}^{(\varrho)} p_{\nu_1 \dots \nu_s}^{(\varrho)}.$$

Recalling the properties of the polarization tensors we come to the conclusion that the projection operator coincides with that investigated by C.

⁽⁶⁾ Although some caution is needed, we are going to use the operator p^{-1} defined by

$$p^{-1} f(x) = \int d^4 p (-p_\mu p_\mu)^{-\frac{1}{2}} f(p) \exp [i p_\mu x_\mu].$$

⁽⁷⁾ When $r = 1$, in (2.4) we put $p_{\mu_1 \dots \mu_s}^{(-1)} \equiv 0$.

FRONSDAL ⁽⁸⁾. \mathbf{P} is independent of the chosen base because it is unique ⁽⁹⁾. Also

$$(3.2) \quad P_{\mu_1 \dots \mu_s; \alpha_1 \dots \alpha_s} P_{\alpha_1 \dots \alpha_s; \nu_1 \dots \nu_s} = P_{\mu_1 \dots \mu_s; \nu_1 \dots \nu_s}$$

and

$$(3.3) \quad P_{\mu_1 \dots \mu_s; \mu_1 \dots \mu_s} = 2s + 1.$$

For the vector field we have

$$P_{\mu; \nu} = a_{\mu} a_{\nu} + b_{\mu} b_{\nu} + c_{\mu} c_{\nu} (= p_{\mu}^{(0)} p_{\nu}^{(0)} + p_{\mu}^{(1)} p_{\nu}^{(1)} + p_{\mu}^{(2)} p_{\nu}^{(2)}).$$

It follows from (2.2) and (2.3) that

$$(3.4) \quad P_{\mu; \nu} = \delta_{\mu\nu} + d_{\mu} d_{\nu} = \delta_{\mu\nu} + p^{-2} p_{\mu} p_{\nu}.$$

4. - Constraint equations and free components.

The fact that a given tensor field A satisfies conditions a , b and c , is expressed by the constraint equation

$$(4.1) \quad A_{\mu_1 \dots \mu_s} = P_{\mu_1 \dots \mu_s; \nu_1 \dots \nu_s} A_{\nu_1 \dots \nu_s}.$$

By considering (3.1), we may draw from (4.1) the consequence that

$$(4.2) \quad \left\{ \begin{array}{l} A_{\mu_1 \dots \mu_s} = \sum_{\varrho} p_{\mu_1 \dots \mu_s}^{(\varrho)} p_{\nu_1 \dots \nu_s}^{(\varrho)} A_{\nu_1 \dots \nu_s}, \\ A_{\mu_1 \dots \mu_s} = \sum_{\varrho=0}^{2s} p_{\mu_1 \dots \mu_s}^{(\varrho)} A^{(\varrho)}, \end{array} \right.$$

where

$$(4.3) \quad A^{(\varrho)} = p_{\nu_1 \dots \nu_s}^{(\varrho)} A_{\nu_1 \dots \nu_s}.$$

The $2s+1$ scalar quantities $A^{(\varrho)}$ given by (4.3) may be taken as the free components of the field tensor A , and (4.2) expresses the latter as a function of the former. The presence of the polarization tensors in (4.2) assures the fulfilment of (4.1).

Some physical significance can be ascribed to the decomposition (4.2). The index ϱ is related to the spin orientation of the represented particle, but we are not going to elaborate on this point.

⁽⁸⁾ R. E. BEHREND and C. FRONSDAL: *Phys. Rev.*, **106**, 345 (1957).

⁽⁹⁾ R. E. BEHREND and C. FRONSDAL: *Phys. Rev.*, **106**, 345 (1957), Appendix.

5. - Lagrangians and field equations.

For the sake of simplicity we will consider only real tensor fields. A natural Lorentz invariant Lagrangian for such a field is:

$$(5.1) \quad L = -\frac{1}{2} (m^2 A_{v_1 \dots v_s} A_{v_1 \dots v_s} + \partial_\mu A_{v_1 \dots v_s} \partial_\mu A_{v_1 \dots v_s}).$$

This Lagrangian is essentially unique in the free field case. In order for the equation of motion to be deduced from the action integral, only the independent components of A must be varied. This is necessary if we want to be consistent with the constraints (4.1).

The action integral is

$$\mathcal{A} = - \int d^4x L.$$

By using (4.2) and (5.1), we have ⁽¹⁰⁾,

$$\mathcal{A} = -\frac{1}{2} \int d^4x (m^2 \sum_{\varrho} p_{v_1 \dots v_s}^{(\varrho)} A^{(\varrho)} \sum_{\sigma} p_{v_1 \dots v_s}^{(\sigma)} A^{(\sigma)} + \dots),$$

$$\mathcal{A} = -\frac{1}{2} \int d^4x (m^2 \sum_{\varrho \sigma} A^{(\varrho)} p_{v_1 \dots v_s}^{(\varrho)} p_{v_1 \dots v_s}^{(\sigma)} A^{(\sigma)} + \dots).$$

With the orthonormality property (2.5), we obtain

$$(5.2) \quad \mathcal{A} = -\frac{1}{2} \int d^4x (m^2 \sum_{\varrho} A^{(\varrho)} A^{(\varrho)} + \dots) = \sum_{\varrho} \int d^4x L^{(\varrho)},$$

$$(5.3) \quad L^{(\varrho)} = -\frac{1}{2} (m^2 A^{(\varrho)} A^{(\varrho)} + \partial_\mu A^{(\varrho)} \partial_\mu A^{(\varrho)}).$$

The equations of motion are now easily deduced from (5.2). The independent variations of the free components give the $2s+1$ equations

$$(5.4) \quad (\partial_\mu \partial_\mu - m^2) A^{(\varrho)} = 0$$

or equivalently (cf. (4.2))

$$(5.5) \quad (\partial_\mu \partial_\mu - m^2) A_{v_1 \dots v_s} = 0.$$

The equations of the theory are then the constraint equations (4.1) and the equations of motion (5.5) (or (5.4)).

⁽¹⁰⁾ It can be proved by a Fourier transformation that the polarization tensors may be viewed as hermitian operators.

In the presence of interactions, the Lagrangian is

$$L = \sum_{\varrho} L^{(\varrho)} + L^{(\text{int})},$$

where $L^{(\text{int})}$ has the form

$$(5.6) \quad L^{(\text{int})} = -A_{\mu_1 \dots \mu_s} F_{\mu_1 \dots \mu_s}.$$

F is a tensorial function of the field representing the source. We may now proceed exactly as before, but to speed up deductions we put

$$A_{\mu_1 \dots \mu_s} = P_{\mu_1 \dots \mu_s; \nu_1 \dots \nu_s} B_{\nu_1 \dots \nu_s},$$

where B is a tensor upon which no constraint is imposed.

The projection operator allows only the free components of A to follow the variations of all the 4^s components of B .

The action integral of the interaction is

$$\mathcal{A}^{\text{int}} = - \int d^4x A_{\mu_1 \dots \mu_s} F_{\mu_1 \dots \mu_s} = - \int d^4x P_{\mu_1 \dots \mu_s; \nu_1 \dots \nu_s} B_{\nu_1 \dots \nu_s} F_{\mu_1 \dots \mu_s}.$$

It follows from the variation of all the components of B and the hermitic character of P ⁽¹¹⁾, that

$$(5.7) \quad (\partial_\mu \partial_\mu - m^2) A_{\mu_1 \dots \mu_s} = -P_{\mu_1 \dots \mu_s; \nu_1 \dots \nu_s} F_{\nu_1 \dots \nu_s}.$$

Of course, (5.7) is compatible with the constraint (4.1). (5.7) means that only that part of the source which belongs to the space of P interacts with A .

6. - Quantization.

When a Lagrangian has the form

$$(6.1) \quad L = \frac{1}{2} (m^2 Q Q + \partial_\mu Q \partial_\mu Q)$$

the canonical rules imply the commutation relations

$$(6.2) \quad [Q(x), Q(x')] = -i \Delta(x - x').$$

⁽¹¹⁾ Cfr. footnote ⁽¹⁰⁾.

This is our case because the partial Lagrangian (5.3) has the form (6.1). Therefore

$$(6.3) \quad [A^{(\varrho)}(x), A^{(\sigma)}(x')] = -i\delta^{\varrho\sigma}\Delta(x-x').$$

Multiplying (6.3) with $p_{\mu_1\ldots\mu_s}^{(\varrho)}p_{\nu_1\ldots\nu_s}^{(\sigma)}$ and summing over ϱ and σ , we have (cf. (4.2)):

$$(6.4) \quad [A_{\mu_1\ldots\mu_s}(x), A_{\nu_1\ldots\nu_s}(x')] = -i \sum_{\varrho} p_{\mu_1\ldots\mu_s}^{(\varrho)} p_{\nu_1\ldots\nu_s}^{(\varrho')} \Delta(x-x').$$

In (6.4), $p_{\nu_1\ldots\nu_s}^{(\varrho')}$ operates on the x' variable of $\Delta(x-x')$, but neither the defining equations nor the properties (cfr. (2.1), (2.4)) of $p_{\nu_1\ldots\nu_s}^{(\varrho)}$ are changed if we transform ∂_{μ} into $-\partial_{\mu}$. Consequently

$$(6.5) \quad [A_{\mu_1\ldots\mu_s}(x), A_{\nu_1\ldots\nu_s}(x')] = -i P_{\mu_1\ldots\mu_s; \nu_1\ldots\nu_s} \Delta(x-x'),$$

(4.1), (5.8) and (6.5) show that the projection operators enter the theory in a rather fundamental way.

7. - Example. Vector field.

(3.4) gives the projection operator for the vector field. The corresponding commutation relations are

$$(7.1) \quad [A_{\mu}(x), A_{\nu}(x')] = -i(\delta_{\mu\nu} + p^{-2}p_{\mu}p_{\nu})\Delta(x-x').$$

The invariant function of Pauli and Jordan satisfies the Klein-Gordon equation; *i.e.*

$$(7.2) \quad p^{-2}\Delta(x-x') = \frac{1}{m^2}\Delta(x-x').$$

Then, (7.1) is equivalent to

$$(7.3) \quad [A_{\mu}(x), A_{\nu}(x')] = -i\left(\delta_{\mu\nu} - \frac{\partial_{\mu}\partial_{\nu}}{m^2}\right)\Delta(x-x').$$

We see now that the free field commutation relations do not differ from those usually imposed. It is nevertheless worth mentioning that this is not the case with the vacuum expectation value of the chronological product.

In fact, from

$$\langle 0 | T[A^{(\varrho)}(x), A^{(\sigma)}(x')] | 0 \rangle = -i\Delta_F(x-x').$$

proceeding as in Sect. 6, we shall arrive to

$$(7.4) \quad \langle 0 | T[A_{\mu_1 \dots \mu_s}(x), A_{\nu_1 \dots \nu_s}(x')] | 0 \rangle = -i P_{\mu_1 \dots \mu_s; \nu_1 \dots \nu_s} \Delta(x - x')$$

which for the vector field is

$$(7.5) \quad \left\{ \begin{aligned} \langle 0 | T[A_\mu(x), A_\nu(x')] | 0 \rangle &= -i(\delta_{\mu\nu} + p^{-2} p_\mu p_\nu) \Delta_F(x - x') = \\ &= -i(\delta_{\mu\nu} - p^{-2} \partial_\mu \partial_\nu) \Delta_F(x - x'). \end{aligned} \right.$$

But now the operator p^{-2} must be retained because Δ_F does not satisfy the homogeneous Klein-Gordon equation.

The presence of the projection operator in (7.4) is related to the fact that not only the field operator, but also the propagator must obey the constraint equations.

APPENDIX

In Sect. 2 we defined the polarization tensors by means of the recurrence formulae:

$$(A.1) \quad \left\{ \begin{aligned} p_{\mu_1 \dots \mu_s}^{(2r-1)} &= p_{\mu_1 \dots \mu_{s+1}}^{(2r-2)} a_{\mu_{s+1}} + p_{\mu_1 \dots \mu_{s+1}}^{(2r-3)} b_{\mu_{s+1}}, \\ p_{\mu_1 \dots \mu_s}^{(2r)} &= p_{\mu_1 \dots \mu_{s+1}}^{(2r-2)} b_{\mu_{s+1}} - p_{\mu_1 \dots \mu_{s+1}}^{(2r-3)} a_{\mu_{s+1}}. \end{aligned} \right.$$

A second application of (A.1) gives

$$(A.2) \quad \left\{ \begin{aligned} p_{\mu_1 \dots \mu_s}^{(2r-1)} &= p_{\mu_1 \dots \mu_{s+1}}^{(2r-4)} a_{\mu_{s+1} \mu_{s+2}} + p_{\mu_1 \dots \mu_{s+2}}^{(2r-5)} b_{\mu_{s+1} \mu_{s+2}}, \\ p_{\mu_1 \dots \mu_s}^{(2r)} &= p_{\mu_1 \dots \mu_{s+2}}^{(2r-4)} b_{\mu_{s+1} \mu_{s+2}} - p_{\mu_1 \dots \mu_{s+2}}^{(2r-5)} a_{\mu_{s+1} \mu_{s+2}}. \end{aligned} \right.$$

Where

$$(A.3) \quad \left\{ \begin{aligned} a_{\mu\nu} &= a_\mu b_\nu + a_\nu b_\mu, \\ b_{\mu\nu} &= b_\mu b_\nu - a_\mu a_\nu. \end{aligned} \right.$$

Step by step, the following formulae are arrived to

$$(A.4) \quad \left\{ \begin{aligned} p_{\mu_1 \dots \mu_s}^{(2r-1)} &= p_{\mu_1 \dots \mu_{s+r}}^{(0)} a_{\mu_{s+1} \dots \mu_{s+r}}, \\ p_{\mu_1 \dots \mu_s}^{(2r)} &= p_{\mu_1 \dots \mu_{s+r}}^{(0)} b_{\mu_{s+1} \dots \mu_{s+r}}, \end{aligned} \right.$$

with

$$(A.5) \quad \left\{ \begin{aligned} a_{\nu_1 \dots \nu_r} &= a_{\nu_1 \dots \nu_{r-1}} b_{\nu_r} + b_{\nu_1 \dots \nu_{r-1}} a_{\nu_r}, \\ b_{\nu_1 \dots \nu_r} &= b_{\nu_1 \dots \nu_{r-1}} b_{\nu_r} - a_{\nu_1 \dots \nu_{r-1}} a_{\nu_r}. \end{aligned} \right.$$

For $p^{(0)}$ we have

$$N p_{\mu_1 \dots \mu_t}^{(0)} = c_{\mu_1} \dots c_{\mu_t} + \alpha_1 (P_{\mu_2; \mu_2} c_{\mu_3} \dots c_{\mu_t} + \text{symm.}) + \alpha_2 (P_{\mu_1; \mu_2} P_{\mu_3; \mu_3} c_{\mu_4} \dots c_{\mu_t} + \text{symm.}) + \\ + \dots + \left\{ \begin{array}{l} \alpha_{t/2} P_{\mu_1; \mu_2} \dots P_{\mu_{t-1}; \mu_t} \\ \alpha_{(t-1)/2} P_{\mu_1; \mu_2} \dots P_{\mu_{t-2}; \mu_{t-1}} c_{\mu_t} \end{array} + \text{symm.} \right\} \quad \left. \begin{array}{l} (t = \text{even}), \\ (t = \text{odd}). \end{array} \right\}$$

$P_{\mu; \nu}$ is the projection operator (3.4). $\alpha_1, \alpha_2, \dots$ are constants to be determined so as to nullify the trace of $p_{\mu_1 \dots \mu_t}^{(0)}$. N is the normalization constant. «symm.» means symmetrizing terms.

Obviously, $p_{\mu_1 \dots \mu_t}^{(0)}$ is symmetric, traceless and perpendicular to d_μ .

RIASSUNTO (*)

Nel presente lavoro si considerano come equazioni restrittive da imporre all'intensità del campo le condizioni occorrenti a descrivere una particella elementare per mezzo di una grandezza irriducibile nel gruppo di Lorentz. Si ricavano le componenti indipendenti in modo covariante. Le equazioni di campo si deducono da un lagrangiano in cui solo le componenti libere possono variare. Si danno anche le relazioni di commutazione compatibili con le limitazioni. Nella Sez. 1 l'intensità di campo è un tensore; in un prossimo lavoro considereremo tensori spinoriali e spinori di Dirac semplici per i quali proporremo equazioni d'onda del second'ordine.

(*) Traduzione a cura della Redazione.

Absorptions of Negative K-Mesons at Rest in Nuclear Emulsion.

IV. — The Pion Producing Reactions.

Y. EISENBERG (*), W. KOCH, M. NIKOLIĆ (**), M. SCHNEEBERGER
and H. WINZELER

Physikalisches Institut der Universität - Bern

(ricevuto il 22 Ottobre 1958)

Summary. — Absorptions of negative K-mesons at rest in nuclear emulsions have been studied in great detail, using a large emulsion block. Most of the secondary particles came to rest in the stack and were identified. Comparing the results obtained in the present work with those previously obtained by us ⁽¹⁾ in a study of the interactions of fast K⁻-mesons, and with the results obtained by ALVAREZ *et al.* ⁽²⁾, the following conclusions may be drawn: 1) As we already derived in III, also in this experiment the single-nucleon reactions (pion producing captures) show a high rate of direct Λ -production. This result is a straightforward consequence of the observed sign fractions and absorption probabilities, if charge independence holds. It can be explained by the influence of the Fermi momentum. 2) The multi-nucleon (not producing pions) K⁻-captures form a large fraction of the total K⁻-captures at rest. It is estimated that as much as (35÷50)% of the captures occur via the multi-nucleon channel. 3) Probably the single-nucleon K⁻-captures at rest are mainly peripheral; thus they lead, because of geometrical reasons, to smaller pion and Σ -hyperon absorption probabilities. Our results mentioned in 2) and 3) verify the results of the European K⁻-Collaboration presented at the Geneva CERN Conference 1958 on Elementary Particles ⁽³⁾.

(*) On leave of absence from the Weizmann Institute, Rehovot.

(**) On leave of absence from the Institute of Nuclear Sciences, Boris Kidrich, Belgrade.

⁽¹⁾ Y. EISENBERG, W. KOCH, E. LOHRMANN, M. NIKOLIĆ, M. SCHNEEBERGER and H. WINZELER: *Nuovo Cimento*, **9**, 745 (1958). Hereafter referred as III. (The notations used in the present work are the same as in III).

⁽²⁾ L. W. ALVAREZ, H. BRADNER, P. FALK-VAIRANT, J. D. GOW, A. H. ROSENFELD, F. T. SOLMITZ and R. D. TRIPP: *Nuovo Cimento*, **5**, 1026 (1957).

1. - Introduction.

In a previous publication ⁽¹⁾ the interaction of fast negative K-mesons with complex nuclei of nuclear emulsion was studied in great detail. In particular, the reaction rates for the absorptions of K^- on single nucleons:

$$(A-1) \quad K^- + p \rightarrow \Sigma^- + \pi^+$$

$$(A-2) \quad \rightarrow \Sigma^+ + \pi^-$$

$$(A-3) \quad \rightarrow \Sigma^0 + \pi^0$$

$$(A-4) \quad \rightarrow \Lambda^0 + \pi^0$$

$$(A-5) \quad K^- + n \rightarrow \Sigma^- + \pi^0$$

$$(A-6) \quad \rightarrow \Sigma^0 + \pi^-$$

$$(A-7) \quad \rightarrow \Lambda^0 + \pi^-$$

were determined. The mean K^- kinetic energy in the above experiment was $\bar{T}_K \approx 86$ MeV, corresponding to a wave length of: $\hbar/p \approx 0.65 \cdot 10^{-13}$ cm. Thus it is to be expected that the K^- -capture should occur primarily on single nucleons, namely via one of the reactions (A-1) to (A-7) above. Indeed in (III) we did not see any evidence for a substantial contribution of the multi-nucleon reactions ((B-1) to (B-7) below) to the absorptions of fast K^- -mesons in emulsions.

The situation in the absorptions of K^- -mesons at rest is entirely different. The K^- could be absorbed by one of the reactions (A-1) to (A-7), or by many nucleons simultaneously. The possible final states having $(Y+N)$ are listed below:

$$(B-1) \quad K^- + nn \rightarrow \Sigma^- + n$$

$$(B-2) \quad K^- + np \rightarrow \Sigma^- + p$$

$$(B-3) \quad \rightarrow \Sigma^0 + n$$

$$(B-4) \quad \rightarrow \Lambda^0 + n$$

$$(B-5) \quad K^- + pp \rightarrow \Sigma^+ + n$$

$$(B-6) \quad \rightarrow \Sigma^0 + p$$

$$(B-7) \quad \rightarrow \Lambda^0 + p$$

Phenomenologically, the reactions (A-1)-(A-7) (from now on referred as 1 N-reactions) and the reactions (B-1)-(B-7) (2 N-reactions) describe comple-

tely the K^- -nucleus interaction, if the inelastic scattering of the hyperons and mesons and also the Fermi motion of the nucleons is taken into account. This phenomenological description, which is equivalent ⁽³⁾ to the final state interaction, will be used in the present work.

The capture stars of the K^- -mesons in nuclear emulsions have already been studied by several authors ⁽⁴⁻⁸⁾. In the present work we have been able to identify most of the particles emitted from the K^- -stars, and the conclusions which we reach are in some points somewhat different from those drawn in most of the previous works. In particular, as was first shown by the K^- -European Collaboration, the percentage of 2 N-reactions ⁽⁶⁾, which formerly was thought to be small is indeed quite large. About 30% of the observed hyperons from the K^- -captures at rest could not, energetically, originate from the 1 N-reactions and must therefore be due to the 2 N-reactions (Figs. 7-9). In fact, from the detailed analysis of our data we obtain a total contribution of about 45% from the 2 N-reactions. This should be compared with the situation in the stars at flight, in which only one hyperon (out of 26) had to be assumed, on energy grounds, to be produced in a 2 N-reaction.

The main purpose of the present work is to separate the (real) pion producing 1 N-reactions from the more complicated multi-nucleon absorptions of K^- -mesons; to derive the reaction rates of the various 1 N-reactions and to compare them with the results previously obtained for the stars in flight. We shall also discuss the possibility of having a substantial peripheral K^- -absorption and its relations to the pion and hyperon absorption probabilities. The 2 N-reactions will be discussed quite briefly and only in order to show that the derived 1 N-reaction rates agree more or less with the stable prong analysis. A detailed work concerning the multi-nucleon absorptions will be published later with improved statistics.

The general observational values are given in Section 2. A detailed discussion of the events emitting charged pions is given in Section 3. In the same section we also present the pion energy spectrum and compare it with a calculated one. The theoretical 2 N-transition rates, assuming charge indepen-

⁽³⁾ Y. YAMAGUCHI: private communication. A detailed work on this subject will be published soon.

⁽⁴⁾ W. F. FRY, J. SCHNEPS, G. A. SNOW, M. S. SWAMI and D. C. WOLD: *Phys. Rev.*, **107**, 257 (1957).

⁽⁵⁾ F. C. GILBERT, C. E. VIOLET and R. S. WHITE: *Phys. Rev.*, **107**, 228 (1957); **109**, 1770 (1958).

⁽⁶⁾ J. HORNOSTEL and G. T. ZORN: *Phys. Rev.*, **109**, 165 (1958).

⁽⁷⁾ F. M. WEBB, E. L. ILOFF, F. H. FEATHERSTON, W. W. CHUPP, G. GOLDBABER and S. GOLDBABER: *Nuovo Cimento*, **8**, 899 (1958).

⁽⁸⁾ K -EUROPEAN COLLABORATION: *High Energy Physics Conf.*, CERN (July 1958). Also E. H. S. BURHOP and C. DILWORTH-OCCHIALINI: private communication.

dence, are given in Section 4, and in Section 5 we attempt a separation of the Σ -hyperon into 1 N- and 2 N-events. Using the results obtained in Sections 3 and 5, and assuming again charge independence, we obtain the 1 N-reaction rates (Section 6). In Section 7 an estimate of the stable prongs to be expected from the 1 N-reaction is presented. Comparing it with the observed 2 N-hyperons, we get an idea what set of multi-nucleon reaction rates will explain the experimental stable prong analysis. The conclusions and comparison of the present results with those obtained in (III) for the stars in flight are given in Section 8.

2. - Observed values.

The details about the experimental set-up, scanning employed etc., were already published before (¹). In the present analysis were included 548 K^- -meson captures at rest in nuclear emulsions (excluding free proton absorptions). The secondary tracks were followed until the particles came to rest in the stack, left the stack, decayed or made nuclear interactions. Thus, most of the particles could be identified. The following table gives the raw observational values:

TABLE I.

Type of event	Numbers observed of			
	« clean » events (*)	events with at least one fast proton (**)	events having no fast protons	total
$(\pi^\pm, 0\Sigma)$	13	8	20	41
$(\pi^+, 0\Sigma)$	4	3	17	24
(π^+, Σ^-)	3	0	3	6
$(\pi^-, 0\Sigma)$	6	31	33	70
(π^-, Σ^+)	20	0	7	27
$(\pi^-, \text{Ex. Fr.})$	2	2	0	4
$(\pi^\pm, \text{Ex. Fr.})$	0	0	3	3
$(0\pi, \Sigma^+)$	1	0	1	2
$(0\pi, \Sigma^-)$	3	3	2	8
$(0\pi, \Sigma^\pm)$	3	11	6	20
$(0\pi, \text{Ex. Fr.})$	1	7	8	16
$K\varrho$	67	—	—	67
Stable prongs only	—	163	97	260
All	—	—	—	548

(*) A « clean » event means here a K^- absorption giving rise only to unstable charged particles and no other visible prongs.

(**) A fast proton will be defined in this work as a proton having ≥ 20 MeV kinetic energy.

In some of the (π, Σ) -events listed in Table I only one particle was actually identified, and the charge of its partner was inferred (meaning that charge exchange scattering of pions was assumed to be small). This procedure is justified since in most of the cases the charge of the hyperon and meson were identified, and in no case (Σ^-, π^-) - or (Σ^+, π^+) -events were seen.

It should be recalled that in identifying the Σ^- -hyperons we followed here exactly the procedure outlined in (III); namely, we have taken as Σ^- -hyperons only those tracks which give rise to 2 or more prongs (longer than 2-3 grains) capture stars at the end of their ranges, and which are not hyperfragments or π^- -mesons (the elimination of hyperfragments and π^- -stars is discussed in III). Thus we have to correct for 1 and zero prong Σ^- -capture stars. The correction factor is $16/5 = 3.2$ (see III). Each Σ^- at rest identified according to the above criterion stands therefore for 3.2 Σ^- -hyperons. The details of the hyperon events are given in Table II, Section 5.

3. - Pion energy spectra and sign fraction.

Out of 548 K^- -capture stars at rest, 175 emitted single (charged) pions (see Section 2). Most of the pions were identified by following them to the end of their ranges in the stack. Only 44 pions could not be identified because they either escaped the stack before coming to rest, or made a nuclear interaction in flight. The energy spectra of the charged pions are given in Figs. 1-5.

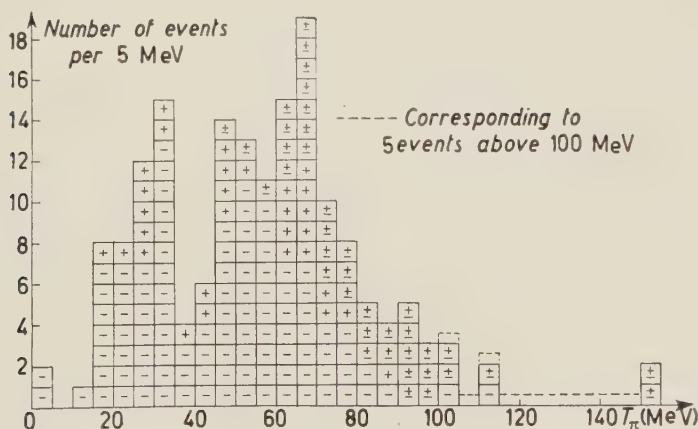


Fig. 1.

The 5 events whose energy could not be exactly determined, (only a lower limit of 100 MeV could be set) were plotted as equally distributed between 100 and 150 MeV.

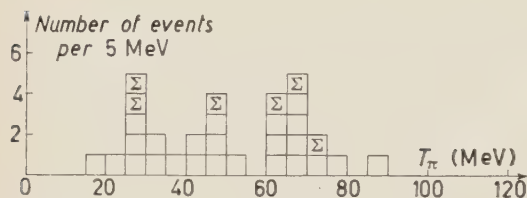


Fig. 2.

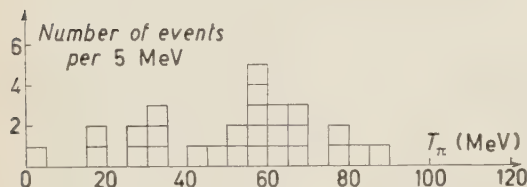


Fig. 3.

this possible Σ^- trapping process plays an important role as far as the pions are concerned, because a) we have actually identified 2 out of the 15 pions above 95 MeV, and

in both cases they turn out to be negative, and b) two other pions have energies above 150 MeV, and thus also could not originate from the Σ^- -trapping process. The energy of these two pions was determined by combined range, scattering and ionization measurements. They are plotted in the energy spectrum (Fig. 1) between 150 and 155 MeV. The limits of error are ± 5 and ± 10 MeV, respectively.

Besides, it should be recalled that the Σ^- -trapping mechanism was originally suggested ⁽⁵⁾ in order to account for the disagreement between the emulsion results and the bubble chamber observations ⁽²⁾ of K^- -absorp-

The total number of observed pions with kinetic energies above 95 MeV is 15. The upper limit of the energy of the pions produced in the (Σ, π) reactions is 95 MeV. Pions from the (Λ, π) reaction may have energies extending up to 170 MeV. It has been suggested that positive pions emitted in the (Σ^-, π^+) -reaction may have energies extending up to ≈ 130 MeV, as a result of the capture of the Σ^- into a negative energy state ⁽⁵⁾. We have no reason to believe that

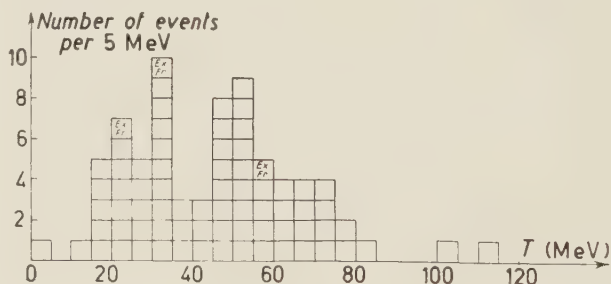


Fig. 4.

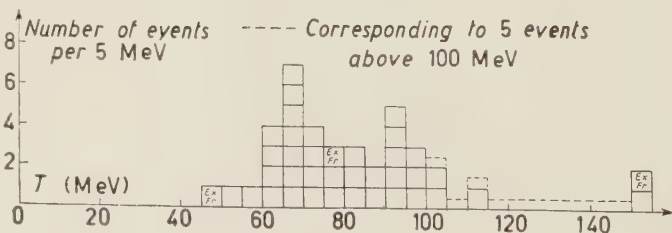


Fig. 5.

tions at rest. But, as was mentioned before ⁽¹⁾, such an agreement should not exist, since the two experiments are not physically the same, because of the Fermi motion of the nucleons in the heavy nuclei of the emulsion.

Thus it seems that the 15 events in which $T_\pi \geq 95$ MeV are examples of reaction (A-7), namely $K^- + n \rightarrow \Lambda^0 + \pi^-$. We shall later on present some support to the fact that K^- -absorptions at rest leading to the 1 N-reactions are peripheral. This fact enables us to estimate the contribution of the reaction (A-7) to the

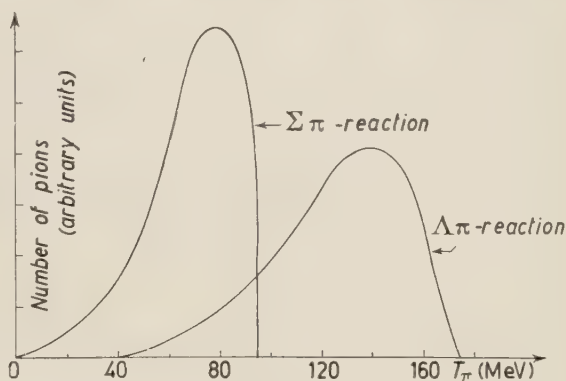


Fig. 6.

1 N-reactions. By the pion energy spectra at production (Fig. 6) we see that $\frac{2}{3}$ of the pions produced in the (Λ^0, π^-) -reaction should have energies above 95 MeV. If the K^- -interaction is peripheral, about 50% of the pions should escape without going through much nuclear matter and without suffering great inelastic scatterings ⁽⁹⁾. Thus, about $\frac{1}{3}$ of the pions from the (Λ^0, π^-) -reaction should still have energies above 95 MeV. This means that the total number of pions emitted from the (Λ^0, π^-) -reaction should be about: $3 \times 15 = 45$ — in agreement with the estimate of 67 events, obtained by an entirely different method in Section 6.

π^+/π^- sign fraction: We have observed 30 positive pions, 101 negative ones and 44 pions with undetermined sign (π^\pm). By the arguments presented before, we may assume that all π^\pm 's above 95 MeV are indeed negative pions from the (Λ^0, π^-) -reaction. As for the pions below 95 MeV, we shall follow the procedure adapted in III, namely, the π^\pm in each energy interval will be divided according to the observed π^+ and π^- frequencies in that interval. We thus obtain that the 44 π^\pm 's contain 9 π^+ 's and 35 π^- 's. The total charge ratio is then:

$$\frac{\pi^+}{\pi^-} = \frac{39}{136} = 0.29 \pm 0.05.$$

⁽⁹⁾ G. PUPPI: *Suppl. Nuovo Cimento*, **11**, 438 (1954). This article contains a summary of all previous results on the subject. See also A. E. IGNATENKO: *CERN Symposium* (1956).

We thank also Prof. M. G. MESCHERIAKOV for communicating us results of B. NIKOLSKY about π^+ and π^- inelastic scattering.

This by itself already proves that K^- -captures at rest in heavy elements differ substantially from captures on free protons (ALVAREZ *et al.* ⁽²⁾), since by assuming charge independence the extrapolated values from ALVAREZ *et al.* experiment to emulsion is ~ 0.7 .

Pion absorption probability and the absorption mechanism of K^- at rest: In the analysis of the stars in flight in III we got 6 examples of (Σ^+, π^-) associated emission and 6 $(\Sigma^-, 0\pi)$ events. Since most of the stars in flight are 1 N-absorptions (see Section 1), in which a Σ^+ could be produced only in association with a π^- (via reaction (A-2) above), the negative pion absorption probability, which we defined (*) as:

$$A_{\pi^-} = \frac{(\Sigma^+, 0\pi)}{(\Sigma^+, 0\pi) + (\Sigma^+, \pi^-)},$$

was

$$A_{\pi^-} \approx \frac{6}{12} = 0.5,$$

in approximate agreement with the value of 0.67 obtained from the entire analysis given in III. In the present experiment we had 19 (1 N) Σ^+ -hyperons decaying at rest and all but one were associated with a π^- ! Thus, A_{π^-} for the stars at rest is ≤ 0.1 . The value $A_{\pi^-} = 0.1$ was adopted in the present work, since it was obtained with better statistics by the European Collaboration ⁽⁸⁾. This big change in A_{π^-} cannot be explained by a mere change in the π -nucleon cross-section ⁽¹⁰⁾ as a function of the pion energy. Thus we have evidence here that the nature of the K^- -absorptions at rest is different from the absorption mechanism in flight. The change in A_{π^-} can be understood if we assume, for example, that the K^- -absorptions at rest leading to the 1 N-reactions are peripheral. In such a case $\sim 50\%$ of the pions will escape without going through much nuclear matter and the other 50% will have a reduced A_{π^-} as compared with the stars in flight, because of the smaller interaction cross-section at smaller pion energies ⁽¹⁰⁾. Using this simple 1 N-absorption model and following CAPP's ⁽¹¹⁾ calculations we have found that an $A_{\pi\Sigma}$ -value, *i.e.* the value of A_{π} for π 's produced together with a Σ , of 0.1 leads to an $A_{\pi\Lambda}$ -value

(*) It should be remarked that this definition of A_{π} has a straightforward meaning only if we are dealing with absorptions on one kind of nuclei. If we have several different nuclei which have different Σ -absorption probabilities, the connection between A_{π^-} defined above and the absorption probabilities of the various nuclei is a bit more complicated. In that case the above A_{π^-} should be considered as some kind of an average of the A_{π} 's of the various nuclei.

⁽¹⁰⁾ H. A. BETHE and F. DE HOFFMANN: *Mesons and Fields*, vol. 2 (1954).

⁽¹¹⁾ R. H. CAPP: *Phys. Rev.*, **107**, 239 (1957).

of 0.2 (because of the higher energies which the pions have when produced in association with a Λ -hyperon; see Fig. 2) and to an average absorption probability for the pions from the stars in flight of ~ 0.5 —in agreement with the value obtained experimentally in III.

Now this model is certainly over-simplified. In particular, the meaning of peripheral 1 N-absorptions is not clear. It could mean literally peripheral absorptions or else a uniform absorption with a very small (about zero) A_{π}^{1N} and A_{Σ}^{1N} in the light elements (C, N, O) which are practically only peripheral and larger absorption probabilities in the heavy elements (*i.e.* $A_{\pi\Sigma} \approx 0.3$ and $A_{\Sigma} \approx 0.8$). These two interpretations of peripheral absorptions would lead to identical experimental observations to a large extent, and differ only in small details. In the present work we have adopted the first interpretation even though we could not rule out the second one. It is hoped that when better detailed statistical information concerning the distribution of stable prongs emitted together with the various unstable particles will be available, one could perform a more precise analysis which will lead to a better understanding of the K^- -absorption mechanism.

Finally we wish to remark that we have no reason to believe that the multi-nucleon absorptions are peripheral. In fact, it is more likely that they are not peripheral, because they involve more than one nucleon and the probability of having many nucleons close to each other is bigger in the center of the nucleus than at its periphery (see also Section 7).

4. - The 2 N-matrix elements.

Before attempting the actual analysis of the data it will be useful to write down the various possible 1 N- and 2 N-reactions and matrix elements leading to them, obtained under the assumption of charge-independence.

In (III) we have already derived the 1 N-reaction rates. We shall only summarize them here for the sake of completeness:

	Reaction	Rate (\sim cross-section)
(A-1)	$K^- + p \rightarrow \Sigma^- + \pi^+$	$r^2 + \frac{2}{3} + 2\sqrt{\frac{2}{3}}r \cos \varphi$,
(A-2)	$\rightarrow \Sigma^+ + \pi^-$	$r^2 + \frac{2}{3} - 2\sqrt{\frac{2}{3}}r \cos \varphi$,
(A-3)	$\rightarrow \Sigma^0 + \pi^0$	$\frac{2}{3}$,
(A-4)	$\rightarrow \Lambda^0 + \pi^0$	$2r_{\Lambda}^2$,
(A-5)	$K^- + n \rightarrow \Sigma^- + \pi^0$	$2r^2$,
(A-6)	$\rightarrow \Sigma^0 + \pi^-$	$2r^2$,
(A-7)	$\rightarrow \Lambda^0 + \pi^-$	$4r_{\Lambda}^2$,

where $r \cdot e^{i\varphi} = A_1/A_0$, and $r_\Lambda = A_{1\Lambda}/A_0$. The A_i 's are the matrix elements in the various isotopic spin T -states, namely:

$$\begin{aligned} A_1 &= \langle T=1 | H^\Sigma \text{ inter} | T=1 \rangle \\ A_0 &= \langle T=0 | H^\Sigma \text{ inter} | T=0 \rangle \\ A_{1\Lambda} &= \langle T=1 | H^\Lambda \text{ inter} | T=1 \rangle. \end{aligned}$$

In the 2 N-case the situation is a bit more complicated. The K^- -2 N wave functions are:

$$\begin{aligned} (K \text{ nn}) &= \left(\frac{3}{2}, -\frac{3}{2}\right), \\ (K^- \text{ np})_s &= \sqrt{\frac{2}{3}}\left(\frac{3}{2}, -\frac{1}{2}\right) + \sqrt{\frac{1}{3}}\left(\frac{1}{2}, -\frac{1}{2}\right)_s, \\ (K^- \text{ pp}) &= \sqrt{\frac{1}{3}}\left(\frac{3}{2}, \frac{1}{2}\right) + \sqrt{\frac{2}{3}}\left(\frac{1}{2}, \frac{1}{2}\right)_s, \\ (K^- \text{ np})_a &= \left(\frac{1}{2}, -\frac{1}{2}\right)_a. \end{aligned}$$

The numbers in brackets are the (T, T_3) -values, and the subscripts «s» and «a» stand for the symmetric and antisymmetric 2 N-states which can both contribute to a final state having $T=\frac{1}{2}$. Similarly, the $\bar{Y}N$ -systems can be written as:

$$\begin{aligned} (\Sigma^- \text{ n}) &= \left(\frac{3}{2}, -\frac{3}{2}\right), \\ (\Sigma^0 \text{ n}) &= \sqrt{\frac{2}{3}}\left(\frac{3}{2}, -\frac{1}{2}\right) + \sqrt{\frac{1}{3}}\left(\frac{1}{2}, -\frac{1}{2}\right), \\ (\Sigma^- \text{ p}) &= \sqrt{\frac{1}{3}}\left(\frac{3}{2}, -\frac{1}{2}\right) - \sqrt{\frac{2}{3}}\left(\frac{1}{2}, -\frac{1}{2}\right), \\ (\Sigma^0 \text{ p}) &= \sqrt{\frac{2}{3}}\left(\frac{3}{2}, \frac{1}{2}\right) - \sqrt{\frac{1}{3}}\left(\frac{1}{2}, \frac{1}{2}\right), \\ (\Sigma^+ \text{ n}) &= \sqrt{\frac{1}{3}}\left(\frac{3}{2}, \frac{1}{2}\right) + \sqrt{\frac{2}{3}}\left(\frac{1}{2}, \frac{1}{2}\right), \\ (\Lambda^0 \text{ n}) &= \left(\frac{1}{2}, -\frac{1}{2}\right), \\ (\Lambda^0 \text{ p}) &= \left(\frac{1}{2}, \frac{1}{2}\right). \end{aligned}$$

Since the symmetric and antisymmetric states do not interfere with each other, we can write the reaction-rates as:

	Reaction	Rate (\sim cross-section)
(B-1)	$K^- \text{ nn} \rightarrow \Sigma^- \text{ n}$	p^2 ,
(B-2)	$K^- \text{ np} \rightarrow \Sigma^- \text{ p}$	$\frac{2}{9}p^2 + \frac{2}{9}q^2 + \frac{2}{3}s^2 - \frac{4}{9}pq \cos \delta$,
(B-3)	$\rightarrow \Sigma^0 \text{ n}$	$\frac{4}{9}p^2 + \frac{1}{9}q^2 + \frac{1}{3}s^2 + \frac{4}{9}pq \cos \delta$,
(B-4)	$\rightarrow \Lambda^0 \text{ n}$	$\frac{1}{3}q_\Lambda^2 + s_\Lambda^2$
(B-5)	$K^- \text{ pp} \rightarrow \Sigma^+ \text{ n}$	$\frac{1}{9}p^2 + \frac{4}{9}q^2 + \frac{4}{9}pq \cos \delta$,
(B-6)	$\rightarrow \Sigma^0 \text{ p}$	$\frac{2}{9}p^2 + \frac{2}{9}q^2 - \frac{4}{9}pq \cos \delta$,
(B-7)	$\rightarrow \Lambda^0 \text{ p}$	$\frac{2}{3}q_\Lambda^2$.

The notations used here are:

$$\langle T = \frac{3}{2} | H_{\Sigma}^{2N} | T = \frac{3}{2} \rangle = p \exp[i\alpha],$$

$$\langle T = \frac{1}{2} | H_{\Sigma}^{2N} | T = \frac{1}{2} \rangle_s = q \exp[i\beta],$$

$$\langle T = \frac{1}{2} | H_{\Sigma}^{2N} | T = \frac{1}{2} \rangle_a = s \exp[i\gamma],$$

and $\delta = \alpha - \beta$. The definition of q_{Λ} and s_{Λ} is similar to that of q and s ; only H_{Λ}^{2N} is substituted for H_{Σ}^{2N} .

5. - The Σ -events.

5.1. *Introduction.* - Evidence for the existence of a substantial 2 nucleon reaction ((B-1) to (B-7) above) in the K^- -absorptions at rest in nuclear emulsion can be obtained directly by inspecting the Σ -hyperon energy spectra. In Figs. 7 and 8 we plot the energy spectrum of the hyperons accompanied by a pion (being clearly 1 N-reactions) and in Fig. 9 are plotted the hyperons not accompanied by pions.

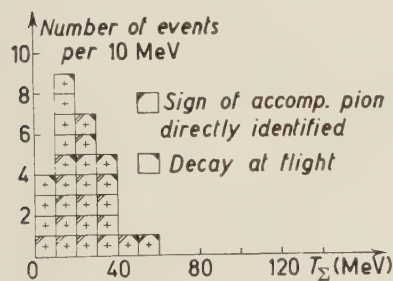


Fig. 7.

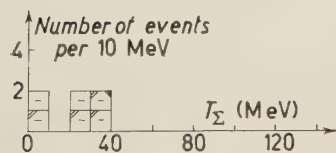


Fig. 8.

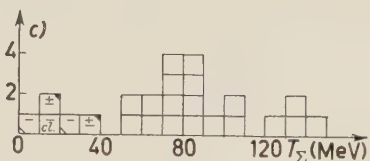
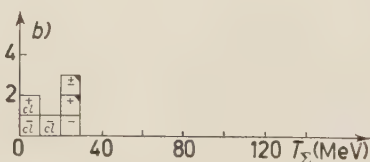
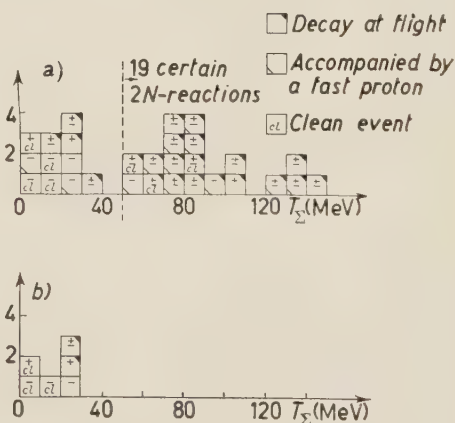


Fig. 9.

These spectra agree with those obtained by the European Collaboration⁽⁸⁾. It is clear that T_{Σ} in the (Σ, π) -events (Figs. 7, 8) is cut sharply at about 60 MeV, whereas the Σ -hyperon kinetic energy in the $(\Sigma, 0\pi)$ events (Fig. 9a)

extends up to 150 MeV. The qualitative conclusions which can be drawn by comparing Figs. 7, 8 with Fig. 9 are the following:

a) The relatively few slow Σ -hyperons not accompanied by pions suggest that the pion absorption probability is small (see Section 3).

b) The relatively large number of hyperons among the $(\Sigma, 0\pi)$ events with energy above the (Σ, π) «cut-off» suggests a substantial contribution from the 2 N-reactions. Taking into account the possible high energy tail in the 1 N-energy spectra and the low energy tail of the 2 N-energy spectra, we get that about 19 (of a total of 63 observed) Σ -hyperons *must* be due to the 2 N-K⁻-absorptions.

These points will be discussed in detail in the next sections.

5.2. *The Σ -hyperons.* — As was mentioned before, this work will be primarily concerned with the 1 N-reaction. It is convenient to start the separation of the observed 1 N-events from the observed 2 N-events by considering first the hyperon events.

The Σ -hyperons observation values are summarized in the following table.

TABLE II.

	Total number	Stable prong data		
		no stable prongs (« clean » events)	fast p's $T_p > 20$ MeV	evaporation only
$\pi^- + \Sigma^+$ (decay at rest)	18	14	0	4
$0\pi + \Sigma^+$ (decay at rest)	1	1	0	0
$\pi^- + \Sigma^+$ (decay in flight)	9	6	0	3
$0\pi + \Sigma^+$ (decay in flight)	1	0	0	1
$\pi^+ + \Sigma^-$ (capture at rest ≥ 2 prong stars)	5	2	0	3
$0\pi + \Sigma^-$ (capture at rest ≥ 2 prong stars)	7	3	3	1
$\pi^+ + \Sigma^-$ (decay in flight)	1	1	0	0
$0\pi + \Sigma^-$ (decay in flight)	1	0	0	1
$0\pi + \Sigma^\pm$ (decay in flight)	20	3	11	6

It should be remembered that we have recorded only those Σ^- -hyperons at rest which give rise to a 2 or more prong capture star. Thus the total number of «observed» hyperons after employing the 3.2 correction factor (see III for details) becomes 89.

We shall now perform the separation of the pion producing reaction from the multi-nucleon reactions which, according to our terminology, do not give rise to pions.

Clearly, the 33 hyperons from the (Σ, π) -events belong to the 1 N-reactions, and the 19 fast Σ 's from the $(\Sigma, 0\pi)$ events belong to the 2 N-reactions (see Figs. 7, 8, 9). However, the 11 slow hyperons of the type $(\Sigma, 0\pi)$ could, in principle, originate in a 1 N- or 2 N-reaction. The division of these 11 events will be considered now.

The Σ^+ -hyperons. The number of 1 N- Σ^+ -hyperons among the above mentioned 11 $(\Sigma, 0\pi)$ events could be estimated by considering the mean kinetic energy of the 1 N- Σ^+ -hyperons (which give the mean moderation time) and the Σ^+ life time. An unbiased sample of 1 N- Σ^+ -hyperons is obtained by considering those Σ -hyperons whose accompanying pion has been identified as negative. Of the 20 hyperons of this type (namely, $\Sigma^+ + \pi^-$ and (Σ^\pm, π^-) events) observed in the present work, 13 decayed at rest and 7 decayed in flight. (The mean energy of these 20 hyperons was ~ 26 MeV.) Among the 11 doubtful $(\Sigma, 0\pi)$ events, only one Σ^+ decayed at rest. Since, in a first approximation, the 1 N- Σ^+ mean energy should be the same for the $(\Sigma, 0\pi)$ and (Σ, π) groups, we get that at most ~ 1 Σ^+ -decay in flight of the 11 $(\Sigma, 0\pi)$ could be due to the 1 N-reactions. (This is only an upper limit since in principle one could have some slow Σ^+ -hyperons from the 2 N-reactions.) Thus we may conclude that the total number of 1 N- Σ^+ hyperons is 27 (Σ^+, π^-) and 2 ($\Sigma^-, 0\pi$)—namely, altogether 29.

The Σ^- -hyperons. The situation with the 6 Σ^- 's among the mentioned 11 cases is less clear. We get an approximate idea about their division into 1 N- and 2 N-reactions only by suitable extrapolation of the spectrum of the certain 2 N-cases to the low energy side. Furthermore it is in principle possible to divide them by using experimental criteria as: number of «clean» events, number of events with fast protons ⁽¹²⁾, mean life-time and energy distributions. The use of these criteria led us to the result shown in Fig. 9c. Once more we must emphasize that the division used is rough, but that this is not of large importance, since the main contribution to the observed hyperons comes from two groups which can be clearly separated.

As a result of these considerations we give the next table which now concerns *only* the 1 N-reactions.

⁽¹²⁾ Percentage of fast protons when pions are absorbed, see for instance R. E. MARSHAK: *Meson Physics* (New York, 1952).

TABLE III. — *Observed and emitted values of 1N-reactions after separation of the 1N- and the 2N-reactions (*)*.

Classification	Raw 1N-observation	π^\pm divided in π^+ and π^-	3.2-correction applied on stopping Σ^-	Emission values Σ^\pm divided in Σ^+ and Σ^-
$(\pi^+, 0\Sigma)$	24	32	21	21
$(\pi^-, 0\Sigma)$	70	103	103	103
$(\pi^\pm, 0\Sigma)$	41	—	—	—
(π^+, Σ^-)	6	6	17	17
(π^-, Σ^+)	27	27	27	27
$(\pi^+, \text{Ex. Fr.})$	0	1	1	1
$(\pi^-, \text{Ex. Fr.})$	4	6	6	6
$(\pi^\pm, \text{Ex. Fr.})$	3	—	—	—
$(0\pi, \Sigma^+)$	2	2	2	2
$(0\pi, \Sigma^-)$	3	3	10	11
$(0\pi, \Sigma^\pm)$	1	1	1	—
$(0\pi, \text{Ex. Fr.})$ } $(0\pi, 0\Sigma)$ }	118	118	111	111

(*) The total number of 1N-reactions is obtained in Sect. 6.

6. — 1 N-production values.

In the last section we have obtained a division of the observed Σ -events into 1 N and 2 N-reactions. With the help of the results obtained in Section 3 we can now attempt to get a set of production values for the reactions (A-1)–(A-7).

6.1. *Pion absorption probability.* — In Section 3 we have shown that the absorption probability of negative pions produced in the (π, Σ) -reaction $A_{\pi\Sigma}$ is ≈ 0.1 , the value obtained by the European K^- Collaboration ⁽⁸⁾. The fundamental pion-deuterium cross-section ⁽¹⁰⁾ seems to be equal for π^+ and π^- mesons having the same energy. However, both cross-sections depend strongly upon the pion energy. As was mentioned in Section 3, using the pion production energy spectra (Fig. 2) and following Capp's calculations, we expect the average absorption probability of the pions produced in the (Λ^0, π^-) -reaction to be $A_{\pi\bar{\Lambda}} \approx 0.2$. The absorption probabilities of the neutral pions are not important as far as the reaction rates are concerned. They will be used, however, in the stable prong analysis (Section 7). Since this analysis is quite rough we need not worry about not knowing A_{π^0} to a better accuracy. We shall assume that $A_{\pi\Sigma} \approx 0.3$; this leads to $A_{\pi\bar{\Lambda}} \approx 0.5$. The higher π^0 -absorption probability takes into account that the neutral pion

has more absorption channels than the charged ones. With improved statistics the stable prong analysis will become more accurate, but so will also A_{π^0} which in principle can be obtained by the analysis of the « clean » events.

6'2. Σ -hyperon absorption probability (1 N-reaction). — In Sections 3 and 5 we have seen that the corrected total number of π^+ -mesons obtained by us was 39, and that 21 of these were accompanied by a Σ^- -hyperon. Since a π^+ is always produced in association with a Σ^- -hyperon (reaction (A-1)), using the definition of absorption probability given in Section 3 (see remark concerning this definition; footnote, p. 358) we obtain for the absorption probability of Σ^- -hyperons produced in the 1 N-reactions the value: $A_{\Sigma^-}^{1N} \approx 0.5$ (*). Following the same procedure in the analysis of the stars in flight (III), we got: $A_{\Sigma^-} \approx 0.9$. This fact, taken at face value would mean that the absorption of Σ -hyperons increases with increasing Σ kinetic energy (for mean Σ -energy compare Figs. 8, 9 of this work with Fig. 3 of III). However, we have by now pretty strong indications that the 1 N-K⁻-absorptions are peripheral (Section 3). So, the smaller value of $A_{\Sigma^-}^{1N}$ obtained in the present experiment may be due to a geometrical reason rather than to the real physical phenomenon of a large change of the Σ -interaction with increase of its energy. It is very likely then, that the Σ -nucleon cross-section is rather large, which leads to a very short mean-free-path in nuclear matter and large absorption probability. In a first approximation, it is independent upon the Σ -energy.

Under this approximation, $A_{\Sigma^+}^{1N}$, $A_{\Sigma^-}^{1N}$ and $A_{\Sigma^0}^{1N}$ are not expected to differ very much from each other. In the forthcoming analysis we shall assume that $A_{\Sigma^{+,0}}^{1N} \approx 0.5$. In any case, the Coulomb correction (**) of A_{Σ^+} is expected to bring it down only to ~ 0.4 so that no large error is made by the above assumption.

6'3. A) The 1 N-reaction rates. — With the absorption probabilities obtained above, and assuming charge independence we can now reconstruct the production values of the reactions (A-1)–(A-7).

(A-1): (Σ^-, π^+). We have 39 π^+ 's emitted. By the above $A_{\pi_{\Sigma^-}}$ -value, the number of produced π^+ 's becomes 43. Since π^+ 's can be produced only via reaction (A-1), this number is indeed the production value of (Σ^-, π^+).

(A-2): (Σ^+, π^-). 27 were actually observed. With $A_{\pi_{\Sigma^+}} \approx 0.1$ we added 2 events from the ($\Sigma^+, 0\pi$) in which the π^- was absorbed. Correcting for the Σ^+ -absorption ($A_{\Sigma^+}^{1N} \approx 0.5$) the production value of (Σ^+, π^-) becomes 58.

(*) This value of $A_{\Sigma^-}^{1N}$ is in full agreement with that obtained by the European K⁻ Collaboration (8).

(**) See III and CAPP's work for details.

(A-5): (Σ^-, π^0). A total of 11 ($\Sigma^-, 0\pi$) were emitted (see Section 5, Table III). From these we have to subtract 2 to account for (Σ^-, π^+)-production where the π^+ was absorbed. The remaining 9 are examples of (Σ^-, π^0)-production. This agrees with the stable prong distribution of the ($\Sigma^-, 0\pi$)-events (see Section 5). Since $A_{\Sigma^-} = 0.50$, the production value of (Σ^-, π^0) becomes 18.

(A-6): (Σ^0, π^-). By charge independence (A-5) \equiv (A-6); therefore, the production value of (Σ^0, π^-) is also 18.

(A-3): (Σ^0, π^0). Again by charge independence, the total number of Σ^0 's produced should be one half the numbers of charged Σ 's. In other words, we have the identity:

$$(A-3) + (A-6) \equiv \frac{1}{2}((A-1) + (A-2) + (A-5)) .$$

(A-7): (Λ^0, π^-). The total number of π^- observed was 136 (see Section 5). In 27 events the π^- was accompanied by a Σ^+ (see Section 5). Therefore, ($0\Sigma, \pi^-$) = 109. From these we have to subtract:

a) The number of (Σ^+, π^-) production where the Σ^+ was absorbed (see above) minus those in which the π^- was also absorbed, namely $58 \times 0.5 = 29 - 3 = 26$.

b) The number of (Σ^0, π^-)-productions minus the number of absorptions from those, namely $18 - 2 = 16$. The total number of (Λ^0, π^-) observed thus becomes $109 - 26 - 16 = 67$, and correcting for the π^- -absorption ($A_{\pi^-} = 0.2$) the production value becomes: 80.

(A-4): (Λ^0, π^0). By charge independence, (A-4) $= \frac{1}{2}$ (A-7), thus the number of (Λ^0, π^0) produced is 40.

The production values can be summarized now (Table IV).

TABLE IV.

	Numbers	Production rate (%)
(A-1) ($\Sigma^- + \pi^+$)	43	14.4
(A-2) ($\Sigma^+ + \pi^-$)	58	19.4
(A-3) ($\Sigma^0 + \pi^0$)	42	14.0
(A-4) ($\Lambda^0 + \pi^0$)	40	13.4
(A-5) ($\Sigma^- + \pi^0$)	18	6.0
(A-6) ($\Sigma^0 + \pi^-$)	18	6.0
(A-7) ($\Lambda^0 + \pi^-$)	80	26.8
All	299	100%

The above production values lead to the following set of matrix elements (see Section 4):

$$\begin{aligned} r &\cong 0.4 \\ r_{\Lambda} &\cong 0.55 \\ \cos \varphi &\cong -0.2 \text{ (*)} . \end{aligned}$$

It can be concluded from this, that we have an indication that r_{Λ} increases and $\cos \varphi$ changes sign with increasing K^- -nucleon momentum (**). Physically this means that with increasing P_{rel} we get:

- a) more contribution from the $T=1$ state (more direct Λ^0 production)
- b) a decrease on the Σ^-/Σ^+ ratio in K^- -absorptions on protons.

The last conclusion was recently confirmed by the Berkeley bubble-chamber group ⁽¹³⁾ studying K^- -interactions in flight in hydrogen.

We should like now to estimate the errors (systematic and statistical) of the matrix elements given above. It is rather hard to give an exact figure for the errors.

The direct observed Σ -absorption probability is that of the negative hyperon (see 6'2). In Section 6'2 we stated why we think that $A_{\Sigma^+}^{1N} \approx A_{\Sigma^-}^{1N}$. This assumption would lead to a systematic error. But, even if we assume that the Coulomb effect reduces $A_{\Sigma^+}^{1N}$ to ≈ 0.4 , the matrix elements which we obtain are: $(r, r_{\Lambda}, \cos \varphi) = (0.4, 0.7, 0)$ not much different from our previous set (*).

The production rates of reactions (A-1) and (A-2) (Table IV above) are statistically quite certain. The rate of (A-5) is statistically not so certain since it involves relatively small observational values and large correction factors. But, even if we assume that the true production rate of (A-5) is substantially different from that given in Table IV (6.0 %), we still practically do not change the ratio of proton to neutron 1 N-absorptions. This is essentially because the production rate of (A-7) was obtained (see Section 6'3) by subtracting from the observed number of the $(0 \Sigma, \pi^-)$ -events the production numbers

(*) These are the values as obtained for the self conjugate nucleus.

(**) The detailed shape of momentum dependence of the matrix elements cannot be derived from our experiment. They might possibly change monotonously, but also some kind of resonance cannot be excluded, because of the smoothing effect of the Fermi momentum.

⁽¹³⁾ BERKELEY BUBBLE CHAMBER GROUP: preliminary results, *CERN Meeting* (July 1958).

(*.) According to Capp's ⁽¹²⁾ model, a uniform K^- -absorption having $A_{\Sigma^-}^{1N} \approx 0.5$ leads to $A_{\Sigma^+}^{1N} \approx 0.4$, using a Coulomb potential: $V_c \approx \pm 10$ MeV and a nuclear potential of: $-V_N = (10 \div 15)$ MeV.

of (A-5). A change in (A-5) means, therefore, a change in the opposite direction of (A-7); thus the total 1 N-neutron absorptions and also the total 1 N-reactions remain practically constant.

7. - Stable prong analysis.

In the previous sections we have obtained the 1 N-reaction rates by separating the 1 N-hyperon events from the total number of hyperons observed and by studying in detail the events in which a charged pion was emitted. We have thus concluded that K^- -absorptions at rest in nuclear emulsions proceed in about 55% of the cases via the 1 N-channel and in about 45% via the 2 N-channel. We shall now attempt, by studying the systematics of the stable prongs emitted in the K^- -absorption stars, to estimate the characteristics of the stable prongs expected to be associated with a 1 N and 2 N K^- -absorption and compare it with the observed stable prongs. This will eventually give us a rough idea about the reaction rates of the 2 N-absorption channel (reactions (B-1) to (B-7)). A detailed and statistically more meaningful analysis of the 2 N-events will be presented in a next publication (In ref. ⁽⁸⁾ a similar analysis was attempted.)

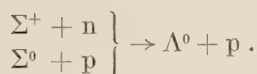
A list of the visible prongs associated with the various types of events observed is given in Table II. By studying the systematics of Table II some very interesting conclusions concerning the emission of fast protons and « clean » events (namely protons with kinetic energies above 20 MeV) can be drawn:

1) Out of the 33 associated (Σ, π)-events observed, *not a single one* had a fast proton; in fact, only 25% contained evaporation prongs and 75% were « clean » events. Hence it may be concluded that when particles escape which are produced via the 1 N-reaction, only in 25% of the cases the nucleus is excited to emit visible prongs and in no case a fast proton is emitted. This is not necessarily true for 2 N-events because of the possible different origin of the 1 N- and 2 N-absorptions (see end of Section 3). In fact, only $\sim 30\%$ of the 2 N-hyperon events are « clean »! (Meaning (Σ^-, p) or (Σ^\pm, n) only).

2) Three of the 24 ($\pi^+, 0 \Sigma$)-events had an associated fast proton and 4 of the 24 were « clean » events (π^+ only). Since a π^+ can be produced only in association with a Σ^- (reaction (A-1)), the above 24 events must be composed of 2 classes: a) Σ^- absorbed, b) Σ^- escapes but makes at its end a zero or one prong capture star. According to our observed number of Σ^- -stars giving rise to 2 or more prongs, we estimate that about 8 of the 24 ($\pi^+, 0 \Sigma$)-events must belong to class b). Since the mean 1 N- Σ^- energy was 18 MeV, we may conclude that Σ^- -absorptions quite seldom lead to fast p's, and in

about 25 % of the events lead to zero prong stars. This is to be expected since the Σ^- absorption mechanism is via the reactions $\Sigma^- + p \rightarrow \begin{cases} \Lambda^0 + n \\ \Sigma^0 + n \end{cases}$ which, primarily gives only neutral particles.

3) About 40 % of the $(\pi^-, 0 \Sigma)$ -events are associated with fast p's. Thus absorption of Σ^+ and Σ^0 may lead quite often to an emission of fast p's, mainly via the reactions:



4) Among the 15 events having pions with $T_\pi \geq 95$ MeV, which must be due to the (Λ^0, π^-) -reaction (Section 3) only one had an associated fast proton. Thus the absorption (or escape) of Λ^0 seldom involves production of fast protons.

In the analysis of the stable prongs we shall also use, in addition to the above conclusions based upon our own observation, the following results obtained by other authors (^{9,12}):

- a) The absorption of a fast > 20 MeV positive pion gives in about 85 % of the cases a fast proton.
- b) The absorption of negative pions yields in about 25 % of the cases zero prong stars and in about 30 % a fast proton.

Since the absorption of Σ^+ and Σ^- proceeds probably via a mechanism similar to that of π^+ and π^- respectively (namely $\pi^+ + n \rightarrow p$, and $\pi^- + p \rightarrow n$ as only possible absorption channels) as far as the stable prongs are concerned, we may assume that the yield of fast p's is the same in both cases. In fact, our own observations verify that Σ^- -absorptions similarly to π^- -absorptions (compare 2) above to b)) yield a very small number of fast protons. For the present analysis we have assumed that they roughly give the same amount of fast protons.

We can summarize now the absorption probabilities and yields of fast protons upon absorption for the various particles, as was deduced above (Table V).

We have to estimate now the contribution of the $1 N - \Lambda^0$ events to the stable prongs. Since the K^- -absorptions seem to be peripheral, about 50 % of Λ^0 's will escape without going through much nuclear matter. By (1) above, 75 % of these will give « clean » events. The other 50 % of the Λ^0 's which will traverse nuclear matter may be assumed to behave like neutrons from π^- -absorptions—thus 30 % of them will still give rise to fast p's, and 25 % will give rise to « clean » events.

We may proceed now and calculate the numbers of fast p's and « clean » events expected from each of the 1 N- and 2 N-reactions, and compare it with our observations.

TABLE V.

Absorption probabilities	Upon absorption yield of:	
	fast protons ($T_p \geq 20$ MeV) (%)	« clean » events (%)
$A_{\pi_{\Sigma}^-} = 0.1$	30	25
$A_{\pi_{\Sigma}^+} = 0.1$ (*)	85	0
$A_{\pi_{\Sigma}^0} = 0.3$	40	12
$A_{\pi_{\Lambda}^-} = 0.2$ (**)	30	25
$A_{\pi_{\Lambda}^0} = 0.5$	42	12
$A_{\Sigma^{1N}-} = 0.5$	30	25
$A_{\Sigma^{1N}+} = 0.5$	85	0
$A_{\Sigma^{1N}0} = 0.5$	42	12
$A_{\Sigma^{2N}-} = 0.8$ (***)	30	25
$A_{\Sigma^{2N}0} = 0.8$	85	0
$A_{\Sigma^{2N}+} = 0.8$	42	12

(*) $A_{\pi_{\Sigma}^+} = A_{\pi_{\Sigma}^-}$ assumed (see text), by this assumption, $A_{\pi_{\Sigma}^0} = 0.3$ deduced. (Sect. 5).

(**) Calculated (see Sect. 3).

(***) The value $A_{\Sigma^{2N}} \cong 0.8$ was assumed, because we obtained this value for the stars in flight (III) whose Σ 's have about the same energy as the 2N- Σ 's in stars at rest, and since we have no reason to believe that the 2N-absorptions are peripheral (see remark end of Sect. 3).

A) 1 N-reactions. With the help of the absorption probabilities, yield of fast protons and « clean » events listed in Table V above, we can now estimate the frequency of occurrence of various types of stable prongs to be associated with the seven 1 N-reactions. The expectation values thus obtained are listed in the following Table VI.

The expected and observed stable prongs, from the 1 N-reactions are summarized below. (The « clean » events and fast p's observed in association with a π^\pm (see Table I) were all assumed to belong to π^- -events, since: a) of the

TABLE VI.

Reaction	Pro- duc- tion rate	(Y+ π) escape			π -absorbed						Y-absorbed π -escapes		
		Y-escapes			Y-absorbed								
		No.	Yield of		No.	Yield of		No.	Yield of		No.	Yield of	
			f. p's	clean		f. p's	clean		f. p's	clean		f. p's	clean
(1) $\Sigma^- + \pi^+$	43	20	0	15	2	2	0	2	2	0	20	6	5
(2) $\Sigma^+ + \pi^-$	58	26	0	19	3	1	0	3	2	0	26	22	0
(3) $\Sigma^0 + \pi^0$	42	15	0	11	6	2	0	6	3	0	15	6	2
(4) $\Lambda^0 + \pi^0$ (*)	40	9	0	6	12	5	1	12	7	0	7	2	2
(5) $\Sigma^- + \pi^0$	18	6	0	5	3	1	0	3	2	0	6	2	1
(6) $\Sigma^0 + \pi^-$	18	8	0	6	1	0	0	1	0	0	8	3	1
(7) $\Lambda^0 + \pi^-$ (*)	80	32	0	25	8	2	1	8	3	0	32	10	7

(*) The Λ^0 's were assumed to escape in 50 % of the events, and go through nuclear matter and interact with it in the other 50 % of the events. Y absorbed means in the Λ^0 -events a big chance for interaction.

41 π^\pm 's only ≈ 8 are expected to be π^+ , b) positive pions do not have many associated fast p's, and do not appear often as « clean » events).

The agreement between the expected and observed events given in Table VII above is quite good. The disagreement in the « clean » (π^- , 0 Σ)-events could be explained by assuming that more than 30 % of the Λ^0 's which go through nuclear matter produce fast protons and less than 25 % of them give rise to

TABLE VII.

	Fast protons		« Clean » events	
	Expectation incl. correction for loss of Σ^-	Observation	Expectation incl. correction for loss of Σ^-	Observation
(π^- , 0 Σ)	35	39	39	14
(π^+ , 0 Σ)	11	3	13	9
(π^- , Σ^+)	0	0	19	20
(π^+ , Σ^-)	0	0	7	3
(0 π , Σ^+)	1	0	0	1
(0 π , Σ^-)	1	2	2	2
(0 π , 0 Σ)	39	(*)	27	(*)

(*) The expected numbers of fast protons and « clean » events ($K\bar{p}$'s) associated with (0 π , 0 Σ)-events will be added to the estimated contribution from the 2N-reactions, since for this type of events there is no way to separate between 1N- and 2N-reactions.

«clean» events. This assumption is not unreasonable, since the Λ^0 -energy spectrum at production extends up to 180 MeV and thus they may be more effective in producing fast p's, and less effective in giving rise to «clean» events, then π^- -mesons.

We may conclude the stable prong analysis of the 1 N-events by saying that this analysis agrees with the determination of the reaction rates which was given in Section 6.

B) 2 N-reactions. So far we have been able to separate the 1 N-reactions and give a consistent scheme of the 1 N-reaction rates. We thus know the total number of the 2 N-reactions (about 250 out of 550 events). We also know the total number of 2 N- Σ -hyperons emitted, namely (see Section 5): $20 + 4 \times 3.2 = 33$. With the help of the 2 N- Σ -absorption probabilities given in Table V and by assuming again charge independence we can get the total 2 N- Σ -production and 2 N- Λ -production. Qualitatively we obtain that the 2 N- Σ -production is larger than the Λ -production. More quantitative and statistically improved results concerning the 2 N-reactions will be given in a next publication.

A very rough idea of the 2 N-reaction rates can, however, be obtained by considering the details of the 2 N-hyperon events (Table VIII below). No definite fast Σ^+ -hyperon decay into a pion or proton was identified. Thus we may conclude that the reaction $K^- pp \rightarrow \Sigma^+ n$ is not very abundant. Also since most of the identified 2 N- Σ^- -hyperons have an associated fast proton, the rate of the reaction ($\Sigma^- n$) is probably smaller than the rate of the reaction ($\Sigma^- p$).

TABLE VIII. - Raw 2N- Σ -hyperons observational data.

Raw 2 N- Σ - hyperons observational data

Hyperon type	with fast p	no fast p	clean	all
Σ^- at rest, giving ≥ 2 prong capture stars	3	0	1	4
Σ^- decay in flight	0	1	0	1
Σ^+ decay at rest or in flight	0	0	0	0
$\Sigma^\pm \rightarrow \pi^\pm$ in flight	9	7	3	19

Using the above ideas concerning the 2 N-reactions and the yield of fast protons and «clean» events given in Table VIII we get good agreement between the observed numbers of stable prongs (fast protons and «clean» events) and the calculated numbers.

8. - Discussion and conclusions.

A first indication that the multi-nucleon mode of K^- capture at rest in nuclear emulsion is quite large, can be obtained by comparing directly the energy spectra of the Σ -hyperons accompanied by a π -meson (Figs. 7, 8, Section 5) with the spectra of Σ -hyperons not accompanied by pions (Fig. 9, Section 5). From this comparison the following quantitative conclusions may be reached.

- a) Out of the 63 charged hyperons observed about 24 originate in a 2 N-reaction.
- b) The pion absorption probability and the production rate of reaction (A-5) (Σ^-, π^0) are relatively small, since the number of slow Σ^\pm -hyperons not accompanied by a pion is small (Fig. 9, Section 5).

Upon a more detailed analysis of the pion events (Section 3) and the Σ -events (Section 5) we reached the conclusion that the negative pion absorption probability (defined in Section 3) is small. We have adopted the value 0.1 from the European K^- Collaboration. This small value of A_π as compared with the value obtained in III for the stars in flight (≈ 0.7) could be understood if we assume an entirely different 1 N-capture mechanism for the K^- -stars at rest, namely peripheral absorption (see Section 3 and 7). Supporting the hypothesis that K^- -absorptions at rest by single nucleons are mainly peripheral, is the agreement obtained in Section 3 between the calculated and observed pion energy spectra and (Λ^0, π^-)-reaction rates (see Section 3), and also the overall agreement obtained in the stable prong analysis (Section 7).

As for the multi-nucleon K^- -captures (reactions (B-1) to (B-7)), we have no reason to assume that they are peripheral. On the contrary, they should be expected to occur well inside the nucleus where the density of nucleons is highest.

Knowing the pion absorption probability (Section 3) and the 1 N- Σ -absorption probability (Section 6) enables us to estimate the entire 1 N-production rates (Section 6). We have thus obtained that the 1 N-absorption occurs in about 55% of the cases, and the multi-nucleon at about 45%. The 1 N-reaction rates given in Section 6'3 depend naturally upon the value of A_π which is used. But the total number of 1 N-absorptions is quite insensitive to the exact value of A_π , being determined essentially by the total number of pions actually observed (see Section 6'3). For example, assuming that $A_{\pi\Sigma} = 0.2$ and $A_{\pi\Lambda} = 0.4$ (instead of the values 0.1 and 0.2, respectively, which were used in Section 6) we get that 65% of the K^- -absorptions are 1 N- and 35% 2 N-reactions. Thus, we can quite safely conclude that the multi-nucleon

K^- -absorption occurs in about $(35 \div 50)\%$ of the K^- -captures at rest in nuclear emulsions.

The reaction rates of the 2 N-reactions can be determined only when statistically improved data will be available. The observed values presented in Table VIII seem to indicate that the $T = \frac{3}{2}$ K^-NN -state is less probable than the $T = \frac{1}{2}$ state (see Section 4). This was suggested by the European Collaboration⁽⁸⁾.

It should be remarked that the entire analysis would be considerably simplified if some relations between the 1 N-matrix elements and the 2 N-matrix elements (Section 4) could be derived.

We wish to compare the results obtained in the present work with those obtained in III for the interactions of fast K^- -mesons (T_K was ≈ 86 MeV) in nuclear emulsion. In Section 6'3 we have derived the 1 N-reaction rates and matrix elements. As for the stars in flight also for the pion producing reactions of the capture stars at rest the contribution of the direct Λ -production is quite respectable and is very different from the fraction of direct Λ 's from K^- -capture at rest by free protons⁽²⁾. The detailed shape of the momentum-dependence of the reaction rates cannot be obtained by this analysis, and any possible resonance of the matrix elements would probably not be detected since the Fermi effect would smooth it out.

The pion absorption probability is much smaller in the present experiment (≈ 0.1) as compared with the value obtained in III (≈ 0.7). This difference is probably due to two physical phenomena (see Section 3):

- a) The increase of the pion interaction cross-section with increasing pion energy⁽¹¹⁾, and
- b) The different nature of the 1 N- K^- -captures at rest (namely peripheral absorptions).

As was argued in Section 1, the K^- -absorptions in flight are expected to occur primarily via the 1 N-channel. Thus, the Σ -hyperon absorption probability obtained for the 1 N- Σ 's (see Section 6'2) could be directly compared with A_Σ obtained in III. Again we see a significant change: $A_\Sigma^{IN} \approx 0.5$ here, compared with 0.8 in the stars in flight. This difference cannot, however, be taken as evidence for a real change of the Σ^- -interaction cross-section with change of its energy, because of the different K^- -capture mechanisms in the two experiments. Indeed it is likely that the Σ -hyperon interaction cross-section is very large, and that its mean free path in nuclear matter is extremely short. This will account for the value $A_\Sigma \approx 0.8$ obtained in III. The reason for the smaller value obtained for A_Σ^{IN} in the present work will be then geometric: due to the peripheral 1 N-capture, about 50% of the Σ 's escape without going through much nuclear matter. The other 50% of the Σ 's are emitted in the direction of the nucleus and are mostly absorbed.

The 2 N- Σ -absorption probability was assumed to be the same as A_Σ in the stars in flight, (≈ 0.8), since

- a) the Σ -production spectrum is similar in both cases, and
- b) as was mentioned before, we have no reason to believe that the 2 N-captures are peripheral.

The value $A_\Sigma^{2N} \approx 0.8$ gave reasonable predictions for the 2 N-reaction rates and the stable prong distribution (see Section 4).

Finally we wish to remark something about the Λ^0 -hyperfragment formation probability. In III we have seen that the number of hyperfragments observed per Λ^0 produced (directly and indirectly via Σ -absorption) was $\approx 5\%$. In the present experiment (see Table I) we had 7 (π^\pm , H.F.)'s and 16 (0π , H.F.)'s. By the value of A_π and by charge independence, the number of hyperfragments produced with π^{+-0} is ≈ 12 . From Table IV we get that the number of Λ^0 's (produced directly or indirectly) in 1 N-reactions which go through nuclear matter is ≈ 150 (sum of all « Y absorbed » events, Table IV). Thus the fraction of hyperfragments per 1 N- Λ^0 is $\approx 8\%$. Similarly, for the 2 N- Λ^0 's we get $\approx 5\%$. In principle, since the Λ^0 -energy spectrum is different in the stars in flight (see III, ref. (1), p. 759) and in the 1 N- and 2 N-absorptions of the K^- -captures at rest (in the latter case \bar{T}_{Λ^0} is smallest) one could get the Λ^0 -energy dependence of the hyperfragment formation probability by the above analysis. However, at the moment the data are statistically too poor, so that no conclusion concerning the hyperfragment formation probability can be reached.

* * *

We wish to express our thanks to Drs. LOFGREN, JAUNEAU and TEUCHER who exposed the stack for us at the Bevatron, and we are much indebted to Profs. DE SHALIT and YAMAGUCHI for their stimulating discussions, to Profs. DILWORTH-OCCHIALINI and BURHOP who speedily communicated to us the preliminary results of the European Collaboration, and to Prof. PEY-ROU and THIRRING for their continuous interest in our work.

Dr. LOHRMANN gave many inspiring suggestions and took part in the early stage of this work.

Our special thanks are due to Prof. HOUTERMANS for his support and encouragement. We thank also Dipl. Phys. PESSIA ABRAHAMSON who during her stay in Bern took part in the investigation. Finally we acknowledge our indebtedness for the efficient work done by our scanning staff which includes: Mrs. BARBARA ALBRECHT, EVA KOCH, CHRISTIANE PLUMETTAZ, TRUDI RIESEN,

IRENE RITSCHARD and SONJA SCHILT. Mrs. ALBRECHT and PLUMETTAZ also contributed certain precise measurements.

Our further thanks are due to the Schweizer Nationalfonds for financial help.

RIASSUNTO (*)

L'assorbimento dei mesoni K negativi a riposo in emulsioni nucleari è stato dettagliatamente studiato in un grosso pacco di emulsioni. La maggior parte delle particelle secondarie venne a riposo nel pacco e fu identificata. Confrontando i risultati ottenuti nel presente lavoro con quelli ottenuti da noi precedentemente ⁽¹⁾ in uno studio delle interazioni di mesoni K^- veloci e con i risultati di ALVAREZ *et al.* ⁽²⁾ si possono trarre le seguenti conclusioni: 1) Come già riferito in III, anche nel presente esperimento le reazioni mononucleari (catture con produzione di pioni) mostrano un tasso elevato di produzione Λ diretta. Tale risultato è la diretta conseguenza delle percentuali di segno e delle probabilità di assorbimento osservate se è valida l'indipendenza dalla carica. Il fenomeno può spiegarsi con l'influenza del momento di Fermi. 2) Le catture K multinucleari (senza produzione di pioni) formano una larga frazione del totale delle catture K a riposo. Si stima che il $(35 \div 50)\%$ delle catture avvengano per via multinucleare. 3) Probabilmente, le catture K^- mononucleari a riposo sono prevalentemente periferiche; conducono pertanto, per ragioni geometriche, a minori probabilità di assorbimento dei pioni e degli iperoni Σ . I nostri risultati di cui ai punti 2) e 3) confermano i risultati della European K-collaboration presentati a Ginevra al Congresso CERN 1958 sulle particelle elementari ⁽⁸⁾.

(*) Traduzione a cura della Redazione.

Highly Directional Detector for Cosmic Ray Particles.

G. W. HUTCHINSON

Physics Department, University of Birmingham - Birmingham

(ricevuto il 7 Novembre 1958)

Summary. — A relatively simple Čerenkov detector is described which will respond to relativistic charged particles only when their directions lie within a well-defined cone. The limits of the cone are determined by the critical reflection of Čerenkov light from parallel faces of the radiator. The semi-angle of the cone may be chosen at will by varying the refractive indices used. It is suggested that the detector might be useful for attempts to detect a directional flux of uncharged primary particles at high altitudes.

1. — Introduction.

A Čerenkov counter has recently been described by BOOTH, HEREFORD and HUTCHINSON ⁽¹⁾ in which a sharp energy discrimination for protons of energy of the order of 1 GeV was achieved by using the critical reflexion condition from the parallel faces of thin slabs of a radiating material. The counter has been made and tested in a preliminary form. By a simple modification, this counter can be made to have well-defined directional properties. It is intended here to draw attention to its potential usefulness in this form.

2. — Description.

The principle of operation of the counter is shown in Fig. 1. Čerenkov light is produced by relativistic charged particles in a series of parallel slabs of refracting material of refractive index n_1 , surrounded by a medium of re-

⁽¹⁾ N. E. BOOTH, F. L. HEREFORD and G. W. HUTCHINSON: *Nucl. Inst.* **3**, 229 (1958).

fractive index n_2 . If the light strikes the surface of the slabs at an angle greater than the critical angle θ_c , defined by n_1 and n_2 , it is completely internally reflected and is collected by photomultipliers placed around the edges of the

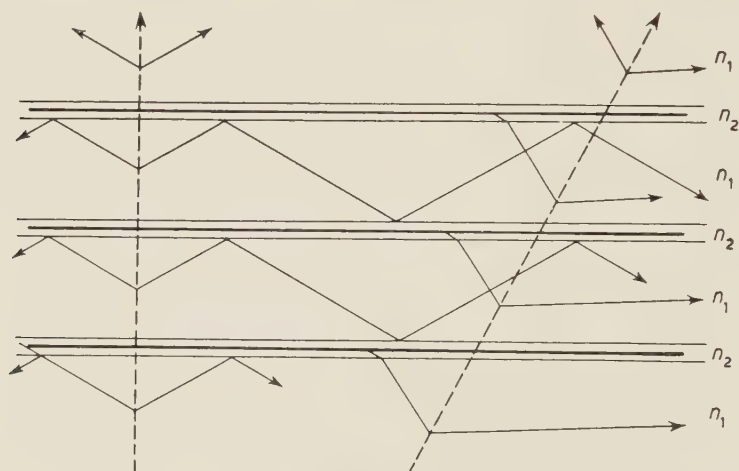


Fig. 1. — Principle of operation. Typical rays of Čerenkov light are shown from two charged particle trajectories (shown dotted).

slabs. If it reaches the surface at an angle less than the critical angle, then a large proportion of the light will pass to the medium n_2 in which it is absorbed by black surfaces. The cut-off at the critical angle is sharp because of the multiple reflections necessary before the light can reach the photomultipliers and because of the direction of polarization of the Čerenkov light.

In the instrument tested, the media n_1 and n_2 were polystyrene and air, the absorbing surfaces were black paper, and the light was collected by two photomultipliers in optical contact with two opposite edges of the slabs. The signals from the two multipliers were added in a linear network and the resulting pulse height was recorded. The limitations on the energy resolution of this arrangement have already been discussed (*loc. cit.*).

In particular it was required that the trajectory of the particles should be very closely perpendicular to the plane of the slabs. A particle travelling at an angle to this direction would produce a cone of Čerenkov light tilted with respect to the slab face normal. If its velocity was such that the Čerenkov angle was close to θ_c , a fraction of the cone could be critically reflected while the remainder was lost. To adapt the detector for angle sensitivity it is only necessary to require coincidence from the signals of several photomultipliers receiving light from different positions around the edges of the slabs. Particles of sufficiently high velocity travelling normally to the slab faces will

then produce signals from all the multipliers, but as the direction of the particle and hence the direction of the axis of the Čerenkov cone is tilted, there will be a well-defined angle at which one or more of the multipliers will cease to receive light. Charged particles of velocity βc will, in fact, be detected when their velocities are directed within a cone of semi angle α where

$$\alpha = \cos^{-1} \frac{1}{n_1} - \sin^{-1} \frac{n_2}{n_1}.$$

The values of α as a function of n_1 and n_2 are shown in Fig. 2, for the most interesting case in which $\beta = 1$. For a very simple form of the detector using perspex (lucite) sheets in air, α is about 6° .

The amount of Čerenkov light and hence the size of the photomultiplier pulses relative to noise could be made fairly large by increasing the thickness and the number of slabs, and by choosing a high value of n_1 and a correspondingly high value of n_2 . The thickness of the refracting slabs should be chosen so as to give a large number of internal reflections before the light reaches the multipliers and to minimize the area around the edges of the slabs from which light could reach the multipliers without internal reflection. Provided that the surfaces of the slabs were of good optical quality and well polished, there should be little loss of light at the many multiple reflections. The maximum useful area of the slabs would be determined by the absorption coefficient of the medium. For a clear medium such as perspex it should be possible to make them of the order of 1 metre in diameter.

The sharpness of the cut-off for angles greater than α will be determined by the same factors as those previously discussed for energy sensitivity. In principle, the same possibilities exist for finding achromatic combinations for the two refracting media, but in practice this might be difficult. It would be important to remember in choosing the refracting media, that the effective refractive indices are those for the wavelengths at which the product of the Čerenkov spectrum intensity and the sensitivity of the photomultipliers is greatest. If the device were to be used at high altitudes it would also be important to remember that the refractive indices are in general a function of temperature.

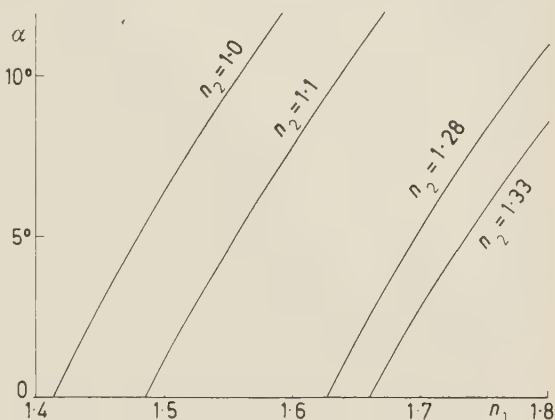


Fig. 2. — The semi-vertical angle (α) of the acceptance cone as a function of n_1 for various values of n_2 .

A very flexible method of design would be to use a liquid for the medium n_1 and either a liquid or a gas for the medium n_2 , separating them by thin sheets of glass or perspex. Mixtures of water and glycerine give refractive indices between 1.33 and 1.47, and mixtures of decalene and tetralene give indices between 1.48 and 1.54 (for the D line of the sodium spectrum). Intermediate and higher indices can be had with various inorganic aqueous solutions and lower indices with fluorochemicals (OSBORNE and CALDWELL ⁽²⁾) A glass could also be used for the medium n_1 . For instance, a counter using a glass of refractive index 1.65 combined with a fluorochemical of index 1.28 would have a half angle of acceptance of about 1.6° , and a relatively high light output.

The disposition of the multipliers around the slabs should not be critical provided that a sufficient fraction of the light was collected and that not too much light was reflected from one multiplier into another. Four or more evenly spaced multipliers should define a symmetrical acceptance cone sufficiently well, but the multipliers need to be distributed symmetrically. For instance, the apparatus could be made sensitive to direction in one plane but not very sensitive to direction in the perpendicular plane, by having multipliers only on two opposite sides of the slabs. The simplest arrangement is to have the multiplier faces in optical contact with the slabs, but for a large detector it might be more convenient to include some optical focussing between the slabs and the multipliers.

3. - Applications.

It has been suggested by the author (HUTCHINSON ⁽³⁾) that there would be considerable interest in looking for an uncharged component of cosmic rays using directional sensitive apparatus at high altitude. In particular one would like to know whether there are any sources of such radiation associated with the sun, the galactic centre and the known sources of radio noise. A similar suggestion has recently been made again by MORRISON ⁽⁴⁾. It appears that the present apparatus is eminently suitable for such an investigation because of its relative simplicity, compactness and flexibility of design. The detector by itself could be used to investigate the direction of incidence of charged primaries, but by using it in anti-coincidence with other counters

⁽²⁾ L. S. OSBORNE and D. O. CALDWELL: *M.I.T. Lab. for Nuclear Science Progr. Rep.* (Nov. 30th. 1957).

⁽³⁾ G. W. HUTCHINSON: *Phil. Mag.*, **43**, 847 (1952).

⁽⁴⁾ P. MORRISON: *Nuovo Cimento*, **7**, 858 (1958).

along its axis, it should be possible to discriminate against these and to collect information about any residual uncharged flux.

The angular definition of the direction of γ -rays should be good since it would be blurred only by the opening angle of the showers which they produce. The angular definition of neutron directions would be less good, unless the neutrons were of very high energy.

The experiment could be most conveniently done in an earth satellite, but it might also be possible to do it at balloon altitudes provided that the back scattering of particles from the atmosphere were not too great.

Although the total flux of incoming uncharged particles is believed to be not more than a few percent of the total flux of the charged particles, the fluxes may well be comparable over small angular regions. This would be the case, for instance, if the preponderance of charged primaries was due chiefly to their confinement in regions of magnetic field. The experiment might therefore be not too difficult and if it produced a positive result, this would be of great importance in the discussion of the origin of cosmic rays.

The detector could also be used for directional studies at ground level, but here its advantages over more bulky, but conventional, counter arrays are not so decisive.

RIASSUNTO (*)

Si descrive un contatore di Čerenkov relativamente semplice che rivela le particelle cariche relativistiche solo se le loro direzioni cadono entro un cono ben definito. I limiti del cono sono determinati dalla riflessione critica della luce di Čerenkov sulle facce parallele del radiatore. La semiapertura del cono può essere scelta a piacere variando gli indici di rifrazione dei materiali usati. Si suggerisce di usare l'apparecchio nei tentativi di rivelare un flusso direzionale di particelle primarie scariche a grandi altezze.

(*) Traduzione a cura della Redazione.

Some Calculations on the Proton Magnetic Resonance Shift Due to Hydrogen Bonding of Ammonia Molecules (*).

H. F. HAMEKA (**)

Department of Chemistry, Carnegie Institute of Technology - Pittsburgh, Penn.

(ricevuto il 18 Novembre 1958)

Summary. — The effect of hydrogen bonding on the proton magnetic shielding constants in the ammonia molecule has been calculated from gauge invariant atomic orbitals. Following SCHNEIDER, BERNSTEIN and POPLE, the effect is regarded as made up of two contributions: *a*) the inter-molecular shift, which is caused by the induced electronic currents in the adjacent molecule, and *b*) the polarization shift, which is caused by the polarization of the N-H bond due to the electrostatic field of the adjacent molecule. The computed intermolecular shift is $-1.02 \cdot 10^{-6}$, the computed polarization shift is $-0.45 \cdot 10^{-6}$. The experimental value of the total effect is $-1.05 \cdot 10^{-6}$.

1. — Introduction.

The increasing accuracy in nuclear magnetic resonance measurements is pleasing. Not more than ten years ago it became possible to observe the small variations (of the order of magnitude of 10^{-5}) in proton resonance shifts in different molecules. Recently SCHNEIDER, BERNSTEIN and POPLE have reported still more accurate measurements on the proton shielding in various

(*) Research supported by a grant from the Alfred P. Sloan Foundation to Carnegie Institute of Technology.

(**) Present address: Philips Research Laboratories, Eindhoven. Requests for reprints should be directed to C.I.T.

simple molecules in the gaseous and liquid states (¹). From their data they found it possible to determine to what extent the proton shielding constants are affected by hydrogen bonding; this effect they named the liquid association shift. In these experiments it was found that liquid association may change the proton shift by amounts which are roughly between 1 and 10% of the total proton shift. The liquid association shifts were measured with an accuracy of about 1% which means an accuracy of about 10^{-8} in the proton resonance measurements. The remarkable result of these measurements is that formation of hydrogen bonds tends to decrease proton shielding.

According to SCHNEIDER, BERNSTEIN and POPLE (¹), if one considers a hydrogen bond between a molecule X-H and another system Y, forming the associated systems X-H...Y, and if one assumes that there is no inter-molecular charge transfer, the liquid association shift is caused by two contributions:

- A) A magnetic field will be induced at the position of the proton due to the direct effect of electronic currents in molecule Y.
- B) The electrostatic field of molecule Y will slightly polarize the electrons of the X-H bond, which in turn will affect the shielding of the proton.

SCHNEIDER, BERNSTEIN and POPLE (¹) gave a qualitative theoretical discussion of their results, which is based on a theoretical discussion of proton shielding constants by POPLE (²). In this discussion POPLE simplified the quantum mechanical description of proton shielding constants by neglecting overlap charges and by introducing the concept of anisotropic susceptibilities. The quantum mechanical description was thus finally reduced to a semi-classical model based on the concepts of electronic ring currents and anisotropic magnetic susceptibilities. The most important advantage of POPLE's discussion (²) is that it offers a very general understanding of the main features of proton shielding. On the other hand, we believe that many of the more subtle aspects of proton shielding are not described satisfactorily in Pople's theory because of the many approximations. Therefore we feel that a theoretical discussion of liquid association shifts which is based on Pople's general theory (²) should be considered with some reservation.

For the case of linear molecules SCHNEIDER, BERNSTEIN and POPLE (¹) have estimated the magnitudes of effect A (inter-molecular shift) and effect B (polarization shift) on the basis of Pople's general theory. They find that effect A gives a shift in a direction opposite to the experimental one. Then

(¹) W. G. SCHNEIDER, H. J. BERNSTEIN and J. A. POPLE: *Journ. Chem. Phys.*, **28**, 601 (1958).

(²) J. A. POPLE: *Proc. Roy. Soc., A* **239**, 541, 550 (1957).

in effect B they argued that it is great enough, in the right direction, to produce the observed shift.

We believe that our description of proton shielding constants which was developed in two previous papers (^{3,4}) is more adequate for a discussion of liquid association shifts than Pople's theory (²) because our theory permits a more detailed consideration of the electronic charge distribution in molecules. In this paper we will use this approach to calculate the effect of hydrogen bonding on the proton shielding constants in the ammonia molecule.

2. - The quantum mechanical description of the ammonia molecule.

Although fairly accurate descriptions of the ammonia molecule have been reported (^{5,6}) we will make use of a simplified wave function, analogous to the wave functions which we have used for the hydrogen halides (⁴). Let h_1 , h_2 and h_3 be the three hydrogen ($1s$) functions, s' the $1s$ function of the nitrogen, t_1 , t_2 and t_3 hybrid (sp^3) orbitals, pointing in the directions $N \rightarrow H_1$, $N \rightarrow H_2$, and $N \rightarrow H_3$ and let t_4 be the hybrid (sp^3) orbital which is orthogonal to t_1 , t_2 , and t_3 . Then it will be assumed that the ground state of the ammonia molecule may be described by means of the properly anti-symmetrized form of the function

$$(1) \quad \left\{ \begin{array}{l} \Psi = s'(1)s'(2)u_1(3)u_1(4)u_2(5)u_2(6)u_3(7)u_3(8)t_4(9)t_4(10), \\ u_i = (1 + 2\lambda\Delta + \lambda^2)^{-\frac{1}{2}}(h_i + \lambda t_i), \\ \Delta = \int t_i h_i d\tau, \end{array} \right.$$

where λ is an electronegativity parameter. The value of the overlap integral $\Delta = 0.5955$. For the sake of simplicity it will be assumed that the four orbitals t_i have tetragonal symmetry.

It might be profitable to discuss in detail the atomic orbitals which will be used in our calculations. Our intention is to make use of Hartree-Fock functions (⁷), whereas in some parts of the calculations we will approximate the Hartree-Fock functions by Slater atomic orbitals. The Hartree-Fock

(³) H. F. HAMEKA: *Mol. Phys.*, **1**, 203 (1958).

(⁴) H. F. HAMEKA: *Mol. Phys.*, **2**, 64 (1959).

(⁵) A. B. F. DUNCAN: *Journ. Chem. Phys.*, **27**, 423 (1957).

(⁶) H. KAPLAN: *Journ. Chem. Phys.*, **26**, 1704 (1957).

(⁷) D. R. HARTREE and W. HARTREE: *Proc. Roy. Soc., A* **193**, 299 (1948).

functions are defined by

$$(2) \quad \begin{cases} 2s & (1/4\pi)^{\frac{1}{2}} r^{-1} s(r), & 2p_z & (3/4\pi)^{\frac{1}{2}} r^{-1} p(r) \sin \theta \cos \varphi, \\ 2p_x & (3/4\pi)^{\frac{1}{2}} r^{-1} p(r) \cos \theta, & 2p_y & (3/4\pi)^{\frac{1}{2}} r^{-1} p(r) \sin \theta \sin \varphi. \end{cases}$$

The Slater atomic orbitals are defined by

$$(3) \quad \begin{cases} \tilde{s} = (q^5/96\pi)^{\frac{1}{2}} r \exp[-\frac{1}{2}qr], & \tilde{p}_x = (q^5/32\pi)^{\frac{1}{2}} r \sin \theta \cos \varphi \exp[-\frac{1}{2}qr], \\ \tilde{p}_y = (q^5/32\pi)^{\frac{1}{2}} r \sin \theta \sin \varphi \exp[-\frac{1}{2}qr], & \tilde{p}_z = (q^5/32\pi)^{\frac{1}{2}} r \cos \theta \exp[-\frac{1}{2}qr]. \end{cases}$$

All lengths in (2) and (3) are expressed in atomic units and $q = 3.90$.

Following the method previously employed (4), if we determine the value of λ in such a way as to yield the correct value for the dipole moment; we find

$$(4) \quad \frac{\mu}{ea_0} = \frac{(1 + 2\lambda A)\alpha + (2\lambda A + \lambda^2 - 1)R_{\text{NH}} - 4\lambda\beta}{1 + 2\lambda A + \lambda^2},$$

where μ is the dipole moment of the ammonia molecule, R_{NH} is the NH distance in atomic units and

$$(5) \quad \begin{cases} \alpha = \int r s(r) p(r) dr, \\ \beta = \pi^{-\frac{1}{2}} \int \left(\frac{1}{2} \tilde{s} + \frac{1}{2} \sqrt{3} \tilde{p}_z \right) z \exp[-(r^2 + R_{\text{NH}}^2 - 2rR_{\text{NH}} \cos \theta)^{\frac{1}{2}}] d\tau. \end{cases}$$

The integral α may be calculated numerically and the integral β may be obtained from the tables of MULLIKEN *et al.* (8). It is then found that $\alpha = 1.350$, $\beta = 0.657$, whereas $R_{\text{NH}} = 1.909$. Then

$$(6) \quad \mu = (1.909\lambda^2 + 1.246\lambda - 0.559)ea_0/(1 + 1.191\lambda + \lambda^2).$$

In order to reproduce the experimental value $\mu = 1.43 D$ we take $\lambda = 0.724$.

Now the wave function (1) with the value of λ determined from the dipole moment, may be used for a calculation of the liquid association shift. The two contributions which were listed in Section 1 will be calculated separately. As has been indicated already, we will refer to the first effect as the *intermolecular magnetic shift*, to the second as the *polarization shift*.

(8) R. S. MULLIKEN, C. A. RIECKE, D. ORLOFF and H. ORLOFF: *Journ. Chem. Phys.*, **17**, 1248 (1949).

3. - The inter-molecular magnetic shift.

In order to calculate the inter-molecular magnetic shift we assume that one of the protons of the first molecule and the lone pair of the second molecule form a hydrogen bond in such a way that both nitrogen nuclei and the proton in question lie on the axis of symmetry of the lone pair of electrons and we set out to compute the shielding at this proton due to the electronic distribution in the second molecule. This situation is represented in Fig. 1. According to PAULING ⁽⁹⁾ the N ... H distance is then $4.5a_0$.

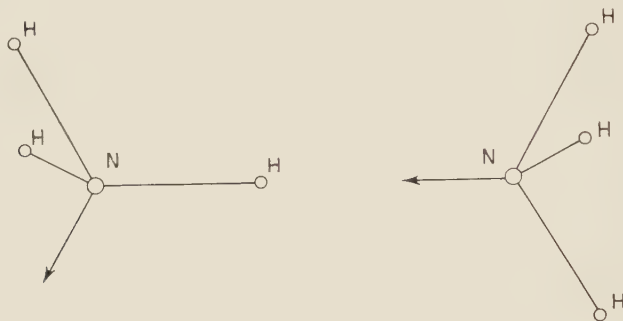


Fig. 1. - Configuration of two ammonia molecules connected by a hydrogen bond.

The first order perturbation term of the inter-molecular magnetic shift depends mainly on the total charge distribution of the second molecule. According to the Mulliken approximation ^(10,11) we assume that the overlap charges $t_i h_i$ may be replaced by

$$(7) \quad t_i h_i = \frac{1}{2} \Delta (t_i^2 + h_i^2).$$

Then the total charge distribution on the second molecule is

$$(8) \quad \begin{aligned} q &= q_N + \sum_i q_{Hi} \\ q_N &= \frac{(\lambda^2 + \lambda) r^{-2} \{s^2(r) + 3p^2(r)\}}{2\pi(1 + 2\lambda\Delta + \lambda^2)} + \\ &\quad + \frac{(1 + \lambda\Delta) r^{-2} \{s^2(r) + 6s(r)p(r)\cos\theta + 9p^2(r)\cos^2\theta\}}{8\pi(1 + 2\lambda\Delta + \lambda^2)}, \\ q_{Hi} &= \frac{2(1 + \lambda\Delta)h_i^2}{1 + 2\lambda\Delta + \lambda^2}, \end{aligned}$$

⁽⁹⁾ L. PAULING: *The nature of the chemical bond* (New York, 1942).

⁽¹⁰⁾ R. S. MULLIKEN: *Journ. Chim. Phys.*, **46**, 497 (1949).

⁽¹¹⁾ K. RUEDEBERG: *Journ. Chim. Phys.*, **19**, 1433 (1951).

where the polar co-ordinates are referred to the nitrogen nucleus as origin with the lone pair electrons on the z axis and the Hartree functions $s(r)$ and $p(r)$ are defined by (2).

The calculation of shielding constants has been discussed at length in previous work ^(3,4). The forms of the operators may be derived from the first paper. Then

$$(9) \quad \sigma' = \frac{e^2}{3mc^2a_0} \left[\frac{\lambda^2 + \lambda\Delta}{1 + 2\lambda\Delta + \lambda^2} \int_R^\infty \frac{2s^2(r) + 6p^2(r)}{r} dr + \frac{1 + \lambda\Delta}{8\pi(1 + 2\lambda\Delta + \lambda^2)} \right. \\ \left. + \int \frac{r^2 - Rr \cos \theta}{(r^2 + R^2 - 2Rr \cos \theta)^{3/2}} \{s^2(r) + 6s(r)p(r) \cos \theta + 9p^2(r) \cos^2 \theta\} \sin \theta dr d\theta d\varphi + \right. \\ \left. + \frac{1 + \lambda\Delta}{1 + 2\lambda\Delta + \lambda^2} \int_{R'}^\infty \frac{6h^2(u)}{u} du \right],$$

where

$$(10) \quad h(u) = 2u^{-1}e^{-u}$$

and where R , the distance between the proton for which the shielding is calculated and the nitrogen nucleus of the second molecule, is $4.50a_0$ and R' , the distance between the proton for which the shielding is calculated and one of the protons of the second molecule, is $5.43a_0$. From the appendix of our previous paper ⁽⁴⁾ follows that this expression may be reduced to

$$(11) \quad \sigma' = \{e^2/6mc^2a_0(1 + 2\lambda\Delta + \lambda^2)\} \left[2(\lambda^2 + \lambda\Delta) \int_R^\infty \{2s^2(r) + 6p^2(r)\} r^{-1} dr + \right. \\ \left. + (1 + \lambda\Delta) \int_R^\infty s^2(r) r^{-1} dr - 2(1 + \lambda\Delta) \int_0^R r s(r) p(r) R^{-2} dr + \right. \\ \left. + 4(1 + \lambda\Delta) \int_R^\infty R s(r) p(r) r^{-2} dr - \{12(1 + \lambda\Delta)/5\} \cdot \int_0^R r^2 p^2(r) R^{-3} dr + \right. \\ \left. + \{3(1 + \lambda\Delta)/5\} \int_R^\infty (6R^2 r^{-3} + 5r^{-1}) p^2(r) dr + 12(1 + \lambda\Delta) \int_{R'}^\infty h^2(r) r^{-1} dr \right].$$

Because of the fact that R and R' are relatively great, (11), may be approxi-

mated by

$$(12) \quad \sigma' = -\frac{e^2}{6mc^2a_0(1+2\lambda\Delta+\lambda^2)} \left\{ 2(1+\lambda\Delta) \int_0^R \frac{rs(r)p(r)}{R^2} dr + \right. \\ \left. + \frac{12(1+\lambda\Delta)}{5} \int_0^R \frac{r^2p^2(r)}{R^3} dr - 4(\lambda^2+\lambda\Delta) \int_R^\infty \frac{s^2(r)+3p^2(r)}{r} dr \right\}.$$

(Compare our considerations on the hydrogen atom ⁽¹²⁾). It should be observed here that the last integral forms only a small correction to the total value. After evaluation of the integrals this becomes

$$(13) \quad \sigma' = -\frac{\{0.1985(1+\lambda\Delta) - 0.0093(\lambda^2+\lambda\Delta)\} \cdot 1.775 \cdot 10^{-5}}{2(1+2\lambda\Delta+\lambda^2)},$$

so that, making use of the λ value which we obtained in Section 2, $\sigma' = -1.02 \cdot 10^{-6}$.

The second order perturbation term of the inter-molecular magnetic shift is clearly negligibly small.

4. - Polarization of the N-H bond due to hydrogen bonding.

Although it seems that the polarization of a molecule due to liquid association is rather difficult to calculate, in our description the change of λ due to hydrogen bonding may be estimated without many difficulties. To this end we will closely follow a formalism which has been derived by PARKS and PARR ⁽¹³⁾ for a description of separated electron pairs. It will be assumed that the positions of the two ammonia molecules with respect to each other are given by Fig. 1. Furthermore it may be observed that it is rather immaterial in this case which value is assigned to λ since we are only interested in changes in λ . Therefore it will be assumed that λ is close to unity; this enables us to obtain a close analogy between our case and the general description of PARKS and PARR ⁽¹³⁾. Consequently we replace λ by

$$(14) \quad \lambda = 1 + q$$

⁽¹²⁾ H. F. HAMEKA: *Nuovo Cimento*, **11**, 395 (1959).

⁽¹³⁾ J. M. PARKS and R. G. PARR: *Journ. Chem. Phys.*, **28**, 335 (1958).

and neglect higher powers of q . From (1) it follows then that the wave function of the electron pair which forms the N-H bond is given by

$$(15) \quad \Psi_i(1, 2) = (2 + 2A)^{-1}(1 + q)^{-1}[\{h_i(1)h_i(2) + h_i(1)t_i(2) + \\ + t_i(1)h_i(2) + t_i(1)t_i(2)\} + q\{h_i(1)t_i(2) + t_i(1)h_i(2) - 2t_i(1)t_i(2)\}]$$

so that our description is to a first approximation, equivalent to the method of Parks and Parr⁽¹²⁾, if it is assumed that in their equations (38)

$$(16) \quad A_1 = 1, \quad A_2 = q(1 - A^2)^{\frac{1}{2}}/2(1 + q)(1 + A), \quad A_3 = 0.$$

It is now possible to make use of the results which were obtained by PARKS and PARR in Section 8. To this end it should be borne in mind that we are only interested in the change of λ due to the perturbation of the second molecule; the operator which represents this electrostatic field will be represented by \mathcal{H}' . Now it follows directly from equations (81), (87) and (95) of Parks and Parr that the variation δA_2 , due to \mathcal{H}' , is given by

$$(17) \quad \delta A_2 = \frac{\langle h | \mathcal{H}' | h \rangle - \langle t | \mathcal{H}' | t \rangle}{\sqrt{2}(1 - A^2)^{\frac{1}{2}}E'}.$$

Here h is the ($1s$) orbital on the hydrogen for which the liquid association shift is calculated and t is the (sp^3) orbital which points from the nitrogen nucleus towards this hydrogen nucleus, $\langle h | \mathcal{H}' | h \rangle$ and $\langle t | \mathcal{H}' | t \rangle$ are the energies of electrons in the orbitals h and t respectively in the electrostatic field of the second molecule, and E' is the energy difference between a bonding and an anti-bonding σ electron in the N-H bond. Now E' may be estimated from the N-H bond energy; if the latter quantity is called E_b , then $E' = 2E_b/(1 - A)$. Furthermore it follows from (12) that

$$(18) \quad \delta q = 2\delta A_2(1 + A)/(1 - A^2)^{\frac{1}{2}}.$$

Consequently

$$(19) \quad \delta q = \frac{\langle h | \mathcal{H}' | h \rangle - \langle t | \mathcal{H}' | t \rangle}{\sqrt{2}E_b}.$$

According to COTTRELL's book⁽¹⁴⁾ $E_b = 0.1344$ atomic units.

(14) T. L. COTTRELL: *The strengths of chemical bonds* (London, 1954).

In order to calculate the matrix elements $\langle h | \mathcal{H}' | h \rangle$ and $\langle t | \mathcal{H}' | t \rangle$ we make use again of the approximation of equation (7) to describe the charge distribution of the second molecule. Then \mathcal{H}' may be written as

$$(20) \quad \mathcal{H}' = 2V_1 + 3\alpha V_b + 3\beta V_H - 5V_N,$$

where

$$(21) \quad \beta = (1 + \lambda^2)/(\lambda^2 + 2\lambda A + 1), \quad \alpha = (2\lambda^2 + 2\lambda A)/(\lambda^2 + 2\lambda A + 1),$$

V_1 is the electrostatic field of the lone pair of electrons, V_b is the field of one of the charge clouds t_i^2 , and V_N and V_H are the fields of point charges at the positions of the nitrogen and hydrogen nuclei respectively. Now from KOTANI's book ⁽¹⁵⁾ and Roothaan's tables ⁽¹⁶⁾ it is found that (in atomic units)

$$\begin{aligned} h | V_1 | h \rangle &= 0.259174 \\ h | V_b | h \rangle &= 0.209232 \\ \langle t | V_1 | t \rangle &= 0.196164 \\ \langle t | V_b | t \rangle &= 0.166835. \end{aligned}$$

The remaining matrix elements may be calculated from

$$\begin{aligned} \langle h | V_i | h \rangle &= R_i^{-1} \{1 - \exp[-2R_i](1 + R_i)\} \\ \langle t | V_i | t \rangle &= \frac{q}{a_i} \left[\left\{ \left(1 + \frac{5}{a_i} + \frac{9}{a_i^2}\right) - \exp[-a_i] \left(\frac{9}{a_i^2} + \frac{23}{2a_i} + 8 + \frac{7a_i}{2} + a_i^2 + \frac{a_i^3}{6} \right) \right\} - \right. \\ &\quad \left. - (1 - \cos \theta_i) \left\{ \frac{5}{2a_i} - \exp[-a_i] \left(\frac{5}{2a_i} + \frac{5}{2} + \frac{5a_i}{4} + \frac{3a_i^2}{8} + \frac{a_i^3}{16} \right) \right\} - (1 - \cos^2 \theta_i) \cdot \right. \\ &\quad \left. \cdot \left\{ \frac{27}{2a_i^2} - \exp[-a_i] \left(\frac{27}{2a_i^2} + \frac{27}{2a_i} + \frac{27}{4} + \frac{9a_i}{4} + \frac{9a_i^2}{16} + \frac{3a_i^3}{32} \right) \right\} \right], \end{aligned}$$

$$a_i = qR_i', \quad i = H, N,$$

$$(22) \quad \begin{cases} R_N = 4.50 & R_N' = 6.40 & \cos \theta_N = 1 \\ R_H = 5.05 & R_H' = 7.26 & \cos \theta_H = 0.93877. \end{cases}$$

⁽¹⁵⁾ M. KOTANI, A. AMEMIYA, E. ISHIGURO and T. KIMURO: *Table of molecular integrals* (Tokyo, 1955).

⁽¹⁶⁾ C. C. J. Roothaan: Special Technical Report, Department of Physics, The University of Chicago (1955).

Hence

$$(23) \quad \left\{ \begin{array}{l} \langle h | V_H | h \rangle = 0.184139 \\ \langle t | V_H | t \rangle = 0.150929 \\ \langle h | V_N | h \rangle = 0.222071 \\ \langle t | V_N | t \rangle = 0.174157 \end{array} \right.$$

Furthermore, with $\lambda = 0.724$ we find

$$(24) \quad \left\{ \begin{array}{l} \alpha = 0.800615 \\ \beta = 0.199385 \end{array} \right.$$

so that

$$(25) \quad \left\{ \begin{array}{l} h | \mathcal{H}' | h \rangle = 0.020680 \\ t | \mathcal{H}' | t \rangle = 0.011934 . \end{array} \right.$$

From (19) it follows then that $\delta q = 0.0460$.

5. - The polarization shift.

In order to calculate the polarization shift the dependence of the proton shielding of the ammonia molecule on the value of λ should be investigated first. It is not our intention to calculate the total value of σ explicitly but only the small change in σ due to a small variation in λ , so that some simplifying assumptions may be made for the calculation of σ :

- 1) It will be assumed that small variations of λ will be reflected in the first order perturbation term only, because the second order perturbation term is relatively much smaller and does not depend so strongly on λ ⁽⁴⁾.
- 2) It will be assumed that the total charge distribution of the ammonia molecule may be described with the aid of Mulliken's approximation (7) ^(10,11), where overlap charges are expressed in terms of one-center charge clouds.

The charge distribution of the ammonia molecule is thus represented as a sum of charge distributions which are centered on the nitrogen, the hydrogen for which the shielding constant is calculated, their overlap charge and charge distributions on the other protons:

$$(26) \quad \varrho = \varrho_N + \varrho_H + \varrho_{NH} + \varrho'_H + \varrho''_H ,$$

where

$$\begin{aligned}
 (27) \quad \left\{ \begin{aligned}
 q_N &= \frac{(\lambda^2 + \lambda\Delta)r^{-2}\{s^2(r) + 3p^2(r)\}}{2\pi(1 + 2\lambda\Delta + \lambda^2)} + \\
 &+ \frac{(\lambda\Delta + 1)r^{-2}[s^2(r) - 2s(r)p(r)\cos\theta + p^2(r)\{\cos^2\theta + 8\sin^2\theta\cos^2\varphi\}]}{8\pi(1 + 2\lambda\Delta + \lambda^2)} - \\
 &- \frac{\lambda\Delta r^{-2}\{s^2(r) + 6s(r)p(r)\cos\theta + 9p^2(r)\cos^2\theta\}}{8\pi(1 + 2\lambda\Delta + \lambda^2)}, \\
 q_H &= \frac{2h_i^2}{1 + 2\lambda\Delta + \lambda^2}, \\
 q_{NH} &= \frac{2\lambda h_1\{s(r) + 3p(r)\cos\theta\}}{(4\pi)^{\frac{1}{2}}(1 + 2\lambda\Delta + \lambda^2)}, \\
 q_H' &= \frac{2(1 - \lambda\Delta)h_2^2}{1 + 2\lambda\Delta + \lambda^2}, \\
 q_H'' &= \frac{2(1 + \lambda\Delta)h_3^2}{1 + 2\lambda\Delta + \lambda^2},
 \end{aligned} \right.
 \end{aligned}$$

where h_1 is the (1s) orbital of the hydrogen for which the shielding constant is calculated and h_2 and h_3 are the (1s) orbitals of the other protons.

The contributions of these various charge clouds to the protons shielding constant will be denoted by σ_N , σ_H , σ_{NH} , σ_H' and σ_H'' respectively. They are

$$\begin{aligned}
 (28) \quad \left\{ \begin{aligned}
 \sigma_N &= \frac{e^2}{3mc^2a_0(1 + 2\lambda\Delta + \lambda^2)} \left[(\lambda^2 + \lambda\Delta) \int_0^\infty \frac{2s^2(r) + 6p^2(r)}{r} dr + \right. \\
 &+ \frac{\lambda\Delta + 1}{2} \int_0^\infty \frac{s^2(r)}{r} dr + 2(\lambda\Delta + 1) \int_0^\infty \frac{p^2(r)}{r} dr + \\
 &+ \frac{4\lambda\Delta + 1}{6} \left\{ 2 \int_0^\infty \frac{rs(r)p(r)}{u^2} dr - 4 \int_0^\infty \frac{us(r)p(r)}{r^2} dr \right\} + \\
 &- \frac{4\lambda\Delta + 1}{6} \left\{ \frac{12}{5} \int_0^\infty \frac{r^2 p^2(r)}{u^3} dr - \int_0^\infty \left(\frac{18u^2}{5r^3} + \frac{r}{3} \right) p^2(r) dr \right\} \Big], \\
 \sigma_H &= \frac{2e^2}{3mc^2a_0(1 + 2\lambda\Delta + \lambda^2)},
 \end{aligned} \right.
 \end{aligned}$$

$$\begin{aligned}
 \sigma_{\text{NH}} = & \left[\frac{2\lambda e^2}{3mc^2a_0(1+2\lambda A+\lambda^2)} \left[\frac{2e^{-u}}{u} \int_0^u (\sinh r) s(r) dr + \right. \right. \\
 & + \frac{2 \sinh u}{u} \int_u^\infty e^{-r} s(r) dr + \frac{3(u+1)e^{-u}}{u^2} \int_0^u \frac{(r-1)e^r - (r+1)e^{-r}}{r} p(r) dr + \\
 & \left. \left. + \frac{3\{(u-1)e^u - (u+1)e^{-u}\}}{u^2} \int_u^\infty \frac{(r+1)e^{-r}}{r} p(r) dr \right] \right], \\
 \sigma'_H = \sigma''_H = & \frac{8(1+\lambda A)}{1+2\lambda A+\lambda^2} \int_v^\infty \frac{e^{-r}}{r} dr,
 \end{aligned}
 \tag{28}$$

where u is the N-H distance and v is the H---H distance within the molecule. All integrals may be calculated numerically without many difficulties; it is then found that

$$\begin{aligned}
 \sigma_N &= (1+2\lambda A+\lambda^2)^{-1} [(\lambda^2+\lambda A)0.5543 + (\lambda A+1)(0.0270+0.1116) + \\
 &\quad + (\tfrac{2}{3}\lambda A + \tfrac{1}{6})(0.24024-0.0659)] \cdot 1.7748 \cdot 10^{-5}, \\
 \sigma_H &= (1+2\lambda A+\lambda^2)^{-1} \cdot 2 \cdot 1.7748 \cdot 10^{-5}, \\
 \sigma_{\text{NH}} &= (1+2\lambda A+\lambda^2)^{-1} \lambda (0.8241+1.6476) \cdot 1.7748 \cdot 10^{-5}, \\
 \sigma'_H = \sigma''_H &= (1+2\lambda A+\lambda^2)^{-1} (1+\lambda A) 0.0024 \cdot 1.7748 \cdot 10^{-5},
 \end{aligned}
 \tag{29}$$

so that

$$\sigma = \frac{(0.5543\lambda^2 + 2.9604\lambda + 2.1704) \cdot 1.7748 \cdot 10^{-5}}{\lambda^2 + 1.1910\lambda + 1}.
 \tag{30}$$

By making use of the value of λ which was obtained in Section 2 and of the value of $\delta\lambda$ which was obtained in Section 4 it is found that in the gaseous state $\sigma = 3.381 \cdot 10^{-5}$ and furthermore that the polarization shift is $-0.45 \cdot 10^{-6}$.

6. - Discussion.

From a combination of the results of Sections 3 and 5 $\delta\sigma$ is calculated to be $\delta\sigma = -1.46 \cdot 10^{-6}$ whereas the experimental value as reported by SCHNEIDER, BERNSTEIN and POPLE ⁽¹⁾ is $\delta\sigma = -1.05 \cdot 10^{-6}$. In view of our approximations it may be concluded that the agreement between theory and experiment seems satisfactory.

It seems profitable at this point to compare our treatment of the liquid association shift in ammonia to the theoretical considerations of SCHNEIDER, BERNSTEIN and POPLE⁽¹⁾ for HF, which are mainly based on POPLE's description of chemical shifts by means of induced currents. SCHNEIDER, BERNSTEIN and POPLE concluded that for hydrogen fluoride the main contribution to the liquid association shift results from the polarization shift, whereas our considerations show that in the case of ammonia the inter-molecular shift is the main effect. Since these two different calculations refer to two different cases it may be that no essential discrepancies exist between the considerations of SCHNEIDER, BERNSTEIN and POPLE⁽¹⁾ and of this paper. We believe however as we pointed out in the introduction that the calculations of SCHNEIDER, BERNSTEIN and POPLE should be considered with some reservation. Although Pople's theory has a more general nature than our calculations we believe that it contains too many simplifications to account in a proper way for the quantitative aspects for as subtle an effect as the liquid association shift. Furthermore, we believe that the value of the electric field which has been inserted into equation (5) of the paper of SCHNEIDER, BERNSTEIN and POPLE is too large.

Although we cannot offer a rigid proof for the following statement we believe that also in general the intermolecular shift is the predominating term of liquid association shifts and that there is some doubt as to whether or not the theoretical conclusions of SCHNEIDER, BERNSTEIN and POPLE are entirely correct.

* * *

I wish to express my gratitude to Dr. ROBERT G. PARR for many stimulating discussions and in particular for some valuable suggestions for calculating the N-H bond polarization.

RIASSUNTO (*)

L'effetto del legame idrogeno sulle costanti dello schermo magnetico dei protoni nella molecola dell'ammoniaca è stato calcolato in base agli orbitali atomici invariante rispetto al gauge. Secondo SCHNEIDER, BERNSTEIN e POPLE, si ritiene che l'effetto sia la somma di due contributi: a) lo sfasamento intermolecolare, causato dalle correnti elettroniche indotte nella molecola adiacente, e b) lo sfasamento della polarizzazione causato dalla polarizzazione del legame N-H dovuta al campo elettrostatico della molecola adiacente. Lo sfasamento intermolecolare calcolato è $-1.02 \cdot 10^{-6}$, lo sfasamento della polarizzazione calcolato è $-0.45 \cdot 10^{-6}$. Il valore sperimentale dello sfasamento totale è $-1.05 \cdot 10^{-6}$.

(*) Traduzione a cura della Redazione.

Nuclear Magnetic Shielding at Large Distances of a Hydrogen Atom in an Electric Field (*).

H. F. HAMEKA (**)

Department of Chemistry, Carnegie Institute of Technology - Pittsburgh, Penn.

(ricevuto il 18 Novembre 1958)

Summary. — The nuclear magnetic shielding constant of a hydrogen atom in a uniform electric field is calculated at a point P which is situated at a large distance from the nucleus in the direction of the electric field. The main term of the screening constant is found to be proportional to the first power of the electric field and to the inverse second power of the distance between P and the hydrogen nucleus.

1. — Introduction.

In a recent paper ⁽¹⁾ the present author obtained some results, which, as it seems, are not readily acceptable on a classical physical basis, namely, it was found that at large distances the shielding due to an ammonia molecule may contain terms which are proportional to the inverse square of the distance R to the center of the ammonia molecule. In order to clarify this point we will consider in this paper a symple system, which contains all the essential features of our original problem and which may be calculated in a straightforward way. We will set out to compute the magnetic shielding due to a hydrogen atom in a uniform electric field for a point which is situated at a large distance R from the hydrogen nucleus in the direction of the electric field.

(*) Research supported by a grant from the Alfred P. Sloan Foundation to Carnegie Institute of Technology.

(**) Present address: Philips Research Laboratories, Eindhoven. Requests for reprints should be directed to C.I.T.

⁽¹⁾ H. F. HAMEKA: *Nuovo Cimento*, **11**, 382 (1959).

Actually this paper is only a slight extension of a recent paper of MARSHALL and POPLE ⁽²⁾ in which the nuclear magnetic shielding at the nucleus of a hydrogen atom in an electric field was calculated. The method which was employed by MARSHALL and POPLE ⁽²⁾ and which will also be followed here was originally introduced by COULSON ⁽³⁾.

2. - Calculations.

In this calculation two different cases will be considered:

- A) A hydrogen atom in a uniform electric field F in the z direction and in a uniform magnetic field H in the x direction, in combination with a magnetic dipole μ at a point $-R$ on the z axis, so that the dipole points in the x direction.
- B) A hydrogen atom in a uniform electric field F in the z direction and in a uniform magnetic field H in the z direction, in combination with a magnetic dipole μ at a point $-R$ on the z axis, so that the dipole points in the direction of the magnetic field.

In both cases the origin is chosen as the hydrogen nucleus.

Instead of using the parameters F , H and μ we will introduce the parameters

$$(1) \quad \begin{cases} A = a_0^2 F / e, \\ B = e a_0^2 H / 2 \hbar c, \\ C = \hbar \mu / m c a_0^2 e, \end{cases}$$

where a_0 is the Bohr radius. It will be assumed that the three dimensionless parameters (R is expressed in atomic units) are small with respect to unity.

The solutions which we set out to compute may now be expanded in terms of A , B , C and $(1/R)$. We will limit ourselves to first powers of A , B , C and no higher powers than the third of $(1/R)$. If we now divide the Schrödinger equation by (e^2/a_0) and express all lengths in terms of a_0 it may be written as

$$(2) \quad \begin{cases} (\mathcal{H} - E)\psi = 0, \\ \mathcal{H} = \mathcal{H}_{0,0,0} + A\mathcal{H}_{1,0,0} + B\mathcal{H}_{0,1,0} + CR^{-3}\mathcal{H}_{0,0,1} + BCR^{-3}\mathcal{H}_{0,1,1}. \end{cases}$$

⁽²⁾ T. W. MARSHALL and J. A. POPLE: *Mol. Phys.*, **1**, 199 (1958).

⁽³⁾ C. A. COULSON: *Proc. Roy. Soc. Edinb.*, A **61**, 20 (1941).

In case A) we have then

$$(3) \quad \left\{ \begin{array}{l} \mathcal{H}_{0,0,0} = -\frac{1}{2} \Delta - \frac{1}{r}, \\ \mathcal{H}_{1,0,0} = z, \\ \mathcal{H}_{0,1,0} = i \left(y \frac{\partial}{\partial z} - z \frac{\partial}{\partial y} \right), \\ \mathcal{H}_{0,0,1} = i \left(1 - \frac{3z}{R} \right) \left(y \frac{\partial}{\partial z} - \{z + R\} \frac{\partial}{\partial y} \right), \\ \mathcal{H}_{0,1,1} = \left(1 - \frac{3z}{R} \right) \left(y^2 + \{z + R\} z \right), \end{array} \right.$$

and in case B)

$$(4) \quad \left\{ \begin{array}{l} \mathcal{H}_{0,0,0} = -\frac{1}{2} \Delta - \frac{1}{r}, \\ \mathcal{H}_{1,0,0} = z, \\ \mathcal{H}_{0,1,0} = i \left(x \frac{\partial}{\partial y} - y \frac{\partial}{\partial x} \right), \\ \mathcal{H}_{0,0,1} = i \left(x \frac{\partial}{\partial y} - y \frac{\partial}{\partial x} \right), \\ \mathcal{H}_{0,1,1} = x^2 + y^2, \end{array} \right.$$

If we now substitute in equation (2):

$$(5) \quad \left\{ \begin{array}{l} \psi = \psi_{0,0,0} + A\psi_{1,0,0} + B\psi_{0,1,0} + C\psi_{0,0,1} + AB\psi_{1,1,0} + \\ \quad \quad \quad + AC\psi_{1,0,1} + BC\psi_{0,1,1} + ABC\psi_{1,1,1} + \dots, \\ E = E_{0,0,0} + AE_{1,0,0} + BE_{0,1,0} + CE_{0,0,1} + ABE_{1,1,0} + \\ \quad \quad \quad + ACE_{1,0,0} + BCE_{0,1,1} + ABCE_{1,1,1} + \dots, \end{array} \right.$$

it is possible to solve successively the equations

$$(6) \quad \left\{ \begin{array}{l} (\mathcal{H}_{0,0,0} - E_{0,0,0})\psi_{0,0,0} = 0, \\ (\mathcal{H}_{1,0,0} - E_{1,0,0})\psi_{0,0,0} + (\mathcal{H}_{0,0,0} - E_{0,0,0})\psi_{1,0,0} = 0, \\ (\mathcal{H}_{0,1,0} - E_{0,1,0})\psi_{0,0,0} + (\mathcal{H}_{0,0,0} - E_{0,0,0})\psi_{0,1,0} = 0, \\ \dots \end{array} \right.$$

In this way it is possible to obtain exact solutions for the functions $\psi_{i,j,k}$ and the energy values $E_{l,m,n}$. It should be borne in mind that the energies are expressed in terms of (e^2/a_0) .

In case A) it now follows that

$$(7) \quad \left\{ \begin{array}{l} \psi_{0,0,0} = \pi^{-\frac{1}{2}} \exp[-r], \\ \psi_{1,0,0} = \frac{1}{2} \pi^{-\frac{1}{2}} (zr + 2z) \exp[-r], \\ \psi_{0,1,0} = 0, \\ \psi_{0,0,1} = \frac{1}{2} i \pi^{-\frac{1}{2}} R^{-3} (2Ry - 3yz) \exp[-r], \\ \psi_{1,1,0} = 12^{-1} i \pi^{-\frac{1}{2}} (2yr^2 + 11yr + 22y) \exp[-r], \\ \psi_{1,0,1} = 12^{-1} i \pi^{-\frac{1}{2}} R^{-3} (12z^2y + 8r^2y + 17ry + 34y + Ryzr) \exp[-r], \\ \psi_{0,1,1} = 12^{-1} i \pi^{-\frac{1}{2}} R^{-3} \cdot \\ \cdot (10y^2r + 15y^2 - 14z^2r - 21z^2 - 2r^2 + 6Rzr + 12Rz) \exp[-r] \end{array} \right.$$

and

$$(8) \quad \left\{ \begin{array}{l} E_{0,0,0} = -\frac{1}{2}, \\ E_{0,1,1} = -R^{-3}BC, \\ E_{1,1,1} = -(71ABC/12R^2). \end{array} \right.$$

The other energy values are all zero.

In case B) it follows that

$$(9) \quad \left\{ \begin{array}{l} \psi_{0,0,0} = \pi^{-\frac{1}{2}} \exp[-r], \\ \psi_{1,0,0} = \frac{1}{2} \pi^{-\frac{1}{2}} (zr + 2z) \exp[-r], \\ \psi_{0,1,0} = 0, \\ \psi_{0,0,1} = 0, \\ \psi_{1,1,0} = 0, \\ \psi_{1,0,1} = 0, \\ \psi_{0,1,1} = 12^{-1} \pi^{-\frac{1}{2}} R^{-3} (2x^2r + 3x^2 + 2y^2r + 3y^2 + 2r^2) \exp[-r] \end{array} \right.$$

and

$$(10) \quad \dots \dots \dots E_{0,1,1} = 2R^{-3}BC.$$

The other energy values are all zero. The shielding constant at the point $(-R, 0, 0)$ is obtained from

$$(11) \quad \sigma = \frac{1}{3} \left[2 \sum_{k=0}^{\infty} E_{k,1,1}^{(A)} + \sum_{k=0}^{\infty} E_{k,1,1}^{(B)} \right] (H\mu)^{-1}$$

so that

$$(12) \quad \sigma = - (71 e^2 / 36 m c^2 a_0) (A/R^2)$$

which is correct up to the first power in A .

3. - Discussion.

The essential feature of our results is that at large distances on the z axis there results a magnetic shielding which is proportional to the first power of the electric field F . If the charge cloud is displaced towards the point for which the shielding is calculated the shielding constant is negative. This result confirms our calculations on the ammonia molecule.

It should be observed that the classical argument, which says that on applying a uniform magnetic field on a charge cloud there results a magnetic dipole which gives a secondary field proportional to R^{-3} at large distances apparently breaks down in the presence of an electric field.

It might be profitable to make some general remarks at this point. In molecules where there are strong local electric fields the atomic charge clouds are not any more spherically symmetric. Often a molecular charge cloud may be represented as a sum of charge clouds of the type

$$(13) \quad \varrho(\mathbf{r}_a) = \alpha(b_1 r_a^2 + b_2 z_a r_a + b_3 z_a^2) \exp[-q r_a].$$

Following a method which was previously discussed^(4,5) it may now be found that to a first approximation at large distances along the z axis such a charge cloud will give rise to a negative magnetic shielding; the effect due to the first term of (13) is zero, the effect of the second term is proportional to R^{-2} and the effect of the third term is proportional to R^{-3} , if R is the distance between the charge cloud and the point for which the shielding is calculated.

Therefore, the contributions of asymmetric atoms and lone pair electrons to proton shielding at large distances may conveniently be described by

$$(14) \quad \sigma = \lambda R^{-2} + \lambda' R^{-3}.$$

⁽⁴⁾ H. F. HAMEKA: *Mol. Phys.*, **1**, 203 (1958).

⁽⁵⁾ H. F. HAMEKA: *Mol. Phys.*, **2**, 64 (1959).

Although in many cases the constants λ and λ' may be computed without many difficulties from atomic structure ⁽⁵⁾, they may also be considered as semi-empirical parameters.

* * *

The author is indebted to Dr. ROBERT G. PARR and to Dr. WALTER KOHN for discussions on the subject.

RIASSUNTO (*)

La costante di schermo magnetico dell'atomo di idrogeno in un campo elettrico uniforme è calcolata in un punto P situato a grande distanza dal nucleo nella direzione del campo elettrico. Si trova che il termine principale della costante di schermo è proporzionale alla prima potenza del campo elettrico e all'inverso della seconda potenza della distanza di P dal nucleo di idrogeno.

(*) Traduzione a cura della Redazione.

On the X-Ray Diffraction in Water-Dioxane and Water-Ethyl Alcohol Mixtures.

F. CENNAMO and E. TARTAGLIONE

Istituto di Fisica Sperimentale dell'Università - Napoli

(ricevuto il 20 Novembre 1958)

Summary. — From the behaviour to X-ray diffraction of water-dioxane and water-ethyl alcohol mixtures, it is shown that the molecular associations of water are attenuated by dioxane, whereas they are favored by ethyl alcohol.

1. — We have studied, by the same method described in previous papers ⁽¹⁾, the variation of intensity and maximum position for the X-ray beam diffracted by water-dioxane and water-ethyl alcohol mixtures.

It is already known that these mixtures both show an interesting behaviour, namely:

The variation of density, vapour tension, surface tension and refractory index as functions of concentration, appears remarkably unlinear in the case of water-dioxane mixtures ⁽²⁾ for which, therefore, a structural research in the X-ray field looks quite interesting. For instance one finds that the above quantities diverge most from the linear law in the mixture of 15% dioxane molecules, where an eutectic point is reached at -15°C , and that is considerably lower than the solidification points of the pure components (0°C for water and $+11,75^{\circ}\text{C}$ for dioxane).

⁽¹⁾ F. CENNAMO: *Nuovo Cimento*, **10**, 395 (1953); *Rend. Acc. Lincei*, **10**, 475 (1951).

⁽²⁾ HOVORKA, SCHAEFER and DREISBACH: *Journ. Am. Chem. Soc.*, **58**, 2264 (1936).

For water-ethyl alcohol also, the above quantities do not follow the linear law of ideal mixtures. On the other hand a difference can be relieved: the polar molecules of water, strongly associated when in the pure state, are found mixed in one case, with an apolar liquid like dioxane and in the other case, with a polar liquid like ethyl-alcohol.

From the velocity values, determined by R. PARSHAD ⁽³⁾, C. J. BURTON ⁽⁴⁾ and others, of the ultrasonic waves propagating through the said mixtures and from the density measurements taken, the adiabatic compressibility values β have been obtained as plotted in Fig. 1, where the curve *a*) refers to water-dioxane and *b*) to water-ethyl alcohol.

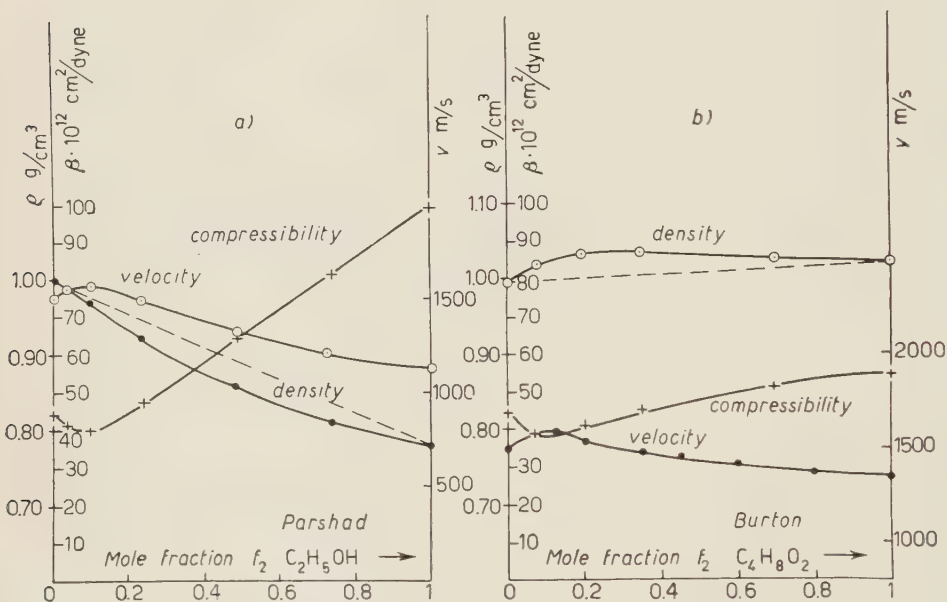


Fig. 1.

It should be noted that letting concentration vary, both systems show a rather pronounced compressibility minimum, but their density variations differ, as may be seen in the same graphs above, where the corresponding values have been plotted: water-ethyl alcohol densities are definitively, even though slightly, lower than those belonging to the ideal law, while, on the contrary, water-dioxane density reaches a maximum at nearly 12% dioxane.

⁽³⁾ R. PARSHAD: *Ind. Journ. Phys.*, **15**, part V, 313 (1941).

⁽⁴⁾ C. J. BURTON: *J.A.S.A.*, **20**, 186 (1948).

2. - In this structural research the Cu K_α X-ray wavelength has been used ($\lambda = 1.54 \text{ \AA}$), the liquid being contained in a flat box 0.5 mm thick, with mica ends. Diffraction rings have been so obtained which were quite different in both intensity and diameter, according to the mixture studied.

Fig. 2 shows the intensity distribution as a function of the diffraction angle in rad. for the diffracted X-rays: in curve *a*) by water, *f*) by dioxane, *b*) ... *e*) by some other mixtures here analyzed, namely those corresponding to the following mole fractions

$f_1 = 0.95$	$f_2 = 0.05$	<i>b</i>) curve
» = 0.85	» = 0.15	<i>c</i>) »
» = 0.72	» = 0.18	<i>d</i>) »
» = 0.40	» = 0.60	<i>e</i>) »

where f_1 and f_2 indicate the mole fractions of water and dioxane respectively.

Each intensity distribution has been calculated from the microphotometer curve plotted by the method quoted above⁽¹⁾, that is: to expose the corresponding plates in the same experimental conditions and to transform measurements of blackening into relative intensities.

As shown in the diagram the diffraction band one obtains under a 15 min exposure for pure water and for pure dioxane has one maximum at 0.45 rad and 0.31 rad respectively, being much denser and narrower in the latter case. The ratio of the water to the dioxane bandwidth, measuring at half the maximum value of intensity, is about 2.2; that between the corresponding intensities at maximal intensities is 0.133.

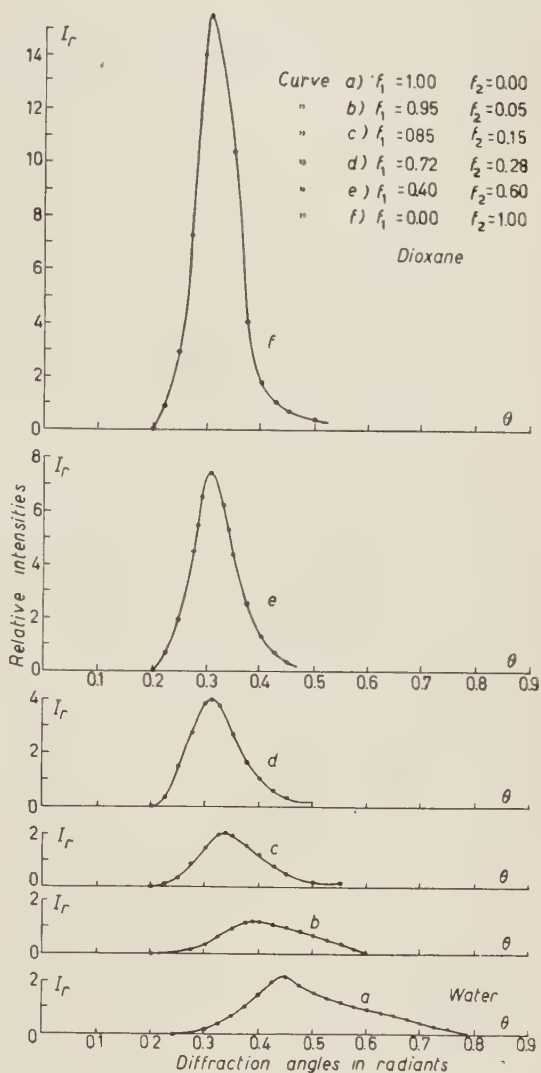


Fig. 2.

Several series of measurements at various concentrations, but in exactly the same experimental conditions, have been repeated, keeping furthermore the same time exposures constant for each series.

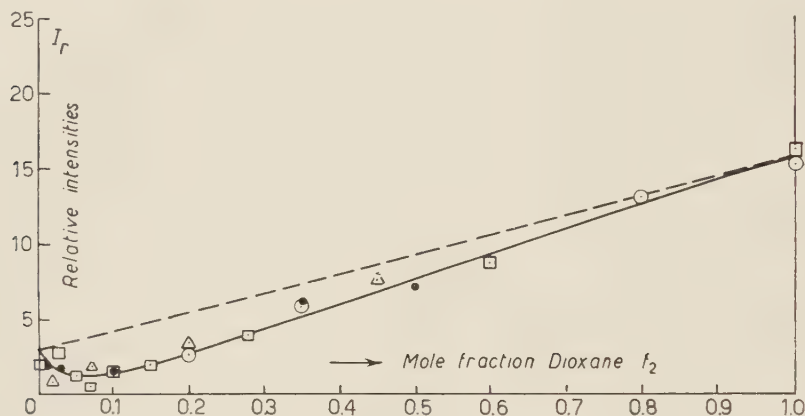


Fig. 3.

Fig. 3 shows the relative intensity—as a function of the dioxane mole fraction—when measured at the diffraction maximum of each mixture: one sees that the curve, starting from the point $f_1 = 1$, $f_2 = 0$ of the pure water, shows a decreasing trend with a minimum at $f_2 = 0.07$, while behaving quite linearly from the point $f_2 = 0.15$ on, till $f_2 = 1$.

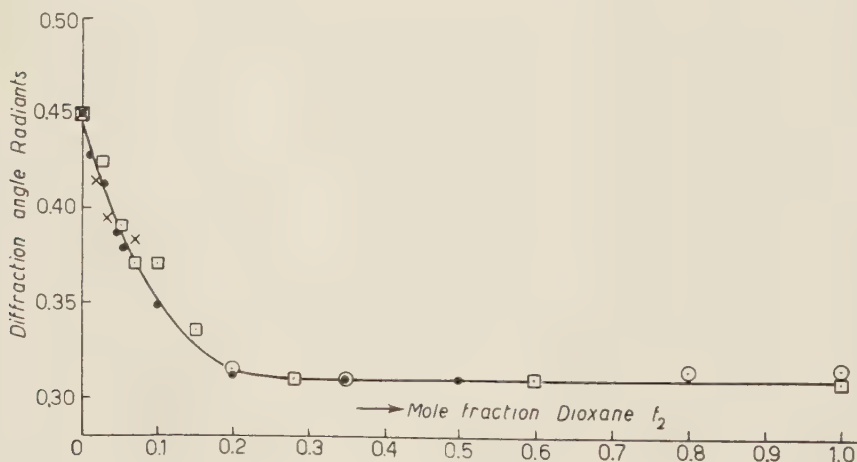


Fig. 4.

Fig. 4 shows—as a function of the dioxane mole fraction—the diffraction angle when measured at the intensity maximum of the diffracted X-rays; a

net decrease in the diffraction angle can be noticed for the mixtures from the value $f_2 = 0$ to $f_2 = 0.20$; from here on the diffraction angle remains constant at the value proper for dioxane.

These results show clearly that the diffraction ring characteristic for water is destroyed (or, at least, much weakened) by adding small fractions of dioxane; actually, complete

vanishing of the ring takes place in the 15% dioxane mixture, where—as already said—the eutectic point is reached. One interesting point: the band intensity distribution for mixtures with dioxane

mole fractions between $f_2 = 0$ and $f_2 = 0.2$ differs considerably from the additive behaviour we would expect, should the two causes co-exist which produce the two corresponding characteristic rings (Fig. 5); this obviously shows that dioxane exerts a weakening—or almost destroying—action on the water molecular associations, which are replaced, even though partly, by associations of the water-dioxane type.

On the other hand the diffraction bands of those water-dioxane mixtures whose dioxane mole fractions exceed the value 0.20, present, not only a maximum corresponding to that of pure dioxane, but also the same diffraction band

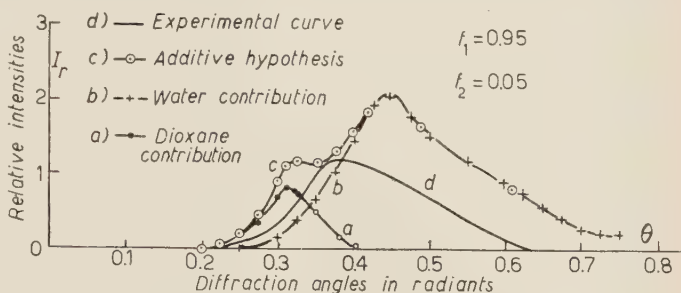


Fig. 5.

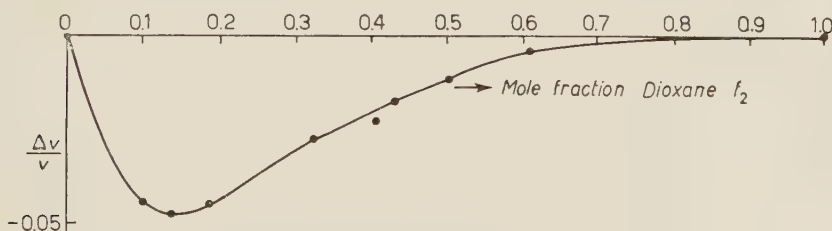


Fig. 6.

characteristic for it, though, of course, with a lower intensity (Fig. 2); which fact would confirm the hypothesis that molecular order, the essential cause for the appearance of rings, is only to be found with dioxane, in those mixtures with water fractions not reaching the value 0.80; that is at these fraction values water molecules behave as if in the vapour state. Let us point out that letting the dioxane mole fraction vary, the density behaviour considerably

diverges from the linear law: according to our measurements, and in agreement with BURTON's, we have the maximum variation of the specific volume for the mixture with the value $f_2 = 0.15$ (Fig. 6). The water-ethyl alcohol mixtures have been studied by exactly the same methods: The diffraction

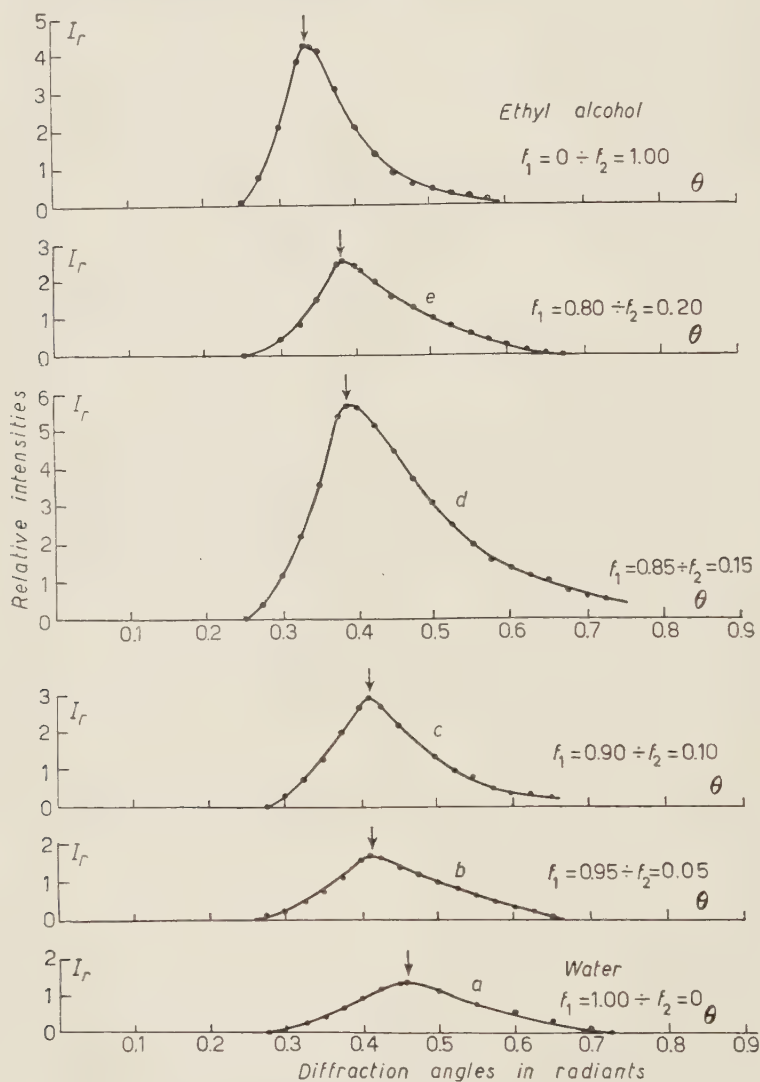


Fig. 7.

bands obtained for either liquid at the pure state furnish the following data: the diffraction maximum is reached at $\theta = 0.45$ rad in water and at $\theta = 0.34$ rad in ethyl alcohol; furthermore, differently from the water-dioxane case, the

two band intensities measured correspondingly appear to be of the same order of magnitude, namely in the ratio 1:2.

Fig. 7 shows the intensity distribution of X-rays diffracted, at varying diffraction angles, by water (curve *a*), by ethyl-alcohol (curve *b*) and by the mixtures of both here quoted

$f_1 = 0.95$	$f_2 = 0.05$	curve <i>b</i>)
$f_1 = 0.90$	$f_2 = 0.10$	» <i>c</i>)
$f_1 = 0.85$	$f_2 = 0.15$	» <i>d</i>)
$f_1 = 0.80$	$f_2 = 0.20$	» <i>e</i>)

where f_1 and f_2 represent the mole fraction for water and ethyl-alcohol respectively.

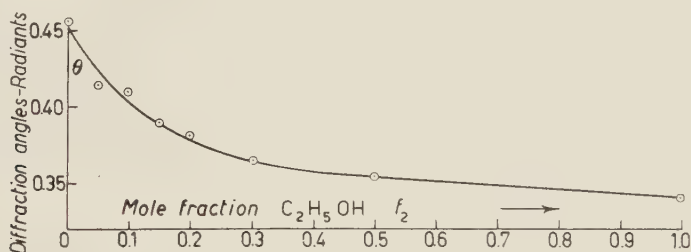


Fig. 8.

Next, taking the ethyl-alcohol mole fraction as abscissa, there are shown: in Fig. 8, the diffraction angle at which the intensity maximum is reached and in Fig. 9, the corresponding intensity of the X-rays diffracted by the pure components and some mixtures of both.

Now the two mixtures water-dioxane and water-ethyl alcohol, while behaving alike—as said—with respect to compressibility, are found to differ when analysed with X-rays.

It is then confirmed that dioxane, even if present in very small percentages destroys water polymeries, in agreement with inferences one may make from the adiabatic compressibility curve (Fig. 1) showing an upward concavity; which fact, precisely, according to PARSHAD ⁽³⁾ would let us think that the molecular associations of both components have been destroyed, at the same time a few associations of the water-dioxane type being produced.

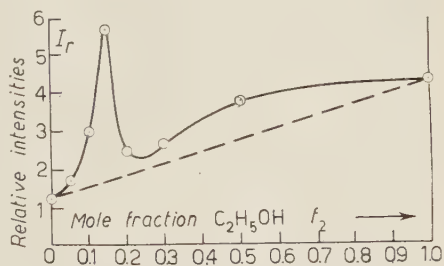


Fig. 9.

The above results agree with those of GORDY ⁽⁵⁾, who has studied the infrared absorption of water-dioxane mixtures, relieving for the water therein contained a behaviour very near to that of the vapour state. It may be remarked that GORDY's research has been made exclusively on high dioxane concentrations, namely for values of f_2 between 0.20 and 1.00, for which we do not actually find, under X-ray diffraction, any contribution from water.

As for the water-ethyl alcohol mixtures, the position of the X-ray diffraction maximum varies continuously from one to the other component, not staying constant in any interval of the concentration axis; by which fact it is shown that associations existing in both components at the pure state are destroyed in the process and replaced by some other of the water-ethyl alcohol type. In fact, looking at the diagram of intensity for the diffracted X-rays maximum, one sees the whole curve above the straight line expected for in the case of ideal mixtures, showing, moreover, a considerably pointed maximum at the value $f_2 = 0.12$ for the ethyl alcohol mole fraction.

It is of interest to note that, according to BUTLER ⁽⁶⁾, the interaction energy between the ethyl alcohol molecular OH group and one water molecule exceeds that between two water molecules, which explains how, by adding ethyl alcohol molecules, water-water associations are split up, to be replaced by some other of the water-ethyl alcohol type.

Following BUTLER's calculations, every association of the water-water type, in such mixtures where each ethyl alcohol molecule is wholly surrounded by water molecules and each water molecule is in contact with some ethyl alcohol one, would be destroyed.

It is worth remarking that the above condition is realized with the mixture whose ethyl alcohol mole fraction has the value $f_2 = 0.11$ for which mixture the diffracted X-rays intensity, reaching actually the value 5.8 instead of the theoretical one 1.5, differs considerably from the ideal behaviour. On the other hand the cohesive energy reaches its maximum value in the said mixture ⁽⁷⁾, which explains the adiabatic compressibility minimum.

One more fact worth remarking: according to some researches by one of the authors ⁽⁸⁾ on the Raman spectrum of ethyl alcohol mixtures, small percentages of ethyl alcohol molecules added to water produce in the band complex at about 3400 cm^{-1} , which is characteristics for water a noticeable decrease of the band at $\lambda = 3620\text{ cm}^{-1}$. Such a band is thought of as due to simple molecules, as it does not appear in ice, in crystallisation water of CaSO_4 , etc., that is in all those water states where presence of simple molecules is to be excluded.

⁽⁵⁾ W. GORDY: *Journ. Chem. Phys.*, **4**, 769 (1936).

⁽⁶⁾ C. C. BUTLER: *Trans. Farad. Soc.*, **33**, 229 (1937).

⁽⁷⁾ D. SETTE: *La ricerca scientifica* (1949), p. 338.

⁽⁸⁾ F. CENNAMO: *Nuovo Cimento*, **15**, 9 (1938).

That once more confirms the results obtained with X-ray diffraction by which water-water and alcohol-alcohol associations in a mixture are replaced by associations of the water-alcohol type.

* * *

The authors express their thanks to Prof. ANTONIO CARRELLI, director for Experimental Physics of the Naples University, for the means made available and the stimulating discussions held on this research.

RIASSUNTO

Dallo studio del comportamento alla diffrazione dei raggi X dei miscugli acqua-diossano ed acqua-alcool etilico si nota che, mentre il diossano attenua le associazioni molecolari dell'acqua, l'alcool etilico tende a favorirle.

The $^{35}\text{Cl}(\gamma, n)^{34}\text{Cl}$ and $^{35}\text{Cl}(\gamma, n)^{34}\text{Cl}^m$ Reactions Investigated up to 31 MeV.

F. FERRERO, S. FERRONI, R. MALVANO, S. MENARDI and E. SILVA (*)

Istituto di Fisica dell'Università - Torino
Istituto Nazionale di Fisica Nucleare - Sezione di Torino

(ricevuto il 24 Novembre 1958)

Summary. — The paper concerns measurements of photoneutron cross sections for activation of the 1.58 s ground state and of the 32 min isomeric state in ^{34}Cl . The branching ratio is found to be of the order of unity. A tentative explanation of the peculiar behaviour of the b.r. in the region of the giant resonance is given.

1. — Introduction.

In the region of the light elements there are few cases where isomeric states are excited through a (γ, n) process. An already well known case is ^{27}Al , that loosing a neutron gives rise to the two states of ^{26}Al , the ground state (5^+) and the 0.25 MeV isomeric state (0^+) respectively. It has been possible by residual activity to study easily the short lived isomeric state activation cross-section, while the 5^+ ground state could not be studied directly but only by total neutron counting and subtraction of the isomeric activation curve. The branching ratio (isomeric state/ground state) has been found to be ~ 0.3 , becoming very small for γ -ray energies above 25 MeV.

The case of ^{35}Cl can be considered complementary to the case of ^{27}Al : the bigger angular momentum level is above the smaller one. Besides the two

(*) Fellow of the National Council of Research, Brasil. On leave of absence from the University of S. Paolo.

levels can be studied directly by residual activity because both states have convenient half lives.

Actually the existence of a 3^+ isomeric state 0.142 MeV above the ^{34}Cl ground state (0^+) has been reported by P. M. ENDT ⁽¹⁾. Both states are β^+ emitters with half lives of 32 min and 1.58 s respectively.

We have investigated the above reactions using the X-rays from a 31 MeV betatron, measuring the annihilation radiation arising from the β^+ residual activities.

2. - Experimental apparatus.

Samples of high purity fused NaCl were used in the experiment. The 32^mCl β^+ residual activity from the isomeric state has been measured detecting the 0.51 MeV rays by means of a NaI(Tl) scintillator and a single channel pulse height analyzer.

The technique used to measure the short lived β^+ activity from the ground state is fully described in the references ^(2,3) and the fast photoneutron yield from chlorine was measured with a $^{28}\text{Si}(n, p)^{28}\text{Al}$ threshold detector ⁽⁴⁾ computing the difference between the measurements carried out independently with samples of NaCl and metallic Na.

3. - Experimental results and discussion.

In Fig. 1 are shown the excitation functions for the isomeric state and for the ground state of ^{34}Cl . In the same figure the fast photoneutron yield from chlorine is plotted. Their absolute values were obtained by comparison with copper ⁽⁵⁾ except for the fast neutron yield, that was determined comparing the yields of Na and NaCl with the known yield of Al ⁽³⁾ at 30 MeV.

The excitation functions were analyzed by the PENFOLD-LEISS ⁽⁶⁾ method and the cross-sections are presented as histograms in Fig. 2.

⁽¹⁾ P. M. ENDT, and I. C. KLUYVER: *Rev. Mod. Phys.*, **26**, 95 (1954).

⁽²⁾ U. FARINELLI *et al.*: *Photoexcitation of $^{207}\text{Pb}^m$* . In publication on *Phys. Rev.*

⁽³⁾ F. FERRERO *et al.*: *Nucl. Phys.*, **9**, 32 (1958).

⁽⁴⁾ F. FERRERO *et al.*: *Nuovo Cimento*, **4**, 418 (1956).

⁽⁵⁾ L. KATZ, and A. G. W. CAMERON: *Can. Journ. Phys.*, **29**, 518 (1951).

⁽⁶⁾ A. S. PENFOLD and J. E. LEISS: *Phys. Rev.*, **95**, 637 (1954).

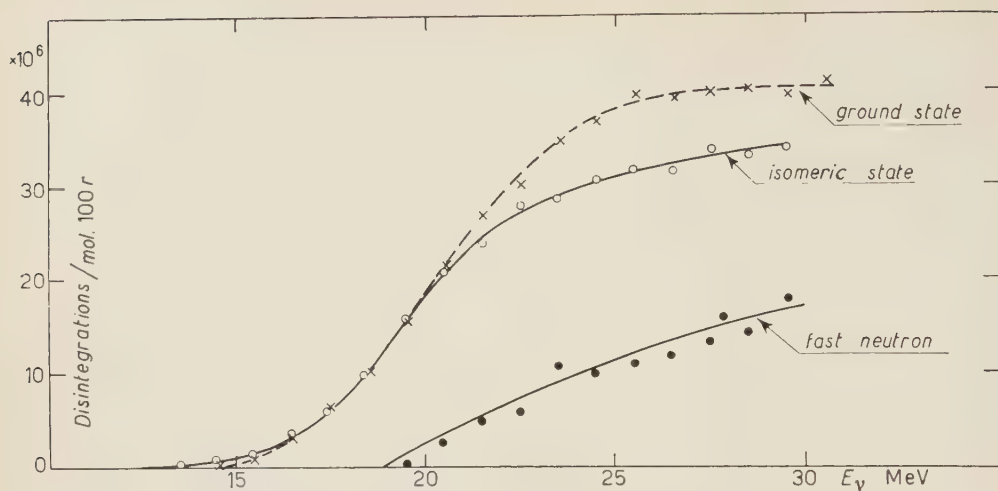


Fig. 1. — Excitation functions for isomeric state, ground state of ^{34}Cl and for fast neutron emission from chlorine. The yields were taken using a 5 cm Al ionization chamber (4).

The principal features of the experimental results are collected in Table I: as a matter of fact the total integrated cross-section (isomeric state+ground state) up to 23 MeV agrees very well with the result of J. GOLDBERG and

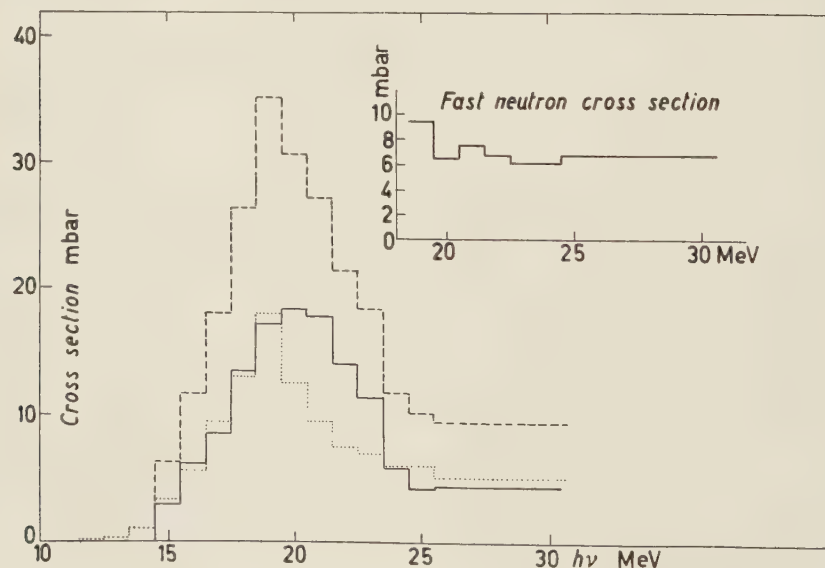


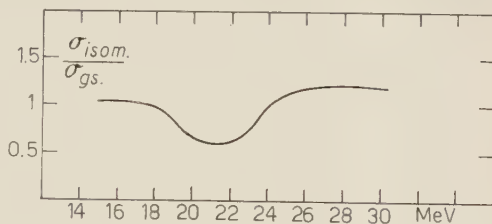
Fig. 2. — Cross sections from $^{35}\text{Cl}(\gamma, n)^{34}\text{Cl}$ ground and isomeric state calculated with the Penfold-Leiss method (..... isomeric state; — ground state, --- g.s.+i.s.). The inset shows the fast neutron cross section in natural chlorine.

L. KATZ⁽⁷⁾ obtained measuring the total neutron yield from chlorine. It would be particularly interesting to extend this measurements to higher energy than was previously done in order to evaluate the contribution from higher order processes $(\gamma, 2n)$, (γ, np) to the total photon-neutron cross-section. Actually we have concluded in a previous paper that *e.g.* in ^{27}Al this contribution is not very great while in ^{32}S direct experiments indicate that the integrated (γ, np) cross-section up to 30 MeV is an important fraction of the total absorption.

TABLE I.

	Γ (MeV)	σ_{peak} (mb)	E_{peak} (MeV)	$\int_0^{30} \sigma dE$ (MeV-mb)
$^{35}\text{Cl}(\gamma, n)^{34}\text{Cl}$ g.s.	6	18.3	20	141
$^{35}\text{Cl}(\gamma, n)^{34}\text{Cl}$ i.s.	5	18	19	125
$^{35}\text{Cl}(\gamma, n)^{34}\text{Cl}$ (g.s.+i.s.)	6.5	35.2	19.5	266

In Fig. 3 is plotted the ratio of the i.s. over g.s. cross-sections (branching ratio, b.r.). The general behaviour of the b.r. versus γ -ray energy can be interpreted qualitatively in the following way. Its value nearly constant and equal to one up to the top of the giant resonance, suggests that the evaporation from ^{35}Cl leads with equal probability to the isomeric state (3^-) and to the ground state (0^+) of ^{34}Cl . On the other hand the high value of the b.r. above 25 MeV, where certainly the contribution from direct neutron emission predominates (this statement is confirmed actually by the behaviour of the fast neutron cross-section), is explained by the fact that such a direct process can leave the residual nucleus with many units of angular momentum. Therefore, only for simple reasons of statistical weight, these direct transitions tend to enhance the 3^+ isomeric level, while in the Al the ground state is enhanced.

Fig. 3. — Branching ratio (b.r.) i.s./g.s. as a function of γ -ray energy.

(7) J. GOLDEMBERG and L. KATZ: *Can. Journ. Phys.*, **32**, 49 (1954).

The value of the b.r. in the intermediate region is more difficult to understand; however it could be explained admitting the existence of a direct transition located at ~ 22 MeV, that feeds directly the ground state and leaves, therefore, the nucleus with a small value of angular momentum. Such a type of transition could be the $2s_{\frac{1}{2}} \rightarrow 2p_{\frac{3}{2}}$. The energy of this transition cannot be easily calculated, however, because a simple application of the shell model with finite well and spin orbit coupling does not take into account the distortion of the potential caused by the unpaired $1d_{\frac{3}{2}}$ proton and by the incomplete $1d_{\frac{3}{2}}$ neutron subshell.

* * *

One of us (E.S.) would express his gratitude to Prof. G. WATAGHIN, director of the Physical Institute of Turin, for the kind hospitality.

RIASSUNTO

In questo lavoro si riportano le misure sulle sezioni d'urto per l'eccitazione foto-neutronica dello stato fondamentale (1.58 s) e dello stato isomerico (32 min) nel ^{34}Cl . Si trova che il b.r. è dell'ordine dell'unità. Viene data una possibile spiegazione del particolare comportamento del b.r. nella regione della risonanza gigante.

Measurement of the Circular Polarization of the Bremsstrahlung Produced by Electrons from ^{204}Tl .

U. AMALDI jr.

Istituto Superiore di Sanità - Roma

M. BERNARDINI, P. BROVETTO and S. FERRONI

Istituto Nazionale di Fisica Nucleare - Sezione di Torino

(ricevuto il 25 Novembre 1958)

Summary. — The polarization of the external bremsstrahlung produced by the electrons emitted by ^{204}Tl near the top of the spectrum (first order unique forbidden transition) has been measured by means of the usual technique of the forward Compton scattering on magnetized iron. The observed effect agrees, within experimental error (about 10%), with the value expected for $-v/c$ polarized electrons.

1. — Introduction.

The failure of parity conservation involves, for allowed β transitions and also for first order unique forbidden transitions, the well known $-v/c$ law for the electronic polarization ⁽¹⁾. In this connection we have performed a polarization measurement on the β -decay electrons of ^{204}Tl ($\Delta J = 2$, yes; $E_{\text{max}} = 760$ keV) by determining the polarization of the corresponding external bremsstrahlung. McVOY ^(2,3) has shown that the forward bremsstrahlung produced by longitudinally polarized electrons is highly circularly polarized. For example, for 700 keV electrons the polarization of the bremsstrahlung is close

⁽¹⁾ V. B. BERESTETSKY, B. L. IOFFE, A. P. RUDIK and K. A. TER-MARTIROSYAN: *Nucl. Phys.*, **5**, 464 (1958); *Phys. Rev.*, **111**, 522 (1958).

⁽²⁾ K. W. McVOY: *Phys. Rev.*, **106**, 828 (1957).

⁽³⁾ K. W. McVOY: *Phys. Rev.*, **110**, 1484 (1958).

to 80%. The transferred polarization, however, decreases rapidly when the γ -ray energy becomes a small fraction of the energy of the irradiating electron ⁽⁴⁾.

Our polarization measurements were performed adopting the well known technique of the Compton scattering of the bremsstrahlung on magnetized iron. Only the high energy part of the bremsstrahlung spectrum was analyzed, in order to select the γ -rays of high polarization.

2. - Polarimeter.

The experimental set-up is schematically shown in Fig. 1. The source S emits the γ rays to be analyzed. The lead collimators define the geometry of the scattering process and, consequently, the integration limits in the calculation of the expected effect. The γ -rays, emitted from source S having a mean angle $\psi = 18^\circ$ with respect to the symmetry axis of the arrangement, are Compton scattered at a mean angle $\vartheta = 60^\circ$. At such an angle the symmetry of the cross-section against magnetized iron is close to its maximum.

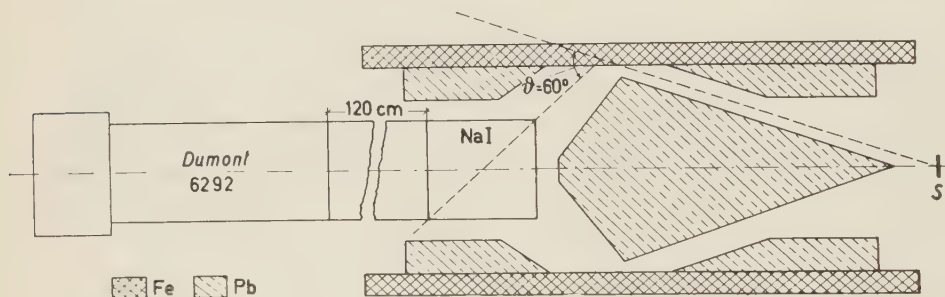


Fig. 1. - Experimental set-up.

The iron scatterer was a cylinder located in the gap of an electromagnet (lines of force parallel to its axis) and was surrounded by ten centimeters of lead to reduce the background. The light pulses, produced in a NaI(Tl) scintillator, were collected by a 6292 Du Mont photomultiplier through a light-pipe 120 cm long and 4.5 cm in diameter. Such a long light-pipe was necessary in order to reduce the influence of the magnetic field on the photomultiplier.

The electronic apparatus was conventional; it consisted of a stabilized power supply, a non-overloading linear amplifier and a single channel pulse analyzer.

⁽⁴⁾ C. FRONSDAL and H. ÜBERALL: *Phys. Rev.*, **111**, 580 (1958).

The magnetic shield of the photomultiplier consisted of four iron plates, each 1 m² area, perpendicular to the axis of the light-pipe, and of two coaxial mu-metal cylinders. By inverting the magnetic field, the variation of the stray magnetic field observed at the position of the photomultiplier was less than 0.02 G. Such a careful shielding was necessary because of the steepness of the bremsstrahlung spectrum. The field measurements were performed by means of a peaking-strip magnetic detector, whose sensitivity is ≈ 0.01 G (5).

The linearity of the experimental equipment was calibrated with the γ -rays of ¹³⁷Cs (661 keV), the annihilation line of ²²Na (511 keV) and the K_{α} X-rays of Pb (75 keV). The resolving power for the ¹³⁷Cs line was 16 %.

A measurement of the magnetic polarization of the iron at saturation performed with a ballistic galvanometer gave a value of (2.08 ± 0.04) weber/m²; on the basis of this figure the fraction of polarized electrons is $f = 1.97/26$.

3. - Scintillator efficiency.

The crystal relative efficiency ϱ depends on the energy and the angle ϑ of the scattered γ -ray. Because ϱ is involved in the calculation of the expected

effect, we measured it accurately by means of a well collimated γ -ray beam emitted by a strong source of ¹³⁷Cs (661 keV). In these measurements the geometry was chosen so that the γ -rays crossed the scintillator along the same path as the γ -rays scattered by the centre of the magnetized iron during the actual experiment. In Fig. 2 the experimental points show the relative efficiency ϱ for seven values of ϑ keeping $\psi = 18^\circ$. ϱ is defined as the ratio of the area of the photopeak measured at each ϑ to that observed at $\vartheta = 60^\circ$.

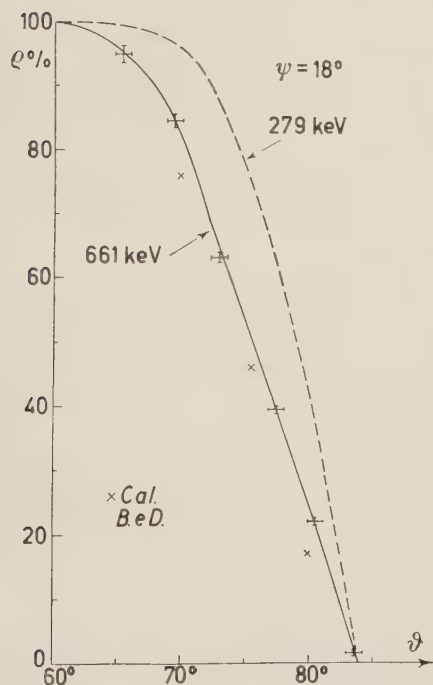


Fig. 2. - The crystal efficiency ϱ versus ϑ . The full line represents ϱ measured at 661 keV. The dashed line represents ϱ calculated at 279 keV by means of M. J. Berger's and J. Dogget's data.

(5) G. GHIGO: unpublished.

It should be noted, however, that the energy of our scattered γ -rays is somewhat lower than 661 keV. Since no strong source of lower energy was available, we adopted the following procedure based on the results of M. J. BERGER and J. DOGGET⁽⁶⁾. Using the Monte Carlo method, these authors have calculated the efficiency of several cylindrical NaI(Tl) scintillators of different dimensions for various γ -rays (e.g. 661 and 279 keV) which were incident perpendicularly to the bases of the scintillators. Our procedure consists in evaluating, for a few conveniently chosen values of ϑ , the dimension of a cylindrical scintillator which would have the same efficiency as our crystal when traversed by the γ -rays in the ϑ direction. The relative efficiencies obtained by such a procedure for 661 keV are plotted as crosses in Fig. 2. The agreement of these computed values with the experimental result is satisfactory. Therefore, for the relative efficiency of our crystal for γ -rays of 279 keV, we felt that we were justified in using the same computation procedure as that used for the 661 keV γ -rays. (The results are given by the dashed line of Fig. 2).

The values of ϱ for intermediate energies have been obtained by linear interpolation.

4. - Measurements.

The source consisted of 20 mC of $^{204}_{81}\text{Tl}$ (as sulfide) covered with a lead target 40 μm thick. The ^{204}Tl nucleus is a pure β^- emitter, with a maximum energy $E_{\text{max}} = 760$ keV; the transition is a first order unique forbidden transition, with $\Delta J = 2$ (yes)^(7,8). The external bremsstrahlung is produced by collisions against either Tl or Pb nuclei, the atomic numbers of which are very similar.

The electrons emerging from the lead target are stopped in a plexiglass plate 4 mm thick.

The bremsstrahlung spectrum, collimated perpendicularly to the lead target within a solid angle of 0.125 steradian is plotted as a function of energy in Fig. 3.

For γ -rays energies of 760 and 600 keV the Compton scattered photons at $\vartheta = 60^\circ$ have energies of 475 and 375 keV respectively. This was the energy range adopted in our measurements in order to restrict the polarization analysis to the upper part of the β^- spectrum.

⁽⁶⁾ M. J. BERGER and J. DOGGET: *Rev. Sci. Instr.*, **27**, 269 (1956).

⁽⁷⁾ T. YUASA and J. LABERRIQUE-FROLOW: *Journ. Phys. et Rad.*, **16**, 39, (1955); **16**, 165 (1955).

⁽⁸⁾ M. GOLDBABER, L. GRODZINS and A. W. SUNYAR: *Phys. Rev.*, **106**, 826 (1957).

The effect on the photomultiplier of the stray magnetic field was checked by measurements on a part of the direct bremsstrahlung spectrum which showed the same slope of the scattered spectrum in the actual experiment. Thus it was shown that the effect of the stray field was negligible: $+ (0.06 \pm 0.08) \%$.

During the polarization measurements the magnetic field was reversed every ten minutes. The counting rate between 375 and 475 keV was about 200 counts per minute, while the background was about 20 counts/min. For all runs the threshold of the discriminator was maintained within the limits (375 ± 5) keV. A subsidiary measurement was made for Compton scattered γ -rays in the range $(275 \div 375)$ keV.

The results of all our measurements are summarized in Table I. The calculation of the expected effect is given in the Appendix.

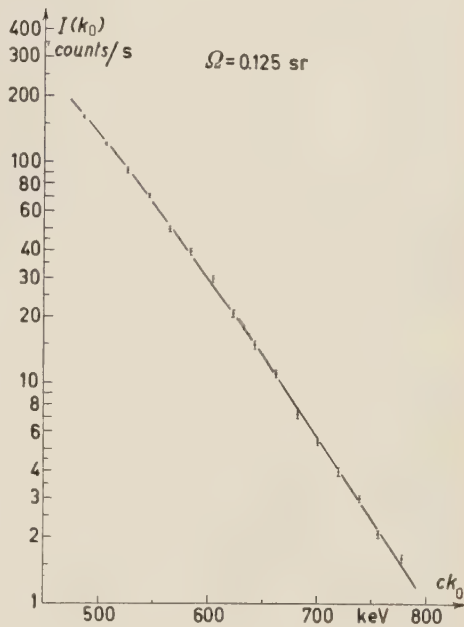


Fig. 3. — ²⁰⁴Tl bremsstrahlung spectrum.

TABLE I. — *Experimental results.* (N_1 and N_2 are the total counts when the magnetic field is directed from the scintillator to the source and viceversa).

Energy range (keV)	Total counting time T min	N_1 counts	N_2 counts	Back-ground b counts	Experimental effect $2 \frac{N_1 - N_2}{N_1 + N_2 - 2b}$	Calculated effect for $-v/c$ polarized electrons
375 \div 475	1 840	349 471	342 032	38 300	$+(2.41 \pm 0.27)\%$	$+ 2.83\%$
275 \div 375	250	281 323	279 208	3 500	$+(0.77 \pm 0.27)\%$	—

5. — Conclusions.

The previous results prove, within the limit of experimental error, that the electrons emitted by ²⁰¹Tl with energy close to E_{\max} have a longitudinal polarization equal to $-v/c$. Because of experimental errors and uncertainties in the computation of the expected effect, we cannot exclude a deviation of

the order of 10% from the $-v/c$ law. This possibility appears in the calculation of reference (1).

Another polarization measurement of β^- -electrons emitted in a first forbidden unique transition was made by other authors in the case of $^{90}\text{Sr}-^{90}\text{Y}$ with similar results (9,10).

* * *

The authors wish to express their gratitude to Prof. M. AGENO for very useful discussion and criticism. Three of us (M.B., P.B., and S.F.) acknowledge the Istituto Superiore di Sanità for its kind hospitality. We acknowledge also Miss F. VALENTE for the help given in collecting the experimental data.

APPENDIX

The calculation of the effect to be expected in the previous described polarization measurements is given here. Initially we assume that the thickness of the iron scatterer is so small that double scattering processes can be neglected. Let us consider the γ -rays emitted by the source (Fig. 4) within a solid angle $d\Omega_1$, with momentum \mathbf{k}_0 at an angle ψ with the symmetry axis of the cylinder and scattered with momentum \mathbf{k} within the solid angle $d\Omega_2$.

Under these conditions, the γ -rays detected by the scintillator, for the two orientations of the magnetic field, are:

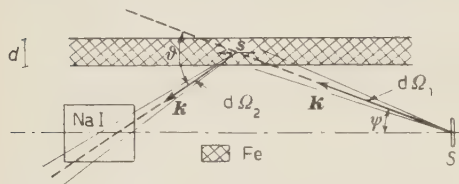


Fig. 4. - Schematic diagram of the experiment.

$$(1) \quad dN^{(\pm)} = I(k_0) dk_0 d\Omega_1 \sigma^{(\pm)} d\Omega_2 \frac{nd}{\sin \psi},$$

where $I(k_0)$ is the bremsstrahlung spectrum per steradian emitted by the source, n is the number of electrons per unit volume of iron, $\sigma^{(\pm)}$

the Compton cross section for the two orientations of electronic spins, d the iron thickness and ϱ the (absolute) efficiency of the scintillator. The Compton cross section can be written:

$$(2) \quad \sigma^{(\pm)} = \sigma_0 \pm fP\sigma_1,$$

where f stands for the fraction of polarized electrons in the iron. The $+$ and $-$ signs refer to the two cases in which the angle between \mathbf{k}_0 and the electronic

(9) A. BISI and L. ZAPPA: to be published.

(10) H. SCHOPPER: *Nucl. Instr.*, **3**, 158 (1958).

spin is smaller or greater than $\pi/2$. P is the absolute value of the degree of circular polarization of the γ -rays. Eq. (2) refers to right circularly polarized γ -rays (*)

Since, in our equipment, the iron magnetization is parallel to the symmetry axis, we have:

$$(3) \quad \sigma_0 = \frac{r_0^2}{2} \left(\frac{k}{k_0} \right)^2 \left[\frac{k_0}{k} + \frac{k}{k_0} - \sin^2 \vartheta \right],$$

$$(4) \quad \sigma_1 = \frac{r_0^2}{2} \left(\frac{k}{k_0} \right)^2 \left[\left(\frac{k_0}{k} - \frac{k}{k_0} \right) \cos \vartheta \cos \psi + \left(1 - \frac{k}{k_0} \right) \sin \vartheta \sin \psi \cos \varphi \right],$$

where r_0 stands for the classical electronic radius, ϑ and φ are the polar angles of \mathbf{k} in the coordinate system in which \mathbf{k}_0 is the z axis and the plane of \mathbf{k}_0 and the symmetry axis is the xz plane. The expected effect is then:

$$(5) \quad \varepsilon = 2 \frac{N^{(+)} - N^{(-)}}{N^{(+)} + N^{(-)}},$$

and is obtained by integration of eq. (1). For this it is necessary to take into account the limits imposed by the geometry of the experimental set-up and by the energy discrimination. The latter was chosen so that only rays with momentum between $k_1 = 375$ keV/c and $k_2 = 475$ keV/c were detected. The integration with respect to k_0 must be performed between the limits $k_{0,1}(\vartheta)$ and $k_{0,2}(\vartheta)$, which are related to k_1 and k_2 through the Compton relation. Then, from eqs. (1), (2) and (5), we obtain:

$$(6) \quad \varepsilon = 2f \frac{\int_{\Omega_1}^{\Omega_2(\psi)} \frac{d\Omega_1}{\sin \psi} \int_{k_{0,1}(\vartheta)}^{k_{0,2}(\vartheta)} d\Omega_2 \int I \varrho P \sigma_1 dk_0}{\int_{\Omega_1}^{\Omega_2(\psi)} \frac{d\Omega_1}{\sin \psi} \int_{k_{0,1}(\vartheta)}^{k_{0,2}(\vartheta)} d\Omega_2 \int I \varrho \sigma_0 dk_0}.$$

In the evaluation of eq. (6) the following simplifications have been used.

In performing the integration on k_0 , since the efficiency of the scintillator ϱ in the energy range (375 ÷ 475) keV is nearly constant, one can apply the mean value theorem. Thus the only relevant dependence of ϱ is on ϑ , which can be deduced, even for $\vartheta < 60^\circ$, from the graphs of Fig. 2.

Finally, in the evaluation of the polarization $P(k_0)$ of the bremsstrahlung spectrum the following points have been considered.

The γ -rays of momentum k_0 are produced by electrons of energy between ck_0 and the maximum energy of the β^- decay spectrum. If we denote

(*) According to the optical convention, a photon is called r.e.p. when its angular momentum along the propagation direction is $-\hbar$.

by $p(k_0, E)$ the polarization of the γ -rays of momentum k_0 produced by electrons of energy E and assume a polarization equal to v/c for the electrons, we can write:

$$(7) \quad p(k_0, E) = \frac{v}{c} F\left(E, \frac{ck_0}{E}\right).$$

The function $F(E, ck_0/E)$ has been determined by McVOY^(2,3) for $E = ck_0$ and by FRONSDAL and ÜBERALL⁽⁴⁾ for any value of E . The latter analysis have shown that the following properties of F hold for $E = 2.5$ MeV: *a*) the dependence of F on ck_0/E is practically linear; *b*) the dependence of F on the angle δ of emission of the photon is small, at least for δ smaller than 30° . Assuming, for simplicity, that these properties exist even at our energies we have neglected in eq. (7) the dependence of F on δ .

In order to calculate $P(k_0)$ it would now be necessary to integrate eq. (7) with respect to E taking into account the β spectrum and the bremsstrahlung cross section. It is noticed, however, that $p(k_0, E)$ decreases very little, for a given k_0 , when E increases from ck_0 to the top of the β -ray spectrum. (For example, assuming that property *a*) still holds at our energies, one finds that for $ck_0 = 600$ keV $p(k_0, E)$ decreases by 13% when E increases from 600 to 760 keV).

It follows that an accurate integration on E is not necessary. On the other hand, great accuracy would be insignificant since the actual available calculations on the bremsstrahlung process are performed using the Born approximation.

Finally we write

$$(8) \quad P(k_0) = \alpha(k_0) \frac{v}{c} F(ck_0, 1),$$

where the factor $\alpha(k_0)$ takes into account the integration with regard to E .

As a final result by accurate numerical integrations we obtain:

$$(9) \quad \varepsilon = 2f\bar{\alpha} \cdot 0.218,$$

where $\bar{\alpha}$ is the mean value of $\alpha(k_0)$ coming from the integration appearing in eq. (6). A reasonable evaluation gives $\bar{\alpha} = 0.90$.

We recall that in eq. (6) and consequently also in eq. (9), the finite resolving power of the γ -ray detector (about 15%) has been neglected. This approximation does not appreciably affect our results because the function $I(k_0)$ (Fig. 3) has been determined by means of the same γ -ray detector as in the main experiment. Therefore, this function involves the same resolution as N_1 and N_2 .

Eq. (9) was established by neglecting the depolarization of the β -rays due to the Coulomb scattering within the source, as well as the double Compton scattering of the γ -rays within the magnetized iron.

In our energy range the first effect is negligible. On the contrary the double Compton scatterings affect appreciably the counting rate. But, as pointed out by H. SCHOPPER⁽¹⁰⁾, the final effect on ε is small, because the

dependence of the double scattering on the polarization is very similar to that of the single Compton scattering. Using Schopper's calculation we find that ε_2 (the expected effect taking into account the double scatterings) differs from ε by a factor of 0.95.

From the values of $\tilde{\alpha}$ and f given above we, finally, deduce

$$\varepsilon_2 = + 2.83\%.$$

We should stress the difficulty of evaluating the error affecting this result. One can estimate that it probably does not exceed 5%.

RIASSUNTO

È stata misurata la polarizzazione della bremsstrahlung prodotta contro nuclei di Pb dagli elettroni di energia prossima all'energia massima emessi dal ^{204}Tl (transizione proibita unica). Si è fatto uso della ben nota dipendenza della sezione d'urto per effetto Compton dall'angolo fra la direzione del γ e la direzione di magnetizzazione di un bersaglio di ferro. L'asimmetria osservata coincide, entro gli errori sperimentali (circa il 10%), con quanto ci si attende nel caso che la polarizzazione degli elettroni nel decadimento β sia $-v/c$.

Universal Baryon-Meson Coupling (*).

R. E. BEHREND

Brookhaven National Laboratory - Upton, N.Y.

(ricevuto il 3 Dicembre 1958)

Summary. — A universal baryon-meson coupling which allows for only those particles which are presently known to exist and which depends upon only one bare coupling constant is discussed.

Recently, PAIS ⁽¹⁾ has noted that some of the results predicted by certain baryon-meson interactions with too high a degree of symmetry seem to be in contradiction with experiment. Following this, several authors ⁽²⁻⁴⁾ have suggested baryon-meson interactions which, while retaining a symmetric form, break these unwanted symmetries through certain relative parity assignments. It is the purpose of this note to point out that with certain of these relative parity assignments, it is possible to formulate the baryon-meson coupling such that it does not contradict present experiments and yet depends upon only one bare coupling constant (common to both the K and π) and allows for only those particles which are presently known to exist (except for the Ξ^0 whose existence is assumed).

The present formulation is based on a seven-dimensional charge space, identical with that proposed by TIOMNO ⁽⁵⁾. In order to examine the structure of such a coupling and the effect of certain relative parity assignments, the Lagrangian is initially written with even relative parity assignments for all

(*) Work carried out under the auspices of the U. S. Atomic Energy Commission.

⁽¹⁾ A. PAIS: *Phys. Rev.*, **110**, 1480 (1958).

⁽²⁾ S. BARSHAY: *Phys. Rev. Lett.*, **1**, 97 (1958).

⁽³⁾ F. GÜRSEY: *Phys. Rev. Lett.*, **1**, 98 (1958).

⁽⁴⁾ A. PAIS: *Phys. Rev.*, **112**, 624 (1958).

⁽⁵⁾ J. TIOMNO: *Nuovo Cimento*, **6**, 69 (1957).

the particles.

$$(1) \quad L = \psi^+ \gamma_4 \gamma_\mu \frac{\partial}{\partial x_\mu} \psi + m_0 \psi^+ \gamma_4 \psi + g \psi^+ \gamma_4 \gamma_5 \Gamma_i \psi B_i + B_i (\Box^2 + \mu^2) B_i + \text{h.c.},$$

where $\psi^+ = (N_1^+ N_4^+ N_2^+ N_3^+)$, and

$$N_1 = \begin{pmatrix} p \\ n \end{pmatrix}, \quad N_2 = \begin{pmatrix} \Sigma^+ \\ Y^0 \end{pmatrix}, \quad N_3 = \begin{pmatrix} Z^0 \\ \Sigma^- \end{pmatrix}, \quad N_4 = \begin{pmatrix} \Xi^0 \\ \Xi^- \end{pmatrix},$$

$$Y^0 = (\Lambda^0 - \Sigma^0)/\sqrt{2}, \quad Z^0 = (\Lambda^0 + \Sigma^0)/\sqrt{2},$$

where the symbol for a particle denotes the operator which destroys it. The γ'_μ (Greek indices run from 1 to 4) are Hermitian Dirac matrices for the usual space-time of four dimensions, while the Γ_i (Latin indices run from 1 to 7) are the set of Hermitian 8×8 anticommuting matrices in a Euclidean space of seven dimensions (charge space). The representation of the Γ_i associated with the spinors of (1) are

$$\Gamma_{1,2,3} = 1^2 \times \sigma_{1,2,3} \times \sigma_1, \quad \Gamma_4 = 1^2 \times 1^2 \times \sigma_2, \quad \Gamma_{5,6,7} = \sigma_{1,2,3} \times 1^2 \times \sigma_3,$$

where the σ 's are the usual three Pauli 2×2 spin matrices. B_i is the Hermitian seven-component vector field operator for the meson (μ is the bare meson mass):

$$B = (K_1, K_2, K_3, K_4, \pi_1, \pi_2, \pi_3),$$

where

$$K_1 = (\bar{K}^+ + K^+)/\sqrt{2}, \quad K_2 = (\bar{K}^+ - K^+)/\sqrt{2}i, \quad K_3 = (\bar{K}^0 + K^0)/\sqrt{2},$$

$$K_4 = (\bar{K}^0 - K^0)/\sqrt{2}i, \quad \pi_1 = (\pi^- + \pi^+)/\sqrt{2}, \quad \pi_2 = (\pi^- - \pi^+)/\sqrt{2}i, \quad \pi_3 = \pi^0.$$

g is the bare baryon-meson coupling constant.

Although such a theory, based on a seven dimensional charge space, is unusual, it does possess just the proper number of components to fit the known particles. (There is no room in the present formulation for any new particles such as an isotopic scalar neutral pion.)

If the interaction part of the Lagrangian is written out explicitly, it assumes the form proposed by GELL-MANN⁽⁶⁾ when the magnitudes of all the g 's (K and π) are taken equal⁽⁷⁾. Furthermore, it can easily be seen that the

⁽⁶⁾ M. GELL-MANN: *Phys. Rev.*, **106**, 1296 (1957).

⁽⁷⁾ It might be interesting to note that for this Lagrangian, generalized so that the coupling is only assumed to be non-derivative, *i.e.* where γ_5 is replaced by $a + b\gamma_5$, it is possible to show that CP invariance implies C and P invariance separately. See G. FEINBERG (*Phys. Rev.*, **108**, 878 (1957)) for such a proof in the case of the pion-nucleon coupling.

invariance under rotations in this 7-dimensional space which mix, say, protons and neutrons, or Ξ^0 and Ξ^- , guarantees electric charge independence while the invariance under rotations which mix, say, nucleons and cascade particles, or Σ and Λ particles, guarantees hypercharge independence (*i.e.* the forces between baryon having different hypercharge ($=N+S$) are the same as the forces between baryons having the same hypercharge). It is, of course, the latter symmetry which disagrees with experiment. For example, here all the baryon as well as the meson masses are degenerate.

It is now interesting to note that if the nucleon-cascade and Σ - Λ parities are taken to be opposite ^(2,3), then in the corresponding Lagrangian the symmetry of hypercharge independence is completely broken while that of electric charge independence remains valid. If, in addition, the Σ -K parity relative to the nucleon is taken to be even, as suggested by BARSHAY ⁽²⁾, the new Lagrangian may be written as in (1) with the interaction term $g\psi^+\gamma_4\gamma_5\Gamma_i\psi B_i$ replaced by

$$g\chi^+\gamma_4\gamma_5\Gamma_i\chi B_i$$

where

$$\chi = \begin{pmatrix} ip \\ in \\ \gamma_5\Xi^0 \\ \gamma_5\Xi^- \\ \gamma_5\Sigma^+ \\ (i\Lambda^0 - \gamma_5\Sigma^0)/\sqrt{2} \\ (i\Lambda^0 + \gamma_5\Sigma^0)/\sqrt{2} \\ \gamma_5\Sigma^- \end{pmatrix}$$

The relative signs of the g 's are then ⁽⁸⁾

$$g \equiv g_{N\pi} = g_{\Sigma\pi} = -g_{\Lambda\pi} = -g_{\Xi\pi} = g_{N\Sigma K} = g_{N\Lambda K} = g_{\Xi\Sigma K} = g_{\Xi\Lambda K}.$$

Although there is no adequate theoretical method of calculating with strong interactions, the following qualitative remarks might be made about such a Lagrangian. With the vanishing of the bare baryon mass, m_0 , the relative parity assignments made above may be transformed away, this again making the Lagrangian hypercharge independent. As long as the bare baryon mass

⁽⁸⁾ There still is an ambiguity in the relative sign of the K and π coupling, but this has no physical significance and is but a matter of convention.

is not zero, however, hypercharge independence will not hold and, as a result, the baryon masses as well as the meson masses will be split. That these mass splittings will be correct is not known, although KATSUMORI⁽⁹⁾ has shown that perturbation theory, with the above assignments of relative parity, qualitatively predicts the mass spectrum. Similarly, it is impossible to realistically calculate the effective K and π couplings from the bare coupling g . (In the limit of hypercharge independence, the effective g 's are all equal.) However, it may be stated that, at present, this Lagrangian does not contradict any known experiments.

* * *

The author wishes to thank Dr. F. GÜRSEY for several helpful discussions.

(⁹) H. KATSUMORI: *Progr. Theor. Phys.*, **19**, 342 (1958).

RIASSUNTO (*)

Si discute un accoppiamento barione-mesone universale che consente solo l'esistenza delle particelle attualmente note e che dipende da una sola costante d'accoppiamento nuda.

(*) Traduzione a cura della Redazione.

The Production of Cascade Particles by 5.5 GeV/c Pions (*).

W. B. FOWLER, W. M. POWELL and J. I. SHONLE

Lawrence Radiation Laboratory, University of California - Berkeley, Cal.

(ricevuto il 29 Dicembre 1958)

Summary. — The first observed production of negative cascade particles at an accelerator is reported. A 30 in. propane bubble chamber was exposed to a beam of negative pions of 5.5 GeV/c. Two cascades were identified, indicating a production cross section of $2.3^{+3.1}_{-1.6}$ μb . The Q values found were (49.5 ± 7.9) MeV and (53.6 ± 11.3) MeV. The lifetimes were $(1.9 \pm 0.1) \cdot 10^{-10}$ s and $(5.2 \pm 0.4) \cdot 10^{-10}$ s. Both Ξ 's were produced backwards in the center-of-momentum system. The identification process and background is discussed.

1. — Introduction.

The cascade particle was first observed in a cloud chamber by the Manchester group.⁽¹⁾ However, at that time there was considerable uncertainty as to the nature of this new particle, since they were unable to identify the V^0 . ANDERSON *et al.*⁽²⁾ established that the V^0 was a Λ . Later ARMENTEROS *et al.*⁽³⁾ were able definitely to identify the negative secondary as a pion. Most of the subsequent data have also come from cloud chamber observations of cosmic-ray events. There have been some data reported from emulsion stacks exposed to cosmic rays, but the evidence is less conclusive, since the Λ can not usually be found. Because so few cascades have been observed, very little is known about the particle other than the existence of the one decay mode,

(*) This work was done under the auspices of the U. S. Atomic Energy Commission.

(1) R. ARMENTEROS, K. H. BARKER, C. C. BUTLER, A. CACHON and C. M. YORK: *Phil. Mag.*, **43**, 597 (1952).

(2) C. D. ANDERSON, E. W. COWAN, R. B. LEIGHTON and V. A. J. VAN LINT: *Phys. Rev.*, **92**, 1089 (1953).

(3) R. ARMENTEROS, B. GREGORY, A. LAGARRIGUE, L. LEPRINCE-RINGUET, F. MULLER and C. PEYROU: *Suppl. Nuovo Cimento*, **12**, 327 (1954).

which has been well established. A good summary of our knowledge of cascades is reported in a general strange-particle review article by FRANZINETTI and MORPURGO ⁽⁴⁾.

The production of cascade particles by 5.5 GeV/c pions in propane is reported here as the first observation of cascade production by an accelerator.

2. - Experimental arrangement.

A 30 inch propane bubble chamber operated in a 13 kilogauss magnetic field ⁽⁵⁾ was exposed to a 5.5 GeV/c beam of negative pions from a beryllium target located 14° upstream from the west straight section of the Bevatron. Negative pions at 0° from the beam were deflected by the Bevatron field through a thin window in the vacuum tank. Two 8 inch quadrupole magnets were used for focusing, adjusted to give an image at the chamber of the target

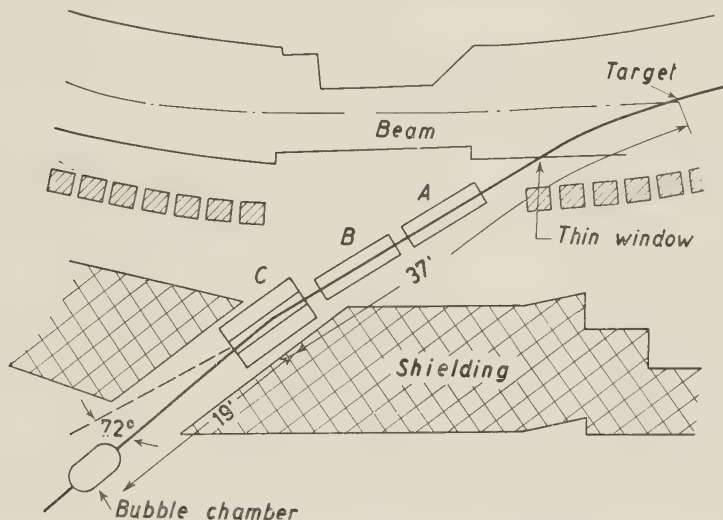


Fig. 1. - Experimental arrangement for directing π^- beam (from Be target in Bevatron) into propane bubble chamber. A and B are 8 in. quadrupole magnets. C is a 5 foot deflecting magnet. The magnet surrounding the bubble chamber is not shown.

1 in. high and 2.8 in. wide. An analyzing magnet deflected the beam 7.2° , so that 5.5 GeV/c pions arrived at the center of the chamber. The dispersion was 80 MeV/c per inch, and the uncertainty at any point due to the target size was ± 125 MeV/c. The total distance from the target to the center of the chamber was 56 feet. Fig. 1 shows the experimental arrangement.

⁽⁴⁾ C. FRANZINETTI and G. MORPURGO: *Suppl. Nuovo Cimento*, **6**, 565 (1957).

⁽⁵⁾ W. M. POWELL, W. B. FOWLER and L. O. OSWALD: *Rev. Sci. Instr.*, **29**, 874 (1958).

All together, 31,500 stereo-pairs of pictures were taken on 70 mm film. The film was scanned for all V^0 's with origins visible in the chamber. The scan cards were examined for possible cascade decays, and these events were then examined by a physicist. Those events in which the V^0 could have possibly come from a kink in a secondary track and which lay on the opposite side of the secondary track from the deflected track were measured. The possible cascade decays were not restricted to negative particles. Fifteen events satisfied the visual-appearance criterion, two of them positive.

Two methods of measuring were used, and most events were measured by both. One method was to reproject through an optical system similar to that used on the chamber but with air replacing the propane. A correction for the index of refraction of propane was made. The tracks in the two views were recombined on a ground-glass screen, and angles and curvatures were measured. The curvatures were measured by fitting templates to the tracks in space. The other method of measuring was by the use of a digitized microscope measuring directly on the two negatives. The locations of a series of points along a track in each view were punched directly onto IBM cards. These cards were then processed by an IBM 650 calculator which gave an output of momenta and angles, with errors based on the internal consistency. Allowance was made for the errors in curvature caused by multiple scattering in the propane. The agreement between the two methods of measuring was compatible with the errors given in each case.

3. - Identification.

Of the fifteen events submitted for measurement, only two were found to be consistent with the known properties of a cascade. They are shown in Figs. 2 and 3. The other events are discussed in a later section. For an event to be considered a cascade the following criteria had to be satisfied.

- a) The V^0 had to be identified as a Λ .
- b) The plane of the Λ had to contain the cascade decay point.
- c) The plane of the cascade and its decay pion had to contain the decay point of the Λ .
- d) Transverse momentum of the Λ had to balance about its line of flight.
- e) Transverse momenta of the pion and the Λ at the cascade decay point had to balance.
- f) The relative ionization had to be consistent with the assumption of a cascade decay.
- g) The kinematics had to be compatible with the assumption of

$$\Xi^- \rightarrow \Lambda^0 + \pi^- + \sim 66 \text{ MeV}.$$

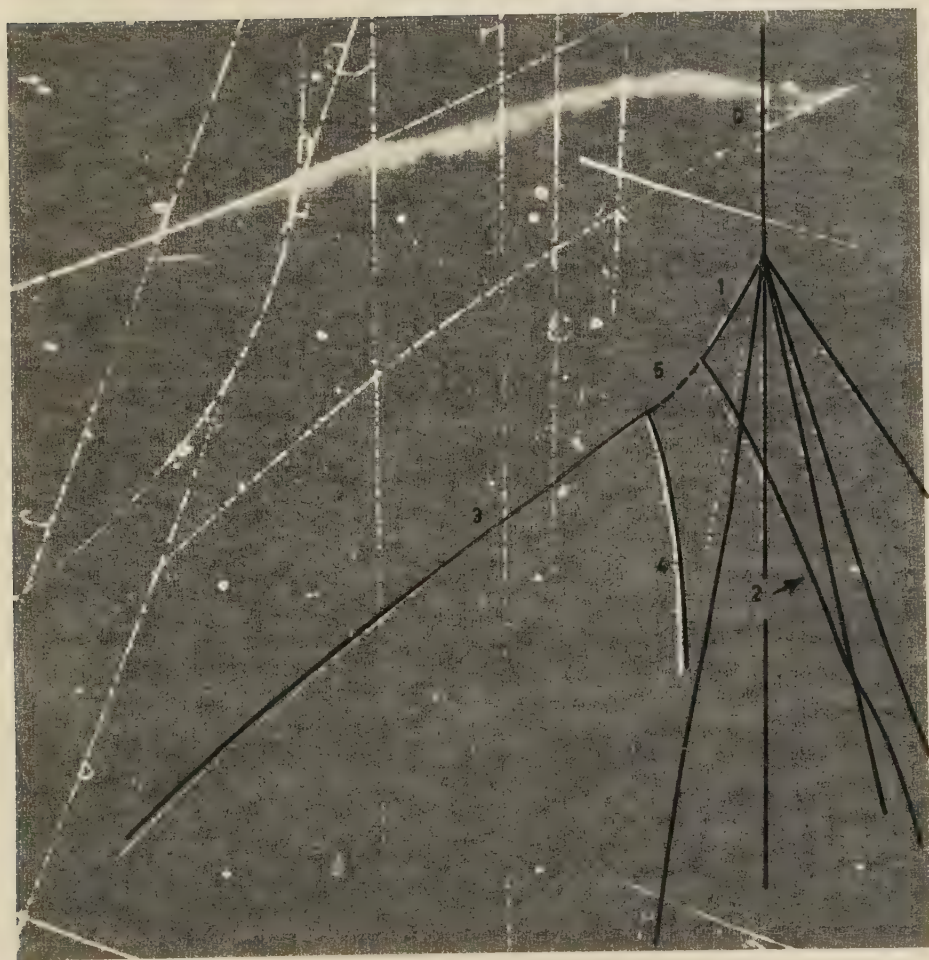


Fig. 2. — Event 17776. Track 0 is the beam π^- . Track 1 is the Ξ^- and 2 is the decay π^- . Track 3 is the proton from the Λ decay which stops in the chamber. Track 4 is the π^- from the Λ decay and leaves the chamber at the top glass. Line 5 is the Λ line of flight.

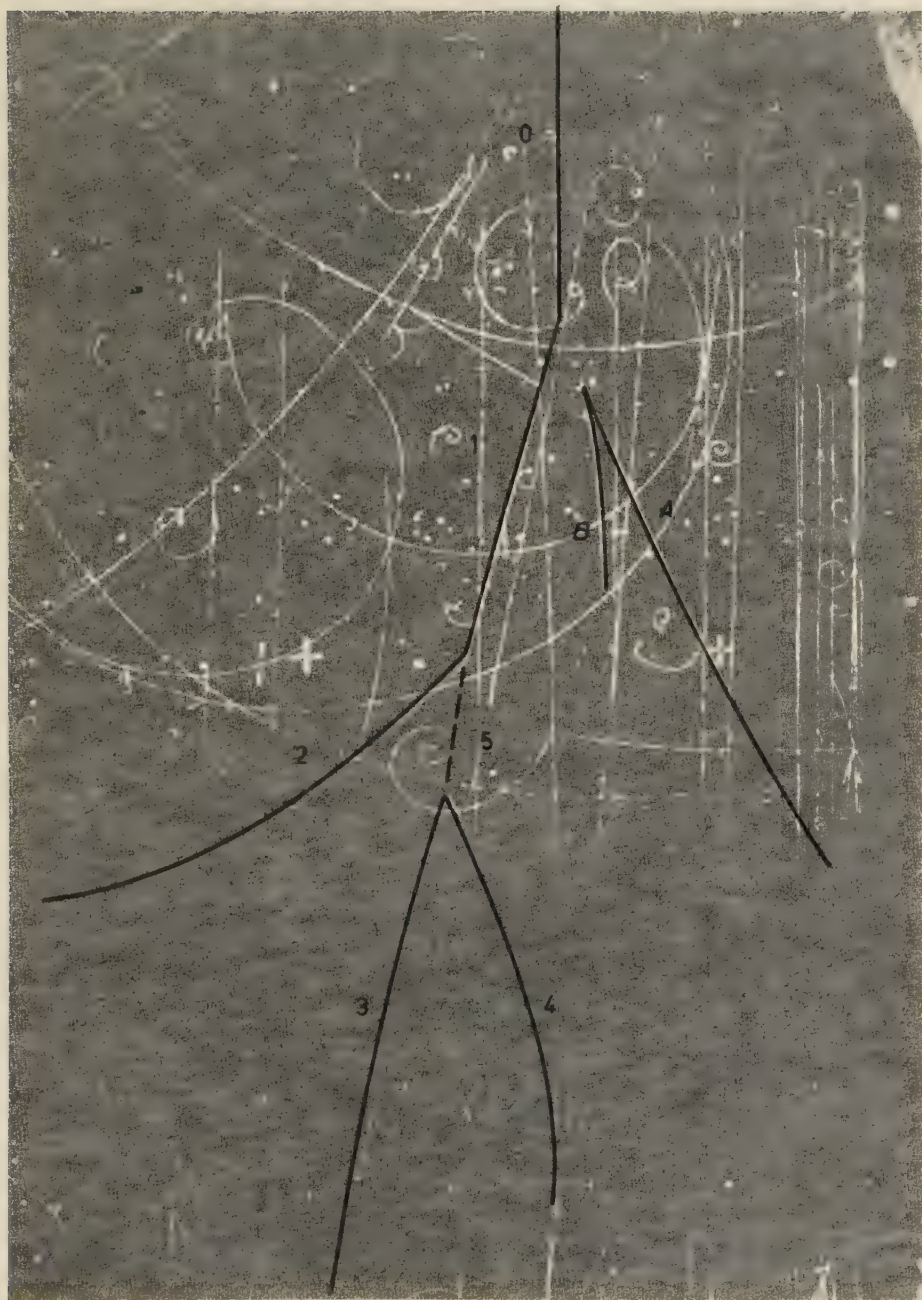


Fig. 3. Event 49837. Track 0 is the beam π^- . Track 1 is the Ξ^- and 2 is the decay π^- . Track 3 is the proton from the Λ decay, and 4 is its π^- which leaves at the bottom glass. Line 5 is the Λ line of flight. Tracks 6 and 7 are the π^- and π^- from a Ξ^0 decay.

Criterion *a*) rules out the identification of possible $\Xi^- \rightarrow n + \pi^-$ modes. Criteria *c*), *e*), and *g*) would eliminate possible leptonic decay modes of cascades.

In general it is not always possible to distinguish a Λ from a θ^0 . No event was rejected solely because the V^0 could not be positively identified as a Λ . However, in both the identified cascades, the V^0 was definitely established as a Λ . In one case (17776) the Λ was identified readily because the positive prong was a stopping proton, and the measured Q -value was 35 ± 6 MeV. In the other case (49837) the measured Q on the assumption of a Λ was (31 ± 7) MeV and on the assumption of a θ^0 was (180 ± 21) MeV, so that the fit to a Λ on Q -value alone was better than to a θ^0 . Ionization estimates from gap counting were decisive for the positive prong's being a proton rather than a positive pion.

Both events satisfied the two coplanarity requirements within the errors. Coplanarity was checked visually on the space reprojector by actually fitting the planes in question, and by spatial reconstruction from the microscope measurements. Both events satisfied transverse momentum balance to within 1.3 standard deviations or less from the unadjusted values. Table I shows the amount of unbalance and the errors. Later an adjustment was made to give exact transverse momentum balance.

In both events the ionization of the tracks was consistent with the particle identities of a cascade decay. Ionization was estimated from comparison with tracks of known ionization in each picture. The positive tracks of the Λ 's could be identified as heavier than pions, and the cascade track in 49837 was definitely heavier than a K^- .

Finally, the Q values calculated for the two events agreed satisfactorily with the present value of (66 ± 3) MeV ⁽⁶⁾.

The only reasonable possible alternative interpretation of both events is $\Sigma^- + n \rightarrow \pi^- + \Lambda + n$, where the outgoing neutron and carbon recoil must have their resultant momentum in essentially the forward direction. Because of the Fermi momentum of the neutron before the reaction and the two unknown outgoing momenta of the neutron and carbon recoil, the problem does not lend itself readily to calculation. If the assumption of an essentially free neutron is made, then a Σ^- of 815 MeV/c would satisfy the visible kinematics for 17776. This interpretation cannot be excluded on the grounds of measured momentum, since the track in question was too short to measure, or on the grounds of ionization, since saturation was reached in this picture at a relative ionization of about two. In 49837, an incoming Σ^- of 1180 MeV/c could satisfy the visible kinematics. This situation is close enough to the observed momentum and ionization that it may not be excluded. However, it is im-

⁽⁶⁾ G. H. TRILLING and G. NEUGEBAUER: *Phys. Rev.*, **104**, 1688 (1956).

TABLE I.

The measured momenta and angles and the constrained values for the various tracks of the two events are given. The track numbers are the same as in Figs. 2 and 3. φ_{ij} refers to the angle between track i and track j . The adjustment parameter τ is the adjustment in a variable divided by the measurement error for that variable. The value listed in brackets under measured momentum for track 5 is the value calculated from the constrained Λ variables. The transverse momentum unbalance at the four decay points is given. The sum of the squares of the adjustment parameter, $\sum (\tau_i)^2$, which indicates the reliability of the adjustment, is given.

Event	Track no.	Measured momentum (GeV/c)	Constrained momentum (GeV/c)	τ	Angle no.	Measured value (e)	Constrained value (e)	τ
17 776	1	—	0.494	—	φ_{34}	83.8 ± 0.8	83.6	-0.25
	2	$0.133 \pm .014$	0.139	0.44	φ_{45}	70.0 ± 2.4	70.5	0.21
	3	$0.407 \pm .012$	0.417	0.84	φ_{25}	74.4 ± 1.5	73.8	-0.41
	4	$0.096 \pm .010$	0.100	0.45	φ_{12}	54.3 ± 3.4	58.1	1.13
	5	($0.440 \pm .012$)	0.437	-0.19	—	—	—	—
49 837	1	$1.181 \pm .100$	1.042	—	φ_{34}	46.5 ± 0.5	46.4	-0.24
	2	$0.215 \pm .021$	0.234	0.91	φ_{35}	39.0 ± 0.7	39.6	0.79
	3	$0.132 \pm .013$	0.155	1.80	φ_{25}	37.4 ± 0.6	37.5	0.18
	4	$0.829 \pm .084$	0.834	0.06	φ_{15}	9.1 ± 0.8	7.9	-1.41
	5	($0.948 \pm .084$)	0.847	-1.21	—	—	—	—
			Transverse momentum unbalance (GeV/c)		$\sum (\tau_i)^2$ for the adjustment			
17 776	Λ decay point		$-0.007 \pm .021$		1.97			
	Ξ decay point		$+0.043 \pm .033$		1.58			
49 837	Λ decay point		$-0.025 \pm .030$		3.92			
	Ξ decay point		$+0.048 \pm .038$		4.40			

probable that two events would occur with their charged prongs satisfying all the identification criteria for cascades. Thus it is concluded that the events in question are cascade decays.

4. — Results.

The following constraints were applied to reduce the errors due to the measurement uncertainties in calculating the Q values of the cascade decays. The momenta and angles of the Λ -decay products were adjusted to give a Q for the Λ of exactly 37.4 MeV and to satisfy transverse momentum balance and coplanarity with respect to the cascade decay point. These adjustments were made with the requirement that the sum of the squares of the adjustment in a variable divided by the measurement error for that variable be a minimum. The Λ momentum was calculated from the adjusted values. At the cascade decay point the adjustment required transverse momentum balance and coplanarity for the Λ and π^- with respect to the cascade-particle line of flight. The amounts of the adjustments are shown in Table I. The Q values of the cascades were then calculated from these adjusted values. Derivatives of the Q value with respect to its parameters were taken. These derivatives were then multiplied by the uncertainties in the variables, and a square root of the sum of the squares was taken to give the error in the Q value.

The Q values thus obtained were (49.5 ± 7.5) MeV for event 17776, and (53.6 ± 11.3) MeV for 49837. The errors are approximately one standard deviation. The times for each particle's life in its own rest system were $(1.9 \pm 0.1) \cdot 10^{-10}$ s for 17776 and $(5.2 \pm 0.4) \cdot 10^{-10}$ s for 49837.

A production cross-section for cascades was found in the following manner. The number of beam-pion tracks entering the scanning region in every hundredth picture was recorded, as well as the number of usable pictures. A picture was considered unusable if there were too many tracks in it for efficient scanning. In some pictures parts of the chamber were not visible, owing either to partial failure of the lights or to a residual bubble. In these cases a suitable correction was made. Not all the tracks entering the scanning region traverse its entire length, since parts of some tracks are removed by interactions. A 10% correction for this effect was made, based on a mean free path of (206 ± 30) cm for all beam-pion interactions in propane. A 6% correction was made for the muon contamination due to decays in flight of the pions. From these figures the path length traversed by the pions was determined.

The scanning efficiency for cascades was estimated as follows. Scanners were instructed to search for V^0 particles and to indicate whether the V^0 particle appeared to be produced in the wall of the chamber or in the propane.

The combined efficiency for finding V^0 particles from visible beam interactions, as determined from two or more successive scans by different scanners, was $(85 \pm 5)\%$. It was felt that the efficiency for associating a V^0 with a kink in a secondary track would be less than for associating it with a beam interaction. A check of one-eighth of the pictures scanned revealed no cases in which a V^0 should have been associated with a kinked secondary track and was not. This check indicated that the scanning efficiency for cascades was not much lower than for V^0 's. A lower limit of 50% was chosen to be conservative. Accordingly, the efficiency for finding cascades was estimated to be $70^{+10}_{-20}\%$.

Since cascades in which the Λ -particles decay via the neutral mode would not be detected by the procedure used, a correction based on the branching ratio for Λ -decay was made.

From these figures the mean free path for the production of a cascade in propane was found to be $3.2 \cdot 10^6$ cm.

An $A^{\frac{2}{3}}$ law was assumed for the shielding of the nucleons in carbon, and a cross-section per nucleon of $2.3^{+3.1}_{-1.6}$ microbarns was obtained. Almost all the error is due to the poor statistics of the small number of events, and represents a confidence coefficient of 0.84.

Since indications are that the lifetime of the Ξ^- is on the order of 1 to $10 \cdot 10^{-10}$ s, a lifetime correction to the cross-section is probably not large for a chamber of this size. A lifetime much different from this would require a considerable correction. No correction was made for possible alternative decay modes. A decay mode with a strangeness change of two, namely $\Xi^- \rightarrow \pi^- + n$ would not have been found by the scanning method used. Any leptonic decay modes would have been rejected by the identification criteria used. This last correction might be on the order of a factor of two, since the leptonic decay rate based on a universal Fermi interaction has been calculated to be possibly of the same order as that for pionic decays. (7).

Both production events were known to have occurred in carbon, since the net outgoing charge was different from zero in both cases. In one event (17776), there were six outgoing charged prongs, two positive and four negative. Only one particle was identifiable by ionization, and that was a negative pion. There were no visible neutral or charged decays associated with the event. Event 49837 had only one outgoing charged prong, that of the cascade itself. There was a 6^0_1 decay associated with the production origin. An analysis for the missing momentum and energy indicated that the kinematics were consistent with there being another particle of a K mass. Thus the observations reported here do not contradict the assignment of $S = -2$ for the cascade. Both particles were produced strongly backwards in the center-of-

(7) G. MORPURGO: *Suppl. Nuovo Cimento*, **6**, 565 (1957).

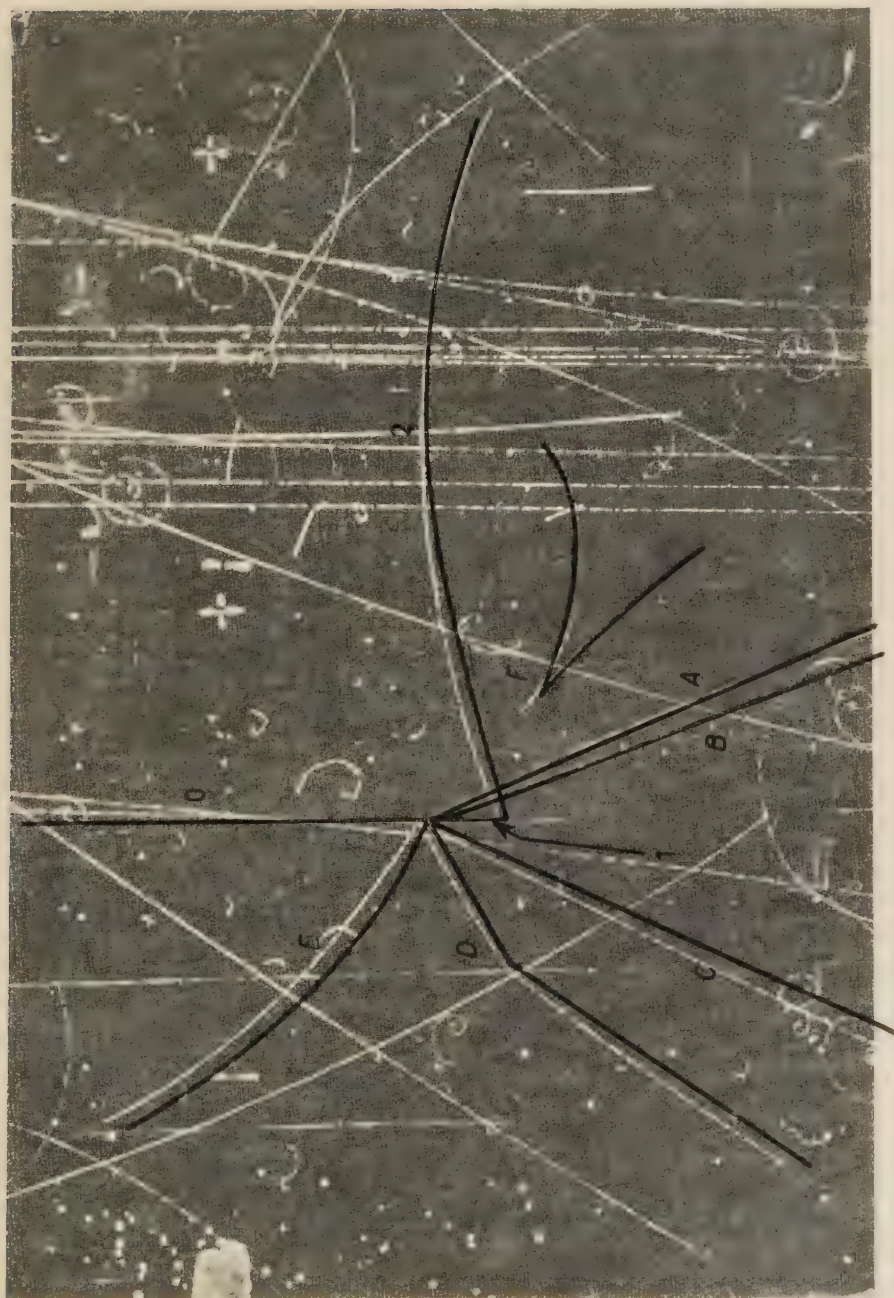


Fig. 4. Event 46709, a possible Ξ decay without a visible Λ decay. Track 0 is the beam π . Track 1 is the possible Ξ . Track 2 is a stopping π from track 1. Track 1 is probably a π by ionization. Tracks B and C are positive and could be protons, π^+ 's, or K^+ 's. Track D is a π^- which scatters and which was identified by ionization. Track E is a π^- which leaves the chamber. F is an electron pair associated with the production origin.

momentum system. One (17776) was at a c.m. angle of about 170 degrees, and the other was at an angle of about 160 degrees.

In addition to the above two events, there was another (46709) that may be interpreted as a cascade, although a K^- or Σ^- decay cannot be ruled out. It is shown in Fig. 4. The production event had six charged prongs with zero net charge. The decay event showed a heavily ionizing negative particle emitting a π^- which then came to rest, allowing an accurate momentum determination to be made. The momentum found was (131 ± 4) MeV/c, and the decay angle $99^\circ \pm 2^\circ$ in the laboratory system. If it is assumed that the decaying particle came to rest or nearly to rest, then these figures are compatible only with a cascade decay. The track was too short for measurement of its momentum, and was at an angle of 43° from the horizontal, so that ionization is difficult to estimate. If the momentum at the decay point is considered a variable, then the decay kinematics are also consistent with both a $K_{\pi^2}^-$ and a Σ^- . A $K_{\mu^2}^-$ decay can be ruled out because the ionization of a $K_{\mu^2}^-$ would not have been consistent with that observed. The other five tracks from the production event were long enough for good momentum measurement, so that a kinematical analysis of the production event was feasible. The kinked positive track was identified by ionization as a π^+ . There were no visible associated decays. Visible transverse momentum was out of balance by about 750 MeV/c, implying at least one neutral particle. Under the assumption that the production event was in hydrogen, energy and momentum conservation could be satisfied only by stretching the measured values somewhat beyond the experimental errors, and then only for the assumption of a $K_{\pi^2}^-$ decay. If the production event is assumed to be in carbon, then the kinematics become far less definitive because of the unknown carbon recoil, and they are consistent with all three of the possible identities of the decaying particle. The $K_{\pi^2}^-$ assumption is unlikely on grounds of lifetime, since the particle would have traveled only 0.015 of a mean life. It is not believed that this event is definitely determined to be a cascade, but it is interesting to speculate that with two cascades found with charged Λ decays, one with a neutral Λ decay should be present. The evidence for the interpretation of this decay as a cascade is of such a nature that it has not been included in any of the statistics.

5. - Background.

Most of the background events could be rejected for failure to comply with two or three of the requirements demanded for cascade identification.

Table II lists the background events and indicates which of the identification criteria were not satisfied. The identity of the V is given whenever

possible. The proper classification of these background events is difficult. In both the positive cases the events are probably K^+ charge exchange: $K^+ + n \rightarrow p + \theta^0$. In two of the events the V^0 particles could be identified as Λ 's,

TABLE II.

Listing of the background events. The sign of the supposed cascade and the identification criteria not satisfied are indicated. The identity of the V^0 is given in those cases in which identification could be made.

Event number	Sign of particle	V^0 not a Λ	Not coplanar	Transverse momentum unbalance	Ionization not consistent	Kinematics not satisfied	V^0 identity
07 529	+	×	×	×	θ^0
27 777	—	×	×	θ^0
28 242	—	...	×	×	...	(^a)	Λ
28 774	—	×	?
30 343	—	×	×	×	×	(^a)	θ^0
33 270	—	×	×	?
39 057	—	×	...	×	...	(^a)	?
39 915	—	×	×	θ^0
42 072	—	×	...	×	?
45 502	—	×	...	(^a)	?
45 781	+	×	×	(^a)	θ^0
46 155	—	×	...	(^a)	Λ
49 697	—	×	...	×	?

(^a) No kinematical calculation was made since it was already apparent that the event was not a Ξ .

and in five of them as θ_1^0 's. In the other six cases no definite identification was possible. In one event the incoming track appeared to be a Σ^- , by ionization. Most of the events probably represent strange-particle interactions of various sorts («strangeness exchange»), although the two with identified Λ 's might possibly be leptonic decays of cascades. Some of the events could be interactions of secondary pions producing strange particles.

* * *

The authors wish to acknowledge the assistance of Dr. E. LOFGREN and the Bevatron staff and thank them for their cooperation during the run. The assistance of all the members of the Cloud Chamber group has been indispensable. Special mention should be made of Dr. R. BIRGE for setting up the beam, H. WHITE for the IBM programming and data reduction, and D. HOTZ for the cross-section normalization and scanning evaluation.

RIASSUNTO (*)

Si riferisce la prima osservazione di particelle negative in cascata prodotte da un acceleratore. Una camera a bolle a propano da 30 pollici è stata esposta ad un fascio di pioni negativi di 5.5 GeV/c. Si sono identificate due cascate indicanti una sezione d'urto di produzione di $2.3^{+3.1}_{-1.6} \mu\text{b}$. I valori di Q trovati sono $(49.5 \pm 7.9) \text{ MeV}$ e $(53.6 \pm 11.3) \text{ MeV}$. Le vite medie $(1.9 \pm 0.1) \cdot 10^{-10} \text{ s}$ e $(5.2 \pm 0.4) \cdot 10^{-10} \text{ s}$. I due Ξ furono prodotti all'indietro nel sistema del centro d'impulso. Si discutono il procedimento di identificazione e il fondo.

(*) Traduzione a cura della Redazione.

LETTERE ALLA REDAZIONE

(La responsabilità scientifica degli scritti inseriti in questa rubrica è completamente lasciata dalla Direzione del periodico ai singoli autori)

Interaction of 4.5 GeV Pions with Emulsion Nuclei.

A. HUSAIN

Physics Department, Rajshahi University - Rajshahi

M. H. SIDDIQUE

Physics Department, Dacca University - Dacca

(ricevuto il 9 Settembre 1958)

For the study of nuclear disintegration produced by very high energy cosmic rays in photographic emulsions it is important to know the energy of the primary particle responsible for the disintegration. But it is found sometimes that the track of the incident primary particle is very steep and, therefore, the available length is too short to make any useful measurements on it. It is thus not possible to get any information about its energy by direct measurements. In the circumstances one has to find an indirect method for the purpose. From a count of the shower tracks produced by a particle one is able to make an approximate estimation of its energy provided there is available a calibration curve obtained by plotting number of shower tracks against energy of the primary particle. Unfortunately there is no such curve available at the moment. The main object of the present work was to provide such a curve.

Just at the time when we were contemplating to undertake the present work there came a report from the University of Chicago, U.S.A. on similar works using 3 GeV negative pions and

5.7 GeV protons. We had at that time 4.5 GeV π^- -meson plates with us and we, therefore, thought it worthwhile to make similar measurements in the hope of getting a calibration curve.

Ionization Measurements.

In the present work ionization was measured by the method of «blob» counts. The track under investigation was at first made parallel to the X or Y motion of the microscope stage with the help of the turntable and then blob counts were made along the whole length of the track available. Since the variations of blob density of tracks with depth of emulsions were observed, depth calibration curves for both the plates used were drawn by using the 4.5 GeV π^- -meson tracks. Then corrections were applied to the tracks under study for the appropriate depths of the emulsion and their blob-densities per unit length *viz.* 90 μm were found. The plateau value for the plate used was found to be 19 blobs per 90 μm . It is estimated that any error due to this

correction is not more than one per cent. Blob counts on all tracks, except the very clogged ones, originating from the stars were then normalized to the plateau (minimum) value.

Depending on the grain-density the tracks were divided into three categories:

a) Shower tracks: These are tracks of singly charged particles with a specific ionization less than or equal to 1.4 times the maximum value.

b) Grey tracks: These are tracks of particles with a specific ionization greater than 1.4 times the minimum value but less than 4 times that value.

c) Black tracks: All other tracks are known as black tracks.

For our present work we are concerned with the first kind only.

For the tracks of 50 stars analysed the total number of prongs was 640 giving an average prong number of 12.8 per star. Of the 640 tracks only 77 were shower tracks giving on the average 1.54 shower tracks per star.

SCHEIN *et al.* ⁽¹⁾ obtained 4.5 prongs and 0.9 shower tracks per star for 3 GeV π^- -mesons and 10.7 prongs and 2.1 shower tracks per star for 5.7 GeV protons.

Thus it would appear that the av-

erage total number of prongs as well as shower tracks per star increases with increasing energy of the incident particle. This relationship is linear as can be seen from Fig. 1 where the average

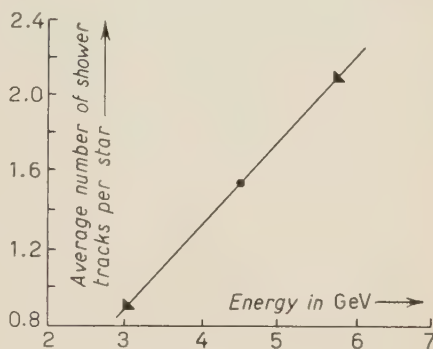


Fig. 1.

number of shower tracks per star has been plotted against the incident energy in GeV. It is hoped that this curve will serve as a calibration curve in the region from 1 GeV to about 10 GeV and will, therefore, be useful in cosmic ray research. It would be interesting to extend the work using higher energy and to test whether the linearity of the curve remains valid beyond 10 GeV as is expected.

It is thought that 80% of the shower particles are generally mesons and hence it may be said that meson production increases with increasing energy of the incident particle.

⁽¹⁾ M. SCHEIN, D.M. HASKIN and R. G. GLASSER: Private Communication (University of Chicago, U.S.A.)

Hydrodynamical Model and Inelasticity in Multiple Production of Particles.

C. ISO

Research Institute for Fundamental Physics, Kyoto University - Kyoto

M. NAMIKI

Department of Applied Physics, Waseda University - Tokyo

(ricevuto il 15 Settembre 1958)

The authors ⁽¹⁾ presented a possible hydrodynamical description of expanding meson-nucleon clouds in the framework of quantum field theory, in which it is shown that such a description is useful if the relaxation time of clouds is very short compared with its diffusion time. Along this line of thought, one could justify the hydrodynamical model of clouds in the period of expansion. But Fermi-Landau's assumption of equilibrium for clouds in the earlier period is involved in other unknown matters.

Following Landau's idea of the hydrodynamical model, secondary interactions at relatively low energies play essential roles to determine the several important quantities; *id. e.* the ratio of the number of K-mesons to that of pions, the transverse momentum and also the energy spectrum. For, secondary interactions determine the space time distribution of the system, mainly depending on the temperature irrespective of the initial details. The multiplicity depends only on the tem-

perature of the initial state but has little relation to interactions at extremely high energies in the initial period of collision. (LANDAU does not consider the dependence on the mechanism of collision to be represented through the impact parameter.) On the other hand one might expect an essential influence of the details of such interactions in the initial period of collision on the important parameter «inelasticity». There we are interested in a problem whether the inelasticity, that is the energy fraction of produced mesons, is mainly determined by the mechanism of collision or by the secondary interactions. Now Landau's model don't permit us to calculate the inelasticity because it handles a one-constituent fluid from the outset. In the present note, it is shown that one may calculate the inelasticity and obtain its values consistent with the experimental ones, under the assumption that the clouds can be represented by the model of a mixed fluid with two constituents, the meson- and nucleon-fluids, and that the front part of the fluid is mainly occupied by the nucleon con-

⁽¹⁾ M. NAMIKI and C. ISO: *Progr. Theor. Phys.*, **18**, 591 (1957); *Nuovo Cimento*, **6**, 245 (1957).

stituent at the end of the expansion. (Here we make use of Fermi-Landau's initial conditions, that is to say, we consider that at the start of the expansion nucleons and pions are in thermal equilibrium with a high temperature irrespective of initial details. We shall not discuss the relations between inelasticity and impact parameter.) The latter assumption will be discussed at the end of this note. From this point of view we intend to infer the possibility that the effect of the mechanism of collision on the inelasticity would be masked by the secondary interactions in the experimental data. It is, however, to be noted that such an effect must be discussed together with the initial conditions given by Fermi and Landau. We shall not enter in it.

In the previous work ⁽²⁾ we calculated the energy fraction a (%) of the front part of the fluid, where a particle occupying the front is considered to be almost a pion. According to the above

in the rest system of the fluid, where ε_{NN} and ε_{π} are energy densities of the nucleon fluid and the meson fluid, and n_{NN} and n_{π} number densities of nucleons and mesons, respectively. Φ , Φ^* , F and F^* are slowly varying functions, defined by BELEN'KIJ and LANDAU ⁽³⁾, of the variable $Z_N = M/T$ or $Z_{\pi} = m/T$, M and m being the masses of nucleon and pion, respectively.

At the final temperature $T \simeq m$ we get

$$E_N \simeq 8m, \quad E_{\pi} \simeq 3.3m,$$

and consequently

$$b = E_N/E_{\pi} \simeq 2.5.$$

Using this value of b , one obtains the inelasticity tabulated in Table I (*).

Now the Bristol group ⁽⁴⁾ considered that 20% of the particles with larger values of energy be K-mesons or nucleons and the remaining 80% be pions. They

TABLE I.

Energy of incident nucleon (in the L. system)	10^{12}	10^{14}	10^{16}	10^{18} eV
Inelasticity (in the C.M. system)	20%	30%	45%	60%

assumption, the front particle should be a nucleon. (The probability of finding pions is neglected there.) Thus the effective elasticity becomes

$$\frac{ab}{(100 - a) + ab},$$

b being the ratio of the energy of a front nucleon to that of a front pion. Now the energies E_N of a nucleon and E_{π} of a pion in the fluid with a temperature T are obtained by

$$E_N = \varepsilon_{NN}/n_{NN} = T\Phi^*(Z_N)/F^*(Z_N),$$

$$E_{\pi} = \varepsilon_{\pi}/n_{\pi} = T\Phi(Z_{\pi})/F(Z_{\pi}),$$

⁽²⁾ S. AMAL, H. FUKUDA, C. ISO and M. SATO: *Progr. Theor. Phys.*, **17**, 241 (1956)

defined the inelasticity K'' by the energy fraction of the latter part. Their experiments show the decrease of this value K'' for the increase of the incident energy. Such an inelasticity K'' can be calculated in the hydrodynamical

⁽³⁾ S. Z. BELEN'KIJ and L. D. LANDAU: *Usp. Fiz. Nauk*, **56**, 309 (1955).

⁽⁴⁾ B. EDWARDS, J. LOSTY, D. H. PERKINS, K. PINKAU and J. REYNOLDS: *Phil. Mag.*, **3**, 237 (1957).

(*) Taking into account the possibility that front particles are other than nucleons, these values of the inelasticity give us its lower limits. Furthermore it is noted that values of the inelasticity in the C. M. system are nearly equal to those in the L. system if the angular distribution is sharp and the inelasticity has small values.

model and is tabulated in Table II. K_{80} or K_{60} stands for the value of the inelasticity that is the energy fraction of particles of 80% or 60% with smaller values of energy in the C.M.S. Here, for the sake of simplicity, we make use of a simple model with one-constituent pion fluid. (One may expect the correct tendency of K'' for the incident energy even in such a simple model.) This result shows the same tendency as the Bristol data (*).

Table II.

E_0 (L. system) eV	K_{80} %	K_{60} %
10^{12}	35	17
10^{14}	24	9
10^{16}	16	6

Finally we discuss the assumption that the front part of the fluid is mainly occupied by the nucleon fluid. The initial hot spot has a number of proto-nucleons, -antinucleons and -pions with energies determined by the rule of thermal equilibrium at the initial temperature. By the above assumption we consider the processes that, during the hydrodynamical expansion of the hot spot, the nucleon-antinucleon constituent of the fluid would outrun the pion fluid and the part of the former overlapping with the latter would transform into pion fluid, leaving the non-overlapping nucleon fluids which are nothing but two nucleons moving at the fronts in opposite directions. Some

mechanism may make it possible to realize such processes. For example we first consider the case that the chemical potential of nucleons becomes very large at the fronts compared with the backs. Then it might be expected that the nucleon density would be predominant at the front. Next we can consider another possible mechanism that the nucleon fluid may outrun the pion fluid because the latter has a viscosity larger than the former. The pion fluid loses its kinetic energy and generates heat in it by its viscosity. This leads to the desired form of the progression of nucleons. The first process is looked on as a reversible one if the mixing effect is disregarded, but it becomes an irreversible one if the mixing effect is taken into account. (This fact is a direct result of the situations that the chemical potential of antinucleons has the same value but the opposite sign as that of nucleons and the chemical potential of pions is vanishing if the mixing effect is disregarded, and that the conservation law of nucleon number holds.) The second process is, of course, an irreversible one. In irreversible processes the entropy of the system increases and consequently the multiplicity becomes larger than the value expected by Landau. Furthermore the viscosity of fluid modifies the angular distribution of produced particles. The discussion whether the expansion of the meson-nucleon clouds is reversible or irreversible will be left till detailed investigations of the multiplicity, the angular distribution of the produced particles and the inelasticity will be available. At any rate it is unfortunate that the calculation offers difficulties for the derivation of numerical results from the hydrodynamical equations of two fluids in the above processes.

(*) Bristol's data are given in the L. system, while our calculation is performed in the C. M. system. But both have nearly the same value because the faster particles carry the most part of the initial energy.

Non-local Interaction and Universal Cut-off.

E. ARNOUS

Centre National de Recherche Scientifique - Paris

W. HEITLER

Seminar für theoretische Physik - Universität Zürich

(ricevuto il 4 Dicembre 1958)

Considerable evidence has accumulated in recent years to show that the present field theories with local interaction have only a limited field of validity which can be expressed by a certain cut-off in momentum space. Whatever quantitative success meson theory was able to show this was achieved by the (non-relativistic) « extended source model », corresponding to a cut-off of the 3-dimensional momentum $|\mathbf{k}| \leq K_0$ where K_0 is of order Mc (for example, papers by CHEW⁽¹⁾ on meson-nucleon scattering etc.). The recent (successful) calculations of the electron-nucleon scattering⁽²⁾ lends further support to this model or its relativistic generalization. In contrast to the earlier renormalization « philosophy » it is almost certain that such quantities as the self-mass of a particle are in some cases observed and exhibit themselves in small mass differences, like $m_{\pi^+} - m_{\pi^0}$ and also the p-n mass difference⁽³⁾. Since it has been proved that at least one renormalization constant is infinite in the local theory, it is most unlikely that such a theory is able to account for the mass differences. The $\pi^+ - \pi^0$ mass difference is again accounted for by a cut-off of the virtual photon momentum of order Mc .

It has been shown in several examples that the non-relativistic extended source can be generalized relativistically and it has also been conjectured that the cut-off value K_0 is universal, *i.e.* the same for all strong interactions⁽⁴⁾ (perhaps even for weak interactions, but there is no evidence). The cut-off prescription was formulated as follows: if a particle with momentum \mathbf{p} dissociates virtually into two particles \mathbf{k} and $\mathbf{p} - \mathbf{k}$, then $|\mathbf{k}|$ is to be restricted to values $\leq K_0$ if $\mathbf{p} = 0$, whilst k_0 ranges as usual from $-\infty$ to $+\infty$. For $\mathbf{p} \neq 0$ the limits of integration are determined by Lorentz transformation. This prescription has proved effective in removing all divergencies (at least so far).

⁽¹⁾ G. F. CHEW: *Phys. Rev.*, **94**, 1755 (1954), and later papers.

⁽²⁾ L. K. PANDIT: *Helv. Phys. Acta*, **31**, 379 (1958); *Nuovo Cimento*, **10**, 534 (1958).

⁽³⁾ L. O'RAIFHEARTAIGH, B. SREDNIAYA and CH. TERREAUX: to be published.

⁽⁴⁾ E. ARNOUS and W. HEITLER: *Nuovo Cimento*, **2**, 1282 (1955).

It is the purpose of the present note to formulate such a cut-off in terms of a non-local interaction with a form factor, specified to a large extent and to discuss this form factor in coordinate space. Consider a non-local interaction between a spinor field ψ and a Bose field φ (interaction representation)

$$H(t) = g \int d^3x \int d^4x' d^4x'' d^4x''' \bar{\psi}(x') \psi(x'') \varphi(x''') F(x - x', x - x'', x - x'''),$$

or in momentum space

$$(1) \quad H(t) = \frac{g}{(2\pi)^3} \int d^4p d^4q d^4k \bar{\psi}(p) \psi(q) \varphi(k) f(p, q, k) \delta^3(\mathbf{p} - \mathbf{q} - \mathbf{k}) \exp[i(p_0 - q_0 - k_0)t],$$

where f is the Fourier transform of F . Operators which may stand between the field quantities (like γ_μ , τ_i = isobaric spin) are omitted. φ is assumed real, but may have several components. For S -matrix problems (including self-energies) f occurs only on the energy-momentum shell $p = q + k$. We therefore consider the form factor

$$f(p, p - k, k) \equiv \varrho(p, k).$$

This must be postulated to be Lorentz-invariant (in contrast to f which need not be so). We first obtain the conditions arising from the hermiticity of H , and the invariance against C , P , T separately. One easily finds:

$$(2a) \quad \text{Hermiticity: } \varrho^*(p - k, -k) = \varrho(p, k),$$

$$(2b) \quad C: \varrho(p, k) = \varrho(-p + k, k),$$

$$(2c) \quad P: \varrho(\mathbf{p}, p_0; \mathbf{k}, k_0) = \varrho(-\mathbf{p}, p_0; -\mathbf{k}, k_0),$$

$$(2d) \quad T: \varrho(\mathbf{p}, p_0; \mathbf{k}, k_0) = \varrho(-\mathbf{p} + \mathbf{k}, p_0 - k_0; \mathbf{k}, -k_0).$$

These conditions, of course, do not suffice to determine ϱ . The essential *physical* condition, which we now add, corresponds to the above cut-off prescription: in the case $\mathbf{p} = 0$, ϱ shall effectively cut down the 3-dimensional momentum $|\mathbf{k}|$ but shall not affect k_0 . This means that in this case ϱ shall be a function $|\mathbf{k}|$ only (and $p_0^2 = +m^2$)

$$(3) \quad \varrho(\mathbf{p} = 0, k) = \varrho(p_0, |\mathbf{k}|).$$

The only invariant function, satisfying (2a)-(2d) and (3) is a real function of one variable only, namely

$$(4) \quad \varrho = \varrho(Q), \quad Q = -p^2 k^2 + (pk)^2 = (p_\mu k_\nu - p_\nu k_\mu)^2.$$

It may be remarked that Lorentz-invariance, (2a), (2d) and (3) suffice to lead to (4) (which may be of interest for the weak interactions). One may for example choose for ϱ something like

$$(4') \quad \varrho = \frac{\lambda^4}{\lambda^4 + Q}.$$

which cuts off Q at λ . If the conjecture that K_0 is universal is true one has to choose $\lambda^4 = K_0^2 m^2$ (m = mass of Fermi particle). It is seen that ϱ satisfies the stronger condition $\varrho(p + \lambda k, k) = \varrho(p, k)$ for any λ and of course, $\varrho(p, k) = \varrho(k, p) = \varrho(-p, k) = \varrho(p, -k)$. A form factor of type (4) or (4') is the natural relativistic generalization of the « extended source » model. The cut-off for processes other than the virtual dissociation is now unambiguously determined, for example for pair creation by the Bose-particle, securing convergence also for vacuum polarization etc. The Hermiticity of $H(t)$ guarantees the unitarity of the S -matrix, if the latter is constructed in the usual manner. So far f is determined only on the energy shell. For the full f one may put, for example

$$f(p, q, k) = \frac{p_0 \varrho(q, k) - q_0 \varrho(p, k) - k_0 \varrho(p, q)}{p_0 - q_0 - k_0},$$

which leads to correct relativistic properties of $H(t)$, and fulfills requirements similar to (2). A form factor similar to (but not identical with) (4) has been suggested by MÖLLER and KRISTENSEN ⁽⁵⁾ but their form factor does not secure convergence in all cases.

We now discuss the corresponding form factor in coordinate space

$$(5) \quad G(x, y) = \frac{1}{(2\pi)^{12}} \int d^4 p d^4 k \exp [+ i(px - ky)] \varrho(p, k).$$

It follows that $G(x, y) = G(x + \lambda y, y)$.

It may be remarked that G occurs only in such a way that x and y are *differences* of 4-coordinates. G is normalized so that $\int d^4 x d^4 y G(x, y) = 1$ which follows from $\varrho(0, k) = \varrho(p, 0) = 1$. From the same property of ϱ it follows that

$$(6) \quad \int G(x, y) d^4 y = \delta^4(x).$$

To obtain a clear picture of the behaviour of G we consider the 2-dimensional case (only one space coordinate). Thus $Q = \varrho(p_1 k_0 - p_0 k_1)^2$. Using the form (4') one can reduce the integrations to a single integral

$$(7) \quad G(x, y) = \frac{\lambda^2}{8\pi^2} \int_{-\infty}^{+\infty} dz \exp \left[-\frac{\lambda^2}{|z|} \right] \exp [iz(x_1 y_0 - y_1 x_0)],$$

which evidently satisfies (6). At first sight it seems that this must give rise to strong a-causal effects because when $x_1 = x_0 = 0$, G is independent of y and diverges. However, G always occurs under a space integral multiplied by field functions, which never behave like δ -functions. Wave packets which are physically meaningful and which might, for example, occur as initial state always have a linear extension not smaller than the nucleon Compton wave length. At any rate, for any useful discussion of causality, we would maintain that a space time description more detailed

⁽⁵⁾ C. MÖLLER and P. KRISTENSEN: *Kong. Dansk. Vid. Selsk.*, **27**, no. 7 (1952).

than to an accuracy of, say \hbar/Mc , is meaningless, since such lengths cannot be measured. Thus, we integrate G over a region δ , say, of x_1 and x_0 such that x_1 extends from $\xi_1 - \delta$ to $\xi_1 + \delta$, say. We find

$$\begin{aligned}
 (8) \quad & \int_{\xi_0 - \delta}^{\xi_0 + \delta} \int_{\xi_1 - \delta}^{\xi_1 + \delta} dx_0 dx_1 G(x, y) d^2x d^2x_0 = \\
 & = \frac{\lambda^2}{2\pi^2} \int_{-\infty}^{+\infty} \frac{dz}{z^2} \exp \left[-\frac{\lambda^2}{|z|} \right] \exp [i(\xi_1 y_0 - \xi_0 y_1)z] \frac{\sin zy_0 \delta \sin zy_1 \delta}{y_0 y_1}.
 \end{aligned}$$

This rapidly decreases for increasing y_0 or y_1 : small values of z do not contribute on account of $\exp[-\lambda^2/|z|]$, and for large z , the sin's are rapidly oscillating unless y_1 and y_0 are very small. Thus, independently of ξ_1 , ξ_0 (8) is restricted to a small region of y_1 and y_0 . Similarly, large x_1 or x_0 do not occur either, when G is averaged over a small region of y_1 and y_0 . The form factor G (7) has very much the properties of an «extended» δ -function $\delta(x_1)\delta(x_0)\delta(y_1)\delta(y_0)$, where the latter is the limiting case of the local theory.

Thus the non-locality of the form factor is such that particles interact only over unobservably small space and time regions (separately).

It appears that the above form-factor is unlikely to show any of the non-causal effects at large distances (which otherwise are feared to occur in non-local theories) whenever averages are taken over unobservably small space-time regions. A violation of causality within regions less than \hbar/Mc or so seems a justifiable sacrifice.

* * *

This work was supported by the Swiss Atomic Energy Commission and the Swiss National Fonds to which we wish to express our gratitude.

Multiple Scattering Corrections in π -Deuteron Scattering.

V. DE ALFARO

Istituto di Fisica dell'Università - Torino
Istituto Nazionale di Fisica Nucleare - Sezione di Torino

R. STROFFOLINI

Istituto di Fisica Teorica dell'Università - Napoli
Scuola di Perfezionamento in Fisica Teorica e Nucleare del C.N.R.N. - Napoli

(ricevuto il 7 Gennaio 1959)

Recently ROCKMORE ⁽¹⁾ has given an evaluation of the corrections to the impulse approximation for the π -deuteron scattering. In particular he calculates the multiple scattering corrections extending the method already used by BRUECKNER ⁽²⁾ in order to take into account also the spin dependence of the pion-nucleon scattering matrix. The Brueckner method essentially consists in assuming that the π -meson propagates as a real particle between two successive scatterings on the two fixed nucleons at r_a and r_b , with a propagator of the form $\exp [ik|\mathbf{r} - \mathbf{r}_y|/|\mathbf{r} - \mathbf{r}_y|]$, ($y = a, b$). This assumption which is correct for the π -meson wave outside the range of the π -interaction with both nucleons, is certainly invalid when the two nucleons are so close together that the interaction regions overlap. In this assumption, indeed, the scattering amplitude for double scattering diverges when the distance between the nucleons $R \rightarrow 0$, while the multiple scattering amplitude tends to zero as R . The structure of the meson propagator produces another difficulty when one takes into account also the spin dependence. In fact the scattering amplitude f is obtained from the solution of a very complicated set of coupled equations for the amplitudes $A, \mathcal{A}, B, \mathcal{B}$, related to f by

$$f = (\mathcal{A} + A \cdot k) \exp [-ik \cdot r_a] + (\mathcal{B} + B \cdot k) \exp [-ik \cdot r_b].$$

An approximate solution is obtained by ROCKMORE ⁽¹⁾ by retaining only the terms « to first order in the propagator in the numerator and to second order in the denominator for A and \mathcal{A} ».

⁽¹⁾ R. M. ROCKMORE: *Phys. Rev.*, **105**, 256 (1957).

⁽²⁾ K. A. BRUECKNER: *Phys. Rev.*, **89**, 834 (1953); **90**, 715 (1953).

It is not clear what this means because in the equations not only the propagator but also its first and second order derivatives appear. Moreover as the real part of the propagator tends to ∞ for $R \rightarrow 0$ (its n -th derivative is infinite of order n) there may be values of R sufficiently small so that the higher order terms in the propagator are bigger than the lowest order ones. At the same time R could still be sufficiently large so that when the scattering amplitude is averaged over the deuteron probability density the contribution from this range is not negligible.

It has seemed therefore worthwhile to reconsider the problem by making use of a π -nucleon scattering matrix with a high momenta behavior such that the propagator does not have singularities at small distance. According to DRELL and VERLET ⁽³⁾ if the propagator is not singular the multiple scattering corrections are negligible in comparison with the double scattering ones: nevertheless this has been verified only for s -wave scattering. When p -wave scattering is important (as it is obviously in our case) one might expect that this is no longer true, because the derivatives of the propagator appear divided by R .

The scattering state

$$(1) \quad \psi_0 = \varphi_0 + \frac{1}{\omega_0 - H_0 + i\varepsilon} (V_a + V_b) \psi_0, \quad \text{with} \quad H_0 \varphi_0 = \omega_0 \varphi_0,$$

describes the scattering of a π -meson of energy ω_0 by the two fixed nucleons. We define, following WATSON ⁽⁴⁾, the operators:

$$(2) \quad \Omega_a = 1 + \frac{1}{\omega_0 - H_0 + i\varepsilon} t_b \Omega_b, \quad \Omega_b = 1 + \frac{1}{\omega_0 - H_0 + i\varepsilon} t_a \Omega_a,$$

where

$$t_\nu = V_\nu + V_\nu \frac{1}{\omega_0 - H_0 + i\varepsilon} t_\nu, \quad (\nu = a, b),$$

is the two body π -nucleon scattering matrix defined also for any initial state whose energy is not equal to ω_0 ⁽⁵⁾. In terms of these operators the scattering matrix \mathcal{T} associated with the scattering state (1) turns out to be:

$$(3) \quad \mathcal{T} = t_a \Omega_a + t_b \Omega_b.$$

We assume a separable π -nucleon interaction, which allows us to obtain exact multiple scattering solutions, of the form

$$(4) \quad \langle \mathbf{k} | V_y | \mathbf{k}' \rangle = 2\pi \frac{v(k)v(k')}{\omega_k \omega_{k'}} [u + v(\boldsymbol{\tau}_y \cdot \mathbf{l}) + \\ + f^2(2i\boldsymbol{\sigma}_y \cdot \mathbf{k} \wedge \mathbf{k}' - 2\boldsymbol{\tau}_y \cdot \mathbf{l} \mathbf{k} \cdot \mathbf{k}')] \exp[i(\mathbf{k}' - \mathbf{k}) \cdot \mathbf{r}_y],$$

where \mathbf{l} is the isotopic spin operator for the π -meson, and $v(k)$ is a Yukawa shaped cut-off $v(k) = k^2/(k^2 + \xi^2)$.

⁽³⁾ S. D. DRELL and L. VERLET: *Phys. Rev.*, **99**, 849 (1955).

⁽⁴⁾ K. M. WATSON: *Phys. Rev.*, **89**, 575 (1953).

⁽⁵⁾ N. C. FRANCIS and K. M. WATSON: *Phys. Rev.*, **92**, 291 (1953).

With this interaction we obtain for t_v the expression

$$(5) \quad \langle \mathbf{k} | t_v | \mathbf{k}' \rangle = - \left(\sum_I h^I(\omega_0) P_v^I + \sum_{I,J} h^{IJ}(\omega_0) \langle \mathbf{k} | P_v^{IJ} | \mathbf{k}' \rangle \right) \frac{v(k)v(k')}{\omega_k \omega_{k'}} \exp [i(\mathbf{k}' - \mathbf{k}) \cdot \mathbf{r}_v],$$

where:

$$h^I(\omega_0) = \frac{2\pi\mu^I}{1 - \frac{\mu^I}{\pi} \int \frac{k'^2 v^2(k') dk'}{\omega_k^2(\omega_k - \omega_0 - i\varepsilon)}}, \quad h^{IJ}(\omega) = \frac{2\pi\lambda^{IJ}}{1 - \frac{\lambda^{IJ}}{\pi} \int \frac{k''^4 v^2(k'') dk''}{\omega_k^2(\omega_k - \omega_0 - i\varepsilon)}}.$$

$$\mu^1 = -u + 2v, \quad \mu^3 = -u - v, \quad \lambda^{1,1} = -\frac{2}{3}f^2, \quad \lambda^{1,3} = \lambda^{3,1} = -\frac{2}{3}f^2, \quad \lambda^{3,3} = \frac{4}{3}f^2,$$

and P^I , P^{IJ} are the projection operators for total isotopic spin I and total angular momentum J .

The parameters u , v , f^2 and ξ^2 have to be so adjusted as to obtain the experimental pion-nucleon phase shifts.

By substituting this result in eq. (2) and defining

$$(6) \quad \begin{cases} \mathbf{A}_i = \frac{1}{(2\pi)^4} \sum_{I,J,I'} h^{IJ}(\omega_0) \langle i | P_a^{IJ} | i \rangle \int \frac{\mathbf{k}'_i}{\omega_{k'}} \exp [i\mathbf{k}' \cdot \mathbf{r}_a] v(k') \langle \mathbf{k}' | \omega_a | \mathbf{k}_0 \rangle d\mathbf{k}', \\ \mathcal{A} = \frac{1}{(2\pi)^4} \sum_I h^I(\omega_0) P_a^I \int \frac{\exp [i\mathbf{k}' \cdot \mathbf{r}_a]}{\omega_{k'}} v(k') \langle \mathbf{k}' | \omega_a | \mathbf{k}_0 \rangle d\mathbf{k}', \end{cases}$$

and two other quantities \mathbf{B} and \mathcal{B} which are obtained by replacing the subscript a with b in the preceding expression, we obtain for \mathcal{C} the expression:

$$(7) \quad \langle \mathbf{k} | \mathcal{C} | \mathbf{k}_0 \rangle = -\frac{2\pi}{\omega_0} v(k) [(\mathcal{A} + \mathbf{A} \cdot \mathbf{k}) \exp [-i\mathbf{k} \cdot \mathbf{r}_a] + (\mathcal{B} + \mathbf{B} \cdot \mathbf{k}) \exp [-i\mathbf{k} \cdot \mathbf{r}_b]],$$

with \mathbf{A} , \mathcal{A} , \mathbf{B} and \mathcal{B} satisfying the following equations, in the case of the scattering of a π^+ -meson:

$$(8) \quad \begin{cases} \mathbf{A} = -\frac{i\eta_{33}}{3k^3 v(k)} T_a (2\nabla + i\boldsymbol{\sigma}_a \wedge \nabla) [\exp [i\mathbf{k} \cdot \mathbf{r}] + (\mathcal{B} - i\mathbf{B} \cdot \nabla) g(|\mathbf{r} - \mathbf{r}_b|)]_{\mathbf{r}=\mathbf{r}_a}, \\ \mathcal{A} = \left[\frac{1}{3kv(k)} (\eta_3 - \eta_1) T_a + \frac{\eta_1}{kv(k)} \right] [\exp [i\mathbf{k}_0 \cdot \mathbf{r}] + (\mathcal{B} - i\mathbf{B} \cdot \nabla) g(|\mathbf{r} - \mathbf{r}_b|)]_{\mathbf{r}=\mathbf{r}_a}, \end{cases}$$

and analogously for \mathbf{B} and \mathcal{B} , where

$$g(r) = \frac{\omega_0}{v(k)(2\pi)^2} \int \frac{\exp [i\mathbf{k} \cdot \mathbf{r}] v^2(k') d\mathbf{k}'}{\omega_{k'}^2(\omega_{k'} - \omega_0 - i\varepsilon)} = \\ = v(k) \left[\frac{\exp [ikr]}{r} - \frac{\exp [-\xi r]}{r} \left(1 + \frac{\xi r}{2v(k)} \right) \right] - \frac{\omega_0}{v(k)\pi r} \int \frac{(2\omega_{k'} + \omega_0) v^2(k') k' \sin k' r dk'}{\omega_{k'}^2(\omega_{k'} + \omega_0)},$$

and, as in ROCKMORE (1),

$$T_a = \begin{pmatrix} 2 & -\sqrt{2} \\ -\sqrt{2} & 1 \end{pmatrix}, \quad T_b = \begin{pmatrix} 2 & \sqrt{2} \\ \sqrt{2} & 1 \end{pmatrix}, \quad \eta_{IJ} = \exp [i\delta_{IJ}] \sin \delta_{IJ}.$$

In deriving eq. (8), we have used the relation

$$(9) \quad \exp[-i\delta_{IJ}] \sin \delta_{IJ} = -\frac{k_0 \omega_0}{2\pi} \langle k_0 | t^{IJ} | k_0 \rangle,$$

and have assumed $\delta_{11} = \delta_{13} = \delta_{31} = 0$. The experimental values of the phase shifts δ_{33} , δ_1 , δ_3 are furnished by eqs. (5) and (9), assuming $f^2 = 0.0246$, $u = 0.075$, $v = 0.130$, $\xi = 12\mu$, (μ is the π -meson mass).

In order to solve these equations we point out that the real and imaginary parts of the products of η_{33}/k^3 or η_3/k or η_1/k times g or g' are small with respect to unity for all the range of R . This is not true for the terms containing g'/R or its powers at least for small values of R . Therefore neglecting terms of higher order in g or g' we obtain for \mathbf{A} the equation:

$$(10) \quad \mathbf{A} = \mathbf{O} + \alpha^2 T_a T_b (2 + i\boldsymbol{\sigma}_a \wedge) \left[(2\mathbf{A} + i\boldsymbol{\sigma}_b \wedge \mathbf{A}) \left(\frac{g'}{R} \right)^2 + (4\mathbf{n} + i\boldsymbol{\sigma}_b \wedge \mathbf{n})(\mathbf{A} \cdot \mathbf{n}) \frac{g'}{R} g_2 + \right. \\ \left. + 2g_2^2 (\mathbf{A} \cdot \mathbf{n}) \mathbf{n} + i \frac{g'}{R} g_2 (\boldsymbol{\sigma}_b \wedge \mathbf{A} \cdot \mathbf{n}) \mathbf{n} \right],$$

with

$$\mathbf{O} = \mathbf{S}_a - \alpha T_a (2 + i\boldsymbol{\sigma}_a \wedge) \left[i\mathbf{n} g' q_b + \frac{g'}{R} \mathbf{S}_b + g_2 \mathbf{n} (\mathbf{n} \cdot \mathbf{S}_b) \right], \\ \mathbf{S}_a = \alpha T_a (2\mathbf{k}_0 + i\boldsymbol{\sigma}_a \wedge \mathbf{k}_0) \exp[i\mathbf{k}_0 \cdot \mathbf{r}_a], \quad q_a = (\beta T_a + \gamma) \exp[i\mathbf{k}_0 \cdot \mathbf{r}_a], \\ \alpha = \frac{\eta_{33}}{3k^3}, \quad \beta = \frac{\eta_3 - \eta_1}{3k}, \quad \gamma = \frac{\eta_1}{k}, \\ \mathbf{n} = \frac{\mathbf{R}}{R}, \quad g' = \frac{dg}{dR}, \quad g_2 = \frac{1}{R} \frac{d}{dR} \left(\frac{g'}{R} \right).$$

By using the easily verifiable relation $i(\boldsymbol{\sigma}_a \wedge \mathbf{A}) = \mathbf{A}$ we obtain (*)

$$(11) \quad \mathcal{A}^1(\mathbf{A})_{11} = \mathcal{A}^1 \left[\frac{1}{1 - 7\alpha^2 (g'/R)^2} (\mathbf{O})_{1,1} + \frac{2i\alpha^2}{1 - 10\alpha^2 (g'/R)^2} \boldsymbol{\sigma}_b \wedge (\mathbf{S}_a)_{1,1} + \right. \\ \left. + \frac{\alpha^2}{1 - 7\alpha^2 (g'/R)^2} \left[\frac{(\mathbf{E})_{1,1}}{1 - \alpha^2 [3(g'/R)^2 + (g'/R)g_2 + 4g_2^2]} + \frac{(\mathbf{F})_{1,1}}{1 - \alpha^2 [3(g'/R)^2 + (g'/R)g_2]} \right] \right],$$

where $\mathcal{A}^1 = \frac{1}{4}(3 + \boldsymbol{\sigma}_a \cdot \boldsymbol{\sigma}_b)$ and $(\)_{1,1}$ means the matrix element between initial and final isotopic singlet nucleon state; moreover:

$$(\mathbf{E})_{1,1} = \left[\left(8 \frac{g'}{R} + 4g_2^2 \right) \mathbf{n} - (\boldsymbol{\sigma}_a \wedge \boldsymbol{\sigma}_b \wedge \mathbf{n}) \frac{g'}{R} g_2 + i \left(4 \frac{g'}{R} g_2 + 2g_2^2 \right) (\boldsymbol{\sigma}_a \wedge \mathbf{n}) + \right. \\ \left. + 2i \frac{g'}{R} g_2 (\boldsymbol{\sigma}_b \wedge \mathbf{n}) \right] \mathbf{n} \cdot (\mathbf{S}_a)_{1,1}, \\ (\mathbf{F})_{11} = i \left[2 \frac{g'}{R} g_2 \mathbf{n} + \frac{g'}{R} (\boldsymbol{\sigma}_a \wedge \mathbf{n}) \right] \cdot (\boldsymbol{\sigma}_b \wedge (\mathbf{S}_a)_{1,1} \cdot \mathbf{n}).$$

(*) Neglecting high order terms.

In the same approximation we obtain

$$(12) \quad \mathbf{A}'(\mathcal{A})_{1,1} = A^1 [q_u + (\beta T_a + \gamma)(gq_b - ig'\mathbf{n} \cdot \mathbf{B})]_{1,1} \cong \\ \cong (q_a)_{1,1} + (\beta + \gamma) \left(g(q_b)_{1,1} - A^1 \frac{i}{1 - 7\alpha^2(g'/R)^2} \mathbf{n} \cdot (\mathbf{S}_b)_{1,1} \right),$$

where we have used for \mathbf{B} the solution corresponding to (11) neglecting terms of higher order.

In order to obtain the scattering matrix for the π -meson-deuteron scattering, we must average the scattering matrix τ on the deuteron probability density (we have used as deuteron wave function the Hulthén function). We have reported in Tables I and II the results of our calculations for the total cross-section (obtained by the optical theorem) and for the elastic differential cross-section at 0° and 180° .

TABLE I. — *Total cross-sections.*

σ_{free} = sum of the free particle cross sections; σ_d = cross section corrected for double scattering σ_m = corrected for multiple scattering.

E_{lab} (MeV)	$\sigma_d/\sigma_{\text{free}}$	$\sigma_m/\sigma_{\text{free}}$
85	1.17	1.34
190	0.94	0.89

TABLE II. — *Elastic differential cross-sections.*

$\sigma_{i,a}(\vartheta)$ = differential cross section in impulse approximation; $\sigma_d(\vartheta)$ = differential cross section corrected for double scattering; $\sigma_m(\vartheta)$ = corrected for multiple scattering.

E_{lab} (MeV)	$\sigma_d(0^\circ)/\sigma_{ia}(0^\circ)$	$\sigma_m(0^\circ)/\sigma_{ia}(0^\circ)$	$\sigma_d(180^\circ)/\sigma_{ia}(180^\circ)$	$\sigma_m(180^\circ)/\sigma_{ia}(180^\circ)$
85	1.12	1.17	1.19	1.13
190	0.89	0.80	0.51	0.31

At $E_{\text{lab}} = 85$ MeV (pion momentum in pion nucleon baricentric system $k = 1.03$) we have taken as value of the phase shift $\delta_{33} = 0.27$, $\delta_3 = -0.12$, $\delta_1 = 0.16$. At $E_{\text{lab}} = 190$ MeV ($k = 1.66$) we have taken $\delta_{33} = \frac{1}{2}\pi$, $\delta_3 = -0.148$, $\delta_1 = 0.176$. The importance of the small phase shifts for the multiple scattering corrections is not easily evaluated since in this case the coupled equations corresponding to eq. (8) become unmanageable.

According to our calculations we conclude that the multiple scattering corrections turn out to be larger than the double scattering corrections. This is essentially a consequence of the fact the real and imaginary parts of $7\alpha^2(g'/R)^2$, appearing in the denominator of eq. (11) become of order of unity for small values of R .

Our results therefore seem to point out that the multiple scattering corrections, when p -waves are explicitly taken into account, differ considerably from the double

scattering ones in disagreement with the assumption made by Drell and Verlet in their calculations. Even if this does not mean that actually the multiple scattering corrections are large, it shows that their magnitude depends strongly on the assumed behavior of the pion nucleon t matrix out of the energy shell. Accordingly we believe that the agreement between experiments and the Rockmore calculations is probably somewhat fortuitous.

* * *

We are grateful to Prof. M. CINI for stimulating discussions. We wish to thank the FIAT Electronic Calculation Center for numerical computations.

Symmetries in K^- -Interaction.

Y. EISENBERG (*) and W. KOCH

Physikalisches Institut der Universität - Bern

(ricevuto il 7 Gennaio 1959)

Recently it has been pointed out ⁽¹⁾ that the interaction of negative K -mesons with nuclear matter could be used for checking the validity of global symmetry in strong interactions ⁽²⁾. The reaction rates (\sim cross-section) for the absorption of s -wave K^- -mesons by single nucleons, calculated by AMATI and VITALE ⁽¹⁾ under the assumption of global symmetry, are given in Table I ⁽³⁾. For a comparison,

TABLE I.

Reactions	Reaction rates assuming	
	Charge independence only	Charge independence and global symmetry
(1) $K^- + p \rightarrow \Sigma^- + \pi^+$	$\frac{3}{2}r^2 + 1 + \sqrt{6}r \cos \varphi$	$1 + b^2 - 2b + (c^2/2) - \sqrt{2}(1-b)c \cos(a_{\frac{3}{2}} - a_{\frac{1}{2}})$
(2) $\rightarrow \Sigma^+ + \pi^-$	$\frac{3}{2}r^2 + 1 - \sqrt{6}r \cos \varphi$	$1 + b^2 + 2b + (c^2/2) + \sqrt{2}(1-b)c \cos(a_{\frac{3}{2}} - a_{\frac{1}{2}})$
(3) $\rightarrow \Sigma^0 + \pi^0$	1	1
(4) $\rightarrow \Lambda^0 + \pi^0$	$3r_{\Lambda}^2$	$b^2 + c^2 - 2\sqrt{2}bc \cos(a_{\frac{3}{2}} - a_{\frac{1}{2}})$
(5) $K^- + n \rightarrow \Sigma^- + \pi^0$	$3r^2$	$2b^2 + c^2 + 2\sqrt{2}bc \cos(a_{\frac{3}{2}} - a_{\frac{1}{2}})$
(6) $\rightarrow \Sigma^0 + \pi^-$	$3r^2$	$2b^2 + c^2 + 2\sqrt{2}bc \cos(a_{\frac{3}{2}} - a_{\frac{1}{2}})$
(7) $\rightarrow \Lambda^0 + \pi^-$	$6r_{\Lambda}^2$	$2b^2 + 4c^2 - 4\sqrt{2}bc \cos(a_{\frac{3}{2}} - a_{\frac{1}{2}})$

(*) On leave of absence from the Weizmann Institute, Rehovoth.

⁽¹⁾ D. AMATI and B. VITALE: *Nuovo Cimento*, **9**, 895 (1958). The single nucleon reaction rates notations used in the present work will be those of AMATI and VITALE.⁽²⁾ M. GELL-MANN: *Phys. Rev.*, **106**, 1297 (1957).⁽³⁾ Note that in ref. ⁽¹⁾ a factor 6 is missing in all the neutron reaction rates when normalized in the same way as the proton reaction rates.

in the same table the reaction rates obtained ⁽⁴⁾ by assuming charge independence only, are also given.

The notations used in Table I are:

$$r \exp [i\varphi] = \frac{\langle T=1 | S^{\Sigma} | T=1 \rangle}{\langle T=0 | S^{\Sigma} | T=0 \rangle}$$

$$r_{\Lambda} = \left| \frac{\langle T=1 | S^{\Lambda} | T=1 \rangle}{\langle T=0 | S^{\Sigma} | T=0 \rangle} \right|.$$

$A = i |A| \exp [i\alpha_{\frac{1}{2}}]$, $B = i |B| \exp [i\alpha_{\frac{3}{2}}]$, $C = i |C| \exp [i\alpha_{\frac{3}{2}}]$ and $b = |B|/|A|$, $c = |C|/|A|$. The α_i 's are the pion-hyperon phase shifts for the $I = \frac{1}{2}$ and $I = \frac{3}{2}$ states respectively ⁽¹⁾.

From Table I we see that from the requirement of charge independence some very simple relations among the various reaction rates follow ^(*):

$$(I) \quad \left\{ \begin{array}{l} (5) \equiv (6) \\ (7) \equiv 2(4) \\ (1) + (2) + (5) = 2[(3) + (6)]. \end{array} \right.$$

In addition to the above equalities, the following inequalities should be satisfied if charge independence holds:

$$(1) + (2) \geq 2(3)$$

and also the stronger relation:

$$(II) \quad 8 \times (3) [(1) + (2) - 2(3)] - [(1) - (2)]^2 \geq 0.$$

This could also be expressed in the form of a triangular inequality ^(**):

$$|\sqrt{(1)} - \sqrt{(2)}| \leq \sqrt{2(5)} \leq \sqrt{(1)} + \sqrt{(2)}.$$

The requirement of global symmetry (second column of Table I) leads to new inequalities, the simplest of which is ⁽¹⁾:

$$(III) \quad [(1) + (2) - 4(3)]^2 + 4[(3) \times (4) - (1) \times (2)] \geq 0.$$

It should be noted that while relations (I) and (II) do not require any special assumptions about the initial state ⁽⁴⁾ (i.e. unique angular momentum state and unique K^- -energy), relation (III) does require such an assumption ⁽¹⁾.

⁽⁴⁾ See, for example, Y. EISENBERG, W. KOCH, E. LOHRMANN, M. NIKOLIĆ, M. SCHNEEBERGER and H. WINZELER: *Nuovo Cimento*, **9**, 745 (1958).

^(*) Bracketed numbers will denote here reaction rates.

^(**) We are grateful to Dr. VITALE for pointing out this to us.

The reaction rates of the two-nucleon K^- -captures (having a nucleon and a hyperon as final states) assuming charge independence only⁽⁵⁾, are given in the first column of Table II. (See ref. (5) for details of the calculations and for the notations.) We shall now calculate the 2 nucleon-reaction rates assuming global symmetry (*). Let the two scattering amplitudes, in terms of which the N-Y and N-Z scattering could be described, be a_0 (for the $I=0$ state) and a_1 (for the $I=1$ state). The nucleon-hyperon system could be in one of the following states:

$$\begin{aligned} N-\Sigma: \quad \varphi_{\frac{3}{2}}, \quad \varphi_{\frac{1}{2}} & \quad (\text{for } T=\frac{3}{2} \text{ and } \frac{1}{2} \text{ respectively}) \\ N-\Lambda: \quad \psi_{\frac{1}{2}} & \quad (T=\frac{1}{2} \text{ only}). \end{aligned}$$

It is easy to show that we have:

$$\begin{aligned} \varphi_{\frac{3}{2}} | S_0 | \varphi_{\frac{3}{2}} &= a_1, \\ \varphi_{\frac{1}{2}} | S_0 | \varphi_{\frac{1}{2}} &= \frac{1}{4} a_1 + \frac{3}{4} a_0, \\ \psi_{\frac{1}{2}} | S_0 | \varphi_{\frac{1}{2}} &= \frac{3}{4} a_1 + \frac{1}{4} a_0, \\ \langle \psi_{\frac{1}{2}} | S_0 | \varphi_{\frac{1}{2}} \rangle &= -\frac{\sqrt{3}}{4} a_1 + \frac{\sqrt{3}}{4} a_0, \end{aligned}$$

where S_0 is the hyperon-nucleon scattering matrix. Obviously the functions $\varphi_{\frac{3}{2}}$, $\varphi_{\frac{1}{2}}$ and $\psi_{\frac{1}{2}}$ do not diagonalize the scattering matrix S_0 . We note, however, that the new functions $\eta_{\frac{1}{2}}$ and $\xi_{\frac{1}{2}}$ which are obtained under the following linear transformation:

$$\begin{aligned} \eta_{\frac{1}{2}} &= \frac{1}{2} \varphi_{\frac{1}{2}} - \frac{\sqrt{3}}{2} \psi_{\frac{1}{2}}, \\ \xi_{\frac{1}{2}} &= \frac{\sqrt{3}}{2} \varphi_{\frac{1}{2}} + \frac{1}{2} \psi_{\frac{1}{2}}, \end{aligned}$$

do diagonalize the nucleon-hyperon scattering matrix. We then have:

$$\begin{aligned} \langle \varphi_{\frac{3}{2}} | S_0 | \varphi_{\frac{3}{2}} \rangle &= a_1 \\ \langle \eta_{\frac{1}{2}} | S_0 | \eta_{\frac{1}{2}} \rangle &= a_1 & \langle \eta_{\frac{1}{2}} | S_0 | \xi_{\frac{1}{2}} \rangle &= 0. \\ \langle \xi_{\frac{1}{2}} | S_0 | \xi_{\frac{1}{2}} \rangle &= a_0 \end{aligned}$$

Now the K^- -2-nucleon system can be in a (symmetric) $T=\frac{3}{2}$ state, a symmetric (with respect to the 2 nucleons) $T=\frac{1}{2}$ state or an anti-symmetric $T=\frac{1}{2}$ state⁽⁵⁾. Let the corresponding wave functions be: $\chi_{\frac{3}{2}}$, $\chi_{\frac{1}{2}}^s$, and $\chi_{\frac{1}{2}}^a$. The reactions: $K^- + N + N \rightarrow Y + N$ can be then described in terms of the following 5 matrix elements, whose dependence upon the hyperon-nucleon scattering phase shifts (subject

⁽⁵⁾ Y. EISENBERG, W. KOCH, M. NICOLIĆ, M. SCHNEEBERGER and H. WINZELER: preprint, (October 1958).

(*) We shall follow here quite closely the calculations of ref. (4).

Concerning the Influence of Radiation in Cyclical Accelerators.

A. A. KOLOMENSKI and A. N. LEBEDEV

P. N. Lebedev Institute of Physics - Academy of Science - Moscow

(ricevuto il 7 Gennaio 1959)

There appeared an article by A. N. MATVEEV in the journal *Il Nuovo Cimento* in which the author questions the validity of the results of our work concerning radiation effects in cyclical accelerators ⁽²⁾.

However, we cannot agree with A. N. MATVEEV's conclusions, and, in view of the practical importance of the problems, we consider it advisable to dwell somewhat on the subject.

Basically, A. N. MATVEEV's position in his article ⁽¹⁾ amounts to the following: He recognizes the correctness of the expressions for the damping decrement of betatron oscillations in the presence of radiation losses and their compensation ⁽²⁾,

$$(1) \quad \xi_{\rho \text{ bet}} = -\frac{1}{2} \frac{n}{1-n} \frac{W}{E}; \quad \xi_z = -\frac{1}{2} \frac{W}{E}$$

obtained by us under the assumption that radiation takes place continuously («adiabatically», as the author expresses it). However, he asserts that the instantaneous quantum character of the photon radiation (*i.e.*, the «non-adiabatic» character of the radiation) completely changes the nature of the damping, reducing it practically to zero.

Such a view appears erroneous. This follows, in the first place, from the fact that the effects under consideration are of a pure classical, non-quantum nature. Within the framework of classical electrodynamics, the concept of «non-adiabatic» radiation is meaningless. At the same time, the correct quantum result should turn into (1) when $\hbar \rightarrow 0$. The results obtained by A. N. MATVEEV do not possess this property, and thus contradict the correspondence principle. A study of this matter shows that this contradiction is the result of certain erroneous assumptions made by the author.

⁽¹⁾ A. N. MATVEEV: *Nuovo Cimento*, **6**, 1296 (1957).

⁽²⁾ A. A. KOLOMENSKI and A. N. LEBEDEV: *Suppl. Nuovo Cimento*, **7**, 43 (1958); *Symposium CERN* (Geneva, 1956), p. 447; *Žurn. Eksp. Teor. Fiz.*, **30**, 1161 (1956).

In deriving formula [11] (*), he contradicts his own pattern of calculation by omitting in formula [10] all non-singular terms, including discontinuous ones. However, the latter yield additional singular terms, in going from [10] to [11], *i.e.*, after second differentiation, and these are not taken into consideration by A. N. MATVEEV.

Below we reproduce the corrected derivation for ξ_{obst} , using A. N. MATVEEV's method and symbols; terms improperly omitted by him are underlined>. We begin with the first relationship on page 1300:

$$(2) \quad \frac{\delta E}{\delta \varphi} = E \left(\frac{1}{\varrho} \frac{\delta \varrho}{\delta \varphi} - \frac{n}{r} \frac{\delta r}{\delta \varphi} \right); \quad \frac{1}{\varrho} \frac{\delta \varrho}{\delta \varphi} = \left(n \frac{\delta r}{\delta \varphi} - \frac{W_{\varphi}}{E} \right).$$

In place of [10] we have

$$(3) \quad \frac{\delta r_i}{\delta \varphi} = \frac{1}{1-n} \left[\frac{n}{r} \frac{\delta r}{\delta \varphi} (1-n)r_i + nr \right] - n \frac{\delta r}{\delta \varphi} - (r_i + nx) \frac{W_{\varphi}}{E}$$

from which we obtain by differentiating again, instead of [11],

$$(4) \quad r_i'' = -\frac{1}{1-n} \left[nx' \frac{W_{\varphi}}{E} + r \frac{W_i}{E} (1-2n)x' - n \frac{W_{\varphi}}{E} x' \right] = \frac{2n-1}{1-n} \frac{W_{\varphi}}{E} x'$$

i.e., the correct expression [6].

Utilising this result, the solution of equations Sect. 4 naturally yields our formula (1) for ξ_{obst} .

The analysis undertaken by A. N. MATVEEV in Sect. 5 for oscillations in the axial direction is also faulty. Moreover, the conclusion here regarding the absence of damping is not based on the «non-adiabatic» nature of the radiation, emphasized in Sect. 3. This conclusion was arrived at as a result of incorrect transformation of time in going from one system of co-ordinates to another. In fact, the solution of equation [19] in a laboratory system yields (1) for ξ_z , as before. At the same time, the relationships for time in a moving system of co-ordinates of the form

$$(5) \quad \dot{\tau} = 1; \quad \ddot{\tau} = 0; \quad \ddot{\tau} = \frac{1}{c^2} W^2,$$

only have meaning close to the given moment $s = s_0$ and merely reflect that

$$(6) \quad \tau(s) = s - s_0 + \frac{1}{c^2} W^2 \frac{(s - s_0)^3}{6} + \dots$$

Therefore, expression [22], being a differential equation obtained by using (5), is valid for only very small durations of time. The criterion for small is given by the

(*) Numbers in square brackets refer to the corresponding formulas in the article by A. N. MATVEEV (1).

ability to neglect the second term in expansion (6), *i.e.*, the condition

$$(7) \quad \frac{W^2}{c^2} (s - s_0)^2 \ll 1 \quad \text{or} \quad \tau \ll \frac{c}{W}$$

Since $\Omega \approx \gamma c/r_i$, $W \approx c^2 \gamma^2/r_i$, this condition is equivalent to

$$(8) \quad \tau \ll \frac{1}{\Omega \gamma} \ll \frac{1}{\Omega}.$$

Consequently, the method of successive approximations used in solving [22] is inapplicable here, and expression [23] obtained by A. N. MATVEEV is incorrect.

A Remark Concerning the Backward-Forward Asymmetry in Λ^0 -Decay (*).

R. A. SALMERON and A. ZICHICHI

CERN - Geneva

(ricevuto l'11 Gennaio 1959)

In the last two years the discovery of parity non-conservation in weak interactions (¹⁻³) aroused a systematic interest in all possible asymmetries in decay processes. One of these processes, on which attention has been focused several times, is the backward-forward asymmetry in the rest frame with respect to the Λ^0 line of flight of the protons emitted in the Λ^0 -decay. Indications about such an asymmetry, which would show a longitudinal polarization of the Λ^0 , seem to be rather controversial. Actually they were found by several groups working on cosmic ray events (⁴⁻⁹), and on the

grounds of particularly good statistics by BLUMENFELD *et al.* (¹⁰). But more recently, on the other hand, no asymmetry has been observed for instance in the production of Λ^0 by π^- mesons of 1.33 GeV/c in carbon (**)

Finally, the quite conclusive evidence of a lack of any significant asymmetry in the decays of the Λ^0 produced in hydrogen (¹¹)

$$(1) \quad \pi^- + p \rightarrow \Lambda^0 + p^0$$

(with π^- momentum of ~ 0.9 to ~ 1.4 GeV/c), has generally been considered adequate enough to rule out any

(*) Part of a paper presented at the 44-th Congress of the Italian Physical Society, Palermo (6-11 November 1958).

(¹) T. D. LEE and C. N. YANG: *Phys. Rev.*, **104**, 254 (1956).

(²) C. S. WU, A. AMBLER, R. W. HAYWARD, D. D. HOPES and R. P. HUDSON: *Phys. Rev.*, **105**, 1413 (1957).

(³) R. L. GARWIN, L. M. LEDERMAN and M. WEINRICH: *Phys. Rev.*, **105**, 1415 (1957).

(⁴) W. B. FRETTER, M. M. MAY and M. P. NAKADA: *Phys. Rev.*, **89**, 168 (1953).

(⁵) H. S. BRIDGE, C. PEYROU, B. ROSSI and R. STAFFORD: *Phys. Rev.*, **91**, 362 (1953).

(⁶) R. ARMENTEROS: *Congrès International sur le Rayonnement Cosmique* (Bagnère de Bigorre, 1953), p. 16.

(⁷) D. B. GAYTHER: *Phil. Mag.*, **45**, 570 (1954).

(⁸) W. A. COOPER, H. FILTHUTH, L. MONTANET, J. A. NEWTH, G. PETRUCCI, R. A. SALMERON and A. ZICHICHI: *Nuovo Cimento*, **8**, 471 (1958).

(⁹) G. ALEXANDER, C. BALLARIO, R. BIZZARRI, B. BRUNELLI, E. DI CAPUA, A. MICHELINI, G. C. MONETI and A. ZICHICHI: *Nuovo Cimento*, **9**, 624 (1958).

(¹⁰) H. BLUMENFELD, W. CHINOWSKY and L. M. LEDERMAN: *Nuovo Cimento*, **8**, 296 (1958).

(**) We are very grateful to Dr. P. FRANZINI for having sent us the data of these carbon events. See also later.

(¹¹) J. STEINBERGER: *Annual International Conference on High Energy Physics*, CERN (1958), p. 147.

possible production of a longitudinal polarization of Λ^0 's produced in any strong interaction. The situation has been considered rather puzzling and many ideas have been floating around to find a plausible explanation of the several somewhat conflicting results. Because so far the asymmetry mentioned above was found mainly in cloud chamber works many opinions and some not too conclusive arguments about possible biases in the selection and evaluation of the pictures involved in the cloud chamber experiments have been presented in several discussions held on this matter during the last year (*) as a good motivation to cast a definite doubt on the real existence of such an asymmetry.

In the following we would like to summarize briefly the arguments that, from our point of view, inclined us to believe that instead this asymmetry may be real and not obviously in contradiction to the results reported by STEINBERGER *et al.* (11).

a) *The question of bias:* Since the problem of bias in selecting the events is decisive for the significance of the results, let us examine first in some detail how we propose to overcome this problem.

The bias arises fundamentally when, among the neutral V-particles of a given experiment, a sample of Λ^0 -hyperons is chosen neither pure nor complete, *i.e.* a sample which contains neutral V-particles which are not Λ^0 's and which does not contain all Λ^0 's produced in that experiment. As the angle of emission of the proton in the Λ^0 rest system is independent of the Λ^0 momentum, the criterion which we propose to avoid bias in the selection of Λ^0 's consists in considering, in a given experiment, all Λ^0 's with momentum less than a fixed max-

imum cut-off momentum. This cut-off must be chosen in one of the following different ways, depending on whether or not we know all data relative to all V^0 -particles of a given experiment:

i) If, in a given experiment, the data corresponding to all V^0 -particles are known, the cut-off must be chosen as follows. Some V^0 -events are identified as Λ^0 -hyperons, others as θ^0 -mesons and others non-identified. The non-identified, if interpreted as Λ^0 -hyperons, show a momentum spectrum with a minimum momentum P . This is the cut-off to be chosen for the Λ^0 momenta. In fact, with this choice, the Λ^0 sample will be pure and complete within the momentum range considered because among all non-identified V^0 -events of the experiment there is no event which, if interpreted as Λ^0 , has momentum less than P .

ii) If in an experiment the data corresponding to all V^0 -particles are not known then the cut-off momentum cannot be chosen as described above, and another criterion must be adopted. This criterion must be chosen in such a way as to allow the selection of Λ^0 's independently of the angle of emission of the proton in the Λ^0 rest system. The choice of this cut-off depends on the lowest value which the ionization can have to be distinguishable from the minimum ionization. We consider that a lowest distinguishable value of the ionization equal to 2.5 times the minimum ionization is a safe choice in all experiments which we have considered. It results that the maximum momentum that a Λ^0 can have is 600 MeV/c in order to give a decay proton with ionization > 2.5 times minimum ionization independently of the angle of emission in the Λ^0 rest system.

(*) Reference is made here to discussions held at the Venice 1957 Conference and at CERN.

A calculation based on the dynamics of the Λ^0 -decay shows that the bias which

may still exist by applying criteria i) and ii) cannot change the result by more than 5% and 10% respectively.

b) *Analysis of experimental data:*
We have applied our selection criteria i) and ii) to Λ^0 data published by six cosmic ray groups ⁽⁴⁻⁹⁾. The results are shown in Table I, which contains the selection criteria and the corresponding cut-off momentum relative to each group's data, the obtained numbers of Λ^0 -particles with backward and forward

1.9 GeV π^- -mesons in lead and in carbon. We do not need to apply our selection criteria to their data because, except in very few cases (about five) they identify all of their V^0 -particles ^(*). In this machine experiment the ratio of number of Λ^0 's with backward to the number of Λ^0 's with forward emitted proton is about the same as that which we obtained from the cosmic ray data with about the same total number of Λ^0 's (see Table I). The cosmic ray plus the machine data together give: 131 back-

TABLE I.

Cosmic ray experiments	Selection criterion	Momentum cut-off (MeV/c)	Number of Λ^0 's with proton emitted			Total number of Λ^0 's	Producing material
			Backward	Forward	Near 90°		
Berkeley ⁽⁴⁾	ii)	600	8	1	1	10	Lead
M.I.T. ⁽⁵⁾	ii)	600	10	7	1	18	Lead
ARMENTEROS ⁽⁶⁾	ii)	600	15	8	—	23	Lead
GAYTHER ⁽⁷⁾	ii)	600	5	5	2	12	Lead
CERN ⁽⁸⁾	i)	700	11	3	3	17	Copper
	ii)	600	10	8	3	21	Lead
Rome ⁽⁹⁾	i)	500	8	3	—	11	Iron
			67	35	10	112	
Machine experiment							
Columbia ⁽¹⁰⁾	—	—	24	8	—	32	Carbon
	—	—	40	31	—	71	Lead
Totals			131	74	10	215	

emitted proton respectively, and the material where the Λ^0 's were produced. The Λ^0 's with proton emitted near 90° have been classified neither backward nor forward. Those cosmic ray data give then 67 events with backwards and 35 with forward emitted proton.

BLUMENFELD *et al.* ⁽¹⁰⁾ at the Cosmotron studied the production of Λ^0 's by

ward with respect to 74 forward, and the ratio:

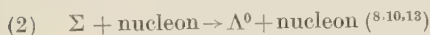
$$\frac{\text{backward}}{\text{forward}} = 1.77 \pm 0.25 .$$

c) As this backward-forward asymmetry seems to exist in Λ^0 's produced in

^(*) We are extremely grateful to Professor L. M. LEDERMAN for this private communication.

complex nuclei and not to exist in Λ^0 's produced in hydrogen, it seems necessary to correlate the asymmetry with the processes in which Λ^0 's are produced in complex nuclei. This difference, as a possible explanation for the apparent inconsistency found between the results reported by STEINBERGER⁽¹¹⁾ and those concerning the Λ^0 -production in complex nuclei, was already pointed out in a previous paper⁽⁸⁾ and also by LEDERMAN during the last CERN Conference⁽¹²⁾.

There are good experimental indications that such Λ^0 's are mostly not produced in the primary collision of the particle which bombards the nucleus, but are produced in great numbers through secondary processes such as:



There is also experimental evidence that Λ^0 -particles produced in complex nuclei have high probability of scattering before leaving the nucleus⁽¹⁴⁾, *i.e.*



This connection between Λ^0 -longitudinal polarization and interactions of the type (2), (3) and (4) is obviously a matter of speculation (*), but it concerns one of

the differences between the events reported by STEINBERGER⁽¹¹⁾ and those obtained in the experiments of references⁽⁴⁻¹⁰⁾. The other difference, is given by the higher energies of the interactions that occurred in these experiments.

In order to show clearly that accepting the criterium applied in collecting the events of Table I, the apparent inconsistency with the STEINBERGER *et al.*⁽¹¹⁾ results seems to be beyond the limits of statistical errors, one may remember that, assuming an angular distribution of the type $1 + a \cos \theta$, from the hydrogen events⁽¹¹⁾ one derives a coefficient

$$a = -0.11 \pm 0.12 .$$

Instead, in the case of Λ^0 's produced in complex nuclei and at high energies, if one agrees on our arguments against unpredictable biases and adds together all the events listed in Table I with an angular distribution of the same type, it is found (on the basis of a total of 205 events)

$$a = -0.56 \pm 0.15 .$$

This would, of course, represent an average value of a corresponding to different ways in which the Λ^0 's used in this analysis have been produced in complex nuclei.

There remains the question of the Λ^0 produced by π^- in carbon (see (*), page 461). For sake of completeness, we have analysed data corresponding to 70 Λ^0 's produced by π^- mesons of momentum 1.33 GeV/c in carbon, which were kindly sent to us by Dr. P. FRANZINI, from Pisa. These events show no asymmetry: 33, backwards, 33 forwards,

(12) L. M. LEDERMAN: *Annual International Conference on High Energy Physics, CERN* (1958), p. 160.

(13) F. M. WEBB, E. L. ILOFF, F. H. FEATHERSTONE, W. W. CHUPP, G. GOLDBABER and S. GOLDBABER: *International Conference on Mesons and Recently Discovered Particles* (Padua-Venice, 1957), p. II-69.

(14) G. D. JAMES and R. A. SALMERON: *Phil. Mag.*, **46**, 571 (1955).

(*) This speculation has been the object of several discussions, including seminars given by one of us (R.A.S.) at Milan and Turin. Lately, a discussion of this type took place at the 44-th meeting of the Italian Physical Society at Palermo, also in connection with a communi-

cation made by Dr. M. BLOCK, regarding information concerning some new evidence of parity violation in strong interactions involving strange particle production found at Berkeley by N. HORWITZ and co-workers.

and 4 near 90° . Here the only difference with respect to the data listed in Table I seems to be the energy. The events presented in this table are largely associated with energies appreciably higher than the 1.3 GeV/c of the events analysed by the Columbia, Bologna, Pisa collaboration. The cosmic ray events are

all produced in interactions of several GeV. Because we are inclined to believe that our criterium against the influence of biases is substantially correct we are also inclined to believe that due to the difference in energy the asymmetry shown by the events listed in Table I is real.

Transport Properties in the Liquid State and the Corresponding State Principle.

G. CINI-CASTAGNOLI, G. PIZZELLA and F. P. RICCI (*)

Istituto di Fisica dell'Università - Roma

Istituto Nazionale di Fisica Nucleare - Sezione di Roma

(ricevuto il 12 Gennaio 1959)

The corresponding state principle for the liquid state has been formulated under well definite hypotheses (¹⁻³). Only,

several different liquids it has been shown that also, Nitrogen, Carbon monoxide, Methane, and Oxygen behave as

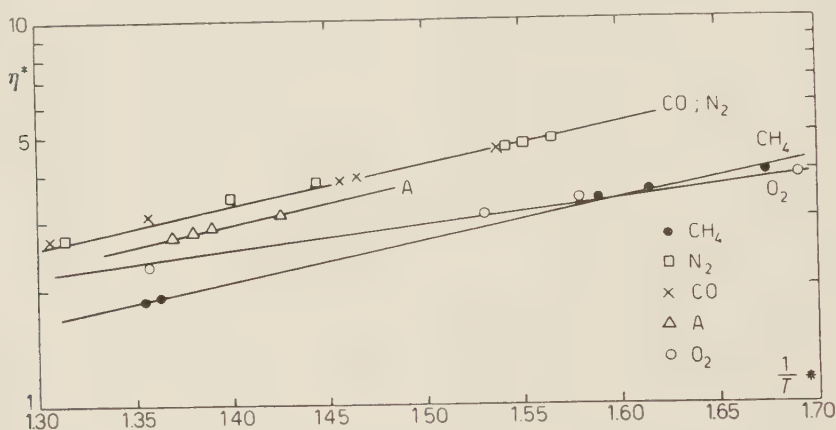


Fig. 1. - Reduced viscosity coefficient η^* against $1/T^*$.

Argon, Krypton, and Xenon meet completely the requirements based on these hypotheses and, therefore, they are called « perfect liquids ». However, examining the equilibrium properties of

perfect liquids with a good approximation (¹⁻²). On account of the considerable usefulness of this principle, we intend to consider to which extent the transport properties of these substances agree with the corresponding state principle.

In Fig. 1, the reduced viscosity (⁴)

(*) Now at C.N.R.N.

(¹) K. S. PITZER: *Journ. Chem. Phys.*, **7**, 583 (1939).

(²) E. A. GUGGENHEIM *Journ. Chem. Phys.*, **13**, 253 (1945).

(³) J. DE BOER: *Physica*, **14**, 139 (1948).

(⁴) J. O. HIRSCHFELDER, C. F. CURTISS and R. B. BIRD: *Molecular Theory of Gases and Liquids* (New York), p. 617.

$\eta^* = \eta(\sigma^2/\sqrt{m\varepsilon})$ is plotted versus the reciprocal of the reduced temperature, $1/T^* = \varepsilon/KT$. All data are given at about the same reduced pressure, $p^* = p(\sigma^3/\varepsilon)$.

Since the value of $(\partial\eta/\partial p)_{T=\text{const}}$ is

purpose: it is possible both to evaluate quantities not yet experimentally measured, when we know the data for one substance and to correlate experimental data concerning various substances.

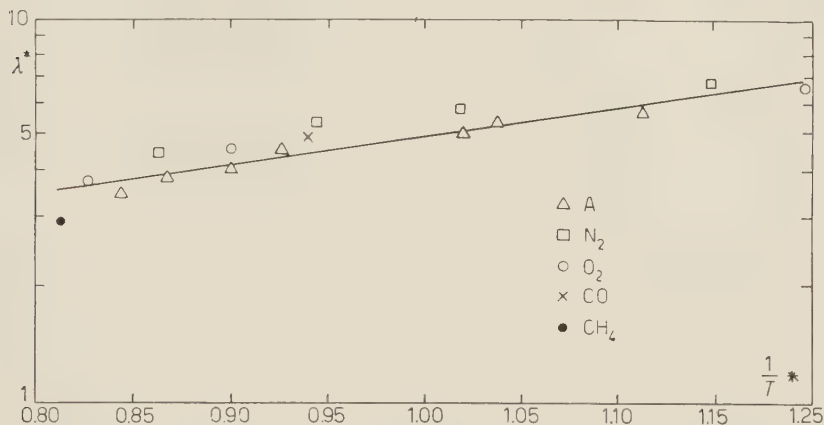


Fig. 2. — Reduced thermal conductivity coefficient λ^* , against $1/T^*$. All the experimental data are taken at $p \simeq 2p_{\text{crit}}$. The data concerning CH_4 and CO are extrapolated data taken at $p_{\text{crit}} < p \leq 2p_{\text{crit}}$. The difference does not change the results.

small the possible deviations are not significant.

In Fig. 2 the reduced thermal conductivity ⁽⁴⁾ $\lambda^* = \lambda(\sigma^2/K)\sqrt{m/\varepsilon}$ is plotted versus $1/T^*$. All data are given at about the same p^* . (The values of ε and σ were taken from J. DE BOER ⁽³⁾. For substances not listed there, the parameters have been calculated from the critical point. (This procedure corresponds to a reduction by means of critical constants).

Figs. 1 and 2 show that the corresponding state principle can be satisfactorily applied to Argon, Nitrogen, Carbon Monoxide and with lower approximation also to Methane and Oxygen.

The deviations, mainly in the viscosity process, from the behaviour of the perfect liquid (*i.e.* Argon) are greater in the case of the transport properties than in the case of the equilibrium properties. However the amount of these deviations cannot be simply related to the kind of molecule. It is well known that the corresponding state principle has a double

From this point of view, some results have been obtained in the case of the diffusion coefficient ⁽⁵⁾.

The following sources of the experimental data have been used:

1) Viscosity:

— A, CO, CH_4 , N_2 by N. S. RUDENKO and L. W. SCHUBNIKOW ⁽⁶⁾.

2) Thermal conductivity:

— A, N_2 by H. ZIEBLAND and J. T. A. BURTON ⁽⁷⁾.

— O_2 by H. ZIEBLAND and J. T. A. BURTON ⁽⁸⁾.

— CO, CH_4 by E. BOROVNIK, A. MATVEV and E. PANINA ⁽⁹⁾.

⁽⁵⁾ G. CINI, G. PIZZELLA and F. P. RICCI: *Nuovo Cimento*, **10**, 300 (1958).

⁽⁶⁾ N. S. RUDENKO and L. W. SCHUBNIKOW: *Phys. Sow.*, **6**, 470 (1934); **8**, 179 (1935).

⁽⁷⁾ H. ZIEBLAND and J. T. A. BURTON: *Brit. Journ. App. Phys.*, **9**, 52 (1958).

⁽⁸⁾ H. ZIEBLAND and J. T. A. BURTON: *Brit. Journ. App. Phys.*, **6**, 417 (1955).

⁽⁹⁾ E. BOROVNIK, A. MATVEV and E. PANINA: *Journ. Tech. Phys. USSR*, **10**, 988 (1940).

Protonic Decay of Σ^+ Hyperon with Associated Electron Pair.

D. H. DAVIS, M. A. SHAUKAT and F. R. STANNARD

Physics Department, University College - London

(ricevuto il 23 Gennaio 1959)

Participating in the European K^- stack collaboration (^{1,3}), we have recently scanned a stack of G-5 emulsion irradiated by the separated K^- meson beam of the Berkeley Bevatron. In the course of this work an unusual decay involving a Σ^+ hyperon was found. This event was previously reported elsewhere (²) and further details are now given.

A star formed by the capture of a K^- meson at rest was seen to give rise to a single fast baryon. After traversing a distance of 2.88 mm, this particle decayed in flight into a proton of range 26.6 mm. From the point of decay there originated an electron pair. The proton made an angle of $23\frac{1}{2}^\circ$ to the direction of the primary track and its energy, 91.6 MeV, was determined from the range.

If the event be interpreted as the decay of a Σ^+ hyperon according to the scheme

$$(1) \quad \Sigma^+ \rightarrow p + \pi^0$$

the energy of the primary can be estimated from the dynamics of the decay. Assuming a Σ^+ mass of 1189 MeV, its energy was calculated to be (60 ± 5) MeV, which is in agreement with an energy determination from blob and hole measurements on the track itself of (69 ± 5) MeV. The interpretation of the event appears well-established.

It was further calculated that the π^0 meson was emitted at an angle of $(93 \pm 6)^\circ$ to the direction of the Σ^+ hyperon and had an energy of (84 ± 5) MeV in the laboratory system. The electron pair, which had an opening angle of the order of 1° , was emitted at an angle of $(51 \pm 6)^\circ$ to the direction of the π^0 meson. Multiple scattering measurements were possible on both electrons and using cells of length 50 μm and 100 μm , the energies of the electrons after correcting for noise were estimated to be (85^{+32}_{-18}) MeV and (28^{+10}_{-6}) MeV, giving for the total energy of the pair, (113^{+35}_{-20}) MeV.

The most probable explanation of this

(¹) EUROPEAN K^- STACK COLLABORATION REPORTS (presented by C. DILWORTH): *Rochester Conference Report VI-19* (1957).

(²) EUROPEAN K^- STACK COLLABORATION REPORTS (presented by D. J. PROWSE): *Padua-Venice Conf. Report II-5* (1957).

(³) EUROPEAN K^- STACK COLLABORATION REPORTS (presented by F. R. STANNARD): *Padua-Venice Conf. Report VIII-10* (1957).

pair is that it arises from the internal conversion ^(4,5) of one of the 2 photons in the normal decay of the π^0 meson, *i.e.*

$$(2) \quad \pi^0 \rightarrow e^+ + e^- + h\nu.$$

by EKSPONG and NILSSON ⁽⁶⁾ who experienced difficulty in obtaining a satisfactory energy balance. They suggested several possible reasons, one of which being another mode of decay for the π^0

TABLE I.

Particle	Dip angle	Energy (MeV)	Method of energy determination
Proton	$1\frac{1}{2}^\circ$	91.5	Range
Σ^+ hyperon	$8\frac{1}{2}^\circ$	69 ± 5 60 ± 5	Blob and Hole Dynamics
Electron pair	$6\frac{1}{2}^\circ$	113^{+35}_{-20} 82 ± 10	Multiple scattering Dynamics

In this case the energy of the converted photon calculated from the dynamics of the event would be (82 ± 10) MeV, which is in agreement with the experimental value. These results are summarized in the Table I.

DALITZ ⁽⁴⁾ predicts that one π^0 meson in about 80 will exhibit the alternative mode of decay into a pair and a photon. The European K^- stack collaboration has this one event compared with 123 protonic decays of Σ^+ hyperons without an associated electron pair.

A similar event has been described

into a pair and more than 1 photon. Our event, however, is quite consistent with a decay scheme for the π^0 meson as given in (2).

* * *

The authors wish to express their thanks to Professor E. J. LOFGREN for exposing the stack to the Bevatron. We are grateful to the other members of the K^- stack collaboration, without whose help this work would not have been possible. Two of us (D.H.D. and F.R.S.) are indebted to the Department of Scientific and Industrial Research and the other (M.A.S.) to the Government of Pakistan for financial support.

⁽⁴⁾ R. H. DALITZ: *Proc. Phys. Soc. (London)*, **A 64**, 667 (1951).

⁽⁵⁾ N. M. KROLL and W. WADA: *Phys. Rev.*, **98**, 1355 (1955).

⁽⁶⁾ A. G. EKSPONG and S. NILSSON: *Phys. Rev. Lett.*, **1**, 36 (1958).

LIBRI RICEVUTI E RECENSIONI

G. HOLTON and D. H. D. ROLLER — *Foundations of Modern Physical Science*. Addison-Wesley Publishing Company, Inc. (1958).

Nell'*Amer. Journ. of Phys.* vol. 25 pp. 417-424 (1957), è pubblicato uno studio intitolato: «Miglioramento della qualità e dell'efficacia dei corsi di introduzione alla fisica». Questo studio rappresenta il resoconto di una conferenza patrocinata dall'American Association of Physics Teachers (AAPT). In esso si auspica che l'insegnamento dei corsi introduttivi di fisica venga focalizzato su «sette principi e concetti basilari» e precisamente: conservazione del momento, conservazione della massa e dell'energia, conservazione della carica, campi, struttura molecolare della materia, ed infine struttura dell'atomo. Questo al fine di permettere un maggiore approfondimento da parte dello studente dei principi generali unificatori della fisica, anche a costo di un sacrificio per ciò che riguarda l'estensione di detto insegnamento. Si raccomanda inoltre in sostanza, di ottenere questo approfondimento degli argomenti trattati anche insegnando i limiti degli «strumenti concettuali» impiegati e lo sviluppo storico delle idee base delle scienze fisiche.

Il libro di G. HOLTON (professore di fisica nella Harvard University) e di D. H. D. ROLLER (professore della storia della scienza nella Oklahoma University) si propone appunto di presentare un corso di fisica generale per studenti in scienze naturali mediche, umanistiche e sociali, che realizzi nel modo migliore le direttive

del congresso dell'AAPT cui sopra abbiamo accennato.

La caratteristica più originale ed interessante è certamente il modo con cui la storia delle scienze fisiche è stata inserita nella esposizione didattica dei principi della fisica. Il criterio adottato, infatti, evita una esposizione secondo un ordine storico cronologico, che non è necessariamente coincidente con quello richiesto dalla logica e coerenza interne dell'argomento trattato. Precisamente l'approfondimento storico è inserito nei vari argomenti, i quali però sono ordinati secondo gli schemi che l'esperienza didattica ha ormai ritenuto più idonei.

La prima e la seconda parte del volume trattano la cinematica e la dinamica con estesi riferimenti al «Dialogo sopra i due massimi sistemi» e al «Discorso intorno a due nuove scienze» di Galileo. La parte III è invece dedicata esclusivamente allo studio dei sistemi planetari, e in essa viene presentato lo sviluppo storico delle varie concezioni dei moti planetari fino alla definitiva introduzione della legge della gravitazione universale, che generalizza l'introduzione di un tipo di forza necessaria per rendere coerenti la cinematica Kepleriana dei moti planetari con la nuova dinamica di Galileo-Newton. Dopo una parte IV dedicata a considerazioni generali sui metodi e la struttura logica della scienza fisica, si ha una parte V dedicata ai fondamentali principi di conservazione (della massa, del momento, dell'energia) ed una parte VI dove si espongono le origini e gli sviluppi della teoria atomistica del secolo XIX. Infine le parti VII, VIII e IX trat-

tano rispettivamente del campo elettromagnetico, dello sviluppo della fisica quantistica della luce e della materia e di alcuni aspetti della moderna concezione del nucleo atomico.

Possiamo dire che gli scopi perseguiti dagli autori siano stati raggiunti? In realtà solo dopo un pratico impiego del libro in un corso di insegnamento si potrebbero trovare gli elementi per una risposta definitiva. Scorrendo il bel volume di HOLTON e ROLLER si ha l'impressione di una esposizione particolarmente chiara e completa, anche tenendo conto dell'estrema elementarità dei mezzi matematici impiegati. Soprattutto va lodato senza riserve lo sforzo fatto dagli autori per la storicizzazione degli argomenti e la chiarificazione dei problemi umanistici e filosofici posti dalla scienza moderna.

Troppo spesso s'incontrano studenti convinti che i più importanti scopi della meccanica siano quelli di spiegare il periodo di oscillazione di un pendolo o la traiettoria di una palla da cannone, mentre nella loro mente la meccanica celeste ha un posticino, seppur ne ha uno, praticamente inapprezzabile. Pensiamo pertanto che questo volume sia di un grande interesse didattico, e formuliamo la fondata speranza che possa venire presentato in versione italiana da qualche nostro editore di buona volontà.

G. DIAMBRINI-PALAZZI

Symposium No. 6 of the I.A.U. Electromagnetic Phenomena in Cosmical Physics. Edited by B. LEHNERT, Cambridge University Press, 1958, pp. 545, 50 scellini.

Negli ultimi dieci anni le ricerche di astrofisica sono state caratterizzate da un crescente interesse verso fenomeni di carattere elettromagnetico. Da un lato molti lavori sono stati dedicati alla

magnetoidrodinamica (l'idrodinamica di fluidi conduttori in presenza di campi magnetici ed elettrici), dall'altro si è intensificato lo studio teorico e sperimentale del plasma in campo magnetico.

Espressione di questi nuovi interessi è stato il VI Symposium della International Astronomical Union, tenuto a Stoccolma nel 1956, di cui il presente volume contiene il resoconto.

Gli argomenti trattati possono venire classificati nelle seguenti categorie: a) « magnetoidrodinamica fondamentale », che nonostante il carattere prevalentemente teorico della maggioranza dei lavori, comprende lavori sperimentali di B. LEHNERT e di W. H. BOSTICK; b) « magnetismo stellare », con lavori in cui osservazione e teoria sono strettamente collegate; c) « fenomeni elettromagnetici all'interno del sistema solare », che comprendono i seguenti argomenti: l'elettrodinamica solare, cioè i problemi riguardanti il campo magnetico solare, le sue perturbazioni, i brillamenti, ecc. (T. G. COWLING presenta a questo proposito, un'esposizione chiara e concisa dello sviluppo storico delle teorie, dai tempi di Hale fino ad oggi); le tempeste magnetiche, per le quali V. C. A. FERRARO espone lo stato attuale della teoria corpuscolare; le aurore boreali; l'importantissimo studio delle condizioni elettromagnetiche dello spazio interplanetario per mezzo dell'analisi delle variazioni, sia in intensità che in energia, dei raggi cosmici.

Il volume comprende inoltre tre lavori di scienziati sovietici sulla produzione di scariche gassose ad altissima intensità di corrente, in relazione al problema della realizzazione in laboratorio di reazioni termonucleari controllate.

Il presente volume dà una chiara idea dello stato attuale delle nostre conoscenze sulle questioni di elettromagnetismo che interessano l'astrofisica. C'è però da rammaricarsi che la pubblicazione sia avvenuta ben due anni dopo il Symposium.

In particolare, per quanto riguarda i raggi cosmici, il trascorso anno Geofi-

sico Internazionale ha fornito dati ulteriori che mettono in nuova luce i modelli dello spazio interplanetario descritti nel 1956 a Stoccolma.

S. SEGRE

J. SHARPE and D. TAYLOR - *Mesure et détection des rayonnements nucléaires*, pag. XI+321. Dunod, Paris (1958).

L'editore Dunod di Parigi ha avuto la felice idea di riunire in un unico volume la traduzione francese (adattata da J. CHATELET) di due volumetti precedentemente pubblicati dalla Methuen di Londra nella sua ottima collezione di brevi monografie informative. I due volu-

metti, riuniti in questo unico volume, sono già noti al pubblico nell'edizione inglese e si presentano di facile lettura dando un quadro chiaro e ben impostato dei problemi relativi alla tecnica di rivelazione e di misura delle radiazioni nucleari.

L'esposizione è ricca di dati e di dettagli sperimentali illustrati da numerosi grafici e disegni. Tutto questo rende la lettura particolarmente utile a chi voglia rapidamente acquistare un succinto ma essenziale aggiornamento sugli argomenti trattati.

La buona bibliografia che segue ogni capitolo e la considerevole quantità di informazioni ivi raccolte consentono una utile consultazione di questo libro anche da parte dello specialista.

A. ALBERIGI

PROPRIETÀ LETTERARIA RISERVATA

Direttore responsabile: G. POLVANI

Tipografia Compositori - Bologna

Questo fascicolo è stato licenziato dai torchi il 28-II-1959.

tano rispettivamente del campo elettromagnetico, dello sviluppo della fisica quantistica della luce e della materia e di alcuni aspetti della moderna concezione del nucleo atomico.

Possiamo dire che gli scopi perseguiti dagli autori siano stati raggiunti? In realtà solo dopo un pratico impiego del libro in un corso di insegnamento si potrebbero trovare gli elementi per una risposta definitiva. Scorrendo il bel volume di HOLTON e ROLLER si ha l'impressione di una esposizione particolarmente chiara e completa, anche tenendo conto dell'estrema elementarità dei mezzi matematici impiegati. Soprattutto va lodato senza riserve lo sforzo fatto dagli autori per la storicizzazione degli argomenti e la chiarificazione dei problemi umanistici e filosofici posti dalla scienza moderna.

Troppo spesso s'incontrano studenti convinti che i più importanti scopi della meccanica siano quelli di spiegare il periodo di oscillazione di un pendolo o la traiettoria di una palla da cannone, mentre nella loro mente la meccanica celeste ha un posticino, seppur ne ha uno, praticamente inapprezzabile. Pensiamo pertanto che questo volume sia di un grande interesse didattico, e formuliamo la fondata speranza che possa venire presentato in versione italiana da qualche nostro editore di buona volontà.

G. DIAMBRINI-PALAZZI

Symposium No. 6 of the I.A.U. Electromagnetic Phenomena in Cosmical Physics. Edited by B. LEHNERT, Cambridge University Press, 1958, pp. 545, 50 scellini.

Negli ultimi dieci anni le ricerche di astrofisica sono state caratterizzate da un crescente interesse verso fenomeni di carattere elettromagnetico. Da un lato molti lavori sono stati dedicati alla

magnetoidrodinamica (l'idrodinamica di fluidi conduttori in presenza di campi magnetici ed elettrici), dall'altro si è intensificato lo studio teorico e sperimentale del plasma in campo magnetico.

Espressione di questi nuovi interessi è stato il VI Symposium della International Astronomical Union, tenuto a Stoccolma nel 1956, di cui il presente volume contiene il resoconto.

Gli argomenti trattati possono venire classificati nelle seguenti categorie: a) « magnetoidrodinamica fondamentale », che nonostante il carattere prevalentemente teorico della maggioranza dei lavori, comprende lavori sperimentali di B. LEHNERT e di W. H. BOSTICK; b) « magnetismo stellare », con lavori in cui osservazione e teoria sono strettamente collegate; c) « fenomeni elettromagnetici all'interno del sistema solare », che comprendono i seguenti argomenti: l'elettrodinamica solare, cioè i problemi riguardanti il campo magnetico solare, le sue perturbazioni, i brillamenti, ecc. (T. G. COWLING presenta a questo proposito, un'esposizione chiara e concisa dello sviluppo storico delle teorie, dai tempi di Hale fino ad oggi); le tempeste magnetiche, per le quali V. C. A. FERRARO espone lo stato attuale della teoria corpuscolare; le aurore boreali; l'importantissimo studio delle condizioni elettromagnetiche dello spazio interplanetario per mezzo dell'analisi delle variazioni, sia in intensità che in energia, dei raggi cosmici.

Il volume comprende inoltre tre lavori di scienziati sovietici sulla produzione di scariche gassose ad altissima intensità di corrente, in relazione al problema della realizzazione in laboratorio di reazioni termonucleari controllate.

Il presente volume dà una chiara idea dello stato attuale delle nostre conoscenze sulle questioni di elettromagnetismo che interessano l'astrofisica. C'è però da rammaricarsi che la pubblicazione sia avvenuta ben due anni dopo il Symposium.

In particolare, per quanto riguarda i raggi cosmici, il trascorso anno Geofi-

and of the artificial coloring of biotites by means of experimental irradiation ⁽³⁾ has confirmed this fact.

The curve of coloration, up to its inversion as a function of the dose of α (in arbitrary units), was obtained by JEDRZEJOWSKI ⁽⁴⁾ (Fig. 1). The inversion of the coloration has been attributed ⁽⁵⁾ to the progressive metamictization of the biotite, the α , at the end of their paths displacing the atoms from their lattice sites.

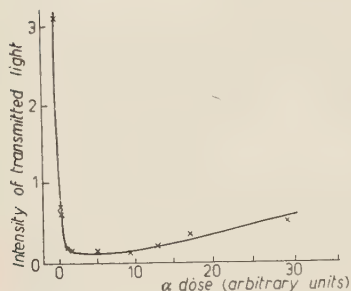


Fig. 1. — Blackening of a biotite of pegmatite by the action of the α -particles (after H. JEDRZEJOWSKI).

The determination of the quantitative relation existing between the halo colour and the α irradiation doses, which is the object of this note, presents an interest both for an understanding of the phenomena of coloration and in the application of the haloes for an estimation of the ages of rocks ⁽⁶⁾.

This determination has become possible only since the perfection of the technique of photographic emulsions used in nuclear research, which permits an evaluation of the very low concentrations of uranium and thorium (of the order of 10^{-10} ÷ 10^{-13} uranium) contained in the radioactive minerals (inclusions) around which the haloes are formed.

Using microphotometric measurements, we have deduced this relation from the study of the coloration of the halo profiles in rocks of known ages ⁽⁶⁾.

The photoregistered profiles of the haloes give the relation between the intensity of the light transmitted across the irradiated biotite and that across the non irradiated biotite as a function of the distance from the inclusion. The increase in optical density at any point across the halo is easily deduced, being evaluated across a thickness of 30 μ m, which is the mean thickness of the thin sections of rock used.

The variation of ΔD across a profile is parallel to and explained by the variation of the number of ions per unit of volume as a function of distance from the inclusion.

For our study, we have chosen haloes with inclusions which may be considered as thick layers ($> 40 \mu$ m), in order that the coloration be independent of the form and size of the inclusion.

⁽³⁾ G. KURTI: *Ber.*, IIa, **174** (Wien, 1938), p. 401.

⁽⁴⁾ H. JEDRZEJOWSKI: *Compt. Rend.*, **135**, (1928).

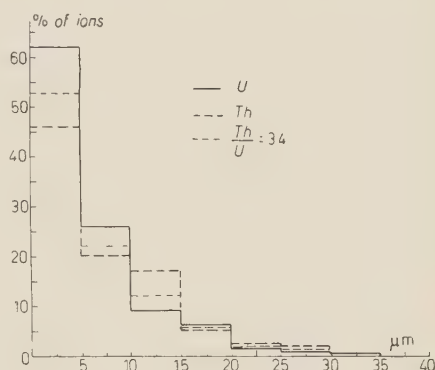
⁽⁵⁾ P. HURLEY and H. FAIRBAIRN: *Bull. Geol. Soc. Am.*, **64**, 659 (1953).

⁽⁶⁾ S. DEUTSCH, D. HIRSCHBERG and E. PICCIOTTO: *Bull. Soc. Belg. Géol.*, **65**, 267 (1956); S. DEUTSCH, P. KIFFER and E. PICCIOTTO: *Nuovo Cimento*, **6**, 796 (1957).

1. - The variation of the number of ions with respect to distance from the source.

The variation of the number of ions with respect to the distance from the source, in α -thick layer emission may be calculated after EVANS (7). Fig. 2 gives the distributions p_x^{x+5} of the number of ions formed in 5 μm thick bands of biotite (~ 1 cm air) as a function of their distance from a source containing either one of the U or Th families in equilibrium, or a mixture of the two families in the ratio $\text{Th}/\text{U} = 3.4$. Bragg's law has here been considered valid for solids, which implies that the total number of ions formed by the α -particles, as well as their distribution, are the same in the biotite and in the air, taking into account the relative α -stopping power of biotite to air which is of the order of 2000.

Fig. 2. - Distribution of the number of ions P , formed in the biotite as a function of their distance from an α -thick radioactive source.



2. - The curves of ΔD with respect to the number of ions per unit volume.

The halo profiles having been divided into 5 μm wide bands, the mean optical density increase ΔD has been evaluated for every band. The total number of α per unit surface being known (Q_T), the number of ions N_i per unit volume follows:

$$N_i = 2 \cdot 10^3 \cdot P_x^{x+5} \cdot q \cdot Q_T \text{ cm}^{-1},$$

q is the mean total number of ions formed per α emitted from a thick layer, being of the order of 10^5 for $\text{Th}/\text{U} = 3.4$. The factor $2 \cdot 10^3 \text{ cm}^{-1}$ appears in the equation due to the fact that the number of ions has been calculated for a band of 5 μm .

Fig. 3 gives ΔD as a function of N_i for the biotites of the dated granites of Kalule (Congo, 1000 My.), Allt Mhoille (Scotland, 310 My.), St. Amarin, St^e Marie (Vosges, 230 My.), La Bresse (Vosges, 340 My.) and Elba (Italy,

(7) R. EVANS: *Phys. Rev.*, **45**, 29 (1934).

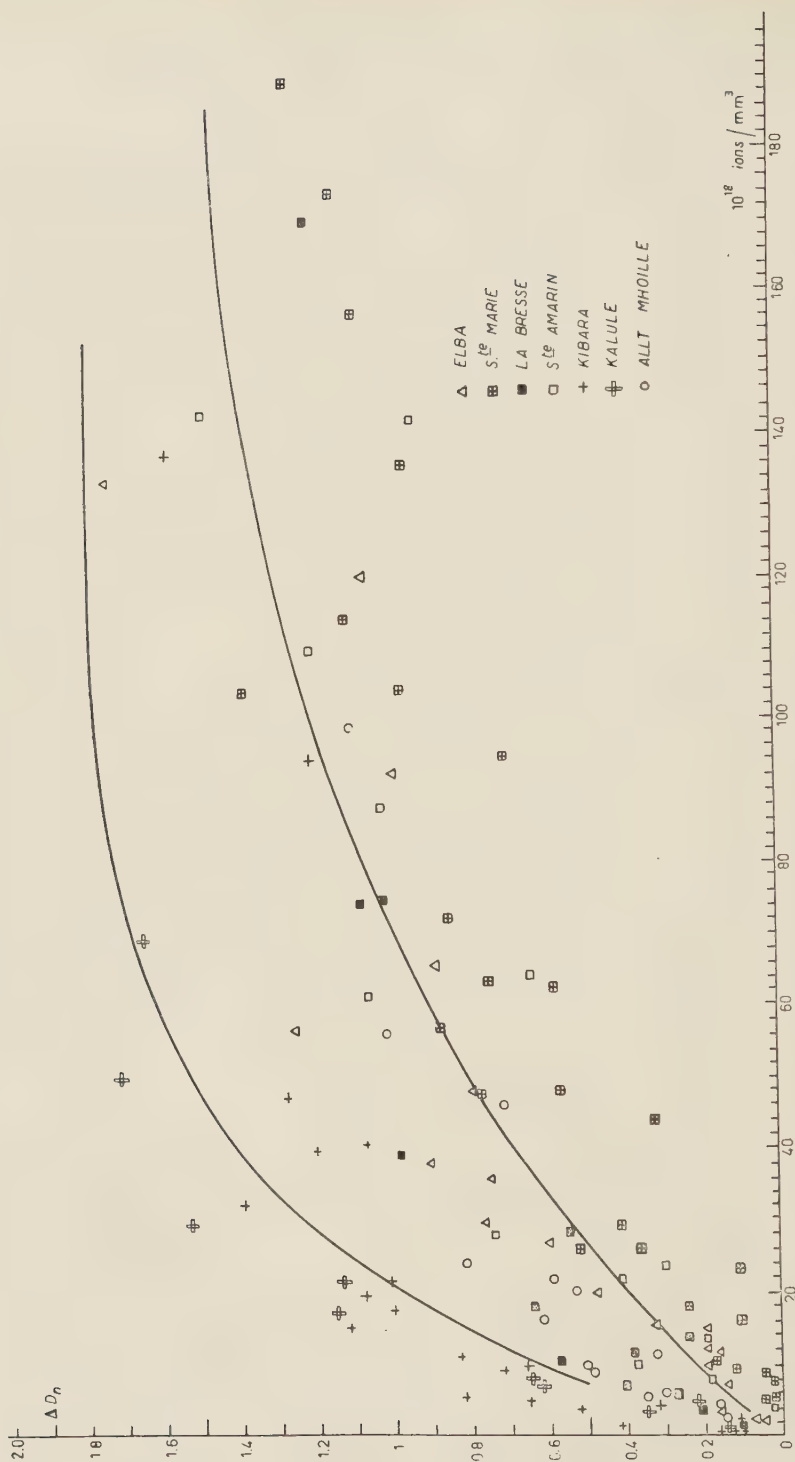


Fig. 3. -- Increase in optical density of the haloes as a function of the number of ions per mm^3 .

30 My.), which have been previously studied (⁶). The various sets of points thus obtained fall in the vicinity of curves of the form

$$\Delta D = \Delta D_{\max}(1 - \exp[-\varrho N_i]),$$

where ΔD_{\max} is the optical density corresponding to saturation of the coloration, this value being easily deduced from saturated haloes, ϱ is the fraction of the total number of colour centers formed per ion per unit volume.

A parameter S may be introduced where $S = 0.69/\varrho$ is the number of ions necessary in order to obtain an increase in density equal to $\Delta D = \Delta D_{\max}/2$.

Table I gives the values of this parameter for the biotites in question.

TABLE I. — *The parameters ϱ , S and ΔD_{\max} for the curves of increasing optical density as a function of the number of ions per unit volume in the haloes.*

Rock	ΔD_{\max}	ϱ 10 ⁻²⁰ mm ³ /ions	S 10 ¹⁸ ions/mm ³
Kalule	1.8	4	18
Kibara			
Allt Mhoille	1.2	3.7	20
St-Amarin	1.4	1.4	50
Ste Marie			
La Bresse	1.5	1.7	40
Elba	1.8	1.9	36

It is noted that the higher the values of ΔD_{\max} and ϱ , the higher is the sensitivity of the biotite to α irradiation. The commencement of the coloration appears for doses of the order of 10¹⁸ ions/mm³. The values set out cannot be given more precisely because:

- 1) The ratio Th/U of the inclusion is not measurable.
- 2) The uncertainties in the α activity and in the age of the rocks are, at best, of the order of 10%.
- 3) A part of the coloration is due to the displacement of the atoms at the end of the α -particle path, when the particle has ceased to cause ionization.

The distribution of the α path endings, with respect to their distance from a α -thick source, may be calculated after FINNEY and EVANS (⁸) (Fig. 4). The

(⁸) G. FINNEY and R. EVANS: *Phys. Rev.*, **48**, 503 (1935).

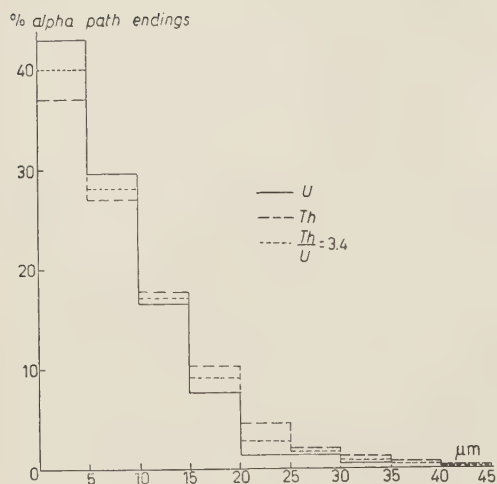


Fig. 4. — Distribution of the number of α -particles V ending in the biotite as a function of their distance from an α -thick radioactive source.

3. — Inversion of the coloration.

An analysis of the profiles of inversed haloes gives us information on the curve of the coloration of the biotite, with respect to the ionization caused by strong doses of α , an inversed halo being a halo which presents an inversion of coloration, at least at the beginning of its radius.

Fig. 5 presents the typical appearance of the profile of an inversed halo. The halo itself is shown in the Fig. 6, which is focussed on the biotite, through the nuclear emulsion, the α -particles emitted by the inclusion being visible as well.

It has been shown ⁽⁶⁾ that approximately 10^{17} α /cm² are necessary in order

ratio of the number of α endings to the number of ions per unit volume remains relatively constant for all distances from the source; the α path ending effect cannot, therefore, be evaluated from a study of the profiles of non-angular haloes.

The biotites thus indicate different sensitivities to α irradiation, the order of sensitivity being Congo > Allt Mhoille > Elba > Bresse > St. Marie. In Fig. 3, two curves only have been traced in order to demonstrate this more clearly: the curve corresponding to the granites of the Congo, and a mean curve for the other biotites.

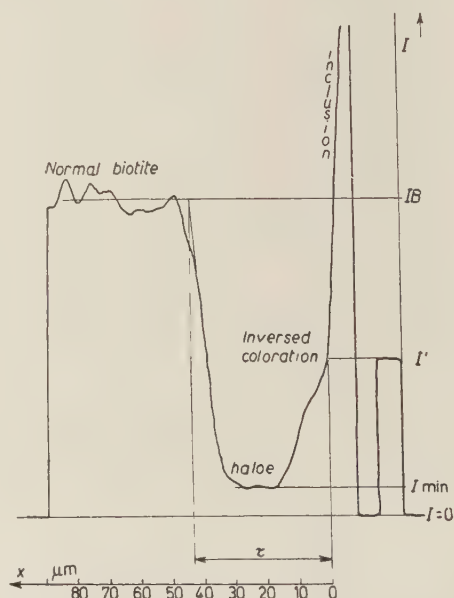


Fig. 5. — Photoregistered profile of the inversed halo shown in photo 6.



Fig. 6.

to form an inversed halo in the case of rocks from the Vosges and from Scotland.

Figs. 7a and 8a show the increase in optical density ΔD with respect to

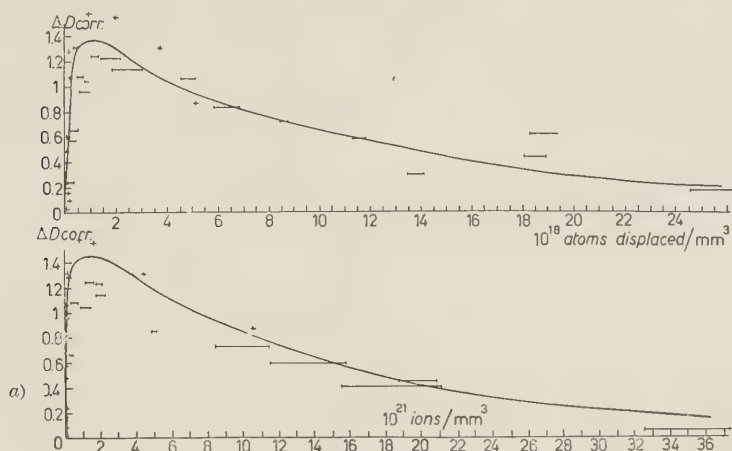


Fig. 7a, b. — a) Increase in optical density as a function of the number of ions produced per mm^3 , after the inversed haloes of La Bresse; b) Increase in optical density as a function of the number of atoms displaced per mm^3 after the inversed haloes of La Bresse.

the number of ions per unit volume for the granites of La Bresse and St. Amarin; haloes of a radius $> 40 \mu\text{m}$ have been considered as due to either $\text{Th}/\text{U} = 3.4$ or Th alone.

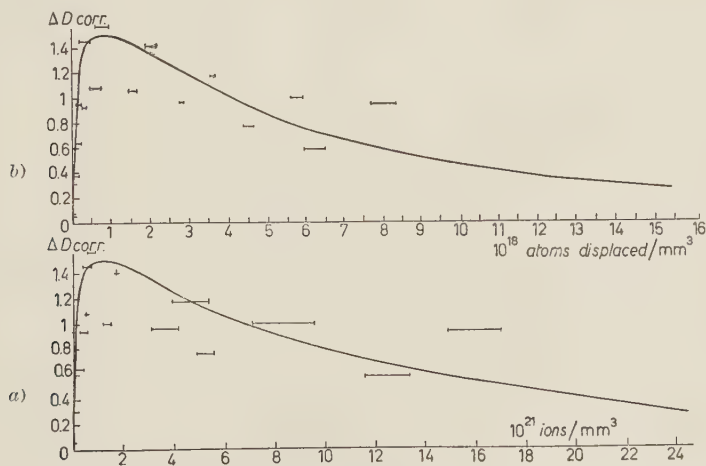


Fig. 8a, b. — a) Increase in optical density as a function of the number of ions produced per mm^3 , after the inversed haloes of St. Amarin; b) Increase in optical density as a function of the number of atoms displaced per mm^3 after the inversed haloes of St. Amarin.

A halo with a radius $r = 36$ (RaC') was attributed to the action of the α -particles due to the uranium family alone.

ΔD with respect to the number of ions per unit volume shows a rapid increase, which is studied in detail in the case of non inversed haloes, followed by a saturation and then a slow decrease.

The value of the ratio U/Th has an important influence on the value of N_i , and the uncertainty in this ratio prohibits anything but a numerical order of the importance of N_i to be given.

The saturation exists for doses of from $2 \cdot 10^{20}$ to $2.4 \cdot 10^{21}$ ions/mm³ according to an exponential curve of the type

$$\Delta D = \Delta D_{\max} \exp \left[-\frac{0.69}{S'} N_i + 0.166 \right],$$

where S' is of the order of 10^{22} ions/mm³ for the biotites of La Bresse and St. Amarin. This dose corresponds to a diminution of the optical density $\Delta D = \Delta D_{\max}/2$, obtained after the saturation. The inversion of the coloration in the biotite is a slower phenomenon than the coloration which explains the paucity of totally inversed haloes.

The shape of the coloration curve of the granitic biotites deduced from their haloes is seen to resemble the curve obtained by the experimental irradiation of the biotites of pegmatite by JEDRZEJOWSKI.

4) a) An approximative evaluation of the number of atoms displaced by an α -particle of energy E , penetrating into a solid, may be carried out according to the theoretical considerations of SEITZ⁽⁹⁾. We use his notations in the following text. The number of atoms displaced by an incident α -particle is thus:

$$(I) \quad N_{(E)} = \frac{R_d \cdot E_c}{\sqrt{E \cdot E_d}} = \left(\frac{E_c}{E_d} \right) \sqrt{\frac{\bar{E}}{E_d}} \cdot \frac{1}{\log E/E^*},$$

where E_c is the amount of energy lost by the α -particle in displacing atoms. E_c depends on the mean ionization energy of the medium and on ε_i , the threshold of electronic excitation, of a numerical order of a fraction of the lowest energy of excitation of the material traversed.

E_d : the minimum energy necessary in order to displace an atom from his lattice site;

E^* : the minimum energy which the α -particle can transmit to an atom;

\bar{E} : the mean kinetic energy transmitted to a displaced atom.

⁽⁹⁾ F. SEITZ: *Disc. Farad. Soc.*, **5**, 271 (1949).

Certain parameters which can be determined with great difficulty intervene in the expression for $N_{(E)}$. In order to indicate the extreme limits of the values, we have calculated (I) for an ensemble of values for these parameters, in the case of the biotite E lying between 0.5 and 10 MeV and $E_d = 10, 25, 50$ eV.

It appears that the second factor

$$\sqrt{\frac{E}{E_d}} \cdot \frac{1}{\log E/E^*},$$

remains practically constant in the region considered, and has a value of 0.16.

On the other hand, the first factor depends on the three values E , E_d , E_c or ε_t .

We have determined the value of the mean ionization energy from the path-energy relation of the α -particles in the biotite, and found it to be 240 eV. The energy ε_t is difficult to determine, we have chosen the values 0.1, 0.25, 0.50, 0.75, 1.0 and 1.50 eV in our calculations.

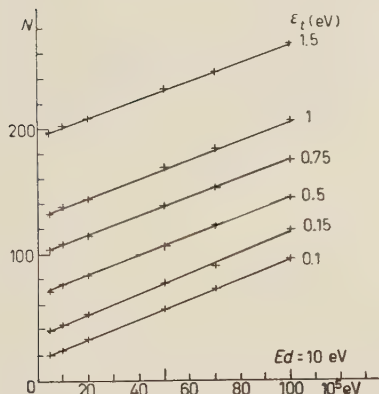


Fig. 9. — Number of the displaced atoms as a function of the energy of the α for $E_d = 10$ eV and different values of ε_t .

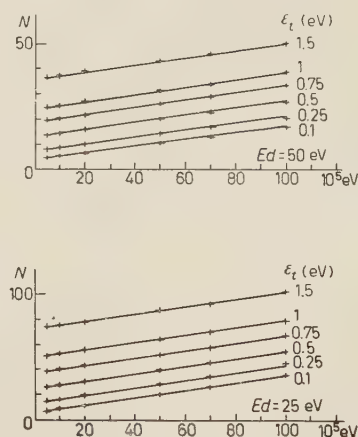


Fig. 10. — Number of the displaced atoms as a function of the energy of the α for $E_d = 50$ eV and 25 eV and different values of ε_t .

The results of these calculations are presented in the three graphs relative to the values of $E_d = 10, 25$ and 50 eV (Figs. 9, 10).

We have, here, shown N as a function of E for the different values of ε_t .

It will be noted that, for a certain medium (E_d and ε_t remaining constant), the number of atoms ejected increases in proportion to the energy E of the particle.

On the other hand, N depends on the values of E_d and ε_t , the former of which depends essentially on the composition of the medium, the latter, on its structure also.

By comparison with analogous elements, the most reasonable values appear to be $E_d = 25$ eV and $\varepsilon_t = 0.75$ eV, which, for α of 5 MeV in the biotite gives a value of N equal to

$$N = (55 \pm 25) \text{ displaced atoms.}$$

b) ΔD may be evaluated as a function of the number of atoms displaced in every 5 μm thick band of the inversed haloes (from the number of α endings). The Figs. 7*b* and 8*b* show such a function for the biotites of La Bresse and St. Amarin. It is seen that S_d , the number of atoms displaced corresponding to an inversion of the coloration such as $\Delta D = \Delta D_{\text{max}}/2$, is of the order of $0.5 \cdot 10^{19}$ displaced atoms per mm^3 , or, in other words, about $1.5 \cdot 10^{18}$ atoms per milligram of biotite. As 1 mg of biotite contains $9 \cdot 10^{19}$ atoms, the fraction of atoms displaced is of the order of 2%. The same line of reasoning applied to the almost complete effacement of the coloration, which is due to the displacement of about $2 \cdot 10^{19}$ atoms per mm^3 , attributes this effacement to the displacement of about 10% of the total number of atoms. Such a small fraction of displaced atoms invalidates an explanation of the inversion of the coloration as a result of the phenomenon of metamictization, which only appears when at least 25% of the atoms have been displaced. This reasoning concords with the approximate evaluations of PELLAS⁽¹⁰⁾.

4. - Conclusions.

The microphotometric study of the haloes, and the measurement of the activity of the inclusions, in rocks of known age, has enabled the determination of a quantitative law governing the increase in the coloration of the biotite as a function of the number of ions formed. The curve of the optical density increase ΔD consists of three parts:

1) An increasing part: the coloration increases according to an approximate law of the form

$$\Delta D = \Delta D_{\text{max}} \left(1 - \exp \frac{-0.69 N_i}{S} \right),$$

where N_i is the number of ions formed per mm^3 .

⁽¹⁰⁾ P. PELLAS: *Bull. Soc. Fr. Min. et Crist.*, **77**, 447 (1954).

S is the number of ions per mm^3 necessary in order to obtain an increase in optical density equal to

$$\Delta D = \frac{\Delta D_{\max}}{2},$$

ΔD_{\max} is the increase in density corresponding to the saturation of the coloration.

The coloration commences after the formation of about 10^{18} ions/ mm^3 .

The parameters S and ΔD_{\max} vary from one biotite to another; S being of the order of 10 to $50 \cdot 10^{18}$ ions/ mm^3 , and ΔD_{\max} lying between 1.2 and 1.8 for a photometered thickness of 30 μm .

2) A horizontal part: the coloration being saturated for doses from $2 \cdot 10^{20}$ to $2.4 \cdot 10^{21}$ ions/ mm^3 .

3) A decreasing part: the coloration diminishing for doses from $2.4 \cdot 10^{21}$ to $7 \cdot 10^{22}$ ions/ mm^3 . This inversion cannot be explained as a metamictisation of the biotite as the inversion of the coloration is almost complete with only about 10% of the lattice atoms having been displaced.

* * *

We are indebted to Mr. P. KIPFER and E. PICCIOTTO for many helpful discussions.

RIASSUNTO (*)

È stata esaminata la colorazione delle biotiti da parte delle particelle α come funzione del numero di atomi dislocati. Tale numero è stato calcolato in base alla teoria di F. Seitz. La colorazione aumenta, si satura e diminuisce con numero crescente di ioni.

(*) Traduzione a cura della Redazione.

An Experimental Analysis of Two Large Cosmic Ray Jets.

F. A. BRISBOUT and C. B. A. MCCUSKER (*)

*The F.B.S. Falkiner Nuclear Research and Adolph Basser Computing Laboratories,
School of Physics (**), The University of Sydney - Sydney N.S.W.*

(ricevuto il 2 Ottobre 1958)

Summary. — The true primary energy of two large jets has been estimated from a study of the secondary interactions and the electromagnetic cascades resulting from the decay of π^0 -mesons. This is compared with the energy estimated from $\gamma_p = 2/tg^2 \eta$ and found, in both cases, to be much greater. However, good agreement with the estimate of primary energy obtained using the tunnel theory of jets is found.

1. — Introduction.

One of the predictions of the tunnel theory ⁽¹⁾ of cosmic ray jets is that, in many cases (particularly those where a central collision with silver and bromine has occurred), the true primary energy will be much greater than the energy estimated from formulae (such as $\gamma_p = 2/tg^2 \eta$) which assume nucleon-nucleon collisions. Until about 1955 the only way in which this prediction could be in any way verified was by the good fit obtained on a $\log f$ - $\log E$ diagram (see ref. ⁽¹⁾) of all jets, or the comparison of events at the same γ_p such as the Bristol jets, $0+4p$ and $0+28p$ at $\gamma_p = 2000$. With the coming of larger stacks however the possibility arose of getting an independent esti-

(*) Visiting Professor from the Institute for Advanced Studies, Dublin.

(**) Also supported by the Nuclear Research Foundation within the University of Sydney.

⁽¹⁾ F. C. ROESLER and C. B. A. MCCUSKER: *Nuovo Cimento*, **10**, 127 (1953).

mate of the true primary energy either from relative scattering of the secondaries or from a study of the secondary interactions or the electromagnetic cascades. The first method was possible with the Turin jet ^(2,3). The second method is applied to two large jets in this paper. The jets are of the type $18+56p$, $\gamma_p = 2500$ (P_4) and $23+152p$, $\gamma_p = 7000$ (P_8). Because of the importance of the correct derivation of the primary energy in the study of the jets themselves, in the verification of the tunnel theory, and in the study of the cosmic ray energy spectrum, the methods used are given in some detail.

2. - Selection of events.

In order to determine the primary energy with some accuracy by a study of the electromagnetic cascades and of the secondary interactions, it is necessary to select events which have as large a number of cascades and interactions as possible. This means, in practice, that the method is applicable to jets with a large number of shower particles which themselves traverse a considerable quantity of emulsion. It is a fortunate circumstance that jets of large n_s are most likely to arise from central collisions with silver or bromine, for in this case the discrepancy between the energy estimated assuming a nucleon-nucleon collision and the true primary energy will be greatest and also the effects of a possibly large elasticity in the individual nucleon-nucleon collisions will be greatly reduced.

Two of the available jets, namely P_4 and P_8 ⁽⁴⁾ satisfied these criteria.

3. - The angular distribution of the shower tracks.

The angular distributions of the shower tracks for P_4 and P_8 are shown in Fig. 1 and 2. Target diagrams for the more centrally emitted tracks are given in Fig. 3 and 4. The values of γ_p , calculated from the median angle using

$$\gamma_p = \frac{2}{\text{tg}^2 \eta},$$

are 2500 for P_4 and 7000 for P_8 .

⁽²⁾ A. DEBENEDETTI, C. M. GARELLI, L. TALLONE and M. VIGONE: *Nuovo Cimento*, **4**, 1142 (1956).

⁽³⁾ C. B. A. McCUSKER and F. C. ROESLER: *Nuovo Cimento*, **5**, 1136 (1957).

⁽⁴⁾ F. A. BRISBOUT, C. DAHANAYAKE, A. ENGLER, Y. FUJIMOTO and D. H. PERKINS: *Phil. Mag.*, **1**, 605 (1956).

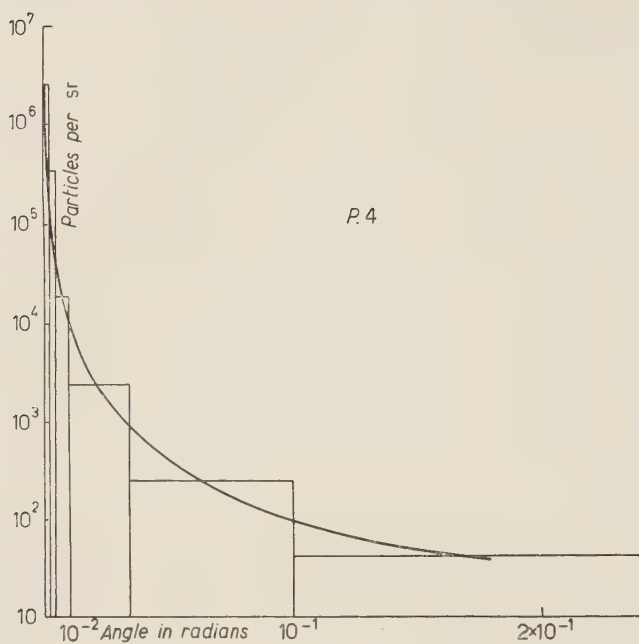


Fig. 1. — The angular distribution of the shower tracks in P_4 .

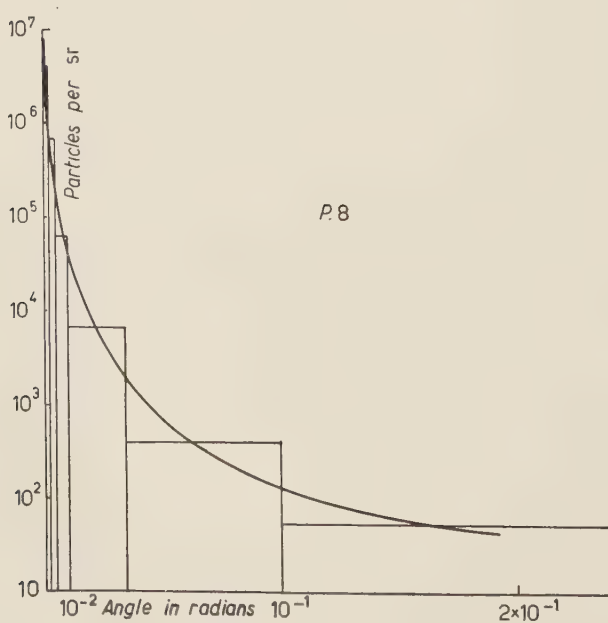
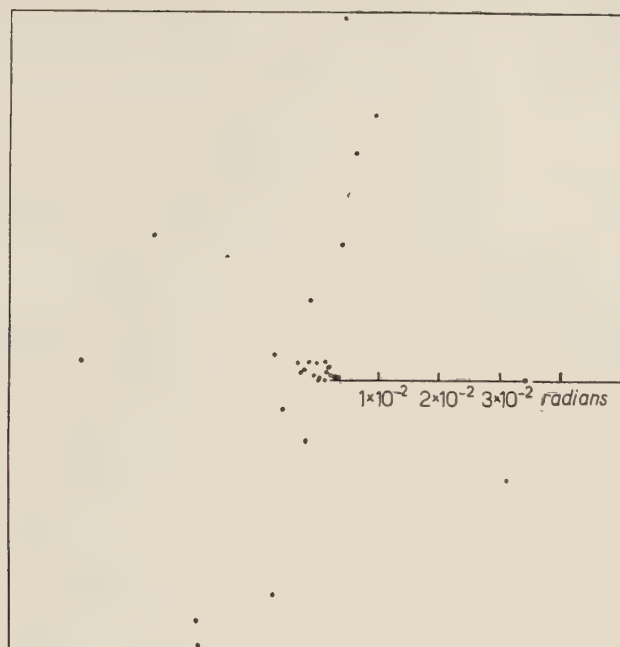


Fig. 2. — The angular distribution of the shower tracks in P_8 .

Fig. 3. - Target diagram for P_4 .

It is of interest to compare these two jets with others of similar γ_v . For instance DANIEL *et al.* ⁽⁵⁾ found two jets with $n_s = 7$ and γ_v respectively 2200

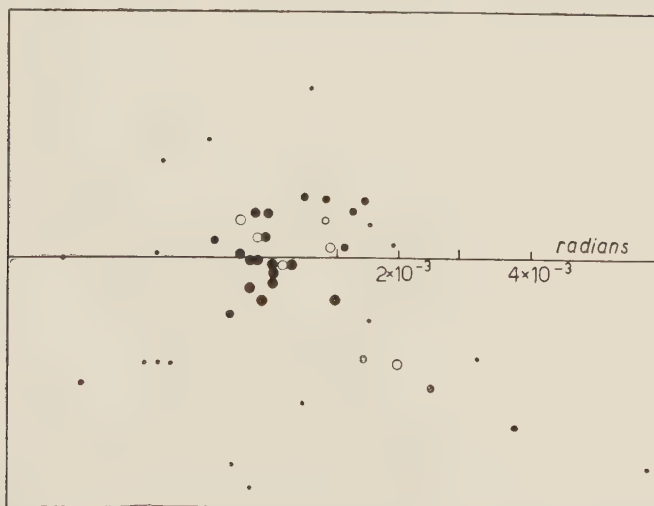


Fig. 4. - Target diagram for P_8 . Open circles correspond to particles producing a secondary interaction. The size of the circle is a rough indication of the energy of the particle.

⁽⁵⁾ R. R. DANIEL, J. H. DAVIES, J. H. MULVEY and D. H. PERKINS: *Phil. Mag.*, **43**, 753 (1952).

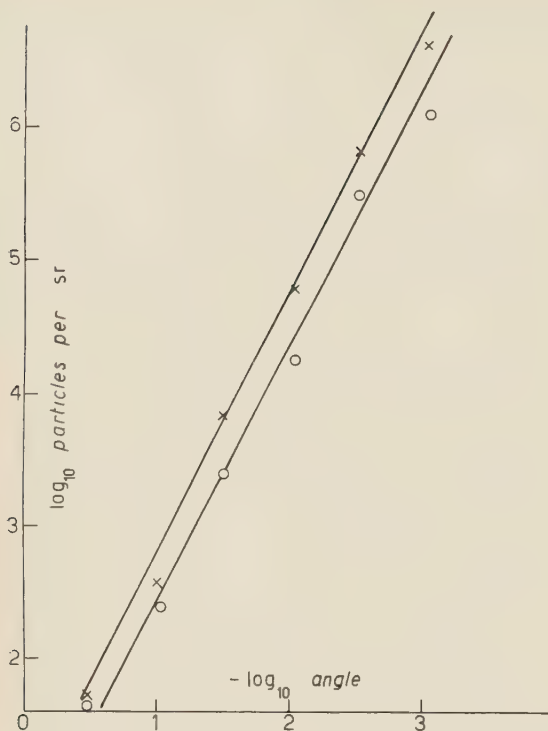


Fig. 5. — A double logarithmic plot of the angular distributions in P_4 and P_8 . The lines represent a law of the form $\text{Density} \propto 1/\theta^2$.

and 2300 and KAPLON and RITSON ⁽⁶⁾ found a jet with $n_s = 14$ and $\gamma_p = 7200$.

It can be seen from Fig. 5 that the number of tracks per steradian falls off approximately as the inverse square of the angle of emission in both cases. The average energy of the particles, as will be shown later, also falls off rapidly with the angle of emission. In such circumstances, if one wishes to get a reasonably accurate value for the total energy by estimating an average and then multiplying this by the number of particles, one must split the target diagram into a number of annuli, carry out this procedure separately for each and then sum the separate values.

For this reason the target diagram in both cases was subdivided as shown in Fig. 6

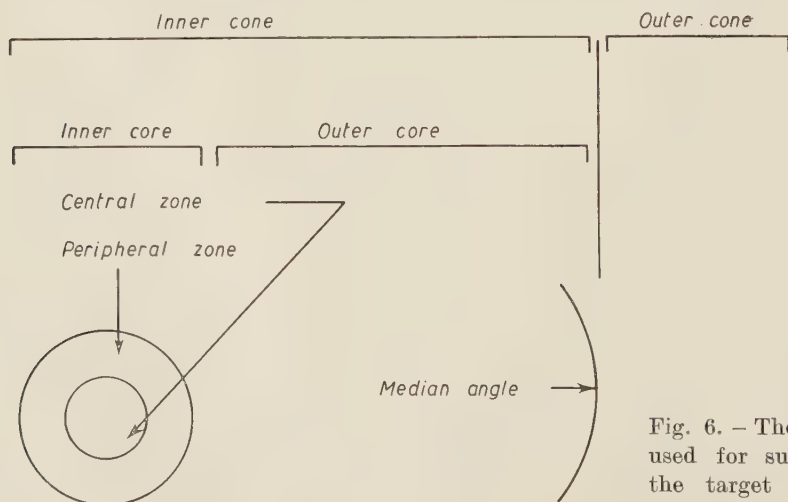


Fig. 6. — The method used for subdividing the target diagram.

⁽⁶⁾ M. F. KAPLON and D. RITSON: *Phys. Rev.*, **88**, 386 (1952).

The median angle is used to define two areas known as the inner and outer cones. The inner cone was then further subdivided into the inner and outer cores on the basis of the observed density of tracks. The inner core was then split into the central and peripheral zones, the central zone containing the particles of very high energy. Inspection of the average energies of the particles in the various annuli in Table I will make it obvious that this rather involved procedure is necessary.

TABLE I. — *This gives the angle of emission and γ_s for the various secondary interactions of jets P_4 and P_8 and the average γ_s for the various zones.*

Jet	Annulus	Secondary interaction	Angle of emission in rad	γ_s	Average γ_s
P_4	Inner Core				
	Central zone	$P_4S_{26}(5+23p)$ $P_4S_{27}(4+34p)$ $P_4S_{29}(12+20p)$	$2 \cdot 10^{-4}$ $4 \cdot 10^{-4}$ $6 \cdot 10^{-4}$	2 400 400 300	1 000
	Peripheral zone	$P_4S_{20}(13+8p)$ $P_4S_{22}(15+10p)$ $P_4S_{24}(10+15p)$	$2.0 \cdot 10^{-3}$ $2.1 \cdot 10^{-3}$ $2.6 \cdot 10^{-3}$	900 200 100	400
	Outer Core				
		$P_4S_{36}(0+5p)$	$1.7 \cdot 10^{-2}$	30	—
P_8	Inner Core				
	Central zone	$P_8S_{11}(11+14p)$ $P_8S_{22}(x+>7p)$ $P_8S_{30}(x+23p)$	$0.5 \cdot 10^{-4}$ $1 \cdot 10^{-4}$ $3 \cdot 10^{-4}$	5 000 > 1 000 500	2 800
	Peripheral zone	$P_8S_7(16+32p)$ $P_8S_5(3+25p)$ $P_8S_8(23+25p)$	$8 \cdot 10^{-4}$ $9 \cdot 10^{-4}$ $9 \cdot 10^{-4}$	300 200 100	200
		$P_8S_9(8+9p)$	$2.3 \cdot 10^{-3}$	3 000	3 000
	Outer Core				
		P_8S_6 P_8S_3	$2.3 \cdot 10^{-3}$ $3.9 \cdot 10^{-3}$	80 40	— —

4. — The determination of the primary energy from the secondary interactions.

The inner cones of jets P_4 and P_8 were scanned for secondary interactions using the methods of BRISBOUT *et al.* (4). It is essential that only second gene-

ration interactions be included. For events produced by charged shower particles one can make sure of this by tracing back the primary. For interactions produced by neutral particles this is not so and hence these were excluded. Table I shows the various interactions observed, the angles of emission of their primaries, their γ_s and the average γ_s for the various annuli. Two of the secondary interactions require some comment. The interaction P_8S_R occurred in an emulsion sheet which was destroyed when the stack landed. The shower tracks of the inner core were observed in the next emulsion and an estimate of γ_s was made from there, and also by means of relative scattering measurements on the primary tracks of P_8S_R and P_8R_{11} .

Event P_8S_9 occurred near the very noticeable « side core » seen at the target diagram shown in Fig. 7. It is of anomalously high energy for a track at such an angle and has been classed as being in the central zone.

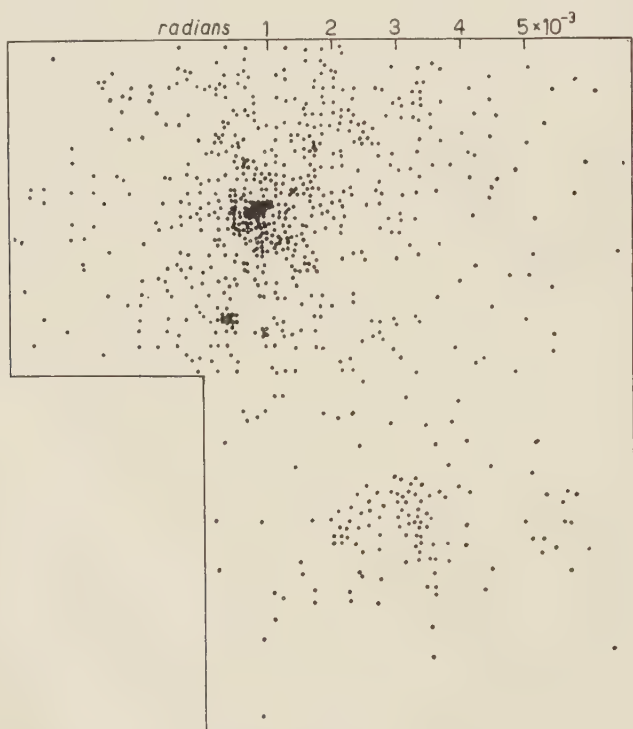


Fig. 7. — Diagram showing the development of the electromagnetic cascade in P_8 at a distance of about four cascade units from the origin.

Having obtained the average energy of the particles in each annulus it is then necessary, if one wishes to obtain the total energy, to multiply these averages by the number of particles in each annulus. Since only the charged

particles leave visible tracks, the number of charged particles in each annulus must be multiplied by a factor to allow for the neutral particles. The total number of shower particles n_T is given by

$$n_T = n_s \{1 + 0.4 + 0.25\} \approx 1.7 n_s,$$

where the second and third factors give the numbers of neutral pions and non pions respectively.

Using this factor and the values for $\langle \gamma_s \rangle$ given in Table I then, the primary energies of P_4 and P_8 are calculated in Table II.

TABLE II. — *The table shows the number of shower particles, their average γ_s and the total energy for each annulus. The total energy for the two jets is also given. The particles in the outer cone are neglected because of their very low average energy.*

Jet	Annulus	n_s	$\langle \gamma_s \rangle$	$1.7n_s \langle \gamma_s \rangle$
P_4	Central zone	6	1 000	10 200 GeV
	Peripheral zone	9	400	6 100
	Outer core	13	20	440
		Total		16 740
P_8	Central zone	7+1	2 800	38 100
	Peripheral zone	16	200	5 400
	Outer core	54	50	4 600
		Total		48 100

5. — The determination of the primary energy from the electromagnetic cascades.

For each jet target diagrams of all tracks were made at intervals of about one conversion length (~ 4 cm). One target diagram for P_8 is shown in Fig. 7. In the case of P_4 and the outer core of P_8 each cascade was traced back to its parent electron pair (*). The cascades from the parent electron pairs in P_4

(*) This method of detecting parent electron pairs was checked against that of BRISBOUT *et al.* and found to be 100% efficient.

which materialized before the first secondary interactions were analyzed with respect to their lateral spreads (⁷), using a radius of about 50 μm and suitable background corrections. The γ -ray energies thus obtained are shown in Table III. It proved to be impossible to treat P_8 in this detailed manner, because the cascades intermixed at too early a stage.

TABLE III. — *This gives the γ -ray and π^0 -meson energies for ten cascades of P_4 . The average energy for each annulus is also given.*

Jet	Annulus	Cascade	γ -ray energy	π^0 -meson energy	Weighted mean zone energy	Minimum π -meson energy from spatial angle between pairs
P_4	Central zone	1	500 \div 600 GeV	paired	(1 000 \div 1 200) GeV	1 000 GeV
		2	500 \div 600 GeV			
		3	400 GeV	paired	600 GeV	500 GeV
		4	200 GeV			
	Peripheral zone	5	200 GeV	paired	300 GeV	200 GeV
		7	100 GeV		200 GeV	—
		6	100 GeV	unpaired	taken as twice γ -ray energy	250
		8	100 GeV	unpaired	200 GeV	—
	Outer core	9	low energy 15 GeV	unpaired	30 GeV	20
		10	low energy 5 GeV	unpaired	10 GeV	—

Once again the average energy of a particle in each annulus must be multiplied by the total number of particles in the annulus in order to get the total energy. As before, n_s , the number of charged shower particles must be multiplied by 1.7 to allow for the unseen neutral particles. It is worth noting, that the total energy obtained in this case will probably be an underestimate for there is some evidence that the average energy carried off by pions is less than that carried off by non pions. (⁸). Table IV shows the experimental results for P_4 .

It is, perhaps, worth saying a little more about the cascade development in P_8 . It can be seen from Fig. 7 that there is a very marked «side shower»,

(⁷) K. PINKAU: in the press.

(⁸) B. EDWARDS, J. LOSTY, D. H. PERKINS, K. PINKAU and J. REYNOLDS: *Phil. Mag.*, **3**, 237 (1958).

TABLE IV. — *This gives n_s the number of shower particles and their average energy for each annulus for jet P_4 and the estimated total energy of the jet.*

Jet	Annulus	n_s	$\langle E_{\pi^0} \rangle$	$1.7n_s\langle E_{\pi^0} \rangle$
P_4	Central zone	6	800	8 250 GeV
	Peripheral zone	9	250	3 820 GeV
	Outer core	13	8	170 GeV
	Total			12 240 GeV

that is, there are two *spatially* separated regions of high electron density in the target diagram. The smaller of these regions appear to be associated with the secondary interaction P_8S_9 of anomalously high energy which was previously noted. If phenomena such as this occur at higher energies, they might explain some of the peculiar air shower distributions which have been noted ^(9,10) from time to time.

6. — Determination of the primary energy using tunnel theory.

In determining the primary energy using any cascade theory one must first ascertain, as far as possible, the path length of the cascade through nuclear matter. A very simple method of doing this is given in detail in ref. (1) and (3). Briefly, one takes the two experimental parameters n_s and γ_p and, using the formula given by the theory, one computes f , the multiplicity parameter, and E' , the primary energy on each of the two extreme assumptions, that the event was a nucleon-nucleon collision and that the event was a central collision with silver. From the positions of the two points on a $\log f$ - $\log E'$ plot, the path length through nuclear matter can be estimated. The calculation takes about five minutes.

Treating P_4 in this way one finds that it was due to a central or near central collision with silver. According to the theory the primary energy is then given by

$$E'_{\text{GeV}} = 5.76 \gamma_p = 14\,400 \text{ GeV}.$$

⁽⁹⁾ T. E. CRANSHAW and W. GALBRAITH: *Proc. Oxford Conf.* (1956), A.E.R.E. Report.

⁽¹⁰⁾ C. CLARK, J. EARL, W. KRAUSHAAR, J. LINSLEY, B. ROSSI and F. SHERB: *Nature*, **180**, 353 (1957).

The position with regard to P_8 is rather more complicated. The $\log f$ - $\log E'$ diagram suggests that the path length through nuclear matter was greater than that across the diameter of a silver nucleus. This, of course, is assuming that the primary particle was a proton with the usual geometric interaction cross-section. Two ways out of this difficulty suggest themselves:

a) One can assume that at an early stage in the cascade a particle was scattered at an anomalously wide angle, resulting in the formation of a side tunnel, or an enlargement in one direction of the diameter of the main tunnel or

b) One can assume that the primary was a deuteron ⁽¹¹⁾.

Alternative b) is attractive because on this assumption one obtains an excellent fit on the $\log f$ - $\log E'$ diagram. The possibility of deuterons occurring as the primaries of jets has been envisaged by DILWORTH *et al.* Indeed it seems very likely that the proportion of deuterons in the primary cosmic ray beam is much higher than in the universe as a whole. Deuterons can be found as fragmentation products of heavy nuclei and α -particles in collisions both with interstellar matter and with the atmosphere above the balloon flight level. The proportion of deuterons and tritons in singly charged particles from stars in emulsion is ~ 30 percent ⁽¹²⁾. Assuming that the primary particle was a deuteron, its primary energy per nucleon is given by

$$\frac{1}{2} E'_{\text{GeV}} = 5.29 \gamma_p$$

that is, the total energy was 74 000 GeV. This is considerably higher than the estimate from the secondary interactions, but it must be remembered that this last may well be an underestimate.

7. - Conclusions.

For jet P_4 the primary energy estimated assuming a nucleon-nucleon collision was 2 500 GeV. The energy estimated from a study of the secondary interactions was 16 740 GeV and from a study of the electromagnetic cascades was 12 200 GeV. An application of the Tunnel Theory of jets suggested that the event was a central collision with silver and gave an estimate of 14 400 GeV for the primary energy. The good agreement in the last three cases is obvious.

For P_8 the energy estimated assuming that it was a nucleon-nucleon col-

⁽¹¹⁾ C. C. DILWORTH, S. J. GOLDSACK, T. F. HOANG and L. SCARSI: *Nuovo Cimento*, **10**, 1261 (1953).

⁽¹²⁾ U. CAMERINI, W. O. LOCK and D. H. PERKINS: *Progr. in Cosmic Ray Phys.*, vol. **1**.

lision is 7 000 GeV. The estimate from the study of the secondary interactions is 48 100 GeV and from the Tunnel Theory, assuming that the primary is a proton, 49 000 GeV. In both cases, therefore, it is very difficult to get agreement with the assumption that the events are nucleon-nucleon collisions, but good agreement can be obtained with the energy estimates based on the Tunnel Theory for a central collision with silver.

* * *

We are grateful to Professor H. MESSEL for the hospitality of his laboratories and to Dr. A. J. HERZ for many interesting discussions.

Also one of us (F. B.) wishes to thank Professor POWELL (H. H. Wills Physical Laboratory, Bristol) for the hospitality of his laboratory and Mrs. HERMAN for technical assistance in the analysis of the interactions and electromagnetic cascades.

RIASSUNTO (*)

L'energia primaria vera di due grandi getti è stata ricavata dallo studio delle interazioni secondarie e delle cascate elettromagnetiche risultanti dal decadimento dei mesoni π^0 . Si confronta il risultato con l'energia ricavata dalla formula $\gamma_p = 2/\text{tg}^2 \eta$ e si trova, per ambo i getti, che essa è molto maggiore. Si ha, tuttavia, un buon accordo col valore dell'energia primaria ottenuto in base alla teoria del tunnel applicata ai getti.

(*) Traduzione a cura della Redazione.

On Extended Conformal Transformations of Spinors and Spinor Equations.

H. A. BUCHDAHL (*)

Physics Department, University of Tasmania - Hobart

(ricevuto il 27 Ottobre 1958)

Summary. — This paper deals in the first place with the behaviour of spinors of arbitrary valence, and of their first derivatives, under transformations of the extended conformal group C , whose elements are basically the transformations of the metric according to $'g_{kl} = \lambda g_{kl}$, where λ is an arbitrary positive function of the coordinates. The results obtained are applied to certain relativistic equations for fields associated with particles of arbitrary spin S . It is shown that: (i) if the mass-scalar κ which occurs in them is taken to be a conformal invariant, then the equations cannot be invariant under C for *any* value of S ; (ii) if κ is taken to be a conformal covariant, then the equations can be invariant under C only if they are reflection-invariant and S is half-odd integral, and the subsidiary equations are imposed *after* transformation, *i.e.* they are not themselves required to be invariant; (iii) if the conformal invariance of the subsidiary equations also is required then the only equations which can be invariant under C are Dirac's equations ($S = \frac{1}{2}$) with conform-covariant mass-scalar, the subsidiary equations being absent in this case.

1. — Introduction.

The conformal behaviour of relativistic wave equations has been considered previously on a number of occasions, *e.g.* by DIRAC ⁽¹⁾, BHABHA ⁽²⁾, MCLENNAN ^(3,4), GÜRSEY ⁽⁵⁾, PAULI ⁽⁶⁾, BLUDMAN ⁽⁷⁾, *et al.* Most of these papers,

(*) Present address: Institute for Advanced Study, Princeton, N. J.

(1) P. A. M. DIRAC: *Ann. Math.*, **37**, 429 (1936).

(2) H. J. BHABHA: *Proc. Camb. Phil. Soc.*, **32**, 622 (1936).

(3) J. A. MCLENNAN jr.: *Nuovo Cimento*, **3**, 1360 (1956).

(4) J. A. MCLENNAN jr.: *Nuovo Cimento*, **5**, 640 (1957).

(5) F. GÜRSEY: *Nuovo Cimento*, **3**, 988 (1956).

(6) W. PAULI: *Helv. Phys. Acta*, **13**, 204 (1940).

(7) S. A. BLUDMAN: *Phys. Rev.*, **107**, 1163 (1957).

in particular the first five of those just referred to, deal with the *restricted* conformal group C_0 , which consists of all transformations of co-ordinates which are such that they transform the galilean metric tensor η_{kl} into a metric tensor γ_{kl} whose components differ from those of the former only by a common factor, *i.e.*

$$(1.1) \quad \gamma_{kl} = \lambda \eta_{kl},$$

where λ may be a function of the co-ordinates. As discussed by McLENNAN (⁽⁴⁾, § 4) all the transformations of C_0 can be obtained from the space and time reflections together with the transformations of the restricted proper conformal group C_0^+ . The latter is defined by its fifteen independent infinitesimal transformations

$$(1.2) \quad \left\{ \begin{array}{l} 'x^k = x^k + \beta^k \\ 'x^k = x^k + \omega^k{}_i x^i \quad (\omega_{(kl)} = 0) \\ 'x^k = (1 + v)x^k \\ 'x^k = (1 + 2\alpha_i x^i)x^k - \alpha^k x_i x^i, \end{array} \right.$$

β^k , $\omega^k{}_i$, v and α^k being infinitesimal parameters.

In the context of relativistic wave equations the extended conformal group C seems to have been considered rather more rarely. In particular PAULI (⁽⁵⁾) has examined the behaviour of Dirac's equations under C ; that is, the effect on the equation of the replacement of η_{kl} by $\lambda\eta_{kl}$, where λ is an *arbitrary* (positive) function of the co-ordinates. Given $\lambda('x)$, there will of course in general be no transformation of co-ordinates $'x = f(x)$ such that $\gamma_{kl}('x) = \lambda('x)\eta_{kl}$. In the present paper I consider the conformal behaviour under C of spinors of arbitrary valence and their first derivatives, and of certain general wave equations constructed from them. For this purpose the spinor analysis of INFELD and VAN DER WAERDEN (⁽⁸⁾) will be used (*), since with it the introduction of non-flat metrics is particularly straightforward. More explicitly, let ζ (indices suppressed) be a spinor field of arbitrary valence, defined in a given Riemann space V_4 (of signature -2), whose metrical tensor is $g_{kl}(x)$. Further, let a certain real number r , called its conformal weight, be associated with ζ ; whilst $q(x)$ shall be an arbitrary real function of the co-ordinates. If now Ω (indices suppressed) is a spinor formed of $\gamma_{\mu\nu}$, $\sigma^{k\dot{\alpha}\beta}$, and the covariant derivative of ζ , then what is to be investigated in the first place

(⁽⁵⁾) L. INFELD and B. L. VAN DER WAERDEN: *Sitzber. Preuss. Akad. Wiss.*, 380 (1933).

(*) Their notation will be adhered to except where otherwise indicated.

is the conformal transform $'\Omega$ of Ω , i.e. the form of the quantity $'\Omega$ which results under a transformation T of \mathcal{C} :

$$(1.3) \quad \sigma^{k\dot{\mu}\nu} \rightarrow '\sigma^{k\dot{\mu}\nu} = \sigma^{k\dot{\mu}\nu},$$

$$(1.4) \quad \gamma_{\mu\nu} \rightarrow '\gamma_{\mu\nu} = e^{-a} \gamma_{\mu\nu},$$

$$(1.5) \quad \zeta \rightarrow '\zeta = e^{va} \zeta.$$

(The condition that the metric must be initially galilean has been relaxed for the time being.) If $'\Omega = e^{a\alpha} \Omega$, where a is a real number, then Ω will be said to be conformally covariant, or «a conformal covariant», the term «conformal invariant» being reserved for the special case $a = 0$. It will be noted that the choice of (1.3, 4) ensures that under T $'g_{kl} = e^{2a} g_{kl}$ (cf. EISENHART⁽⁹⁾). No greater generality would have been obtained by choosing (with b real)

$$(1.6) \quad '\sigma^{k\dot{\mu}\nu} = e^{ba} \sigma^{k\dot{\mu}\nu}, \quad '\gamma_{\mu\nu} = e^{-(b+1)a} \gamma_{\mu\nu},$$

for (1.6) results from (1.3, 4) through the spin transformation

$$(1.7) \quad A^\mu_\nu = \delta^\mu_\nu e^{ab\alpha}.$$

Once the effect of conformal transformations on the linear spinor connexion is known (Section 2), one may easily investigate the formation of conformally invariant fundamental spinors on the one hand (Section 3), and the effect of such transformations on a general derived spinor Ω on the other (Section 4). This in turn allows one to examine systematically sets of field equations, linear or quasi-linear, constructed from spinors ξ , η and their first derivatives (Sections 5 and 6), leading to the general results announced in the summary at the beginning of this paper.

2. - The linear connexion.

If the basic hermitian vector spinor $\sigma^{k\dot{\mu}\nu}$, and the metric spinor $\gamma_{\mu\nu}$ be associated with the Riemann space V_4 whose metric tensor is g_{kl} , one has the fundamental relations

$$(2.1) \quad \gamma_{\mu\alpha} \gamma_{\nu\beta} \sigma^{k\dot{\mu}\nu} \sigma^{l\dot{\alpha}\beta} = g^{kl},$$

$$(2.2) \quad \sigma^{k\dot{\mu}\nu}_{;\dot{\mu}} = 0,$$

$$(2.3) \quad \gamma_{\alpha\beta;\dot{\mu}} = 0,$$

(9) L. P. EISENHART: *Riemannian Geometry* (Princeton, 1926), chap. II, § 28.

where subscripts following a semicolon indicate covariant differentiation, the latter being defined with respect to the linear connexion Γ_{kl}^s (*i.e.* the Christoffel symbols of V_4) and the linear spinor connexion $\Gamma_{\nu l}^\mu$ and its complex conjugate $\Gamma_{\bar{\nu} l}^{\bar{\mu}}$. It may be noted that (2.3) has been adopted in place of the weaker equation

$$(2.4) \quad (\gamma_{\mu\alpha}\gamma_{\nu\beta})_{;l} = 0.$$

The former destroys the phase-invariance of the theory, whereas the latter does not. Electromagnetic interactions are however here taken to be absent in any case, for it is known⁽¹⁰⁾ that their presence brings with it special difficulties in the context of fields for particles of spin $S \geq 1$, and with that problem this paper is not concerned.

Now let V_4 be a space in conformal correspondence with V_4 , *i.e.*

$$(2.5) \quad 'g_{kl} = e^{2q} g_{kl},$$

where q is an arbitrary real function of the co-ordinates. If $'\sigma^{k\bar{\mu}\nu}$, $'\gamma_{\alpha\bar{\beta}}$ be the corresponding basic spinors given by (1.3) and (1.4) one has the fundamental relations

$$(2.6) \quad '\gamma_{\mu\alpha}\gamma_{\nu\beta}\sigma^{k\bar{\mu}\nu}\sigma^{l\bar{\alpha}\beta} = 'g^{kl},$$

$$(2.7) \quad '\sigma^{k\bar{\mu}\nu}_{;l} = 0,$$

$$(2.8) \quad '\gamma_{\alpha\bar{\beta};l} = 0,$$

the colon indicating covariant differentiation with respect to the transformed linear connexions $'\Gamma_{kl}^s$ and $'\Gamma_{\nu l}^\mu$. It is convenient to write for either connexion

$$(2.9) \quad \Delta = 'F - F,$$

(indices suppressed). Then it follows from $'g_{kl;s} = 0$ as usual that

$$(2.10) \quad \Delta^s_{kl} = \delta^s_k q_{;l} + \delta^s_l q_{;k} - g_{kl} g^{st} q_{;t}.$$

Now, identically,

$$\begin{aligned} '\sigma^{k\bar{\mu}\nu}_{;l} &= \sigma^{k\bar{\mu}\nu}_{;l} + \Delta^k_{\mu l} \sigma^{t\bar{\mu}\nu} + \Delta^{\bar{\mu}}_{\bar{\lambda} l} \sigma^{k\bar{\lambda}\nu} + \Delta^{\nu}_{\lambda l} \sigma^{k\bar{\mu}\lambda}, \\ e^q (' \gamma_{\mu\nu})_{;l} &= e^q (e^{-q} \gamma_{\mu\nu})_{;l} - \Delta^\lambda_{\mu l} \gamma_{\lambda\nu} - \Delta^\lambda_{\nu l} \gamma_{\mu\lambda}, \end{aligned}$$

the second equation effectively constituting only a single equation for each

⁽¹⁰⁾ *E.g.* M. FIERZ and W. PAULI: *Proc. Roy. Soc., A* **173**, 211 (1939).

value of l . Using (2.2, 3) and (2.7, 8)

$$(2.11) \quad \Delta^k_{\mu\epsilon} \sigma^{t\mu\nu} + \Delta^{\dot{\mu}}_{\dot{\lambda}l} \sigma^{k\dot{\lambda}\nu} + \Delta^{\nu}_{\lambda l} \sigma^{k\dot{\mu}\dot{\lambda}} = 0,$$

$$(2.12) \quad q_{,l} + \Delta^{\dot{\lambda}}_{\dot{\lambda}l} = 0.$$

Multiplying (2.11) throughout by $\sigma_{k\mu\epsilon}$ and using (2.12) it follows easily that

$$(2.13) \quad \Delta^{\nu}_{\epsilon l} = -\frac{1}{2} \sigma_{k\mu\epsilon} \sigma^{t\mu\nu} \Delta^k_{tl}.$$

Inserting (2.10) on the right and making use of the identity

$$(2.14) \quad 2\sigma^{(k}_{\mu\epsilon} \sigma^{l)\dot{\mu}\nu} = \delta^{\nu}_{\epsilon} g^{kl},$$

eq. (2.13) becomes simply

$$(2.15) \quad \Delta^{\mu}_{\nu l} = -\sigma_{l\alpha\nu} \sigma^{t\alpha\mu} q_{,t}.$$

It is sometimes convenient to introduce the spinor

$$(2.16) \quad q^{\dot{\alpha}\beta} = \sigma^{k\dot{\alpha}\beta} q_{,k}.$$

Then (2.15) reads simply

$$(2.17) \quad \Delta^{\mu}_{\nu l} = -\sigma_{l\alpha\nu} q^{\dot{\alpha}\mu}.$$

With this result the investigation of the behaviour of derived spinors under transformations of U becomes quite straightforward.

3. - The conformal curvature spinor.

This section deals briefly with a conformally invariant fundamental spinor which is analogous to the well known conformal curvature tensor C^m_{kls} (*e.g.* EISENHART⁽⁹⁾), and is indeed very closely related to it. From the definition (*)

$$(3.1) \quad \frac{1}{2} P^{\mu}_{\nu kl} = \Gamma^{\mu}_{\nu[l;k]} + \Gamma^{\alpha}_{\nu l} \Gamma^{\mu}_{\alpha k}$$

of the usual spin curvature tensor it follows at once that

$$(3.2) \quad \frac{1}{2} {}'P^{\mu}_{\nu kl} = \frac{1}{2} P^{\mu}_{\nu kl} + \Delta^{\mu}_{\nu[l;k]} + \Delta^{\alpha}_{\nu l} \Delta^{\mu}_{\alpha k}.$$

(*) Brackets enclosing indices act in every case on only one kind of index, *e.g.* here only on the *tensor* subscripts k and l .

Upon making use of (2.15) one is confronted with terms of the kind

$$(3.3) \quad \sigma_{k\dot{\alpha}\nu} \sigma^{s\dot{\alpha}\lambda} \sigma_{l\dot{\beta}\lambda} \sigma^{t\dot{\beta}\mu} q_{;s} q_{;t} ,$$

which may be simplified by means of identities given by HARISH-CHANDRA ⁽¹¹⁾. Thus (3.3) becomes

$$(3.4) \quad \sigma_{k\dot{\alpha}\nu} \sigma^{s\dot{\alpha}\mu} q_{;s} q_{;l} - \sigma_{l\dot{\beta}\mu} \sigma_{k\dot{\alpha}\nu} q_{;t} q_{;t} .$$

With this result one then has

$$(3.5) \quad {}^{\prime}P^{\mu}_{\nu kl} = P^{\mu}_{\nu kl} + 2\sigma^{s\dot{\alpha}\mu} Q_{s[l} \sigma_{k]\dot{\alpha}\nu} ,$$

where

$$(3.6) \quad Q_{st} = q_{;st} - q_{;s} q_{;t} + q_{st} q_{;r} q^{ir} .$$

From (3.5) it may be inferred that

$$(3.7) \quad ({}^{\prime}P^{\mu}_{\nu kl} - P^{\mu}_{\nu kl}) \sigma_r^{\dot{\lambda}\nu} \sigma_{\dot{\lambda}\mu}^r = \frac{1}{2} g_{rk} Q + Q_{rk} ,$$

and hence

$$(3.8) \quad ({}^{\prime}P^{\mu}_{\nu kl} - P^{\mu}_{\nu kl}) \sigma^{k\dot{\lambda}\nu} \sigma_{\dot{\lambda}\mu}^l = 3Q .$$

By means of the last two equations Q_{st} may be eliminated from (3.5), and one has the result that the spin tensor

$$(3.9) \quad \Gamma^{\mu}_{\nu kl} = P^{\mu}_{\nu kl} - 2\sigma^{t\dot{\lambda}}_{\alpha} P^{\alpha\mu}_{[k} \sigma_{l]\dot{\lambda}\nu} - \frac{1}{3} \sigma_{[k}^{\dot{\alpha}\mu} \sigma_{l]\dot{\alpha}\nu} \sigma^{s\dot{\lambda}\beta} \sigma_{\dot{\lambda}\alpha}^s P^{\alpha}_{\beta st}$$

is a conformal invariant. Finally it is possible to show (the details need not be reproduced here) that

$$(3.10) \quad \Gamma^{\mu}_{\nu kl} = \frac{1}{2} \sigma^{s\dot{\alpha}\mu} \sigma_{\dot{\lambda}\nu}^s C_{stkl} .$$

4. - The conformal behaviour of derived spinors.

To investigate the conformal behaviour of relativistic wave equations it is appropriate first to consider the behaviour of certain derived spinors of the form $p^{\dot{\alpha}\beta\xi}$, where ξ (indices suppressed) is a spinor of arbitrary valence $r+s$,

⁽¹¹⁾ HARISH-CHANDRA: *Proc. Ind. Acad. Sci.*, **23**, 152 (1946).

symmetric in its dotted and undotted indices, and

$$(4.1) \quad p^{\dot{\alpha}\beta}(\dots) = \sigma^{k\dot{\alpha}\beta}(\dots)_{;k}.$$

Since it is clearly immaterial whether a given set of indices be written as subscripts or as superscripts, ξ will be taken in the standard form

$$(4.2) \quad \xi = \xi^{\dot{\mu}_1 \dots \dot{\mu}_r \nu_1 \dots \nu_s}.$$

The spinor which results when $\dot{\mu}_t$ is replaced by $\dot{\lambda}$ will be denoted by $\xi^{(\dot{\lambda})_t}$; and $\xi^{(\lambda)_m}$ similarly denotes the spinor which results when ν_m is replaced by λ .

a) Now let ξ have the conformal weight v . Then

$$'(p^{\dot{\alpha}\beta}\xi) = \sigma^{k\dot{\alpha}\beta}(e^{vq}\xi)_{;k} = \sigma^{k\dot{\alpha}\beta}e^{vq}(\xi_{;k} + vq_{;k}\xi + \sum_{t=1}^r \Delta^{\dot{\mu}_t}_{\dot{\lambda}k} \xi^{(\dot{\lambda})_t} + \sum_{t=1}^s \Delta^{\nu_t}_{\lambda k} \xi^{(\lambda)_t}).$$

Introducing (2.17) this becomes

$$(4.3) \quad '(p^{\dot{\alpha}\beta}\xi) = e^{vq}(p^{\dot{\alpha}\beta}\xi + vq^{\dot{\alpha}\beta}\xi - \sum_{t=1}^r q^{\dot{\mu}_t\beta} \xi^{(\dot{\alpha})_t} - \sum_{t=1}^s q^{\dot{\alpha}\nu_t} \xi^{(\beta)_t}).$$

Applying the symmetry operators s and \dot{s} (cf. GÄRDING⁽¹²⁾) one then has

$$(4.4) \quad '(s\dot{s}p^{\dot{\alpha}\beta}\xi) = e^{vq}s\dot{s}(p^{\dot{\alpha}\beta}\xi + (v-r-s)q^{\dot{\alpha}\beta}\xi).$$

Hence: $s\dot{s}p^{\dot{\alpha}\beta}\xi$ is a conformal covariant if and only if $v = r + s$; and its conformal weight is then $r + s$.

b) From (4.3), ($s > 0$), keeping (1.4) in mind,

$$'(p^{\dot{\mu}_{r+1}}_{\nu_s}\xi) = e^{(v-1)q}(p^{\dot{\mu}_{r+1}}_{\nu_s}\xi + vq^{\dot{\mu}_{r+1}}_{\nu_s}\xi - \sum_{t=1}^r q^{\dot{\mu}_t}_{\nu_s} \xi^{(\dot{\mu}_{r+1})_t} + q^{\dot{\mu}_{r+1}}_{\nu_s} \xi),$$

in view of the symmetry properties of ξ . Consequently

$$(4.6) \quad '(\dot{s}p^{\dot{\mu}_{r+1}}_{\nu_s}\xi) = e^{(v-1)q}\dot{s}(p^{\dot{\mu}_{r+1}}_{\nu_s}\xi + (v-r+1)q^{\dot{\mu}_{r+1}}_{\nu_s}\xi).$$

Hence: $\dot{s}p^{\dot{\mu}_{r+1}}_{\nu_s}\xi$ is a conformal covariant if and only if $v = r - 1$; and its conformal weight is then $r - 2$.

c) Proceeding exactly as under b) above one has also that $sp^{\nu_{s+1}}_{\mu_r}\xi$ is a conformal covariant if and only if $v = s - 1$; and its conformal weight is then $s - 2$.

(12) L. GÄRDING: *Proc. Camb. Phil. Soc.*, **41**, 49 (1945).

d) Finally, from (4.3),

$$(4.9) \quad (p_{\dot{\mu}_r v_s} \xi) = e^{(v-2)q} (p_{\dot{\mu}_r v_s} \xi + (v+2) q_{\dot{\mu}_r v_s} \xi) .$$

Hence: $p_{\dot{\mu}_r v_s} \xi$ is a conformal covariant if and only if $v = -2$; and its conformal weight is then -4 .

5. - Linear field equations for particles of any spin and finite rest mass.

a) In galilean space-time R_4 one may take the equations for fields corresponding to particles of finite rest mass and arbitrary spin $S = \frac{1}{2}(r+s)$, ($s > 0$), in the form

$$(5.1) \quad \dot{s} p_{\dot{\mu}_{r+1} v_s} \xi = \kappa \eta ,$$

$$(5.2) \quad s p_{\dot{\mu}_{r+1} v_s} \eta = \kappa \xi .$$

where κ is a constant, together with the subsidiary conditions

$$(5.3, 4) \quad p_{\dot{\mu}_r v_s} \xi = 0 , \quad p_{\dot{\mu}_{r+1} v_{s-1}} \eta = 0 ,$$

required to ensure that the field describe only particles of spin S , i.e. not a mixture of particles of spin $\leq S$. The explicit form of ξ is given by (4.1), whilst $\eta = \eta^{\dot{\mu}_1 \dots \dot{\mu}_{r+1} v_1 \dots v_{s-1}}$. Here the operator $p^{\dot{\alpha}\beta}$ means

$$(5.5) \quad p^{\dot{\alpha}\beta}(\dots) = \sigma^{\dot{\alpha}\dot{\beta}}(\dots)_{,\dot{\beta}} .$$

Because of (5.3, 4) the operators s and \dot{s} could be omitted from (5.1, 2), but it is convenient to retain them here.

Suppose now that fields are contemplated in some V_4 whose curvature tensor does not necessarily vanish. Then it will be laid down that the correct field equations are just (5.1-4) $p^{\dot{\alpha}\beta}$ having the meaning given by (4.2). In other words the view is taken that the equations for an R_4 are the degenerate form of the equations for a V_4 adopted here. (This seems to be generally taken for granted (e.g. reference ⁽⁶⁾), but it will be understood that the inclusion of terms containing the curvature tensors as factors would leave the equations relating to an R_4 unaffected. Such terms would however appear to be necessarily rather artificial.)

Starting, then, with an R_4 the equations (5.1-4) are certainly compatible. For spin $S > \frac{1}{2}$ their compatibility in an arbitrary V_4 is however no longer assured, as I have shown on an earlier occasion ⁽¹³⁾. Thus since $S > \frac{1}{2}$,

⁽¹³⁾ H. A. BUCHDAHL: *Nuovo Cimento*, **10**, 96 (1958). This paper will be referred to as A.

take $s > 1$; then the condition of consistency, corresponding to eq. A(13) for the case $S = \frac{3}{2}$, follows easily:

$$(5.6) \quad \sigma_{\nu_s}^{k\lambda} \sigma_{\lambda\nu_{s-1}}^l \xi_{[kl]} = 0.$$

In terms of the spin curvature this tensor becomes

$$(5.7) \quad S_{\nu_s \nu_{s-1}}^{kl} \left(\sum_{t=1}^r P_{\nu_s}^{k\lambda} \sum_{\alpha k l} \xi^{(\alpha)\lambda} + \sum_{t=1}^s P_{\alpha k l}^{\nu_t} \xi^{(\alpha)\lambda} \right) = 0,$$

where

$$(5.8) \quad S_{\alpha\beta}^{kl} = \sigma_{\alpha}^{[k\lambda} \sigma_{\lambda\beta]}^l.$$

(The first sum is absent if $r = 0$). Now, if the V_4 is conformal to an R_4 then it is a space of constant Riemannian curvature ⁽⁹⁾, Λ , say. This means that

$$(5.9) \quad P_{\nu k l}^{\mu} = -\frac{1}{12} \Lambda S_{k l}^{\mu}{}_{\nu}.$$

One therefore has to consider terms of the kind (i) $S_{\nu_s \nu_{s-1}}^{kl} S_{k l}^{\mu}{}_{\alpha} \xi^{(\alpha)\mu}$ and (ii) $S_{\nu_s \nu_{s-1}}^{kl} S_{k l}^{\nu_t}{}_{\alpha} \xi^{(\alpha)\nu_t}$. Now one has ⁽¹⁴⁾

$$(5.10-11) \quad S^{kl\alpha\beta} S_{kl\mu\nu} = 0, \quad S^{kl\alpha\beta} S_{kl\mu\nu} = 2\delta_{\mu}^{(\alpha} \delta_{\nu}^{\beta)}.$$

Hence without having to invoke the symmetry properties of ξ one concludes already that all the terms above vanish except those of the second type which have $t = s$ or $s - 1$. Omitting irrelevant numerical factors, these terms are $\delta_{(\nu_s \nu_{s-1})\alpha}^{\nu_t} \xi^{(\alpha)\nu_t}$; and they vanish because of the symmetry of ξ . Thus it has been shown that *the field equations are compatible in any V_4 of constant Riemannian curvature*; that is to say, the possibility of conformal invariance of the equations is not impaired by any *a priori* incompatibility in the V_4 .

b) Two alternatives now present themselves in principle, *viz.* (i) either (5.1, 2) alone are required to be conformally invariant, or, (ii) the subsidiary equations (5.3, 4) shall also be invariant.

As regards the first alternative, the subsidiary equations must then be imposed upon the field quantities *after* transformations. (It may be remarked that McLENNAN in his work ⁽⁴⁾ concerning conformal invariance under C_0 does not consider any subsidiary equations.) This procedure is somewhat unnatural; and the first alternative is therefore contemplated largely for heuristic reasons.

Suppose now that the conformal weights of ξ and η are a and b respectively. Then, in view of (4.6), one has in the case of (5.1)

$$(5.12) \quad a = r - 1, \quad b = r - 2,$$

⁽¹⁴⁾ E. M. CORSON: *Tensors, Spinors and Relativistic Wave Equations* (London, 1953), chap. II, § 13.

where the second member of (5.12) follows from the required equality of both members of eq. (5.1). Keeping in mind that, in (5.2,) η has not s but $s-1$ undotted superscripts, one has similarly, with (4.8),

$$(5.13) \quad b = s - 2, \quad a = s - 3.$$

(5.12) and (5.13) are mutually incompatible. Thus without having to draw upon the subsidiary equations at all, it follows that the (linear) field equations associated with particles of arbitrary spin S cannot be invariant under the extended conformal group for any value of S . (The phrase «... cannot be invariant...» is preferred to «... are not invariant...» since invariant equations could be made non-invariant by a different choice of conformal weights. Note also that it has been supposed above that $s > 0$, i.e. $S > 0$; but the non-invariance of the scalar field equations under C is known).

6. - Field equations with conform-covariant mass-scalar.

a) The «mass-scalar» κ was taken to be a constant in (5.1, 2). This condition may be relaxed: without as yet making any hypothesis about the detailed structure of κ one may simply suppose that it has a conformal weight c (cf. PAULI⁽⁶⁾). Then in place of (5.12, 13) one has now

$$(6.1) \quad a = r - 1, \quad b + c = r - 2,$$

$$(6.2) \quad b = s - 2, \quad a + c = s - 3.$$

It follows that

$$(6.3) \quad c = -1, \quad r = s - 1,$$

and incidentally

$$(6.4) \quad a = b = s - 2.$$

The equality of a and b might have been anticipated and might indeed have been imposed from the outset. The second member of (6.3) implies that the field equations must be reflection-invariant (FIERZ⁽¹⁵⁾), the total number of indices and therefore $2S$ being odd. Thus the pair of field equations (5.12) with conform-covariant mass-scalar can be invariant under the transformations of the extended conformal group only if they are reflection-invariant and the particles associated with them have half-odd integral spin.

As regards the structure of κ , one may for example take it to be a power of a suitable invariant K formed bilinearly from ξ and η . Taking into account that $\lambda_{\alpha\beta}$ must enter into it multiplicatively $r+s=2s-1$ times, the con-

⁽¹⁵⁾ M. FIERZ: *Helv. Phys. Acta*, **12**, 3, § 5 (1938).

formal weight of K will be $2(s-2) - (2s-1) = -3$. The first member of (6.3) then requires

$$(6.5) \quad \kappa = K^{\frac{1}{2}}.$$

This result is consistent with that obtained by McLENNAN ⁽⁴⁾, eq. (24).

b) The situation is greatly altered if it be required that the subsidiary equations (5.3, 4) be conformally invariant at the same time. For in accordance with (4.10) one must then have in addition

$$(6.6) \quad a = b = -2,$$

whenever $s > 1$; but (6.6) is incompatible with (6.4). Accordingly the case $s=1$ remains as the only possibility, the subsidiary equations then being absent. Accordingly *the entire set of field equations (5.1-4) cannot be conformally invariant (under C), even when the mass-scalar κ is supposed to be a conformal covariant*. In this sense, then, *the condition of extended conformal invariance distinguishes Dirac's equations (the mass-scalar κ having the conformal weight -1)*

$$(6.7) \quad p^{\mu}_{\nu} \xi^{\nu} = \kappa \eta^{\mu}, \quad p_{\mu}^{\nu} \eta^{\mu} = \kappa \xi^{\nu},$$

from the equations for all other fields associated with particles of integral or half-odd integral spin.

It may be noted that if one adopts (6.5) one is left essentially with just the equations considered by GÜRSEY ⁽⁵⁾ in the context of C_0^+ .

RIASSUNTO (*)

Il lavoro tratta principalmente del comportamento degli spinori di valenza arbitraria e delle loro derivate prime rispetto alle trasformazioni del gruppo conforme esteso C , i cui elementi sono essenzialmente le trasformazioni della metrica secondo $'g_{kl} = \lambda g_{kl}$, dove λ è una funzione positiva arbitraria delle coordinate. I risultati ottenuti si applicano ad alcune equazioni relativistiche per campi associati a particelle di spin arbitrario S . Si dimostra che: (i) se la massa scalare κ che compare nelle stesse si considera conformalmente invariante, le equazioni possono essere invarianti rispetto a C per *qualsiasi* valore di S ; (ii) se κ si considera conformalmente covariante, le equazioni possono essere invarianti rispetto a C solo se sono invarianti rispetto alla riflessione e S è semi intero e le equazioni sussidiarie sono impostate *dopo* la trasformazione, cioè la loro invarianza non è richiesta; (iii) se è richiesta anche l'invarianza conforme delle equazioni sussidiarie, le sole equazioni che possono essere invarianti rispetto a C sono le equazioni di Dirac ($S = \frac{1}{2}$) con massa scalare conformalmente covariante, mancando in tal caso le equazioni sussidiarie.

(*) Traduzione a cura della Redazione.

About the μ -Meson Spin from Ionization Bursts Data.

I. X. ION, N. J. IONESCU-PALLAS and C. C. POTOCEANU

Institute of Atomic Physics of the Rumanian Academy - Bucarest

(ricevuto il 3 Novembre 1958)

Summary. — Accurate calculations of appearance frequencies of bursts generated by muons in a shielding layer of lead at sea level were performed. Cross sections for bremsstrahlung when the screening of the nucleus by the orbital electrons is incomplete, and Furry's distribution model revised by CHRISTY and KUSAKA in order to diminish the fluctuations, were used. Theoretical results fall in good agreement with experimental data in the range $100 \div 1200$ particles, assuming a spin $\frac{1}{2}$ for the μ -meson.

1. — Introduction.

It is well known that the hard component of the cosmic rays, generates ionization bursts in a matter shielded ionization chamber.

If measurements are carried out at sea level, and the protonic component is removed, the process is determined especially by the muons. Muon interactions with shielding matter via knock-on and bremsstrahlung processes, the first process giving a negligible contribution with respect to the last, generates electrono-photon cascade showers.

Cross-sections of both processes are dependent on primary particle spin for energies greater than 10^{10} eV. Hence, a calculation leading to the frequency of ionization bursts, involving a number of particles $\geq S$ may determine (by comparison with experimental data) the value of the muon spin.

The problem was resolved under these conditions, by CHRISTY and KUSAKA ⁽¹⁾ (*) who found spin 0 with an uncertainty implying also the possibility of spin $\frac{1}{2}$, and by CHAKRABARTHY ⁽²⁾ who found spin 1.

(*) We refer to CHRISTY and KUSAKA's work by the abbr. C.K.

⁽¹⁾ R. F. CHRISTY and S. KUSAKA: *Phys. Rev.*, **59**, 414 (1941).

⁽²⁾ S. K. CHAKRABARTHY: *Ind. Journ. Phys.*, **46**, 377 (1942).

The investigations continued (³⁻⁵), most of the results favouring the value $\frac{1}{2}$. The present work continued on the C. and K. line to see if it was possible to find agreement between theoretical results and experimental data (^{7,8}).

In this connection, several sources of possible errors, arising from the uncertainty of the value of some experimental constants used in calculations were eliminated.

Finally, a discussion on C. and K.'s work and on other methods used up to now is given.

2. - Muon spectrum renormalization.

The first difficulty arising in calculations consists in the fact that a power law for the muon energy spectrum leads, according to Wilson's experimental data (⁹) to an energy dependence of the exponential coefficient (we use the differential spectrum coefficient)

$$\alpha \sim 2.9 \text{ for } E_0 < 6 \cdot 10^{10} \text{ eV} \quad \text{and} \quad \alpha \sim 3.4 \text{ for } 6 \cdot 10^{10} < E_0 < 2 \cdot 10^{11}.$$

On the assumption of experimental coefficient variation with energy and because of muon hemispheric isotropy, C. and K.'s expression,

$$(2.1) \quad N(E_0) dE_0 d\Omega = \frac{0.02 (E_0)^{1.9} dE_0 d\Omega}{(E_0 + 1.8 \cdot 10^9 \text{ sec } \theta)^{2.9}},$$

for the differential spectrum (used without changes by other authors) may be modified by a suitable expression for spectrum normalization at an arbitrary value of α . To find with accuracy the total muon number, the spectrum was cut-off at a given energy, which in the present case is $E_0 \sim 0.6 \cdot 10^9 \text{ eV}$. Now the question arises at which energy the spectrum has to be cut-off to obtain precisely, for a given exponential coefficient α , the muon number by means of the power law.

(³) S. HYOKAVA, H. KOMORI and S. OGAVA: *Nuovo Cimento*, **7**, 736 (1956).

(⁴) A. MITRA: *Nucl. Phys.*, **3**, 262 (1957).

(⁵) M. GUPTA: *Nuovo Cimento*, **7**, 39 (1958).

(⁶) B. ROSSI: *Rev. Mod. Phys.*, **20**, 537 (1948).

(⁷) M. SCHEIN and P. S. GILL: *Rev. Mod. Phys.*, **44**, 267. (1939).

(⁸) R. E. LAPP: *Phys. Rev.*, **64**, 255 (1943).

(⁹) J. G. WILSON: *Nature*, **158**, 415 (1946).

Eq. (2.1) may be written:

$$(2.2) \quad N(E_0) dE_0 d\Omega = \frac{(\alpha - 1) I_0 \mathfrak{E}_0^{\alpha-1} g^{\alpha-1}(\alpha) dE_0 d\Omega}{(E_0 + \mathfrak{E}_0 \sec \theta)^\alpha},$$

where I_0 is the muon intensity per unit of solid angle and per second, near the vertical, at sea level and $g(\alpha)$ the ratio E_c/\mathfrak{E}_0 , where $\mathfrak{E}_0 = 1.8 \cdot 10^9$ eV is a spectrum constant. The value assigned to I_0 , namely $I_0 = 0.88 \cdot 10^{-2}/\text{cm}^2 \cdot \text{sr} \cdot \text{s}$ (6) gives a correction of $\sim 12\%$ with respect to $I_0 \approx 10^{-2}/\text{cm}^2 \cdot \text{sr} \cdot \text{s}$, used by C. and K. in their calculations.

By integrating the differential spectrum (2.2) over the upper hemisphere and over all energies and with the condition to obtain C. and K.'s (who took $\alpha \sim 3$) value for the ratio between total intensity and $2\pi I_0$, where I_0 is the vertical intensity, we obtain a transcendent equation for $g(\alpha)$. For $\alpha = 3$ the total spectrum will be

$$(2.3) \quad y = 2\pi I_0 \left(\frac{E_1}{E_{\min}} \right)^2 \left\{ 2 - \frac{E_{\min}}{E_0 + E_{\min}} - 2 \frac{E_0}{E_{\min}} \ln \frac{E_0 + E_{\min}}{E_0} \right\},$$

where $E_{\min} = E_1 - E_0$; $E_1/E_0 = E_1/\mathfrak{E}_0 = g(3)$. Introduction of numerical values in (2.3) gives

$$(2.4) \quad \frac{y}{2\pi I_0} = k = 0.3827 \dots$$

For a given α , eq. (2.2) will be integrated first with respect to energy (the integration limits being E_{\min} and ∞) and second with respect to angles. Therefore

$$(2.5) \quad y = 2\pi I_0 \left(\frac{E_1}{E_{\min}} \right)^{\alpha-1} J_{\alpha-1} \left(\frac{E_0}{E_{\min}} \right),$$

with the same notations as in eq. (2.3) but for a given α , function $J_\lambda(a)$ may be defined by means of the transcendent function

$$(2.6) \quad J_\alpha(a) = \int_0^{\pi/2} \frac{\sin \theta d\theta}{(1 + (a/\cos \theta))^\alpha}.$$

Expanding the integral in a rapid convergent infinite series, we obtain the following infinite degree algebraic equation (see App. I)

$$(2.7) \quad \sum_1^\infty \lambda \frac{x^\lambda}{(\alpha + \lambda)(\alpha + \lambda - 1)} = k_0,$$

where

$$x = \frac{E_{\min}}{E_0 + E_{\min}} = 1 - \frac{1}{g(\alpha)} \quad \text{and} \quad k_0 = \frac{1}{\alpha - 1} \left(\frac{y}{2\pi I_0} - \frac{1}{\alpha} \right).$$

As $k_0 \ll 1$ the real positive root may be given as an expansion in powers of k_0 . Finally the equation relating x to $g(\alpha)$ gives

$$(2.8) \quad g(\alpha) = 1 + \alpha \frac{\alpha + 1}{\alpha - 1} \left(k - \frac{1}{\alpha} \right) + \frac{2}{\alpha + 2} \alpha^2 \left(\frac{\alpha + 1}{\alpha - 1} \right)^2 \left(k - \frac{1}{\alpha} \right)^2 + \\ + \frac{2(\alpha + 6)}{(\alpha + 2)^2(\alpha + 3)} \alpha^3 \left(\frac{\alpha + 1}{\alpha - 1} \right)^3 \left(k - \frac{1}{\alpha} \right)^3 + \dots$$

Very good approximation ($\ll 1\%$) is obtained taking in the whole α variation interval $2.9 \leq \alpha \leq 3.4$ the following expression for $g(\alpha)$

$$(2.9) \quad g(\alpha) \approx 1.335 + 0.870(\alpha - 3).$$

3. - The integral spectrum of muons.

The second difficult task is to obtain a proper expression for the integral spectrum, which may be used in further calculations. As it is impossible to obtain a finite expression for $\alpha \neq 3$, we shall take, instead, a power series of the variable, as rapidly convergent as possible. This difficulty does not arise in C. and K.'s work, who use the following approximation

$$(3.1) \quad N(E_0) dE_0 d\Omega \approx \frac{0.02 (E_c)^{1.9} dE_0 d\Omega}{E_0^{2.9} \left(1 + \frac{1.8 \cdot 10^9 \sec \theta \epsilon}{15\beta S} \right)^{2.9}},$$

in which the energy of the muon generating the shower is replaced by $15(\beta S/\epsilon)$, where ϵ is the energy transfer ratio from the muon to the electron or the photon generating the cascade, and S is the number of particles in the shower. On the assumption that $6\beta S$ (β being the energy at which the multiplication process stops) is the most probable energy of the particle (electron or photon) generating the cascade, as results from Furry's model modified by C. and K., and that the mean value of transfer ratio is $\frac{3}{4}$, we obtained for the muon initiating the process, an energy of $20\beta S$, a too great value with respect to $8\beta S$ resulting from the model and with respect to $13.3\beta S$ obtained without considering the fluctuations.

To resolve this problem, the following change of variable, whose meaning will appear later, will be made

$$(3.2) \quad E_0 = \frac{\mathcal{E}_0}{a},$$

where E_0 is the muon energy and \mathcal{E}_0 the differential spectrum constant (2.2). For simple dimensional reasons, E_0 will be expressed in $15\beta S$ units: $E_0 = 15\beta S E'_0$; $E'_0 = E/\varepsilon$, where E is the energy (in arbitrary units) of the photon or electron generating the cascade. Hence, $\mathcal{E}_0/a = 15\beta S(E/\varepsilon)$ and setting $\xi = 1/E$, we obtain the second important transformation

$$(3.3) \quad \varepsilon = \frac{S}{C_1} a,$$

where

$$(3.4) \quad C_1 = \frac{\mathcal{E}_0}{15\beta} = 8.57142 \dots,$$

and $\beta = 14$ MeV a more correct value than that of 13 MeV given by C. and K.

According to eq. (3.2) and eq. (3.3) the differential spectrum (2.2) will be

$$(3.5) \quad N(\alpha) dE_0 d\Omega = \frac{(\alpha - 1) I_0 a^{\alpha-1} g^{\alpha-1}(\alpha) (d\xi/\xi) d\Omega}{(1 + (a/\cos \theta))^\alpha},$$

where the sign $(-)$ before eq. (3.5) was omitted; it will be taken into account only at the end by reversing the integration limits of the integral with respect to ξ , which gives the shower appearance frequencies. The integral spectrum will now be

$$(3.6) \quad dE_0 \int N(\alpha) d\Omega = 2\pi I_0 (\alpha - 1) a^{\alpha-1} g^{\alpha-1}(\alpha) J_\alpha(a) \frac{d\xi}{\xi},$$

(upper hemi ph.)

where $J_\alpha(a)$ which was defined by eq. (2.6) will not be expressed any more as a series of type (2.7) but, according to the purpose of the present work, as a rapidly convergent asymptotic series (see App. II),

$$(3.7) \quad J_\alpha(a) = 1 + \alpha a \ln a + C_\alpha a - \sum_k (-1)^{k-1} C_{\alpha+k}^{\alpha-1} \frac{a^{k+1}}{k},$$

where C_α is in its turn

$$(3.8) \quad C_\alpha = \alpha(\alpha - 1) \sum_k \frac{1}{(k+1)(k+\alpha)}.$$

For $\alpha = 3$, $C_\alpha = \frac{5}{2}$ and $J_3(a)$ may be written as a finite expression

$$(3.9) \quad J_3(a) = \left\{ \frac{6a^2 + 9a + 2}{2(a+1)^2} - 3a \ln \left(\frac{a+1}{a} \right) \right\}.$$

Using Stirling's formula it may be observed that series (3.7) is rapidly convergent for $0 < a < 1$ and $\alpha > 1$ and both conditions are fulfilled in this case.

4. - Cross section transformations for processes initiating the cascade.

Both for knock-on processes with atomic electrons and for muon bremsstrahlung we shall take the cross-sections given in C. and K.'s work (critical considerations on the applicability limits of these expressions will be given further).

Cross-sections for electron knock-on processes in both cases discussed above (spin 0 and spin $\frac{1}{2}$) are

a) spin 0, magnetic moment 0

$$(4.1) \quad \sigma_0^{(e)}(E_0, \varepsilon) = 2\pi \left(\frac{137}{Z} \right) \left(\frac{\mu}{m} \right)^2 \frac{mc^2}{E_0} \frac{1}{\varepsilon^2} \left(1 - \frac{\varepsilon}{\varepsilon_m} \right).$$

b) spin $\frac{1}{2}$, magnetic moment $e\hbar/2\mu c$

$$(4.2) \quad \sigma_{\frac{1}{2}}^{(e)}(E_0, \varepsilon) = 2\pi \left(\frac{137}{Z} \right) \left(\frac{\mu}{m} \right)^2 \frac{mc^2}{E_0} \frac{1}{\varepsilon^2} \left(1 - \frac{\varepsilon}{\varepsilon_m} + \frac{1}{2} \varepsilon^2 \right),$$

where ε_m is the maximum energy transfer ratio from a muon (of energy E_0) to an electron (of energy E)

$$(4.3) \quad \varepsilon_m \approx \left[1 + \frac{1}{2} \left(\frac{\mu}{m} \right)^2 \frac{mc^2}{E_0} \right]^{-1}.$$

Cross sections are measured in radiation units

$$(4.4) \quad \bar{\varphi} \approx \left(\frac{e^2}{\mu c^2} \right)^2 \frac{Z^2}{137}.$$

Cross-sections for muon bremsstrahlung in the Coulomb field of a nucleus, are

a) spin 0, magnetic moment 0

$$(4.5) \quad \sigma_0^{(\mu)}(E_0, \varepsilon) = \frac{16}{3} \frac{1 - \varepsilon}{\varepsilon} \left\{ \ln \frac{2(1 - \varepsilon)E_0}{(5/6)\mu c^2 Z^{\frac{1}{3}} \varepsilon} - \frac{1}{2} \right\},$$

b) spin $\frac{1}{2}$, magnetic moment $e\hbar/2\mu c$

$$(4.6) \quad \sigma_{\frac{1}{2}}^{(v)}(E_0, \varepsilon) = \frac{16}{3} \left(\frac{3}{y} \varepsilon + \frac{1-\varepsilon}{\varepsilon} \right) \left\{ \ln \frac{2(1-\varepsilon)E_0}{(5/6)\mu c^2 Z^3 \varepsilon} - \frac{1}{2} \right\}.$$

To write eq. (4.1), (4.2), (4.3), (4.5) and (4.6) in the new variables (a, ξ) , changes of variables (3.2) and (3.3) will be used. We have to find first, the expression relating a_m and ε_m to get the variation limit of ε in the « a » scale. From (4.3) it follows that.

$$(4.7) \quad \varepsilon_m \approx \frac{S}{S + C_2 \xi},$$

where

$$(4.8) \quad C_2 = \frac{1}{2} \left(\frac{\mu}{m} \right)^2 \left[\frac{mc^2}{15\beta} \right] = 54.67909 \dots$$

In computing C_2 the precise value $\mu \approx 207m_e$ has been assumed for the muon mass. Writing eq. (3.3) for the limiting values (ε_m, a_m) and using eq. (4.7) we shall find the following equation relating a_m to ξ

$$(4.9) \quad a_m = \frac{C_1 \xi}{S + C_2 \xi},$$

which allows for the reciprocal conversion of these variables. In the limiting case $\xi \rightarrow \infty$

$$(4.10) \quad \lim_{\xi \rightarrow \infty} a_m(\xi) = \max(a_m) = \frac{C_1}{C_2} = 0.15676.$$

Using the equations relating a_m to ξ , and ε_m to ξ and taking ξ from eq. (4.7) and eq. (4.9), we shall obtain

$$(4.11) \quad \varepsilon_m = 1 - \frac{C_2}{C_1} a_m = 1 - 6.3793 \dots a_m,$$

which is the energy transformation. Now the cross-sections of the investigated processes may be expressed only in terms of a and a_m . The great advantage of this transformation consists in the possibility of obtaining—as will be seen further—an integrant for the expression giving the shower appearance frequency, in which the particle number S does not appear. In this connection it is opportune to notice that the relative low value obtained in (4.10) assures a rapid convergence of the series (3.7).

Before writing the cross-sections in the new variables we shall introduce some simplifying notations

$$(4.12) \quad \mathcal{S}(Z) = 2\pi \frac{137}{Z} \left(\frac{\mu}{m}\right)^2 \frac{mc^2}{\mathcal{E}_0} C_1^2,$$

$$(4.13) \quad Q(Z) = \ln \frac{2\mathcal{E}_0}{(5/6)\mu c^2 Z^{\frac{1}{3}}} = \\ = 2.22533 \left\{ 1 - 0.14978 \left(\frac{\delta Z_0}{Z_0} \right) + 0.07489 \left(\frac{\delta Z_0}{Z_0} \right)^2 - 0.04993 \left(\frac{\delta Z_0}{Z_0} \right)^3 + \dots \right\},$$

where

$$Z_0 = 80 \quad \text{and} \quad \delta Z_0 = Z - Z_0.$$

Taking into account all changes between old and new variables (that is ε , E_0 , ε_m and a , ξ , a_m) respectively, we finally obtain

$$(4.14) \quad \sigma_0^{(e)}(a, \xi) = \mathcal{S}(Z) \frac{\xi^2}{S^2} \left\{ \frac{1}{a} - \frac{1}{a_m} \right\},$$

$$(4.15) \quad \sigma_{\frac{1}{2}}^{(e)}(a, \xi) = \mathcal{S}(Z) \frac{\xi^2}{S^2} \left\{ \frac{1}{a} - \frac{1}{a_m} + \frac{1}{2} \left(\frac{1}{a_m} - 6.3793 \right)^2 a \right\},$$

$$(4.16) \quad \sigma_0^{(\gamma)} = \frac{16}{3} \left[\frac{a_m}{a} \frac{1}{1 - 6.3793 a_m} - 1 \right] \left\{ \left(Q - \frac{1}{2} \right) + \ln \left[\frac{a_m}{a} \frac{1}{1 - 6.3793 a_m} - 1 \right] \frac{1}{a} \right\}.$$

$$(4.17) \quad \sigma_{\frac{1}{2}}^{(\gamma)} = \frac{16}{3} \left[\frac{a_m}{a} \frac{1}{1 - 6.3793 a_m} - 1 + \frac{3}{4} \frac{a}{a_m} (1 - 6.3793 a_m) \right] \cdot \\ \cdot \left\{ \left(Q - \frac{1}{2} \right) + \ln \left[\frac{a_m}{a} \frac{1}{1 - 6.3793 a_m} - 1 \right] \frac{1}{a} \right\}.$$

5. - General expressions for cascade shower appearance frequencies as functions of the particle number S .

In order to find these expressions we shall perform the integral

$$(5.1) \quad N_i(S) = \bar{\varphi} N \int_0^\infty dE \int_0^{\varepsilon_m} \frac{d\varepsilon}{\varepsilon} \int F \left(\frac{E}{\varepsilon}, \theta \right) \sigma_i \left(\frac{E}{\varepsilon}, \varepsilon \right) P(E, S) d\Omega,$$

(upper hemisphere)

where $P(E, S)$ is the probability for an electron (or a photon) of energy E of generating a cascade shower which contains more than S particles, σ_i the cross-section of the process in which an electron (or a photon) of energy E is

freed (or created) by a muon of energy E/ε , $F(E/\varepsilon, \theta)$ the meson differential spectrum intensity and N the number of shielding atoms per unit of path (N does not appear in the final result). According to our transformations eq. (5.1) will be written in terms of ξ and a . Let us note

$$(5.2) \quad \mathcal{P}(Z, \alpha) = \frac{2\pi}{C_1} I_0 \bar{\varphi} N x_0 K(\alpha - 1) g^{\alpha-1}(\alpha) = \frac{2\pi}{C_1} I_0 \bar{\varphi} N x_0 K \Xi(\alpha),$$

where K and x_0 are used to express the probability $P(E, S)$, which in the ξ scale will take the form

$$(5.3) \quad P(\xi) = \frac{K x_0}{\sqrt{\xi}} \exp[-\xi];$$

here $K = 13.5$ and x_0 (the shower unit for length) is given by

$$(5.4) \quad x_0 = \left[4 \frac{Z^2}{137} \left(\frac{e^2}{mc^2} \right)^2 N \ln \frac{191}{Z^{\frac{1}{3}}} \right]^{-1}.$$

The probability (5.3) results from Furry's model (for spatial distribution of particles in the shower) modified by C. and K. to diminish its somewhat great fluctuations.

Now we may write for both processes (knock-on and bremsstrahlung) the following general equation giving the frequencies $N(S)$

$$(5.5) \quad \frac{N_i(S)}{S} = \mathcal{P}(Z, \alpha) \int_0^\infty \xi^{-\frac{1}{2}} \exp[-\xi] d\xi \int_0^{a_m} a^{\alpha-1} \sigma_i(a) J_\alpha(a) da,$$

where the subscript i denotes a definite process, $J_\alpha(a)$ is the function defined by eq. (2.6) but in the form (3.7); a_m must be replaced after integration by its expression as a function of ξ (4.9); cross-sections are those given in (4.14)–(4.17).

Cross-sections for the collision process are of the form

$$(5.6) \quad \sigma^{(e)}(\xi, a) = \mathcal{S}(Z) \frac{\xi^2}{S^2} f^{(e)}(a),$$

and if we set

$$(5.7) \quad \mathcal{P}(Z, \alpha) \mathcal{S}(Z) = \Gamma(Z) \Xi(\alpha),$$

shower appearance frequencies for this process will be

$$(5.8) \quad N_{(i)}^{(e)}(S) = \frac{\Gamma(Z)}{S} \Xi(\alpha) \int_0^\infty \frac{\exp[-\xi]}{\sqrt{\xi}} d\xi \int_0^{a_m} a^{\alpha-1} f_{(i)}^{(e)}(a) J_\alpha(a) da,$$

where i now refers to a definite muon spin value, and the functions $\Gamma(Z)$ and $\Xi(\alpha)$ are, respectively

$$(5.9) \quad \Gamma(Z) = \pi^2 \frac{137}{Z} \frac{mc^2}{15\beta} \frac{KI_0}{\ln(191/Z^{1/3})} \simeq \\ \simeq 1.2886 \cdot 10^{-3} \left[1 - 0.91208 \left(\frac{\delta Z_0}{Z_0} \right) + 0.87585 \left(\frac{\delta Z_0}{Z_0} \right)^2 - 0.85360 \left(\frac{\delta Z_0}{Z_0} \right)^3 + \dots \right],$$

and

$$(5.10) \quad \Xi(\alpha) = (\alpha - 1) g^{\alpha-1}(\alpha) \simeq \\ \simeq 3.5644 \{ 1 + 2.0923(\alpha - 3) + 2.2908(\alpha - 3)^2 + 1.7538(\alpha - 3)^3 + \dots \}.$$

For the other process (bremsstrahlung) we may write

$$(5.11) \quad N_{(i)}(S) = ST(Z) \Xi(\alpha) \int_0^\infty \xi^{-\frac{5}{2}} \exp[-\xi] d\xi \int_0^{a_m} a^{\alpha-1} \sigma_{(i)}^{(v)}(a) J_\alpha(a) da,$$

when $T(Z)$ takes the form

$$(5.12) \quad T(Z) = \frac{\pi}{2C_1} \left(\frac{m}{\mu} \right)^2 \frac{KI_0}{\ln(191/Z^{1/3})} \simeq \\ \simeq 1.2776 \cdot 10^{-7} \left\{ 1 + 0.08791 \left(\frac{\delta Z_0}{Z_0} \right) - 0.03622 \left(\frac{\delta Z_0}{Z_0} \right)^2 + 0.02225 \left(\frac{\delta Z_0}{Z_0} \right)^3 - \dots \right\}.$$

Eq. (5.11) may be written similarly to eq. (5.8) by introducing transformed cross-sections

$$(5.13) \quad \tilde{\sigma}_{(i)} = \sigma_{(i)} \left[\frac{1}{a_m} - 6.3793 \dots \right]^2.$$

Thus eq. (5.11) becomes

$$(5.14) \quad N_i^{(v)}(S) = C_1^2 \frac{T(Z)}{S} \Xi(\alpha) \int_0^\infty \frac{\exp[-\xi]}{\sqrt{\xi}} d\xi \int_0^{a_m} a^{\alpha-1} \tilde{\sigma}_i(a) J_\alpha(a) da.$$

Now we must compute the functions G_i and F_i which are the integrals over a in (5.8) and (5.14).

6. - Computation of functions G_i and F_i .

Functions G_0 and $G_{\frac{1}{2}}$ are easily obtained because the series of which they consist may be integrated term by term. Thus, we find

$$(6.1) \quad G_0(a_m) = \frac{a_m^{\alpha-1}}{\alpha(\alpha-1)} \left\{ 1 + \alpha \frac{\alpha-1}{\alpha+1} a_m \ln a_m + \frac{\alpha-1}{\alpha+1} \left(C_\alpha - \frac{2\alpha+1}{\alpha+1} \right) a_m - \right. \\ \left. - \alpha(\alpha-1) \sum_{k=1}^\infty \frac{(-1)^{k-1}}{k} C_{\alpha+k}^{\alpha-1} \frac{a_m^{k+1}}{(k+a)(k+\alpha+1)} \right\},$$

and

$$(6.2) \quad G_{\frac{1}{2}}(a_m) - G_0(a_m) = \frac{1}{2} \frac{a_m^{\alpha-1}}{\alpha+1} (1 - 6.3793 a_m)^2 \left\{ 1 + \alpha \frac{\alpha+1}{\alpha+2} a_m \ln a_m + \right. \\ \left. + \frac{\alpha+1}{\alpha+2} \left(C_\alpha - \frac{\alpha}{\alpha+2} \right) a_m - (\alpha+1) \sum_1^\infty \frac{(-1)^{k-1}}{k} C_{\alpha+k}^{\alpha-1} \frac{a_m^{k+1}}{k+\alpha+2} \right\}.$$

Functions F_i are much more intricate and may not be written as simple power series. Therefore we shall introduce 9 auxiliary functions $g_i(a_m)$, $i = 1, 2, \dots$ in terms of which function F_i will be written,

$$(6.3) \quad g_1(x) = 1 + (\alpha-1)x \ln x + \\ + \frac{\alpha-1}{\alpha} (C_\alpha - 1)x - (\alpha-1) \sum_1^\infty (-1)^{k-1} \frac{C_{\alpha+k}^{\alpha-1}}{k(k+\alpha)} x^{k+1},$$

$$(6.4) \quad g_2(x) = 1 + \frac{\alpha^2}{\alpha+1} x \ln x + \\ + \frac{\alpha}{\alpha+1} \left(C_\alpha - \frac{\alpha}{\alpha+1} \right) x - \alpha \sum_1^\infty (-1)^{k-1} \frac{C_{\alpha+k}^{\alpha-1}}{k(k+\alpha+1)} x^{k+1},$$

$$(6.5) \quad g_3(x) = 1 + (\alpha-1)x \ln x \frac{1 + \frac{\alpha}{\ln(y/x)} \sigma_{\alpha-1}}{1 + \frac{\alpha-1}{\ln(y/x)} \sigma_{\alpha-2}} + \\ + \frac{\alpha-1}{\alpha} (C_\alpha - 1)x \frac{1 + \frac{\alpha}{\ln(y/x)} \left[\frac{C_\alpha}{C_\alpha-1} \sigma_{\alpha-1} + \frac{\alpha \sigma'_{\alpha-1}}{C_\alpha-1} \right]}{1 + \frac{\alpha-1}{\ln(y/x)} \sigma_{\alpha-2}} - \\ - (\alpha-1) \sum_1^\infty (-1)^{k-1} \frac{C_{\alpha+k}^{\alpha-1}}{k(k+\alpha)} x^{k+1} \frac{1 + \frac{k+\alpha}{\ln(y/x)} \sigma_{k+\alpha-1}}{1 + \frac{\alpha-1}{\ln(y/x)} \sigma_{\alpha-2}},$$

$$(6.6) \quad g_4(x) = 1 + \frac{\alpha^2}{\alpha+1} x \ln x \frac{1 + \frac{\alpha+1}{\ln(y/x)} \sigma_\alpha}{1 + \frac{\alpha}{\ln(y/x)} \sigma_{\alpha-1}} + \\ + \frac{\alpha}{\alpha+1} \left(C_\alpha - \frac{\alpha}{\alpha+1} \right) x \frac{1 + \frac{(\alpha+1)}{(C_\alpha - \alpha/(\alpha+1)) \ln(y/x)} (C_\alpha \sigma_\alpha + \alpha \sigma'_\alpha)}{1 + \frac{\alpha}{\ln(y/x)} \sigma_{\alpha-1}} -$$

$$\begin{aligned}
 (6.7) \quad g_5(x) = & 1 + (\alpha - 1)x \ln x + \\
 & - \alpha \sum_1^{\infty} (-1)^{k-1} \frac{C_{\alpha+k}^{\alpha-1}}{k(k+\alpha+1)} x^{k+1} \frac{1 + \frac{k+\alpha+1}{\ln(y/x)} \sigma_{k+\alpha}}{1 + \frac{\alpha}{\ln(y/x)} \sigma_{\alpha-1}}, \\
 & + \frac{\alpha-1}{\alpha} \left(C_{\alpha} - \frac{\alpha-2}{\alpha-1} \right) x \frac{\ln x - \frac{1}{\alpha} \frac{C_{\alpha}-2}{C_{\alpha} - ((\alpha-2)/(\alpha-1))}}{\ln x - \frac{1}{\alpha-1}} - \\
 & - (\alpha-1) \sum_1^{\infty} (-1)^{k-1} \frac{C_{\alpha+k}^{\alpha-1}}{k(k+\alpha)} x^{k+1} \frac{\ln x - \frac{1}{k+\alpha}}{\ln x - \frac{1}{\alpha-1}},
 \end{aligned}$$

$$\begin{aligned}
 (6.8) \quad g_6(x) = & 1 + \frac{\alpha^2}{\alpha+1} x \ln x + \\
 & + \frac{\alpha}{\alpha+1} \left(C_{\alpha} - \frac{\alpha-1}{\alpha+1} \right) x \frac{\ln x - \frac{1}{\alpha+1} \frac{C_{\alpha}-2(\alpha/(\alpha+1))}{C_{\alpha} - ((\alpha-1)/(\alpha+1))}}{\ln x - \frac{1}{\alpha}} - \\
 & - \alpha \sum_1^{\infty} (-1)^{k-1} \frac{C_{\alpha+k}^{\alpha-1}}{k(k+\alpha+1)} x^{k+1} \frac{\ln x - \frac{1}{\alpha+k+1}}{\ln x - \frac{1}{\alpha}},
 \end{aligned}$$

$$\begin{aligned}
 (6.9) \quad g_7(x) = & 1 + \alpha \frac{\alpha+1}{\alpha+2} x \ln x + \\
 & + \frac{\alpha+1}{\alpha+2} \left(C_{\alpha} - \frac{\alpha}{\alpha+2} \right) x - (\alpha+1) \sum_1^{\infty} (-1)^{k-1} \frac{C_{\alpha+k}^{\alpha-1}}{k(k+\alpha+2)} x^{k+1},
 \end{aligned}$$

$$\begin{aligned}
 (6.10) \quad g_8(x) = & 1 + \alpha \frac{\alpha+1}{\alpha+2} x \ln x \frac{1 + \frac{\alpha+2}{\ln(y/x)} \sigma_{\alpha+1}}{1 + \frac{\alpha+1}{\ln(y/x)} \sigma_{\alpha}} + \\
 & + \frac{\alpha+1}{\alpha+2} \left(C_{\alpha} - \frac{\alpha}{\alpha+2} \right) x \frac{\frac{\alpha+2}{(C_{\alpha} - \alpha/(\alpha+2) \ln(y/x))} (C_{\alpha} \sigma_{\alpha+1} + \alpha \sigma'_{\alpha+1})}{1 + \frac{\alpha+1}{\ln(y/x)} \sigma_{\alpha}} - \\
 & - (\alpha+1) \sum_1^{\infty} (-1)^{k-1} \frac{C_{\alpha+k}^{\alpha-1}}{k(k+\alpha+2)} x^{k+1} \frac{1 + \frac{\alpha+k+2}{\ln(y/x)} \sigma_{\alpha+k+1}}{1 + \frac{\alpha+1}{\ln(y/x)} \sigma_{\alpha}},
 \end{aligned}$$

$$\begin{aligned}
 (6.11) \quad g_9(x) = & 1 + \alpha \frac{\alpha + 1}{\alpha + 2} x \ln x + \\
 & + \frac{\alpha + 1}{\alpha + 2} \left[C_\alpha - \frac{\alpha^2}{(\alpha + 1)(\alpha + 2)} \right] x \frac{\ln x + \frac{[2\alpha/(\alpha + 2) - C_\alpha]1/(\alpha + 2)}{C_\alpha - (\alpha^2/(\alpha + 1)(\alpha + 2))}}{\ln x - \frac{1}{\alpha + 1}} - \\
 & - (\alpha + 1) \sum_1^\infty (-1)^{k-1} \frac{C_{\alpha+k}^{\alpha-1}}{k(k + \alpha + 2)} x^{k+1} \frac{\ln x - \frac{1}{k + \alpha + 2}}{\ln x - \frac{1}{\alpha + 1}},
 \end{aligned}$$

where $x = a_m$, $y = 1 - 6.3793 a_m$ and

$$(6.12) \quad \sigma_q(y) = \sum_1^\infty \frac{y^k}{k(k + q + 1)}.$$

The derivative of σ , stressed in the expressions giving g 's is taken with respect to subscript q . (For the derivation of g_i see App. III).

Functions g_i and σ_q allow to write the functions F_0 and $F_{\frac{1}{2}}$ in a relatively simple form

$$\begin{aligned}
 (6.13) \quad F_0(a_m) = & \frac{16}{3} y x^{\alpha-2} \cdot \\
 & \cdot \left\{ \frac{Q - \frac{1}{2}}{\alpha - 1} g_1(x) - \left[\frac{\ln(y/x)}{\alpha - 1} + \sigma_{\alpha+2} \right] g_3(x) - 2 \frac{(\ln x - 1/(\alpha - 1))}{\alpha - 1} g_5(x) \right\} - \\
 & - \frac{16}{3} y^2 x^{\alpha-2} \left\{ \frac{Q - \frac{1}{2}}{\alpha} g_2(x) - \left[\frac{\ln(y/x)}{\alpha} + \sigma_{\alpha-1} \right] g_4(x) - 2 \frac{\ln \alpha - (1/\alpha)}{\alpha} g_6(x) \right\}, \\
 (6.14) \quad F_{\frac{1}{2}}(a_m) - F_0(a_m) = & \\
 = & 4y^3 x^{\alpha-2} \left\{ \frac{Q - \frac{1}{2}}{\alpha + 1} g_7(x) - \left[\frac{\ln(y/x)}{\alpha + 1} + \sigma_\alpha \right] g_8(x) - 2 \frac{\ln x - 1/(\alpha + 1)}{\alpha + 1} g_9(x) \right\}.
 \end{aligned}$$

7. - Numerical data.

Expressions obtained in Sect. 6 for the functions G and F have been derived very clearly—without any approximation—and are therefore, the most precise solutions of the problem discussed above.

Now, the following integrals have to be performed,

$$\int_0^\infty \frac{\exp[-\xi]}{\sqrt{\xi}} G(a_m) d\xi \quad \text{and} \quad \int_0^\infty \frac{\exp[-\xi]}{\sqrt{\xi}} F(a_m) d\xi.$$

As the integrand of both integrals do not contain explicitly the particle number S , functions G and F are quite general, this was of course, the main reason determining us to perform all transformations from Sect. 2 and 3. Function G_0 , $G_{\frac{1}{2}}$ and F_0 , $F_{\frac{1}{2}}$ were tabulated after previous tabulation of functions f_i and g_i . All numerical calculations were performed for $\alpha = 3$ and $Z = 82$ (Pb).

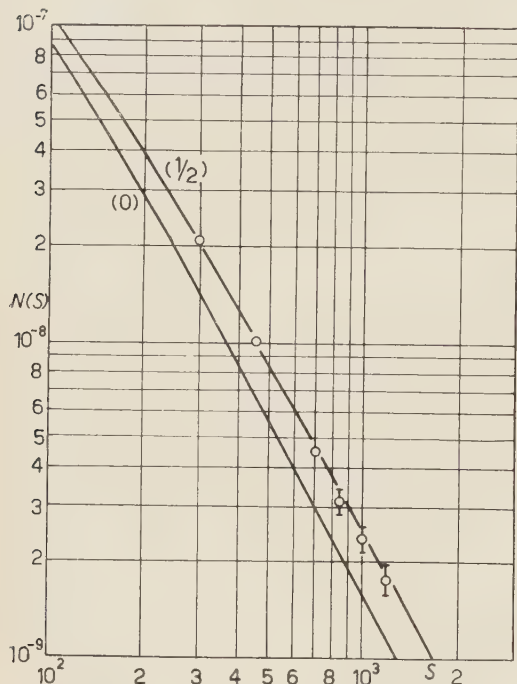


Fig. 1. — Plot of burst frequency against minimum burst size given in terms of the number of particles S of the burst. The circles indicate the experimental points of (7) and (8).

For showers containing no more than 1200 particles, a good agreement was found. Comparison with Schein and Gill's experimental data is also satisfactory.

After plotting G and F to a scale allowing for great precision, we made the conversion from the hyperbolic scale a_m to the linear scale ξ , using transformation (4.9) which was also tabulated. Graphical calculations were performed up to $\xi = 5$; for the remaining interval, adequate tail corrections were made. Frequencies of the two processes (knock-on and bremsstrahlung) generating the cascade are given in the table below, for both values (0 and $\frac{1}{2}$) of the muon spin.

A comparison between total frequencies and Lapp's experimental data is given in Fig. 1.

TABLE I. — *The values of $N(S)$.*

S	$N_0^{(e)}(S)$	$N_{\frac{1}{2}}^{(e)}(S)$	$N_0^{(G)}(S)$	$N_{\frac{1}{2}}^{(G)}(S)$
75	$2.532 \cdot 10^{-8}$	$3.105 \cdot 10^{-8}$	$1.083 \cdot 10^{-7}$	$1.316 \cdot 10^{-7}$
150	$5.713 \cdot 10^{-9}$	$8.286 \cdot 10^{-9}$	$4.039 \cdot 10^{-8}$	$5.003 \cdot 10^{-8}$
300	$1.136 \cdot 10^{-9}$	$1.664 \cdot 10^{-9}$	$1.259 \cdot 10^{-8}$	$1.852 \cdot 10^{-8}$
600	$1.963 \cdot 10^{-10}$	$2.999 \cdot 10^{-10}$	$3.883 \cdot 10^{-9}$	$5.990 \cdot 10^{-9}$
1200	$2.900 \cdot 10^{-11}$	$4.807 \cdot 10^{-11}$	$1.102 \cdot 10^{-9}$	$1.714 \cdot 10^{-9}$

8. — Concluding remarks.

In the present work some sources of errors were removed by introducing in our calculations the precise values for the muon mass, the vertical intensity I_0 and the critical energy β . Errors arising from some approximative calculation methods were also eliminated. C. and K. made the approximation mentioned in (3.1) and took $\varepsilon = \bar{\varepsilon} = \frac{3}{4}$ without discussing the errors introduced in this manner. In more recent works (^{4,5}), the saddle-point method giving an error 20 % is used (*).

A cross-section determined with incomplete shielding has been used for the bremsstrahlung, because its applicability limit is given by

$$E_0 \ll \left(\frac{\mu}{m}\right)^2 \frac{137}{Z^{\frac{1}{2}}} mc^2 \approx 6.78 \cdot 10^{11}.$$

Measurements carried out with the muon spectrum at sea level and theoretical calculations (⁹) show a variation of α with energy

$$\begin{array}{lll} \text{in the range} & (8 \cdot 10^9 - 5.3 \cdot 10^{10}) \text{ eV} & \alpha = 2.8, \\ \text{in the range} & (5.3 \cdot 10^{10} - 10^{12}) \text{ eV} & \alpha = 3.2 \div 3.3. \end{array}$$

As the variation of α with energy is not known, spectrum normalization was performed according to Sect. 2. For $S > 1200$ a value of parameter > 3 is—as results from an estimated calculus—a possible explanation for the data in this domain.

For particle distribution in the shower, we have used Furry's model modified by C. and K., which gives good approximations in the range of $(10^{10} \div 10^{11})$ eV, that is for $S \approx (10^2 \div 10^3)$ particles. Therefore, it may be considered that our results are in agreement with experimental data up to $S = 1200$ particles.

APPENDIX I

Muon spectrum normalization.

Integration with respect to angles over the upper hemisphere and with respect to energies from E_{\min} to ∞ gives

$$(1) \quad \frac{y}{2\pi I_0} = \left(1 + \frac{E_0}{E_{\min}}\right)^{\alpha-1} J_{\alpha-1} \left(\frac{E_0}{E_{\min}}\right) = k.$$

(*) This method applies successfully only when the integrand vanishes rapidly to infinity (e.g. like e^{-x}) and the maximum peak is sufficiently far from the origin. For the integrals present in our work (7.1) the second condition is not fulfilled.

Noting $E_0/E_{\min} = N$; $N \gg 1$ we have according to definition

$$(2) \quad k = (N+1)^{\lambda-1} \int_0^1 \frac{dx}{(1+N/x)^{\alpha-1}} = N(N+1)^{\alpha-1} \int_N^\infty \frac{d\eta}{\eta^2(1+\eta)^{\alpha-1}} = \\ = N(N+1)^{\alpha-1} \sum_1^\infty \lambda \int_N^\infty \frac{d\eta}{(1+\eta)^{\alpha+\lambda}} = N \sum_1^\infty \lambda \frac{1}{\alpha+\lambda-1} \cdot \frac{1}{(N+1)^\lambda}$$

If we set

$$\frac{1}{N+1} = x \quad \text{and} \quad k_0 = \frac{1}{\alpha-1} \left(k - \frac{1}{\alpha} \right),$$

and take into account the identity

$$(3) \quad \sum_1^\infty \lambda \frac{1}{\alpha+\lambda-1} x^\lambda \equiv \frac{1}{\alpha} + (\alpha-1) \sum_1^\infty \lambda \frac{x^\lambda}{(\alpha+\lambda)(\alpha+\lambda-1)},$$

the problem is reduced to finding the real positive root of

$$\sum_1^\infty \lambda \frac{x^\lambda}{(\alpha+\lambda)(\alpha+\lambda-1)} = k_0.$$

If $x = \sum_j K_j k_0^j$ by identification we find

$$(5) \quad \frac{E_{\min}}{E_0 + E_{\min}} = \left(1 - \frac{1}{g(\alpha)} \right) = \alpha \frac{\alpha+1}{\alpha-1} \left(k - \frac{1}{\alpha} \right) - \frac{\alpha^3}{(\alpha+2)} \left(\frac{\alpha+1}{\alpha-1} \right)^2 \left(k - \frac{1}{\alpha} \right)^2 + \\ + \frac{\alpha^4}{(\alpha+2)^2(\alpha+3)} \left(\frac{\alpha+1}{\alpha-1} \right)^3 (\alpha^2 + 3\alpha - 2) \left(k - \frac{1}{\alpha} \right)^3 - \dots,$$

hence

$$(6) \quad g(\alpha) = 1 + \alpha \frac{\alpha+1}{\alpha-1} \left(k - \frac{1}{\alpha} \right) + \frac{2}{\alpha+2} \alpha^2 \left(\frac{\alpha+1}{\alpha-1} \right)^2 \left(k - \frac{1}{\alpha} \right)^2 + \\ + \frac{2(\alpha+6)\alpha^3}{(\alpha+2)^2(\alpha+3)} \left[\frac{\alpha+1}{\alpha-1} \right]^3 \left(k - \frac{1}{\alpha} \right)^3$$

APPENDIX II

Asymptotic expansion of $J_\alpha(a)$.

By definition

$$(1) \quad J_\alpha(a) = \int_0^{\pi/2} \frac{\sin \theta d\theta}{(1+(a/\cos \theta))^\alpha} = \int_0^1 \frac{dx}{(1+a/x)^\alpha}.$$

If we set $x/a = \xi$, $1/a = N$, then

$$(2) \quad J_{\lambda} \left(\frac{1}{N} \right) = \frac{1}{N} \int_0^N \left(1 + \frac{1}{\xi} \right)^{-\alpha} d\xi = 1 - \alpha \frac{\ln N}{N} + \frac{C_{\alpha}}{N} - \sum_1^{\infty} \frac{(-1)^{k-1}}{k} \frac{C_{\alpha+k}^{k+1}}{N^{k+1}}.$$

The integration constant C_{α} is defined so that (2) be an asymptotic series

$$(3) \quad C_{\alpha} = \lim_{N \rightarrow \infty} \left\{ \int_0^N \left(1 + \frac{1}{\xi} \right)^{-\alpha} d\xi - N + \alpha \ln N \right\} = \\ = \int_1^{\infty} \left\{ \left(1 + \frac{1}{\zeta} \right)^{\alpha} - 1 + \frac{\alpha}{\zeta} \right\} d\zeta = \alpha(\alpha-1) \sum_1^{\infty} \frac{1}{(k+1)(k+\alpha)}.$$

Expanding eq. (3) in series, after some straightforward transformations we find around the point $\alpha=3$; $\alpha-3=\varepsilon$

$$(4) \quad C_{\alpha} = \frac{5}{2} + \left\{ \frac{\pi^2}{2} - \left(3 + \frac{1}{4} \right) \right\} \varepsilon + \sum_1^{\infty} \frac{\lambda}{\lambda+3} \frac{(\varepsilon/(\lambda+3))^2}{1 + [\varepsilon/(\lambda+3)]},$$

or using Riemann's function $\zeta(p) = \sum_1^{\infty} 1/k^p$

$$(5) \quad C_{\alpha} = \frac{5}{2} + \left\{ \frac{\pi^2}{2} - \left(3 + \frac{1}{4} \right) \right\} \varepsilon + \sum_1^{\infty} (-1)^{k-1} \cdot \left\{ \zeta(k+1) - 3\zeta(k+2) + 2 + \frac{1}{2^{k+2}} \right\} \varepsilon^{k+1}.$$

APPENDIX III

About the derivation of the functions $g_k(a_m)$.

Functions $g_1, g_2, g_5, g_6, g_7, g_9$ are obtained performing a direct integration of expressions arising from functions $F_0, F_{\frac{1}{2}}$.

Functions g_3, g_4, g_8 — that are similar — may be expressed by means of transcendent functions $Y_p(x)$ and $L_p(x)$

$$(1) \quad Y_{\nu}(a_m) = \int_0^{a_m} x^{\nu} \ln \left[\frac{a_m}{1 - 6.3793 a_m} - x \right] dx,$$

$$(2) \quad L_{\nu} = \frac{\partial}{\partial p} Y_{\nu}(a_m).$$

For $g_3(a_m)$, for example, we obtain

$$(3) \quad g_3(a_m) = 1 + \alpha \frac{L_{\alpha-1}(a_m)}{Y_{\alpha-2}(a_m)} + C \frac{Y_{\alpha-1}(a_m)}{Y_{\alpha-2}(a_m)} - \sum_1^{\infty} \frac{(-1)^{k-1}}{k} C_{\alpha+k}^{\alpha-1} \frac{Y_{\alpha+k-1}(a_m)}{Y_{\alpha-2}(a_m)}.$$

After some transformations of the integrand in eq. (1), we find for $Y_p(x)$:

$$(4) \quad Y_p(x) = -x^{p+1} \left\{ \frac{\ln((1/x) - 6.3793)}{p+1} + \sum_1^{\infty} \frac{(1 - 6.3793x)^k}{k(k+p+1)} \right\}.$$

Introducing in eq. (3) the eqs. (1), (2) and (4), this takes, after some simple algebraic transformations, the form used in calculations.

RIASSUNTO (*)

Si sono eseguiti accurati calcoli delle frequenze dei burst generati dai muoni in uno strato schermante di piombo a livello del mare. Per diminuire le fluttuazioni si sono usati le sezioni d'urto per la bremsstrahlung nel caso di schermatura incompleta del nucleo da parte degli elettroni orbitali e il modello di Furry modificato da CHRISTY e KUSAKA. I risultati teorici risultano in buon accordo coi dati sperimentali nell'ambito di $(100 \div 1200)$ particelle assumendo per mesone μ lo spin $\frac{1}{2}$.

(*) Traduzione a cura della Redazione.

Investigations of Bremsstrahlung of Electrons in the Energy Interval ($10^{11} \div 10^{12}$) eV.

J. BENISZ, Z. CHYLIŃSKI and W. WOLTER

Institute of Nuclear Research - Cracow

(ricevuto il 7 Novembre 1958)

Summary. — Four high energy ($\sim 10^{12}$ eV) electron-photon cascades have been investigated at the first stage of their development. The number and the energy of the electron pairs of the first generation, produced on the first radiation length were estimated and compared with the theoretical values calculated on the basis of the theory of Bethe and Heitler. On the other hand, the same was calculated according to the theories of Landau, Pomerančuk and Ter-Mikaelyan which take into account the influence of the medium on the bremsstrahlung of electrons of very high energy. The experimental results are in better agreement with the predictions of Landau, Pomerančuk and Ter-Mikaelyan than with that of Bethe and Heitler. This fact confirms the results obtained earlier in our laboratory and given in a previous paper ⁽¹⁾.

1. — Introduction.

Up to the present time there were very few experiments investigating the problem of the influence of a dense medium on the probability of emission of bremsstrahlung photons by electrons of very high energies. The point in question is an effect first predicted by LANDAU ⁽²⁾, POMERANČUK and TER-MIKAELYAN ^(3,4) and followed up in papers by MIGDAL ^(5,7). According to

⁽¹⁾ M. MIĘSOWICZ, O. STANISZ and W. WOLTER: *Nuovo Cimento*, **5**, 513 (1957).

⁽²⁾ L. D. LANDAU and I. A. POMERANČUK: *Dokl. Akad. Nauk SSSR*, **92**, 535, 735 (1953).

⁽³⁾ M. L. TER-MIKAELYAN: *Žu. Èksper. Teor. Fiz.*, **25**, 289, 296 (1953).

⁽⁴⁾ M. L. TER-MIKAELYAN: *Dokl. Akad. Nauk SSSR*, **94**, 1033 (1954).

⁽⁵⁾ A. B. MIGDAL: *Dokl. Akad. Nauk SSSR*, **96**, 48 (1954).

⁽⁶⁾ A. B. MIGDAL: *Dokl. Akad. Nauk SSSR*, **105**, 77 (1955).

⁽⁷⁾ A. B. MIGDAL: *Žu. Èksper. Teor. Fiz.*, **32**, 633 (1957).

the theories developed by these authors we ought to expect that for very high energies ($\gtrsim 10^{12}$ eV in nuclear emulsions) the spectrum of bremsstrahlung photons is strongly cut down for low energy photons as compared with the Bethe and Heitler spectrum.

LANDAU, POMERANČUK and TER-MIKAELYAN have called in question the validity of the Bethe and Heitler formulas for very high electron energies and for photons for which $W/E \ll 1$, where W denotes the energy of the emitted photon and E the energy of the radiating electron. According to the LANDAU, POMERANČUK and TER-MIKAELYAN theory which will be further denoted by L-P-T the reason for this is as follows. If W/E is sufficiently small, the change of the momentum of an electron in consequence of an emission of a photon is so small that the uncertainty of the localization of the event due to Heisenberg's principle is much greater than the distances between the scattering centres. If so, in Landau's opinion, the effects due to the particular centres can not be treated additively as in BETHE and HEITLER's (B-H) ⁽⁸⁾ calculations. If this uncertainty range is large enough, the L-P-T theory predicts that multiple Coulomb scattering of the electron on the distance can destroy the coherence between electron and photon waves. It is thus expected that the bremsstrahlung cross-section at high energy will decrease below the B-H value. The polarization of the medium leads also to an analogous « decoherence » effect. The quantitative estimations of these phenomena were made firstly by LANDAU and POMERANČUK (multiple scattering effect) and TER-MIKAELYAN (polarization effect). More rigorous calculations based on a quantum theoretical treatment were given by MIGDAL.

The existence of the effect mentioned above was reported in a previous paper from our laboratory (MIĘSOWICZ *et al.* ⁽¹⁾). To study the quantitative agreement of the observed effect with the theory, more events of very high energy electron-photon cascades were needed, in order to increase the statistical significance of the obtained results.

The aim of this paper is to present an analysis performed on four electromagnetic cascades with primary energies $\sim 10^{12}$ eV. The results obtained, were compared with the theoretical predictions of the B-H and L-P-T theories.

Just before sending our work to print we received a paper by VARFOLOMEEV *et al.* ⁽⁹⁾ (*) in which the discrepancy between the observed development of electron-photon cascades and the development predicted by cascade theory, has been also interpreted on the basis of the L-P-T theory.

⁽⁸⁾ W. HEITLER: *The Quantum Theory of Radiation* (Oxford, 1954).

⁽⁹⁾ A. A. VARFOLOMEEV, R. I. GERASIMOVA, I. I. GUREVIČ, L. A. MAKARINA, A. C. ROMANTSEVA, I. A. SVETLOBOV and S. A. ČUEVA: *Proc. of the International Conference on High Energy Physics at CERN* (Geneve, 1958), Appendix I, p. 297.

(*) We are much indebted to Professor GUREVIČ for sending us the preprint before publication.

2. - Experimental method.

The present analysis concerns four electron-photon cascades. Three of them (cascade *A*, *B*, *C* in Table I) have been generated in a nucleon-nucleon interaction of the type $0+14x$ and energy $3.3 \cdot 10^{14}$ eV/nucleon (CIOK *et al.* ⁽¹⁰⁾). The fourth isolated cascade (cascade *D* in Table I) was described in the paper of MIĘSOWICZ *et al.* ⁽¹¹⁾. The energy of the primary photon of cascade *D* was found to be $(7.0^{+3.4}_{-2.6}) \cdot 10^{11}$ eV.

Since cascades *A*, *B*, *C* originate from decays of π^0 generated in the same nuclear interaction, the mutual radial distances between them are small. In consequence, electron tracks belonging to the different cascades are crossing each other at greater depths than about one radiation length from the point of origin of each primary pair. Therefore there was no possibility of evaluating the energy of each cascade separately. For this reason we have evaluated the mean energy of each cascade under the assumption that there is energy equipartition between primary photons and electrons of the primary pairs. This mean energy has been evaluated from the longitudinal development of the cascade taking into account the correction for lateral distribution according to PINKAU ⁽¹²⁾. From the number of electrons with energies greater than $1 \cdot 10^9$ eV and $4 \cdot 10^8$ eV within two different radii (the values of energies have been received from scattering measurements) at the depth 2.76 rad lengths from the point of interaction we have obtained for the mean energy of the cascade the values $(1.1^{+0.4}_{-0.4}) \cdot 10^{12}$ eV, $(1.3^{+0.8}_{-0.5}) \cdot 10^{12}$ eV respectively. In these calculations we used the cascade tables of JÁNOSSY ⁽¹²⁾ as well as Jánosy's ⁽¹³⁾ standard deviation. In the sequel we have accepted the value $1.2 \cdot 10^{12}$ eV for the mean energy of each cascade.

The mean energy of a π^0 meson (assuming the equipartition of energy between the two photons) equal to $2.4 \cdot 10^{12}$ eV is in good agreement with the energy values of two charged mesons which are contained within the same angle as the cascades. Their energies obtained from the secondary interactions are equal to $1 \cdot 10^{12}$ eV and $2 \cdot 10^{12}$ eV respectively.

Now we investigated the energy spectrum of pairs of the first generation only, generated on a given length from the point of origin of the cascade, and not the energy spectrum of all secondary electrons at a given depth as in cascade theory. By first generation pairs we understand pairs produced by the con-

⁽¹⁰⁾ P. CIOK, M. DANYSZ, J. GIERULA, A. JURAK, M. MIĘSOWICZ, J. PERNEGR, J. VRANA and W. WOLTER: *Nuovo Cimento*, **6**, 1409 (1957).

⁽¹¹⁾ K. PINKAU: *Nuovo Cimento*, **3**, 1285 (1956).

⁽¹²⁾ L. JÁNOSSY and H. MESSEL: *Proc. Roy. Irish Acad.*, A **54**, 217 (1951).

⁽¹³⁾ L. JÁNOSSY: *Acta Phys. Hung.*, **2**, 289 (1952).

TABLE I.

Pair	Distance from the point of origin of the primary pair (rad. lengths)	Obtained from the scattering measurements			Obtained from the angle of divergence	Remarks
		E_1 (eV)	E_2 (eV)	$W = E_1 + E_2$		
C a s c a d e A						
1	0	—	—	—	—	Primary pair (*) $E_1 + E_2 = 1.2 \cdot 10^{12}$ eV
2	0.26	$7.7 \cdot 10^8$	$1.2 \cdot 10^9$	$2.0 \cdot 10^9$	—	First generation
3	0.42	$1.3 \cdot 10^8$	$6.6 \cdot 10^8$	$7.9 \cdot 10^8$	—	The order of generation is unknown
4	0.50	$> 2.4 \cdot 10^9$	$> 2.5 \cdot 10^9$	$> 4.9 \cdot 10^9$	—	First generation
5	0.64	—	—	—	$> 1 \cdot 10^9$	First generation
6	0.81	$(3.0^{+2.5}_{-0.9}) \cdot 10^8$	$(3.5^{+4.0}_{-1.2}) \cdot 10^8$	$(6.5^{+6.5}_{-2.1}) \cdot 10^8$	—	The order of generation is unknown
7	0.92	—	—	—	$> 4.6 \cdot 10^9$	First generation
8	0.96	—	—	—	$> 3.5 \cdot 10^9$	First generation
C a s c a d e B						
1	0	—	—	—	—	Primary pair (*) $E_1 + E_2 = 1.2 \cdot 10^{12}$ eV
2	0.02	$> 1.0 \cdot 10^{10}$	$(7.8^{+10.7}_{-2.7}) \cdot 10^8$	$> 1.0 \cdot 10^{10}$	$\geq 1 \cdot 10^{10}$	First generation
3	0.18	$> 3.8 \cdot 10^9$	$> 3.4 \cdot 10^9$	$> 7.2 \cdot 10^9$	$> 1 \cdot 10^{10}$	First generation
4	0.52	$> 3.5 \cdot 10^9$	—	$> 3.6 \cdot 10^9$	$> 1 \cdot 10^9$	First generation
5	0.93	—	—	—	$> 1 \cdot 10^{10}$	First generation
6	0.94	—	—	—	$> 7 \cdot 10^9$	First generation
C a s c a d e C						
1	0	—	—	—	—	Primary pair (*) $E_1 + E_2 = 1.2 \cdot 10^{12}$ eV
2	0.27	$(1.1^{+0.6}_{-0.3}) \cdot 10^8$	$(1.3^{+2.6}_{-0.5}) \cdot 10^9$	$(1.4^{+2.7}_{-0.5}) \cdot 10^9$	$> 5 \cdot 10^8$ $< 1 \cdot 10^9$	First generation
3	0.57	$> 3.2 \cdot 10^9$	$> 4.8 \cdot 10^9$	$> 8.0 \cdot 10^9$	$> 1 \cdot 10^{10}$	First generation
4	0.57	$(1.3^{+0.5}_{-0.3}) \cdot 10^8$	$(3.0^{+3.6}_{-2.0}) \cdot 10^8$	$(4.3^{+4.1}_{-2.3}) \cdot 10^8$	$< 1 \cdot 10^8$	First generation
5	0.89	$(2.2^{+2.6}_{-0.7}) \cdot 10^8$	$(2.7^{+2.2}_{-0.8}) \cdot 10^8$	$(4.9^{+4.7}_{-1.5}) \cdot 10^8$	—	The order of generation is unknown
C a s c a d e D						
1	0	—	—	—	—	Primary pair (*) $E_1 + E_2 = 7.0 \cdot 10^{11}$ eV
2	0.32	$2.0 \cdot 10^8$	$1.0 \cdot 10^8$	$3.0 \cdot 10^8$	—	First generation
3	0.57	$1.3 \cdot 10^8$	$1.0 \cdot 10^7$	$1.4 \cdot 10^8$	—	First generation
4	0.60	$6.0 \cdot 10^8$	$\geq 7.0 \cdot 10^8$	$\geq 1.3 \cdot 10^9$	—	First generation
5	0.82	$1.3 \cdot 10^8$	$8.0 \cdot 10^7$	$2.1 \cdot 10^8$	—	First generation
6	0.96	$\geq 1.0 \cdot 10^9$	$7.5 \cdot 10^8$	$\geq 1.8 \cdot 10^9$	—	First generation

(*) $E_1 + E_2 = 2E_0$ according to the assumption of equipartition of the energy.

version processes of bremsstrahlung photons emitted by electrons of the primary pair.

We succeeded in evaluating the energy of almost all electron pairs of first generation for each cascade separately. It is obvious that the distance from the point of origin of the primary pair up to the end point where the scanning for electron pairs is stopped, ought to be as long as possible (in our case about one radiation length from the point of origin of each primary pair).

The restriction to electron pairs of the first generation only, was imposed by the conditions of our measurements. As it was mentioned above, the small radial distances between the separate cascades *A*, *B*, *C* do not allow to correlate with the particular cascade any electron pair generated at a rather great distance from the tracks of the primary electron pair. On the other hand, it is known that all the electron pairs of the first generation, in consequence of great energy of the primary electrons, must originate in close proximity of the parent track as apparent tridents. Since the losing of such pairs is rather improbable, we avoid in this way the scanning bias.

In our opinion, investigation performed on electron pairs of the first generation is more sensitive for detecting the L-P-T effect than the investigation of the development of the whole cascade. The L-P-T effect is rather reduced by the degradation of energy, whereas in our procedure such a degradation does not take place.

We have used two criteria, energy and geometry criteria, whether a pair is a first generation one. Such a procedure was successful in all cases except in the case of three electron pairs where there was no possibility to establish the order of generation, *i.e.* in which successive generation each pair was produced. The energy measurements have been performed by scattering, especially the differential one. In cases in which the application of scattering was not possible, we have based on the data derived from the measurements of the angle of divergence.

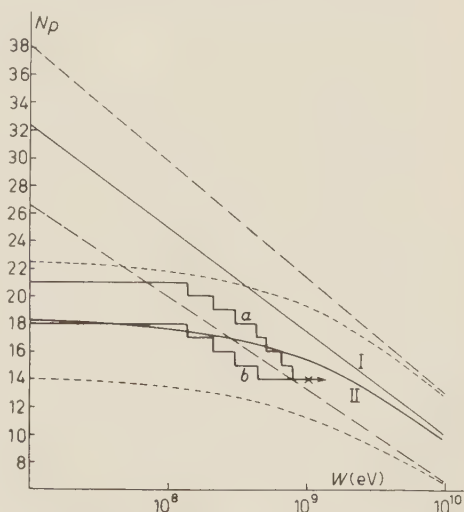


Fig. 1. — Integral energy spectrum of electron pairs of the first generation created in the first radiation length. N_p : number of pairs of energy greater than the given value W . *a*, *b*: experimental histograms. I, II: Bethe, Heitler and Landau, Pomeranchuk, Ter-Mikaelian curves respectively (primary electron energy $5 \cdot 10^{11}$ eV). Curves I and II are given with their standard deviations.

In Table I there are given the results of our measurements performed on four cascades. The energy spectrum of electron pairs of the first generation created on the first radiation length has been done on the basis of the data given in Table I (Fig. 1). The histograms represent the experimental spectrum taking into account the uncertainty of the order of generation of the three electron pairs (histograms *a* and *b*). For energies greater than about 10^9 eV (see the point with an arrow on Fig. 1) the shapes of the histograms are unknown because of the impossibility of evaluating the upper limit of such high energies. Curves I and II represent the B-H and L-P-T spectra respectively for the primary electron energy equal to $5 \cdot 10^{11}$ eV at the depth of one radiation length. This energy value corresponds to the mean energy of eight primary electrons of four cascades under consideration (six primary electrons each of energy of $6 \cdot 10^{11}$ eV and two primary electrons each of energy of $3.5 \cdot 10^{11}$ eV). The dashed curves represent the Poisson deviation from the theoretical curves of B-H and L-P-T.

3. - Discussion on experimental procedure.

We have calculated the average number of electron pairs of first generation with energy greater than W , created by the primary electron of initial energy E_0 on the length t , where t is the distance from the beginning of the electron trajectory. The calculations were made, first on the basis of the B-H formulas and then also performed by means of the L-P-T formulas.

Fig. 2 shows the integral energy spectrum of electron pairs of the first generation obtained from these two theories. Theoretical curves I and II of Fig. 1 have been obtained in the same way as the curves of Fig. 2.

We have taken into account the energy loss of the primary electron resulting from radiation. The energy losses from ionization (about $2 \cdot 10^7$ eV on one radiation length) are in our case negligible in comparison with the energy of about 10^{12} eV.

In our problem we must take into consideration the cross-sections of the following processes which are decisive in forming the energy spectrum of electron pairs.

- 1) Pair production by photons,
- 2) Compton effect,
- 3) Photonuclear reactions,
- 4) Production of tridents.

Processes 1), 2) and 3) are competitive. From the geometry of the experiment, *i.e.* from the fact that the number of pairs is observed on the first radiation length follows that the reduction of the number of pairs caused by 2 and 3 is negligible. The number of pairs of energy $W \sim 10^7$ eV is diminished by about (2 ÷ 3%). The number of pairs of energy $W > 10^8$ eV practically rests unchanged, because in this energy range the cross-sections of processes 2) and 3) are very small in comparison with the cross-section of 1).

The increasing of the mean free path for pair production with the decreasing energy of photons ($\sim 10^7$ eV) results in the same direction. Although this effect and the effects 2) and 3) act in the same direction as the modification of L-P-T, nevertheless they are much smaller than this modification. We have estimated that the whole cumulative influence amounts to only some per cent and so, is negligible in comparison with the L-P-T modification.

So we see that the number of electron pairs of first generation is a sensitive detector of the character of the bremsstrahlung spectrum and quite insensitive to competitive effects, in comparison with the process of pair production.

The number of pairs is of course increased by the trident production, however, this last one does not favour the production of pairs of small energies. Accepting for $E_0 = 5 \cdot 10^{11}$ eV the mean free path for trident production about 3.5 radiation lengths, we obtain a contribution of about 6% of the whole number of pairs produced by the first process. Finally we see that the effects 2), 3) and 4) are of no importance in our problem.

On Fig. 2, representing the results of both theories (B-H and L-P-T), it is interesting to remark that in the B-H energy spectrum we have the dependence of the number of pairs on E_0/W only, while in the analogous curves of L-P-T there is a dependence on both E_0 and W .

Although there is a possibility of large errors in estimating E_0 , the primary energy of the electron, it is important to stress that the change of E_0 even by one order of magnitude, does not change the character of the L-P-T spectrum. From Fig. 2 we see also that the L-P-T spectrum curves have a plateau be-

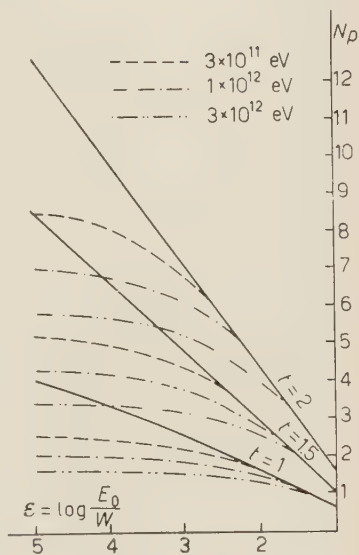


Fig. 2. - Integral energy spectrum of electron pairs of the first generation. N_p : number of pairs of energy greater than that corresponding to the value ε . Full curves: Bethe-Heitler curves for three different depths (1.0, 1.5, 2.0 radiation lengths). Dashed and dotted dashed curves: Landau, Pomerančuk, Ter-Mikaelyan curves for the depths 1.0, 1.5, 2.0 radiation lengths and the primary electron energy $E_0 = 3 \cdot 10^{11}$ eV, $1 \cdot 10^{12}$ eV and $3 \cdot 10^{12}$ eV.

ginning from a certain ε , which feature is not shown by the B-H spectrum curve. This is the main consequence of the L-P-T theory which just expresses the lack of small energy pairs.

4. - Conclusions.

1) The experimental energy spectrum of the electron pairs of the first generation, produced in the first radiation length, shows a statistically significant deviation from the Bethe and Heitler energy spectrum curve.

2) There is rather a good agreement between the experimental results and the curve which represents the energy spectrum of Landau, Pomerančuk and Ter-Mikaelyan.

3) The method of investigation of electron pairs of the first generation only, is in the author's opinion a sensitive tool in detecting the difference between the energy spectrum of Bethe and Heitler and that of Landau, Pomerančuk and Ter-Mikaelyan, since in cascade development there is a degradation of energy of the emitting electron.

* * *

We wish to express our gratitude to Professor M. MIĘSOWICZ for suggesting these investigations, his permanent interest in our work, and many valuable ideas and hints during the progress of this work.

RIASSUNTO (*)

Si sono esaminate quattro cascate elettrofotoniche di alta energia ($\sim 10^{12}$ eV) nel primo stadio del loro sviluppo. Il numero e l'energia delle coppie di elettroni della prima generazione prodotte nella prima lunghezza di radiazione sono stati stimati e confrontati coi valori teorici calcolati sulla base della teoria di Bethe e Heitler. Le stesse grandezze sono state anche calcolate in base alle teorie di Landau, Pomerančuk e Ter-Mikaelyan che tengono conto dell'influenza del mezzo sulla bremsstrahlung di elettroni di altissima energia. I risultati sperimentali sono in miglior accordo colle previsioni di Landau, Pomerančuk e Ter-Mikaelyan che con quelle di Bethe e Heitler, confermando i risultati ottenuti nel nostro laboratorio e comunicati in un precedente lavoro ⁽¹⁾.

(*) Traduzione a cura della Redazione.

Rayleigh Scattering of Polarized Photons.

D. BRINI, E. FUSCHINI, D. S. R. MURTY (*) and P. VERONESI

Istituto di Fisica dell'Università - Bologna

Istituto Nazionale di Fisica Nucleare - Sezione di Bologna

(ricevuto il 22 Novembre 1958)

Summary. — We discuss two criteria for comparing in a decisive manner the theoretical predictions on the Rayleigh scattering deduced by FRANZ and by BROWN and MAYERS. The first deals with the study of the Rayleigh scattering of the polarized photons, the second considers the polarization effects due to the Rayleigh scattering of an unpolarized radiation. In the elastic scattering of polarized photons an asymmetry ratio R can be defined as $(d\sigma_0/d\Omega + \xi_{\parallel} d\sigma_1/d\Omega) / (d\sigma_0/d\Omega + \xi_{\perp} d\sigma_1/d\Omega)$, where the numerator and the denominator represent the Rayleigh cross-section for the same angle of scattering in two orthogonal planes. The quantities ξ_{\parallel} and ξ_{\perp} are the degrees of polarization of the incident beam referred to the previous planes, while $d\sigma_0/d\Omega$ is the cross-section for the unpolarized photons and $d\sigma_1/d\Omega$ is the term sensitive to polarization. The value of R was determined by using a beam of photons of energy 1.28mc^2 scattered on a target of Hg at angles of scattering $\theta_1 = 65^\circ$, $\theta_2 = 90^\circ$ and $\theta_3 = 110^\circ$. The experimental results are in closer agreement with the calculations of BROWN and MAYERS. The polarized beam was obtained by means of a Compton scattering at an angle of 50° of the unpolarized beam coming from a ^{60}Co source.

1. — Introduction.

It is known that in all the experiments performed in order to put in evidence the Delbrück scattering, the knowledge of the contribution of the Rayleigh scattering has a fundamental importance.

(*) On leave from the Physics Department, Osmania University, Hyderabad (India).

In fact it is possible, in principle, to deduce the cross-section of the Delbrück effect by subtracting the THOMSON and RAYLEIGH contributions from the values of the differential cross-section of the elastic scattering. While the THOMSON contribution can be easily calculated, some uncertainty exists for the Rayleigh effect. The theory of the latter effect due to FRANZ ⁽¹⁾ was the only one available until a few years back, and this is based on an atom model and on a simplifying hypothesis which could not be considered completely satisfying to describe the phenomenon. In recent years more precise calculations were made by BRENNER, BROWN and WOODWARD ⁽²⁾ and by BROWN and MAYERS ^(3,4) for different energies of photons but only for the scattering on the *K*-shell electrons of Hg.

Though the calculations of these authors offer a greater confidence of exactness, however, an experimental test is necessary which permits a direct confirmation of the validity of the theory proposed by them in comparison with that of FRANZ ⁽⁵⁻⁸⁾. A comparison of the theories made by means of the measurement of the absolute value of the differential cross-section of the Rayleigh scattering results quite unprecise as shown by the different results of the various authors. The reason for the imprecision lies in the difficulties of evaluation of the corrections for the counter efficiency, the absorption of the scattered radiation in the target, and the evaluation of the number of scattering centers, etc.

Two criteria exist which permit a comparison of the two theories with experiment which eliminate to a large extent the inconveniences cited above. The first criterion consists in the study of the Rayleigh scattering of polarized photons and the second criterion in the experimental verification of the polarization effects produced by the Rayleigh scattering.

The first method was used by us in a previous work as well as in the present measurements ⁽⁹⁾. The second method was successfully used by SOOD ⁽¹⁰⁾ in a very recent experiment and by SOOD and KNAPP ⁽¹¹⁾ in the study of the resonance nuclear scattering.

(1) W. FRANZ: *Zeits. Phys.*, **98**, 314 (1936).

(2) S. BRENNER, G. E. BROWN and J. B. WOODWARD: *Proc. Roy. Soc.*, A **227**, 59 (1954).

(3) G. E. BROWN and D. F. MAYERS: *Proc. Roy. Soc.*, A **234**, 387 (1956).

(4) G. E. BROWN and D. F. MAYERS: *Proc. Roy. Soc.*, A **242**, 89 (1957).

(5) P. KESSLER and P. EBERHARD: *Compt. Rend.*, **245**, 1599 (1957).

(6) M. FEIX, P. KESSLER and P. NICOURD: *Compt. Rend.*, **246**, 3226 (1958).

(7) N. CINDRO and K. ILAKOVAC: *Nucl. Phys.*, **5**, 647 (1958).

(8) K. G. STANDING and J. V. JOVANOVIĆ: *Nature*, **182**, 521 (1958).

(9) D. BRINI, E. FUSCHINI, L. PELI and P. VERONESI: *Nuovo Cimento*, **7**, 877 (1958).

(10) B. S. SOOD: *Proc. Roy. Soc.*, A **247**, 575 (1958).

(11) V. KNAPP and B. S. SOOD: *Proc. Roy. Soc.*, A **247**, 369 (1958).

LOVAS⁽¹²⁾ has recently suggested the same criterion to separate the different components of the elastically scattered radiation, particularly the Delbrück effect.

In the following two sections we examine in some detail the two criteria and report the results of some numerical calculations made following both theories and using the formalism of the Stokes parameters⁽¹³⁾.

2. - Elastic scattering of polarized photons.

By means of a convenient Compton scattering of an unpolarized radiation a partially polarized photon beam is obtained a (*). This beam after a suitable collimation is sent on to a Hg target where the elastic interaction takes place. For a fixed angle of elastic scattering the ratio between the intensity of the scattered radiation in the plane of Compton scattering and the intensity scattered in the orthogonal plane, is expressed by the relation

$$(1) \quad R = \frac{d\sigma_0/d\Omega + \xi_{\parallel}(d\sigma_1/d\Omega)}{d\sigma_0/d\Omega + \xi_{\perp}(d\sigma_1/d\Omega)},$$

where: $d\sigma_0/d\Omega$ is the differential cross-section of Rayleigh scattering for unpolarized photons;

$d\sigma_1/d\Omega$ is the term of the cross-section sensitive to polarization and ξ is the degree of polarization of the incident beam defined as the second Stokes parameter of the Compton scattered beam, making the total intensity equal to unity.

Substituting in (1) the explicit expressions of $d\sigma_0/d\Omega$ and $d\sigma_1/d\Omega$ deduced from the two theories of Franz and of Brown and Mayers one can obtain the corresponding values of R . These values of R can be compared with those obtained from the experiment. In Fig. 1 are plotted the ratios which can be deduced from the two above mentioned theories for the energies of 0.32 mc^2 , 0.64 mc^2 , 1.28 mc^2 and 2.56 mc^2 . The solid curve represents the behaviour

(12) I. LOVAS: *Nucl. Phys.*, **8**, 155 (1958).

(13) U. FANO: *Journ. Opt. Soc. Am.*, **39**, 859 (1949).

(*) It is clear that the Compton scattering is not the only polarizing scattering. All the elastic scatterings give, as we shall see, polarization effects. Here we have considered only that Compton component whose cross-section is high.

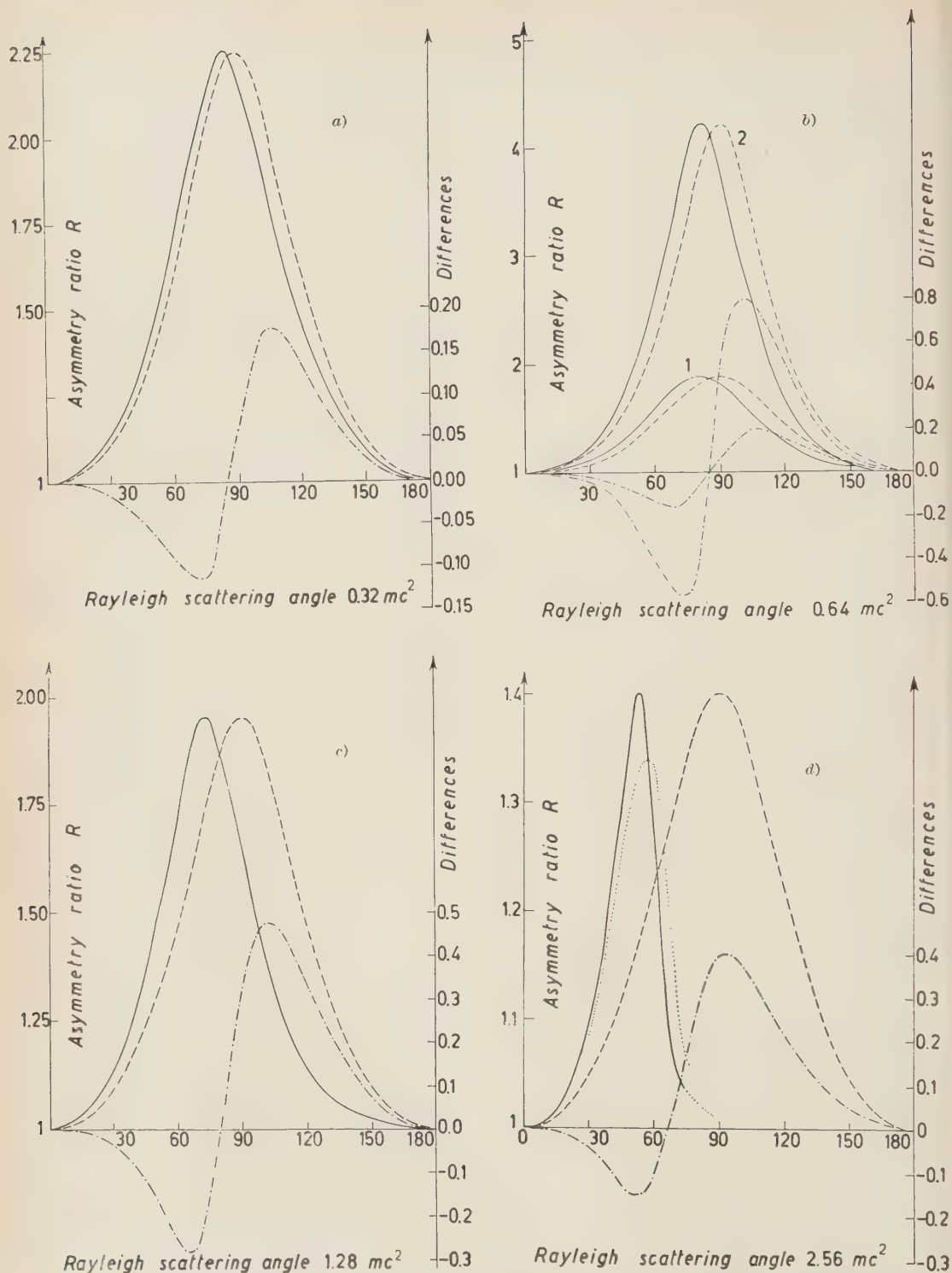


Fig. 1. - Asymmetry ratio in Rayleigh scattering of polarized photons. Solid line: Brown and Mayers theory. Dashed line: Franz theory. Dashed-dotted line: differences between the values of the asymmetry ratios deduced from the two theories. (See Table I).

of R deduced from Brown' and Mayers theory, the dashed curve the behaviour of R from Franz' theory and the dotted-dashed curve gives the difference between the ratios.

TABLE I. — *Data referring to the curves of Fig. 1.*

Energy	Source	Compton scattering angle	Polarization degree
0.32 mc ²	⁵¹ Cr 0.320 MeV	123°	— 0.384
0.64 mc ²	¹³⁷ Cs 0.666 MeV	77°	— 0.615
	⁶⁰ Co { 1.17 MeV	100°	— 0.307
	1.33 MeV		
1.28 mc ²	⁶⁰ Co { 1.17 MeV	50°	— 0.322
	1.33 MeV		
2.56 mc ²	²⁴ Na 2.75 MeV	38°	— 0.167

In the case of the energy of 2.56 mc² we take into account the contribution of the Thomson effect. The dotted line represents the resulting asymmetry ratio.

3. — Polarization effects in the elastic scattering.

We shall confine our consideration briefly to Thomson and Rayleigh scattering. We wish to deduce the expression for the degree of polarization of the scattered radiations as a function of the scattering angle.

3'1. *Thomson scattering.* — Let us consider an unpolarized beam represented by the parameters

$$(2) \quad \begin{pmatrix} 1 \\ 0 \\ 0 \\ 0 \end{pmatrix}.$$

The operator which, applied to the Stokes parameters of a generic γ -ray beam, permits to deduce the relations which describe the Thomson scattering is given by the matrix (*)

$$(3) \quad T = \frac{1}{2} r_0^2 \begin{pmatrix} 1 + \cos^2 \theta & -\sin^2 \theta & 0 & 0 \\ -\sin^2 \theta & 1 + \cos^2 \theta & 0 & 0 \\ 0 & 0 & 2 \cos \theta & 0 \\ 0 & 0 & 0 & 2 \cos \theta \end{pmatrix},$$

(*) The matrix T can be deduced in this classical case, in a very simple way. We omit here the calculations which lead to its determination.

where r_0 is the classical radius of the electron and θ the scattering angle. The Stokes parameters of the scattered beam are then expressed by

$$(4) \quad T \begin{pmatrix} 1 \\ 0 \\ 0 \\ 0 \end{pmatrix} = \frac{1}{2} R_0^2 \begin{pmatrix} 1 + \cos^2 \theta \\ -\sin^2 \theta \\ 0 \\ 0 \end{pmatrix},$$

where we put $R_0^2 = Z^2 e^2 / A c^2$ instead of r_0^2 since this is the equivalent expression for the nucleus.

From (4) it can be seen that the scattered beam is partially linearly polarized in the plane of scattering with a degree of polarization ξ given by

$$(5) \quad \xi = -\frac{\sin^2 \theta}{1 + \cos^2 \theta}.$$

ξ is independent of the energy of the photons, of the scattering material and is symmetric around 90° .

3.2. *Rayleigh scattering.* - Theory of Franz: We recall the expression for the Rayleigh scattering cross-section for a wave linearly and totally polarized deduced from the Franz theory,

$$\frac{d\sigma}{d\Omega} = A^2 r_0^2 \sin^2 \Theta,$$

where A is the form factor and Θ is the angle between the direction of vibration of the incident wave and the direction of the scattering wave.

The theory of Franz for the polarization states of the scattered beam, leads to the same result found for the Thomson scattering; the matrix T in this case results identical to (3) multiplied by the form factor. Consequently the expression of ξ is still given by (5).

Theory of Brown and Mayers: The deduction of the matrix T for the Rayleigh scattering based on Brown and Mayers' theory and valid only for the K shell electrons (calculated specifically for Hg) was made by BÖBEL and PASSATORE (14). It results in the following form:

$$(6) \quad T = r_0^2 \begin{pmatrix} AA^* + BB^* & 2(R)AB^* & 0 & 0 \\ 2(R)AB^* & AA^* + AB^* & 0 & 0 \\ 0 & 0 & AA^* - BB^* & 2(I)A^*B \\ 0 & 0 & 2(I)AB^* & AA^* - BB^* \end{pmatrix},$$

(14) G. BÖBEL and G. PASSATORE: private communication.

where

$$A = M(1', 1) + M(2', 2) \quad \text{and} \quad B = M(1', 2) + M(2', 1).$$

$M(1', 1)$, $M(2', 2)$, $M(1', 2)$ and $M(2', 1)$ are the complex quantities calculated by BROWN and MAYERS in their work (*). Bearing in mind (6), the scattered beam is represented by the parameters

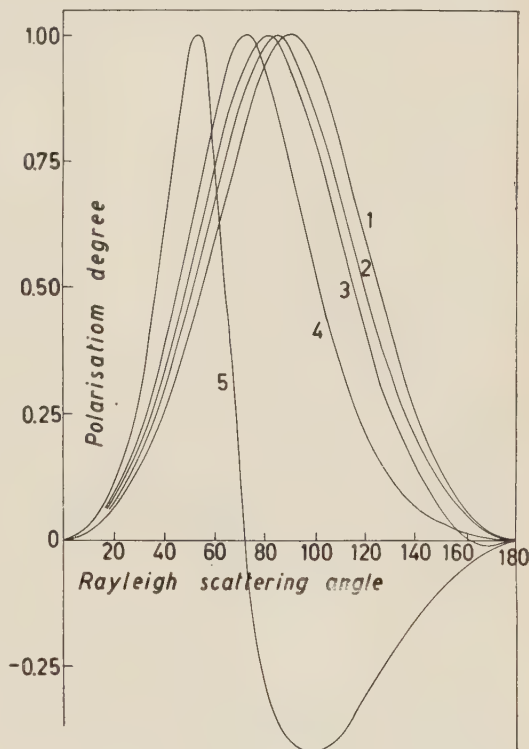
$$(7) \quad T \begin{pmatrix} 1 \\ 0 \\ 0 \\ 0 \end{pmatrix} = r_0^2 \begin{pmatrix} AA^* + BB^* \\ -2(R)AB^* \\ 0 \\ 0 \end{pmatrix}.$$

Remembering the definition of the degree of polarization we can deduce in this case

$$(8) \quad \xi = -\frac{2(R)AB^*}{AA^* + BB^*}.$$

The behaviour of $-\xi$ for the various energies and for both theories is shown in Fig. 2. The curve for 2.56 mc² energy does not take

Fig. 2. — Polarization degree of the Rayleigh scattered radiation as a function of the scattering angle: 1) Franz' theory; 2) Brown and Mayers' theory for the energy of 0.32 mc²; 3) Brown and Mayers theory for the energy of 0.64 mc²; 4) Brown and Mayers theory for the energy of 1.28 mc²; 5) Brown and Mayers theory for the energy of 2.56 mc².



(*) These authors do not report for the energy $h\nu=1.28$ mc² the imaginary parts of the scattering amplitudes. The data which permitted us to calculate these imaginary parts were kindly supplied by the authors in a private communication. In the Appendix we shall report the scattering amplitudes completed with the imaginary parts.

into account the interference contribution due to Thomson scattering, which is not negligible at this energy. The change in the sign of the polarization degree at large angles has not any particular significance. It results only as a consequence of the approximation

with which the numerical calculations of the quantities M were evaluated.

The Fig. 2 shows evidently the different behaviour of the polarization effects deduced from one or the other of the theories. An experimental verification of this fact represents a check very decisive in respect of the two theories.

A Compton scattering of the radiation already polarized in the elastic scattering can be utilized for this purpose. Also in this case an asymmetry ratio R' can be conveniently determined and it results

$$(9) \quad R' = \frac{d\sigma_0/d\Omega + \xi (d\sigma_1/d\Omega)}{d\sigma_0/d\Omega + \xi_{\perp} (d\sigma_1/d\Omega)},$$

where this time the quantities $d\sigma_0/d\Omega$ and $d\sigma_1/d\Omega$ correspond to Compton scattering and are deducible from Fano's matrix ⁽¹³⁾. Choosing for each of the four energies considered the Compton scattering angle for which R' results maximum, it is possible

to calculate its behaviour as a function of ξ , that is, as a function of the angle of the polarizing elastic scattering. Fig. 3 shows the behaviour of R' ; one sees that at low energies the difference between the theory of Franz and that of Brown and Mayers is less significant than at high energies. In the case of 2.56 mc^2 we have considered the interference with the Thomson effect.

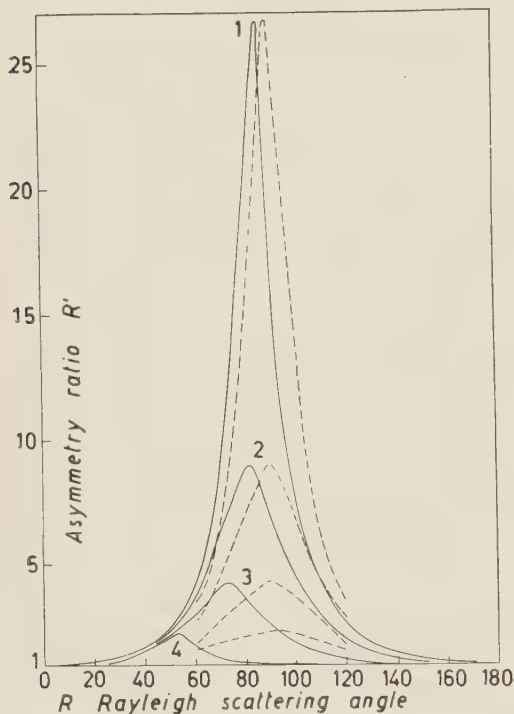


Fig. 3. — Asymmetry ratio R' . Dashed line: Franz' theory. Solid line: Brown and Mayers' theory: 1) 0.32 mc^2 Compton scattering angle $\theta_c = 90^\circ$; 2) 0.64 mc^2 Compton scattering angle $\theta_c = 90^\circ$; 3) 1.28 mc^2 Compton scattering angle $\theta_c = 80^\circ$; 4) 2.56 mc^2 Compton scattering angle $\theta_c = 70^\circ$.

4. - The experiment.

In the previous paper we reported the results of a measurement of R defined by (1) for an energy $h\nu = 0.64 \text{ mc}^2$. In the present paper we report the results of a measurement performed at the energy $h\nu = 1.28 \text{ mc}^2$.

By means of a Compton scattering at 50° of a collimated beam of photons from a ^{60}Co source a partially polarized beam of mean energy 1.28 mc^2 is obtained. The polarization degree averaged over the energies of 1.17 MeV and 1.33 MeV of the incident photons with the criterion already mentioned ⁽⁹⁾ results to have the absolute value

$$\xi = 0.322.$$

In Fig. 4 is shown the spectrum of the Compton scattered radiation after a second collimation along with a spectrum of ^{137}Cs . Observing that the counter resolution is 10% at half-maximum, the dispersion in energy of the polarized beam is 20% since our radiation has an energy of $(1.28 \pm 0.013) \text{ mc}^2$.

The polarized beam is directed to a Hg target on which the investigated Rayleigh scattering takes place. The cross-section of the process may be given in the form

$$\frac{d\sigma}{d\Omega} = \frac{d\sigma_0}{d\Omega} + \xi \frac{d\sigma_1}{d\Omega}.$$

We have calculated the values of $d\sigma_0/d\Omega$ and $d\sigma_1/d\Omega$ from both theories. In Fig. 5 is shown their behaviour as a function of the scattering angle and in units of r_0^2 . In this connection one must observe that comparison between the two theories is valid only for sufficiently large angles to which correspond great transfers of momentum.

From the so calculated cross-section values and taking into account the polarization degree it is possible to evaluate from (1) the asymmetry ratio

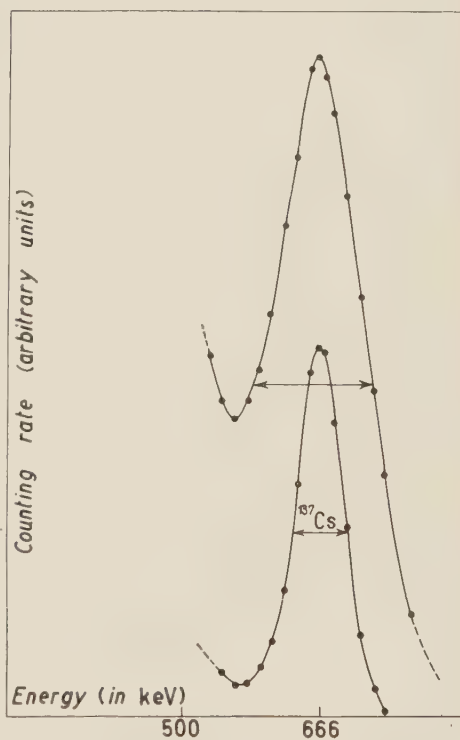


Fig. 4. - Photoelectric peak of the polarized beam and of a ^{237}Cs source.

as a function of the scattering angle. The behaviour of such asymmetry ratio for the theory of Franz as well as for that of Brown and Mayers is shown in Fig. 1.

The asymmetry ratio was measured at angles of 65° , 90° and 110° with a disposition similar to that used in our previous work and by utilizing the

same criterion for the selection of the investigated events from the spurious ones (Fig. 6).

The reason for choosing these angles is that at these values the asymmetry ratio is very significant.

In a manner similar to that followed in the previous work we evaluated the influence of the geometry due to the finite dimensions of the scatterers and detectors. The calculations made to this purpose show that for the angles of 65° and 110° the geometry does not considerably alter the results obtained for the point-like scatterers and detectors, while at 90° the influence of geometry is appreciable.

The eventual asymmetry due to geometry was measured by sending on to the target of Hg an unpolarized beam of photons. The measurements were made in two different ways, once by using a very intense source of ^{60}Co and another time by using a small source of ^{137}Cs ; the results obtained have been averaged.

In Table II is given a summary of the results.

As can be seen the results are in closer agreement with the theory of Brown and Mayers.

In all our evaluations we have disregarded the contribution of the L shell to Rayleigh scattering; although little is known about it, it is generally considered to be very

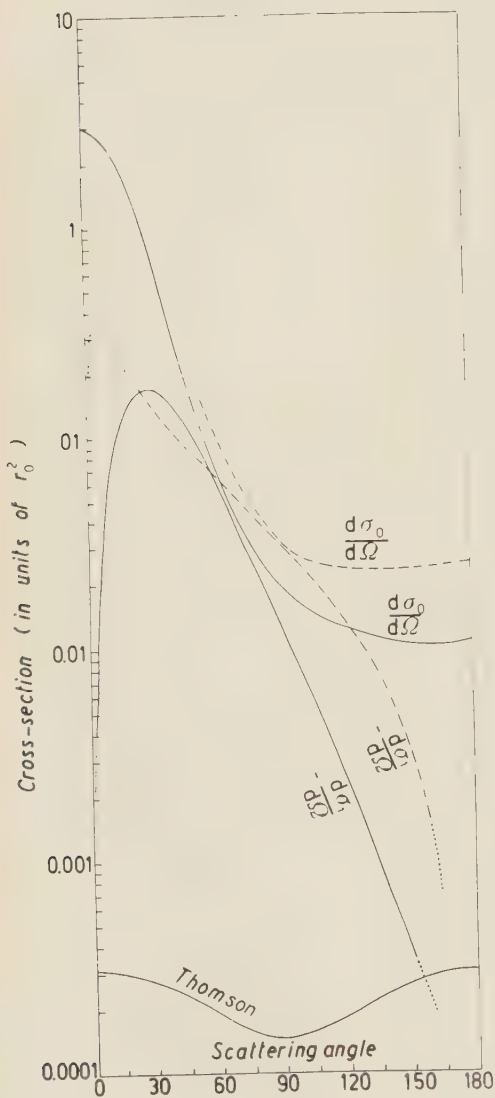


Fig. 5. — Rayleigh and Thomson scattering cross-sections. Solid curve: Brown and Mayers' theory. Dashed curve: Franz' theory.

TABLE II.

Angle	R_{theor}		$R_{\text{corrected}}$		R_{measured}	$R_{\text{geometrical}}$	$R_{\text{effective}}$
	F	B.M.	F	B.M.			
65°	1.575	1.836	1.580	1.855	1.831 ± 0.077	0.980 ± 0.012	1.868 ± 0.082
90°	1.955	1.650	1.880	1.520	$\left\{ \begin{array}{l} 1.602 \pm 0.198 \\ 1.370 \pm 0.120 \end{array} \right.$	$\left\{ \begin{array}{l} 1.115 \pm 0.016 \\ 0.966 \pm 0.005 \end{array} \right.$	1.423 ± 0.104
110°	1.685	1.250	1.660	1.234	1.337 ± 0.211	1.032 ± 0.007	1.295 ± 0.205

small especially at large angles. Similarly we have not taken into account the small percentage of Thomson scattering whose presence, however, acts in favour of Franz' theory.

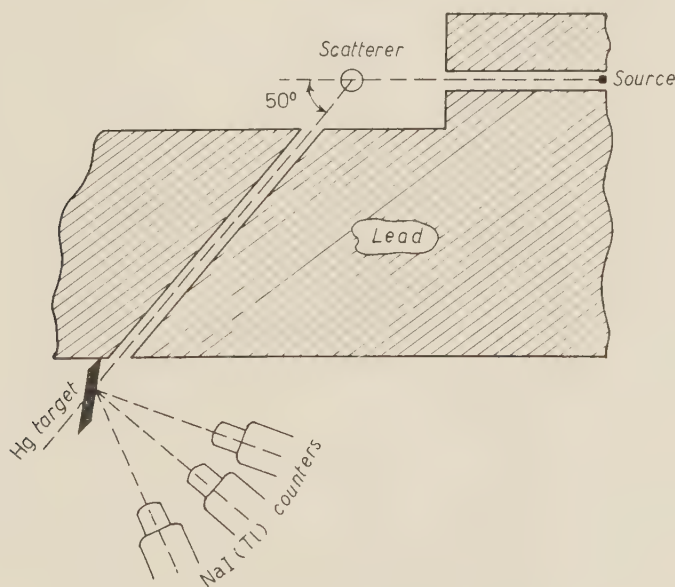


Fig. 6. - Experimental arrangement.

An evaluation of its contribution on our experimental results brings about an yet greater confirmation of the agreement with the theory of Brown and Mayers.

* * *

We are grateful to Mr. G. BUSACCHI and to Mr. R. VOLTA for their continued help in maintaining the electronic equipment.

One of us (D.S.R.M.) wishes to express his grateful thanks to Professor G. PUPPI, Director of the Institute for a fellowship and for the hospitality.

APPENDIX

We report in the following Table the scattering amplitudes on Hg for the energy 1.28 mc^2 . They include the imaginary parts which were not reported in the work of Brown and Mayers.

TABLE III.

Angle	$A = M(1', 1) + M(2', 2)$	$B = M(1', 2) + M(2', 1)$
0	$1.7454 - i 0.1062$	$-0.0000 + i 0.0000$
10	$1.6159 - i 0.0980$	$-0.0158 + i 0.0032$
20	$1.2967 - i 0.0777$	$-0.0531 + i 0.0109$
30	$0.9316 - i 0.0546$	$-0.0914 + i 0.0187$
40	$0.6251 - i 0.0357$	$-0.1182 + i 0.0239$
50	$0.4042 - i 0.0229$	$-0.1319 + i 0.0258$
60	$0.2540 - i 0.0149$	$-0.1374 + i 0.0254$
70	$0.1568 - i 0.0101$	$-0.1373 + i 0.0237$
80	$0.0960 - i 0.0074$	$-0.1335 + i 0.0212$
90	$0.0580 - i 0.0059$	$-0.1280 + i 0.0184$
100	$0.0346 - i 0.0046$	$-0.1223 + i 0.0159$
110	$0.0204 - i 0.0035$	$-0.1170 + i 0.0137$
120	$0.0117 - i 0.0027$	$-0.1123 + i 0.0119$
130	$0.0060 - i 0.0020$	$-0.1082 + i 0.0105$
140	$0.0034 - i 0.0014$	$-0.1040 + i 0.0093$
150	$0.0021 - i 0.0007$	$-0.1017 + i 0.0084$
160	$0.0010 - i 0.0002$	$-0.1013 + i 0.0078$
170	$0.0002 - i 0.0000$	$-0.1022 + i 0.0076$
180	$0.0000 - i 0.0000$	$-0.1029 + i 0.0075$

RIASSUNTO

Si discutono due criteri per confrontare in modo decisivo le previsioni teoriche dello scattering Rayleigh effettuate da FRANZ e da BROWN e MAYERS. Il primo consiste nello studiare lo scattering Rayleigh di fotoni polarizzati, il secondo nel considerare gli effetti di polarizzazione dovuti allo scattering Rayleigh di una radiazione non polarizzata. Nello scattering di fotoni polarizzati si può definire un rapporto di asimmetria $R = (d\sigma_0/d\Omega + \xi_1 d\sigma_1/d\Omega) / (d\sigma_0/d\Omega + \xi_2 d\sigma_1/d\Omega)$, dove il numeratore ed il denominatore rappresentano la sezione d'urto Rayleigh, per uno stesso angolo di scattering in due piani ortogonali. Le grandezze ξ_1 e ξ_2 sono i gradi di polarizzazione del fascio incidente riferiti ai due piani suddetti, mentre $d\sigma_0/d\Omega$ è la sezione d'urto per fotoni non polarizzati e $d\sigma_1/d\Omega$ il termine sensibile alla polarizzazione. È stata eseguita una misura di R nello scattering Rayleigh elastico usando un fascio di fotoni di energia 1.28 mc^2 , scatterati su Hg con angoli di scattering $\theta_1 = 65^\circ$, $\theta_2 = 90^\circ$ e $\theta = 110^\circ$. I risultati sperimentali sono in ottimo accordo con i calcoli di BROWN e MAYERS. Il fascio polarizzato era ottenuto mediante uno scattering Compton ad un angolo di circa 50° di un fascio emesso da una sorgente di ^{60}Co .

A Note on the Trident Process.

P. K. ADITYA (*) (**)

Physics Honours School, Panjab University - Chandigarh

(ricevuto il 2 Dicembre 1958)

Summary. — The mean free path for direct pair production by high energy electrons has been found for electrons of mean energy 20 GeV and 80 GeV. Electrons were obtained from high energy electromagnetic cascades recorded in nuclear emulsion stacks. Pair energies have been determined by using a modified relation for the pair opening angle. The cascade theory has been used to find the correction for spurious tridents. The trident mean free path values obtained at mean energy 20 GeV and 80 GeV are 10.4 ± 1.2 and 7.7 ± 1.9 respectively, measured in terms of the cascade unit. The results are in agreement with the theoretical predictions.

In recent years, some observations on the abnormal development of cascade showers ⁽¹⁾ and the presence of a large number of tridents in them and along cores of high energy disintegrations ⁽²⁾ had raised doubt on the validity of the quantum electrodynamic theory. We have carried out an investigation in this field and in this note describe our method of approach and the results obtained thereof. A detailed survey ⁽³⁾ of all the data known to us reveals

(*) Formerly known as Prem Kumar.

(**) At present at the Institute for Theoretical Physics, University of Copenhagen.

(1) M. SCHEIN, D. M. HASKIN and R. G. GLASSER: *Phys. Rev.*, **95**, 171 (1954); A. DEBENEDETTI, C. M. GARELLI, L. TALLONE and M. VIGONE: *Nuovo Cimento*, **2**, 220 (1955); **3**, 226 (1956); **4**, 1151 (1956); G. WATAGHIN: *Proc. Rochester Conference* (Feb. 1955); L. BARBANTI-SILVA, C. BONACINI, C. DE PIETRI, R. PERILLI-FEDEL and A. ROVERI: *Nuovo Cimento*, **3**, 1465 (1956).

(2) P. S. FREIER and J. E. NAUGLE: *Phys. Rev.*, **92**, 1086 (1953); M. KOSHIBA and M. F. KAPLON: *Phys. Rev.*, **97**, 193 (1955); E. LOHRMANN: *Nuovo Cimento* **3**, 820 (1956).

(3) To be published separately.

that the observed discrepancies arose due to limitations of the experimental approach.

Two parameters entering into the determination of the trident mean free path are *a*) the energy estimation of the parent electrons and *b*) the elimination of spurious tridents. The following has been our method of approach.

a) Energy estimation: Since multiple Coulomb scattering measurements have a limited reliability (up to about 5 GeV for the normally available 500 μm cell size and 0.1 μm noise level), we resorted to the use of pair opening angle versus photon energy relation, taking into account the fact that, for high energy pairs of which the separation is not measurable in the first few mm from origin, the contribution due to multiple Coulomb scattering may not *a priori* be neglected (⁴). Assuming equipartition of energy between the two electrons we have combined the relative scattering contribution to the true opening, using the most probable value given by Borsellino's relation (⁵). Since the separation due to scattering varies as the $\frac{3}{2}$ power of the distance from origin, it predominates over the true opening for all distances beyond 250 μm , at which the two contributions are equal. A few typical energies, plotted in Fig. 1,

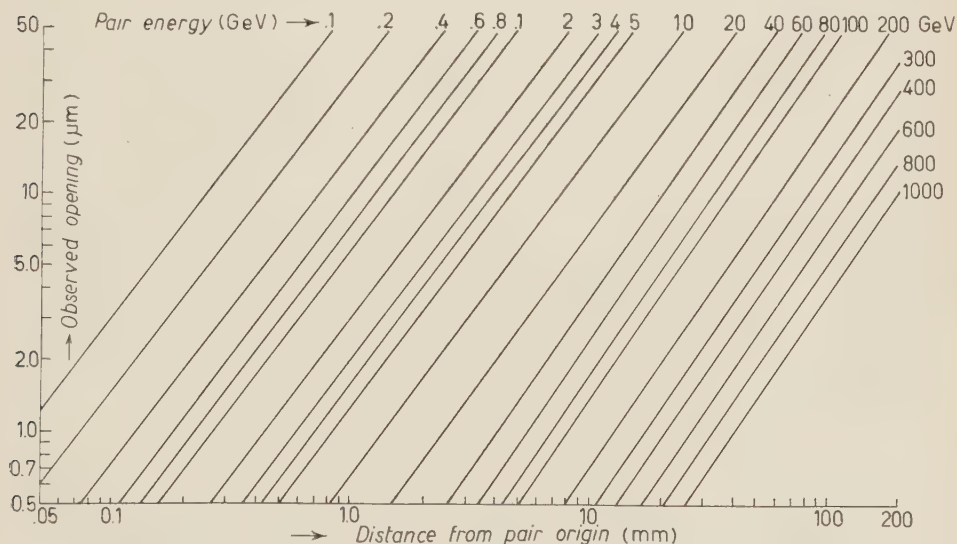


Fig. 1. — Variation of pair separation with distance from pair origin, for pairs of various energies.

(⁴) In two brief communications (¹⁴), the energy estimation was done on these lines, when our attention was drawn to similar arguments already published independently by E. LOHRMANN (*Nuovo Cimento*, **2**, 1029 (1955)). We shall therefore not enter into details.

(⁵) A. BORSELLINO: *Phys. Rev.*, **89**, 1023 (1953).

show the curves between pair opening and distance from origin. One then needs to find pair separation at regular intervals, the interval depending upon pair energy and available length. In general up to ten such readings give a good estimate of the energy. For most part of the energy range we are interested in at present, the reliability of the method has been checked by comparing the energy spectrum of secondary electrons with that theoretically predicted (⁶). Our results are shown in Fig. 2. The availability of a few

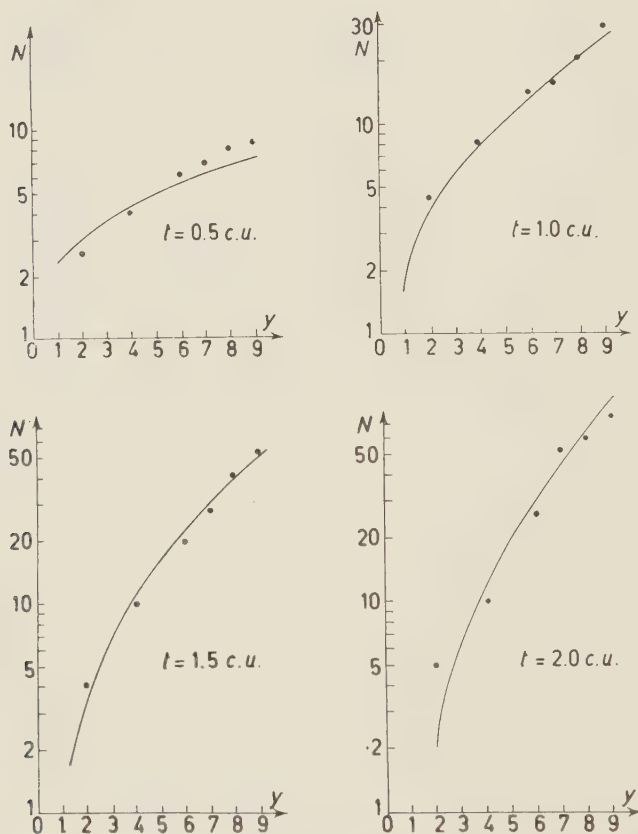


Fig. 2. Mean number N , of secondary electrons of energy greater than E_m , against y , where $y = \ln(E_0/E_m)$, E_0 being the energy of a primary electron. Points beyond $y=7$ are derived from cascades of primary energy greater than 100 GeV.

alternate methods in the high energy region have enabled us to extend the comparison to energies even of the primary order. For six cascades of which

(⁶) H. J. BHABHA and S. K. CHAKRABARTY: *Phys. Rev.*, **74**, 1352 (1948). We are thankful to Professor CHAKRABARTY for the communicated advice and some of his later calculations.

the energy could be found by three or more methods, the comparative statement is given in Table I. For the longitudinal development we have employed the calculations of BHABHA and CHAKRABARTY and CHAKRABARTY⁽⁶⁾. Each of the cascades was followed for more than 2.5 cascade units (one c.u. = 2.9 cm of nuclear emulsion). In order to compensate for the detection inefficiency of low energy pairs (since there is no such effect in case of tridents), an appropriate

TABLE I. - *Energy of the primary pairs (GeV), obtained by various methods.*

Shower designation	Longitudinal development	Lateral development	Decrease of ionization	Present method
K_1	1200	1000	800 ± 100	> 600
K_2	300	300	250 ± 50	$200 \div 300$
N_2	600	—	500 ± 80	$500 \div 600$
N_3	300	300	250 ± 50	—
N_7	250	—	250 ± 50	$250 \div 300$
N_{10}	100	—	100 ± 30	$80 \div 100$
S_3	150	—	100 ± 30	$100 \div 150$

cut-off for the minimum acceptable energy was applied, *e.g.*, at $y = \ln(E_0/E_m) = 7$ for primary energies around 100 GeV. The lateral development of three showers which were geometrically favorable was plotted and the energy estimated after the method of PINKAU⁽⁷⁾. The energy estimate of six pairs was also obtained from the decrease in ionization near the pair origin⁽⁸⁾, by comparing the experimental value of the distance at which the ionization tended asymptotically to the value for two independent electrons, with that expected theoretically. The energy values obtained by us compare reasonably well also with those obtained from relative scattering, as was indicated by LOHRMANN⁽⁹⁾, who found, using our curves, an energy of 70 to 75 GeV for some of the pairs, for which he had obtained a value of 50^{+15}_{-10} GeV by scattering. In regard to Table I, it may be mentioned that the present method may not give a representative energy value for any individual pair, but since it is our aim to find the average energy of electrons classified into a group, the individual uncertainty does not matter, especially since the error would decrease with the increase of statistics.

b) Correction for spurious tridents: Theoretically it is possible to com-

(7) K. PINKAU: *Nuovo Cimento*, **3**, 1285 (1956).

(8) D. H. PERKINS: *Phil. Mag.*, **46**, 1146 (1955); G. YEKUTIELI: *Nuovo Cimento*, **5**, 1381 (1957).

(9) E. LOHRMANN: private communication (June 1956). Thanks are due Dr. LOHRMANN for the measurements and useful comments.

pute the fraction F of bremsstrahlung pairs (B.P.), which would materialize within the least resolvable distance ($0.2 \mu\text{m}$ in projection and $0.4 \mu\text{m}$ in dip) from an electron track and give rise to a spurious trident (S.T.). Results of such a calculation made by KING *et al.* ⁽¹⁰⁾ and by KAPLON *et al.* ⁽¹⁵⁾, indicate

that, for energies $\sim 100 \text{ GeV}$, more than 70% of the observed tridents are spurious. According to Kaplon's procedure that has been widely used, number of S.T. = $F/(1-F)$ times observed B.P., that appear resolved from electron tracks. GREISEN ⁽¹¹⁾ has however suggested the advantage of finding the correction not from the observed number of resolved B.P., but entirely from the electromagnetic theory, *i.e.*, compute the bremsstrahlung spectrum and expected number of both resolvable and unresolvable pairs. This method, though it accepts the measurement of energy and computation of F , is less sensitive to errors, because F would enter linearly rather than as $F/(1-F)$. We have obtained our experimental material from two stacks of stripped emulsions exposed in the stratosphere over India ⁽¹²⁾. Out of a large number of scanned showers, in all 20 cascades of favorable

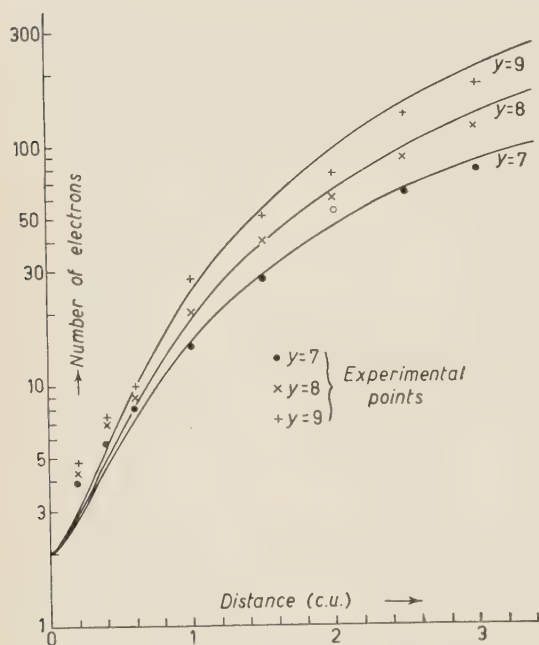


Fig. 3. - Mean number of electrons observed at various distances along the shower axis against distance in cascade units. Theoretically predicted curves are included for values of y from 7 to 9. $y = \ln(E_0/E_m)$, E_0 being the energy of a primary electron, and E_m the minimum acceptable energy for a secondary electron. Points for $y=8$ and 9 are derived from cascades of primary energy greater than 100 GeV.

geometry were selected for detailed investigation. Plots of showers at various stages were made for each cascade. In Fig. 3, the observed development is

⁽¹⁰⁾ M. M. BLOCK and D. T. KING: *Phys. Rev.*, **95**, 171 (1954); **96**, 1627 (1954).

⁽¹¹⁾ K. GREISEN: private communication (August 1956). We are grateful to Professor GREISEN for his excellent suggestions.

⁽¹²⁾ D. LAL, YASH PAL and B. PETERS: *Proc. Ind. Acad. Sci.*, **38**, 277 (1953); R. R. DANIEL, G. FRIEDMAN, D. LAL, YASH PAL and B. PETERS: *Proc. Ind. Acad. Sci.*, A **40**, 151 (1954). We are indebted to Professor PETERS for the loan of a stack and for the facilities of his laboratory where part of this work was done.

plotted over that predicted theoretically ⁽⁶⁾. But for a small though apparent deviation ⁽¹³⁾ within the first 0.5 c.u., the agreement appears to be good. We have not observed any case depicting abnormal behaviour. In fact, what we observed was a slightly too small number of resolved pairs and a large number of tridents, but the correct total.

In earlier brief communications ⁽¹⁴⁾ using the present method of energy estimation, we had corrected for S.T. according to KAPLON *et al.* ⁽¹⁵⁾. Using an along-the-track following procedure, a total of 125 pairs and 49 tridents (including spurious and genuine) were observed along 3.83 metre of emulsion length. The electron track was separated into two energy groups of $(1 \div 10)$ GeV and $(10 \div 100)$ GeV, obtaining the mean free path values $(6.1^{+2.6}_{-1.4})$ c.u., and $(4.0^{+1.4}_{-0.8})$ c.u., respectively. (A cascade unit was there taken equal to 3.0 cm of emulsion).

In view of the above approach to the correction for S.T., it appeared useful to reconsider our previous data as well as to include some more cascades. From the facsimile drawing of 20 showers an electron track length of 70 c.u. was accumulated for an average energy of 20 GeV. In this length 68 possible tridents were observed. Using an appropriate factor F , the proportion of B.P. which would appear as tridents was calculated at 61.3, leaving an excess of 6.7 tridents as genuine.

Reconsideration by KING *et al.* ⁽¹⁰⁾ of the theoretical cross-section for trident processes calculated by BHABHA ⁽¹⁶⁾, has shown it to be in agreement with that of RACAH ⁽¹⁷⁾. Accordingly, the mean free path for an average energy of 20 GeV is 35 cm, such that in 70 c.u. one expects 5.8 true tridents. This number is in fair agreement with our experimental value of 6.7, which gives $\lambda_T = (10.4 \pm 1.2)$ c.u. at 20 GeV.

With a view to find the cross-section at still higher energies, we considered separately the primary pairs up to a distance of 0.5 c.u. from the origin. Such a cut-off has a further advantage, since the number of tridents increases linearly with t , while the correction goes as t^2 . 16 possible tridents were observed along 18.5 c.u., of average energy 60 GeV. The calculated number of S.T., equal to 13.6, left an excess of 2.4 true tridents, leading to a mean free path of (7.7 ± 1.9) c.u., as compared to 8.9 c.u. expected theoretically. Since the small statistics does not allow stress to be laid on this result, our value of 20 GeV

⁽¹³⁾ It may be possible to account for part of this deviation on the basis of a genuine trident contribution likely to be present while the electrons have not lost their primary energy.

⁽¹⁴⁾ P. KUMAR: *Proc. Ind. Sci. Cong.*, III-3 (n. 18, 1955; n. 61, 1956); *Proc. Cosmic Ray Symposium* (Bombay, March 1957, unpublished).

⁽¹⁵⁾ M. KOSHIBA and M. F. KAPLON: *Phys. Rev.*, **100**, 327 (1956).

⁽¹⁶⁾ H. J. BHABHA: *Proc. Roy. Soc.*, A **152**, 559 (1935).

⁽¹⁷⁾ G. RACAH: *Nuovo Cimento*, **14**, 93 (1937).

suggests in general that the theoretical cross-section is not in error and that the observed discrepancies arise as a consequence of the methods applied.

* * *

It is a pleasure to thank Professor B. M. ANAND for his keen interest during the course of the work and for granting leave of absence the Tata Institute of Fundamental Research, Bombay. Financial assistance of the Government of India, Department of Atomic Energy, is gratefully acknowledged.

RIASSUNTO (*)

È stato trovato il cammino libero medio per la produzione di coppie di elettroni di media energia (20 GeV e 80 GeV) da parte di elettroni di alta energia. Gli elettroni sono stati ottenuti da cascate elettromagnetiche di alta energia registrati in pacchi di emulsioni nucleari. L'energia delle coppie è stata determinata servendosi di una relazione per l'angolo d'apertura della coppia modificata. La teoria della cascata è stata utilizzata per trovare la correzione per i tridenti spuri. I valori dei cammini liberi medi dei tridenti ottenuti alle medie energie di 20 GeV e 80 GeV espressi in unità di cascata sono rispettivamente 10.4 ± 1.2 e 7.7 ± 1.9 . I risultati si accordano colle previsioni teoriche.

(*) Traduzione a cura della Redazione.

The Asymptotic Condition for Simple Scattering Systems (*).

J. M. JAUCH (**) and I. I. ZINNES

CERN, Theoretical Studies Division - Geneva

Department of Physics, University of Oklahoma - Norman, Okla.

(ricevuto il 2 Dicembre 1958)

Summary. — Necessary and sufficient conditions are given for an interaction operator of a simple scattering system to admit a scattering operator. The result is applied to the study of radial scalar potentials.

1. - Introduction.

A scattering system is characterized by a certain limiting property of the state vectors in the remote past and the distant future. In a previous publication ⁽¹⁾ we have formulated this property in terms of the unitary operators $U_t = \exp[-iH_0t]$ and $V_t = \exp[-iHt]$ which describe the time development of the free particles and the total system respectively. In these expressions H_0 represents the kinetic energy of the free particles and H the total energy of the system.

The asymptotic condition as we have used it is that the strong limits (**)

$$(1) \quad \Omega_{\mp} = \lim_{t \rightarrow \pm \infty} V_t^* U_t$$

exist for all f in the underlying Hilbert space \mathcal{H} formed by the totality of state vectors of the system.

(*) Supported in part by the National Science Foundation.

(**) On leave of absence from State University of Iowa, Iowa City, U.S.A.

⁽¹⁾ J. M. JAUCH: *Helv. Phys. Acta*, **31**, 127 (1958).

(*) Strong limits means that the numbers $\|(\Omega_{\mp} - V_t^* U_t)f\|$ tend to zero for all f and $t \rightarrow \pm \infty$ respectively.

It is easy to show with simple counter-examples that condition (I) implies certain restrictions on the interaction operator. One of the simplest of such examples is obtained for instance by setting $H = eI + H_0$. In this case $V_t^* U_t = \exp[ict] \cdot I$, and this operator cannot converge for any f as $t \rightarrow \pm \infty$.

The object of this paper is to obtain necessary and sufficient conditions on the interaction operator which are equivalent to the asymptotic condition (I) and to apply them to the study of radial scalar potentials in wave mechanical scattering theory.

Roughly speaking condition (I) means that the motion of any state vector associated with a scattering system approaches in the distant past and the remote future the free motion. This can also be expressed by saying that a state vector in the interaction picture $\varphi(t)$ which is orthogonal to the bound states of H must approach a constant state vector for $t \rightarrow \pm \infty$. Now this state vector satisfies the Schrödinger equation in the interaction picture

$$(1.1) \quad i\dot{\varphi}(t) = V(t)\varphi(t),$$

where

$$(1.2) \quad V(t) \equiv U_t^* V U_t$$

is the interaction operator in the interaction picture. One might therefore be led to believe that such a condition on the interaction operator is that $V(t) \rightarrow 0$ in some sense, as $t \rightarrow \pm \infty$.

However, even if this limit were made precise it would certainly not be enough to guarantee the existence of the scattering operator as may be seen from the following simple example: Let the Hilbert space be one-dimensional so that the state vectors are just complex numbers. Consider $V(t) = 1/t$ so that (1.1) becomes

$$i\dot{\varphi}(t) = \frac{1}{t} \varphi(t),$$

with the solution $\varphi(t) = A \exp[-i \ln t]$. In this case $V(t) \rightarrow 0$ for $t \rightarrow \pm \infty$ but $\varphi(t)$ has no limit for $t \rightarrow \pm \infty$.

In this paper we shall give the necessary and sufficient conditions on the potential for the validity of property (I) in two equivalent forms.

2. - The interaction operator.

We shall assume that we are given a total Hamiltonian H and the corresponding unitary group $V_t = \exp[-iHt]$. If we are dealing with a simple

scattering system we also have an expression for the free Hamiltonian H_0 and the corresponding group $U_t = \exp[-iH_0t]$. We shall now define precisely what we mean by the interaction operator V .

The obvious procedure of setting $V = H - H_0$ is in need of elaboration because of the following circumstance. The operators H and H_0 are, in all physical systems of interest, unbounded operators, which are only definable in everywhere dense linear manifolds D_H and D_{H_0} respectively. The difference $H - H_0$ is therefore only defined on the intersection $D_H \cap D_{H_0}$ of these two manifolds. We shall always agree to define two operators as equal if they have the same domain of definition and if on this domain they have the same value. It is quite possible that the intersection of two dense linear manifolds is empty. In this case the interaction operator is undetermined.

Even in the physically more important case in which the intersection of the two domains is also everywhere dense it is still possible that the operator $H - H_0$ admits an extension. If this extension is to be continuous it is also unique and there is a maximal continuous extension. If $H - H_0$ is uniformly bounded on its domain the maximal extension is to all of \mathcal{H} . In the contrary case it is a dense linear manifold. In either case the maximal extension leads to a uniquely determined closed, self-adjoint but not necessarily bounded linear operator which we shall denote by V and for which we write

$$(2.1) \quad V \supseteq H - H_0.$$

For the discussion of scattering systems the existence and uniqueness of the interaction operator is not enough. In order to formulate necessary and sufficient conditions on V for the existence of the scattering operator it is necessary to have what we shall call *admissible* interaction operators.

We define an admissible interaction operator as one which has the property: There exists a dense linear manifold D'_V on which V and H_0 are defined and which is invariant under the group U_t .

That this is a restriction can easily be verified with examples. We shall not give such examples here, since they have hardly any physical significance. It follows from this definition that $D'_V \subseteq D_H \cap D_{H_0}$.

From now on we shall only consider simple scattering systems with admissible interaction operators. It is obvious that a bounded interaction operator is always admissible with $D'_V = D_H$, $D'_V = D_H \cap D_{H_0} \equiv D_{H_0}$. Such operators already occur for a large group of physically interesting systems. But such important ones as the Yukawa potential and the Coulomb potential are not in this class. It is for this reason that it is necessary to admit unbonded interaction operators in the general theory of scattering and to replace boundedness of V by the weaker condition of admissibility.

3. - The asymptotic property of the transformation operator.

In this section we shall relate condition (I) to an asymptotic property of the transformation operator $V_t = \exp[-iHt]$. We recall that condition (I) ensures the existence of a bounded operator ⁽¹⁾

$$\Omega = \lim_{t \rightarrow \infty} V_t^* U_t$$

defined on all of \mathcal{H} with the upper bound $\|\Omega\| = 1$. We shall prove the following

THEOREM 1: *Let U_t and V_t be two continuous unitary representations of the group of real numbers $(-\infty < t < +\infty)$ in the Hilbert space \mathcal{H} . The necessary and sufficient condition that the strong operator limit*

$$(3.1) \quad \Omega = \lim_{t \rightarrow \infty} V_t^* U_t$$

exists, on all of \mathcal{H} is that the strong limit

$$(3.2) \quad \lim_{t \rightarrow \infty} U_t^* V_\tau U_t = U_\tau$$

exists on all of \mathcal{H} , for all τ uniformly in $\tau \geq 0$.

Proof: We shall first show that (3.2) is necessary. According to the assumption (3.1) there exists for every $f \in \mathcal{H}$ and any $\varepsilon > 0$ a T such that

$$(3.3) \quad \|(V_t^* U_t - V_{t'}^* U_{t'})f\| < \varepsilon \quad \text{for all } t, t' > T.$$

By using the unitary property of V_t and U_t , we can transform the left-hand side with the help of the identity

$$(3.4) \quad \|(V_t^* U_t - V_{t'}^* U_{t'})f\| = \|(U_t^* V_\tau U_t - U_\tau)f\|,$$

where $\tau = t' - t$. Therefore for any fixed τ the right-hand side of (3.4) is $< \varepsilon$ for all t such that $t > T - \tau$ and $t > T$. This proves the existence of the limit (3.2) for all τ . Furthermore the convergence is uniform in $\tau \geq 0$, since $t > T$ implies that $t' = t + \tau > T$, so that by (3.3),

$$\|(U_t^* V_\tau U_t - U_\tau)f\| < \varepsilon \quad \text{for } t > T, \tau \geq 0,$$

independently of τ *q.e.d.*

In order to prove the sufficiency of (3.2) we use the identity (3.4) in reverse.

By assumption the right-hand side of (3.4) is $< \varepsilon$ for fixed f and for all $\tau \geq 0$ and $t > T$. Hence the left side is $< \varepsilon$ for $t > T$, $t' = t + \tau \geq t$. Since it is unchanged upon interchanging t with t' , this is also true for $t' > T$, $t = t' + \tau \geq t'$, that is for all $t, t' > T$. The set of vectors $f_t = V_t^* U_t f$ for arbitrary f satisfy the Cauchy condition and since \mathcal{H} is complete there exists a uniquely defined limit

$$g = \lim_{t \rightarrow \infty} f_t.$$

Thus the operator $V_t^* U_t$ strongly converges with $t \rightarrow \infty$ to

$$\Omega = \lim_{t \rightarrow \infty} V_t^* U_t$$

on all of \mathcal{H} . *q.e.d.*

We remark incidentally that uniform convergence of $U_t^* V_\tau U_t$ to U_τ for $t \rightarrow \infty$ on the half-line $\tau \geq 0$ implies uniform convergence on any half-line $\tau \geq \tau_0$, with τ_0 arbitrary.

In order to show this we may assume $\tau_0 < 0$, since there is nothing to prove if $\tau_0 \geq 0$.

The easily verified identity

$$\|(U_t^* V_\tau U_t - U_\tau) f\| = \|(U_{t+\tau}^* V_{-\tau} U_{t+\tau} - U_{-\tau}) f\|$$

shows that

$$\|(U_t^* V_\tau U_t - U_\tau) f\| < \varepsilon \quad \text{for } t > T \text{ uniformly in } \tau \geq 0$$

implies

$$\|(U_t^* V_\tau U_t - U_\tau) f\| < \varepsilon \quad \text{for } t \geq T + |\tau_0|, \text{ uniformly in } \tau \geq \tau_0$$

and this proves the statement.

We also remark that Theorem 1 has its counterpart for the limit $t \rightarrow -\infty$ with the domain of uniform convergence $\tau \leq 0$. The proof is an obvious modification of the preceding proof and will be omitted.

4. - The asymptotic property of the interaction operator.

In this Section we shall formulate necessary and sufficient conditions for an admissible interaction operator which are equivalent to the asymptotic condition I.

We begin with a few preliminary considerations:

Let $f \in D_H$ and $g \in D_{H_0}$ then the expression

$$(4.1) \quad \Phi_t(f, g) \equiv H V_t f, U_t g - (V_t f, H_0 U_t g)$$

is, for every fixed pair f and g , a continuous function of t for $-\infty < t < +\infty$.

We verify that for instance the first expression on the right is continuous in t . The continuity of the second term may be verified in a similar manner.

Continuity means, for every $\varepsilon > 0$, we can determine a δ such that

$$(4.2) \quad |(HV_{t+\tau}f, U_{t+\tau}g) - (HV_t f, U_t g)| < \varepsilon \quad \text{for } |\tau| < \delta.$$

We have for the left-hand side

$$\begin{aligned} |(HV_{t+\tau}f, U_{t+\tau}g) - (HV_t f, U_t g)| &\leq \\ &\leq |(H(V_{t+\tau} - V_t)f, U_{t+\tau}g)| + |(HV_t f, (U_{t+\tau} - U_t)g)| \leq \\ &\leq \|H(V_{t+\tau} - V_t)f\| \|g\| + \|HV_t f\| \|(U_{t+\tau} - U_t)g\|. \end{aligned}$$

Since H commutes with V_t and $f \in D_H$ we can write for the first term

$$\|(V_{t+\tau} - V_t)Hf\|, \quad \|g\| < \frac{\varepsilon}{2}, \quad \text{for all } |\tau| < \delta_1,$$

because V_t is strongly continuous in t .

For the second term we have

$$\|V_t Hf\|, \quad \|(U_{t+\tau} - U_t)g\| < \frac{\varepsilon}{2}, \quad \text{for all } |\tau| < \delta_2,$$

since U_t is strongly continuous in t .

Consequently we have verified (4.2) for $\delta = \text{Min}\{\delta_1, \delta_2\}$.

Since $\Phi_t(f, g)$ is a continuous function of t it can be integrated on any interval of the real t -line. We define

$$(4.3) \quad \Psi_{t_2, t_1}(f, g) \equiv \int_{t_1}^{t_2} \Phi_t(f, g) dt, \quad f \in D_H, \quad g \in D_{H_0}.$$

We shall now show, that the integral on the right of (4.3) can be evaluated, with the result

$$\Psi_{t_2, t_1}(f, g) = -i(f, (W_{t_2} - W_{t_1})g)$$

and

$$W_t = V_t^* U_t.$$

To this end we use the fact that for every $f \in D_H$ the strong limit

$$(4.4) \quad \lim_{\tau \rightarrow 0} \frac{V_{t+\tau} - V_t}{\tau} f = -iH V_t f,$$

exists ⁽²⁾, and of course a corresponding property for $g \in D_{H_0}$.

This means that for such f and g we can write (4.1) as

$$\Phi_t(f, g) = -i \frac{d}{dt} (V_t f, U_t g) - i \left(V_t f, \frac{d}{dt} U_t g \right).$$

Because of the continuity of the scalar product this can be reduced to

$$\Phi_t(f, g) = -i \frac{d}{dt} (V_t f, U_t g) = -i \frac{d}{dt} (f, W_t g),$$

consequently

$$\int_{t_1}^{t_2} dt \Phi_t(f, g) = -i \int_{t_1}^{t_2} dt \frac{d}{dt} (f, W_t g) = -i (f, (W_{t_2} - W_{t_1}) g).$$

We summarize the result up to this point with the

Lemma 1: For every pair of elements $f \in D_H$ and $g \in D_{H_0}$ we have

$$(4.5) \quad i \int_{t_1}^{t_2} [(H V_t f, U_t g) - (V_t f, H_0 U_t g)] dt = (f, (W_{t_2} - W_{t_1}) g),$$

with

$$W_t = V_t^* U_t.$$

The left-hand side of (4.5) is only defined for $f \in D_H$ and $g \in D_{H_0}$ but the result of the integration shows that it represents a bounded bilinear functional in two dense domains for f and g and can therefore be extended continuously and uniquely to all of \mathcal{H} . Thus even though the *integrand* has only meaning for f and g in these domains the *integral* has a more general meaning after continuous extension.

If we are dealing with an admissible interaction operator, the left-hand side of (4.5) can be further transformed as follows. We assume that $g \in D'_V \subseteq D_{H_0}$ so that the norms of $H_0 U_t g$, $V U_t g$ and $H U_t g$ are all finite. We can then write

$$(H V_t f, U_t g) = V_t f, H U_t g = (f, V_t^* H U_t g).$$

⁽²⁾ See for instance F. RIESZ and B. SZ.-NAGY: *Functional Analysis*, esp. p. 384.

We obtain then

Lemma 2: If the interaction operator V is admissible, we have

$$(4.6) \quad (f, (W_{t_2} - W_{t_1})g) = i \int_{t_1}^{t_2} dt (f, V_t^* V U_t g), \quad \text{for all } f \in D_H, g \in D_V'.$$

Since D_V' is dense in \mathcal{H} we can uniquely again extend the meaning of the integral to a bilinear functional in all of \mathcal{H} . Such a functional always determines a bounded linear operator which we consider the definition of

$$i \int_{t_1}^{t_2} dt V_t^* V U_t = X_{t_2 t_1}.$$

It has the property

$$(f, X_{t_2 t_1} g) = i \int_{t_1}^{t_2} dt (f, V_t^* V U_t g), \quad \text{for all } f \in D_H, g \in D_V'.$$

With this definition of the operator $X_{t_2 t_1}$ we have from (4.6) the following operator relation

$$(4.7) \quad W_{t_2} - W_{t_1} = i \int_{t_1}^{t_2} V_t^* V U_t dt.$$

We are now prepared for the proof of

THEOREM 2: Let H , H_0 and V be the total Hamiltonian, the free Hamiltonian and the admissible interaction operator of a quantum mechanical system.

The necessary and sufficient condition that property I holds is that the operator

$$(4.8) \quad X_{t_2 t_1} = \int_{t_1}^{t_2} V_t^* V U_t dt,$$

converges strongly to a bounded operator for $t_2 \rightarrow +\infty$, $t_1 \rightarrow -\infty$.

Proof: The convergence property of the operator $X_{t_1 t_2}$ may also be stated as follows: For every $f \in \mathcal{H}$ and every $\varepsilon > 0$, there exists a T such that

$$(4.9) \quad \|X_{t_2 t_1} f\| < \varepsilon \quad \text{for all } t_2 > T, t_1 > T,$$

or all $t_2 < -T, t_1 < -T$.

In this form we shall prove the equivalence with I. Let us first assume I. The for every f , $W_t f$ satisfies the Cauchy condition for $t \rightarrow \pm \infty$. Therefore, given $\varepsilon > 0$, there exists a T such that

$$\begin{aligned} \|W_{t_2} f - W_{t_1} f\| &= \|X_{t_2 t_1} f\| & \text{for all } t_2 > T, t_1 > T, \\ &< \varepsilon & \text{for all } t_2 < -T, t_1 < -T. \end{aligned}$$

Let us next assume (4.9). It follows from (4.7) that the elements $W_t f$ satisfy a Cauchy condition for $t \rightarrow \pm \infty$. Since \mathcal{H} is complete they converge strongly to a limit f_{\mp}

$$\lim_{t \rightarrow \pm \infty} W_t f = f_{\mp}.$$

This is the assertion of I. Thus the theorem is proved.

In conclusion of this section we mention a few consequences of Eq. (4.7). Since the limits $t_1 \rightarrow -\infty$, $t_2 \rightarrow +\infty$ exist if we are dealing with a scattering system, we can put

$$(4.10) \quad \Omega_- - \Omega_+ = i \int_{-\infty}^{+\infty} V_t^* V U_t dt.$$

We multiply this from the left with Ω^* and use the relations (*)

$$\Omega_-^* \Omega_- = I, \quad \Omega_-^* V_t = U_t \Omega_-^*, \quad S = \Omega_-^* \Omega_+,$$

and we obtain

$$(4.11) \quad I - S = i \int_{-\infty}^{+\infty} U_t^* \Omega_-^* V U_t dt.$$

In a similar way one obtains

$$(4.12) \quad I - S = -i \int_{-\infty}^{+\infty} U_t^* V \Omega_+ U_t dt.$$

There are corresponding formulae for the operator $S' = \Omega_+ \Omega_-^*$

$$(4.13) \quad E_N - S' = i \int_{-\infty}^{+\infty} V_t^* V \Omega_-^* V_t dt,$$

$$(4.14) \quad E_N - S' = -i \int_{-\infty}^{+\infty} V_t^* \Omega_+ V V_t dt.$$

(*) For the proof of these relations, see ref. (1).

In the last two expressions E_N is the projection operator for the subspace of the continuum states.

The expressions (4.11) and (4.12) are a useful starting point for a study of the convergence of perturbation theory. One obtains for instance the « first Born approximation » of scattering theory from (4.11) by setting $\Omega_- = I$.

5. - The asymptotic condition for a radial potential.

In this section we shall study the implications of the asymptotic condition for a radial potential $V(r)$. The Hilbert space is realized by L^2 -functions $\psi(\mathbf{x})$ over the three-dimensional Euclidean space. The total Hamiltonian is assumed to be of the form

$$(5.1) \quad H = \frac{p^2}{2m} + V,$$

where

$$(5.2) \quad (V\psi)(\mathbf{x}) = V(r)\psi(\mathbf{x})$$

and the operator p^2 has the usual meaning

$$(p^2\psi)(\mathbf{x}) = -\nabla^2(\mathbf{x}).$$

The first question to be investigated is under what condition the interaction operator is admissible in the sense defined in Section 2. The answer is contained in the

THEOREM 3: *If there exists an R and two positive numbers M_1 and M_2 such that*

$$(5.3) \quad \int_0^R r^2 V^2(r) dr < M_1, \quad \int_R^\infty \exp[-r^2] V^2(r) dr < M_2,$$

then V is an admissible interaction operator.

It is satisfactory that the conditions (5.3) of this theorem include the important cases of the Coulomb and the Yukawa potential. But the case $V(r) = 1/r^3$ is excluded by the first of the conditions (5.3). Since these conditions are only sufficient it is not clear whether this case represents a real anomaly or not.

Before we prove this theorem we mention that the conditions (5.3) imply that for any pair R_1 and R_2 such that $0 < R_1 < R_2 < \infty$ and for any bounded

integrable function $\Phi(r)$ in $[R_1, R_2]$ we have

$$(5.4) \quad \int_{R_1}^{R_2} \Phi(r) V^2(r) dr < \infty.$$

We shall omit the easy proof of this statement.

Proof of Theorem 3: In order to prove Theorem 3 we must show that there exists a dense linear manifold D'_V on which V and H_0 are defined and which is invariant under $U_t = \exp[-iH_0t]$.

In order to do this we utilize the displacement theorem of WIENER⁽³⁾ which may be stated as follows:

Let $K_1(x)$ belong to L^2 and be such that its Fourier transform does not vanish except possibly on a set of measure zero, then if $K_2(x)$ belongs to L^2 and $\varepsilon > 0$, there exists an integer N together with a set of real numbers A_n and complex numbers A_n such that

$$\int_{-\infty}^{+\infty} |K_2(x) - \sum_{n=1}^N A_n K_1(x - A_n)|^2 dx < \varepsilon.$$

What this theorem says in brief is that there exist suitable generating functions K_1 , which when displaced and superposed can approximate in the norm any function in L^2 to any desired accuracy.

It is clear that the set of functions

$$\sum_{n=1}^N A_n K_1(x - A_n) = F(x)$$

with all finite N and arbitrary A_n are a linear manifold \mathcal{L} . The theorem says that, if $K_1(x)$ satisfies the conditions of the theorem, then this linear manifold is dense in \mathcal{H} .

As stated above, the theorem refers to functions on the line. By considering the closed linear manifolds formed by products of functions on the line it is possible to extend Wiener's theorem to L^2 -functions defined on a space of three or more dimensions.

We shall not stop to carry this through here.

For the functions which generate the linear manifold we choose the Fourier

(3) N. WIENER: *The Fourier Integral*, (Cambridge, 1933).

transforms of

$$(5.5) \quad \varphi_{k_0}(\mathbf{k}) = \exp[-a^2(\mathbf{k} - \mathbf{k}_0)^2]$$

for fixed real $a > 0$.

This function of \mathbf{k} vanishes nowhere and its norm is

$$(5.6) \quad \|\varphi_{k_0}\|^2 = \int \exp[-2a^2(\mathbf{k} - \mathbf{k}_0)^2] d^3k = \left(\frac{\pi}{2a^2}\right)^{\frac{3}{2}} < \infty.$$

Hence it satisfies the conditions of Wiener's theorem.

Furthermore we have

$$(H_0 \varphi_{k_0})(\mathbf{k}) = \frac{1}{2m} \mathbf{k}^2 \exp[-a^2(\mathbf{k} - \mathbf{k}_0)^2],$$

and therefore

$$\|H_0 \varphi_{k_0}\|^2 = \frac{1}{4m^2} \int \mathbf{k}^4 \exp[-2a^2(\mathbf{k} - \mathbf{k}_0)^2] d^3k < \infty, \quad \text{for all } \mathbf{k}_0.$$

Thus $\varphi_{k_0} \in D_{H_0}$ for all \mathbf{k}_0 and therefore

$$(5.7) \quad \mathcal{D} \in D_{H_0}.$$

For the Fourier transform of $U_t \varphi_{k_0}$ we have

$$(U_t \varphi_{k_0})(\mathbf{x}) = \frac{1}{(2\pi)^{\frac{3}{2}}} \int d^3k \exp[-a^2(\mathbf{k} - \mathbf{k}_0)^2] - \frac{it}{2m} \mathbf{k}^2 + i\mathbf{k} \cdot \mathbf{x}.$$

This can be evaluated in closed form with the result

$$(5.8) \quad (U_t \varphi_{k_0})(\mathbf{x}) = \frac{1}{[2(a^2 + (it/2m))]^{\frac{3}{2}}} \exp \left[-i\mathbf{k}_0 \cdot \left(\frac{t}{2m} \mathbf{k} - \mathbf{x} \right) - \frac{((t/2m)\mathbf{k}_0 - \frac{1}{2}\mathbf{x})^2}{a^2 + (it/2m)} \right].$$

From this we obtain

$$(5.9) \quad \|V U_t \varphi_{k_0}\|^2 = \frac{1}{8\alpha^3} \int V^2(r) \exp \left[-\frac{2a^2}{\alpha^2} \left(\frac{1}{2} \mathbf{x} - \frac{t}{2m} \mathbf{k}_0 \right)^2 \right] d^3x,$$

with

$$\alpha^2 = a^2 + \left(\frac{t}{2m} \right)^2.$$

When we carry out the angle integration in (5.9) we find

$$(5.10) \quad \|VU_t\varphi_{k_0}\|^2 = \frac{\pi}{2\alpha r_0 a^2} \int_0^\infty \exp\left[-\frac{a^2}{2\alpha^2}(r^2 + r_0^2)\right] \sinh\left(\frac{rr_0 a^2}{\alpha^2}\right) r V^2 dr,$$

with

$$r_0 = \frac{t}{m} k_0.$$

By changing to the dimensionless variable

$$\frac{ar}{\alpha} = \varrho,$$

and defining

$$F(\varrho) = V\left(\frac{\alpha\varrho}{a}\right), \quad \varrho_0 = \frac{a}{\alpha} r_0,$$

we obtain finally

$$\|VU_t\varphi_{k_0}\|^2 = \frac{\pi}{2\varrho_0 a^3} \exp\left[-\frac{1}{2}\varrho_0^2\right] \int_0^\infty \exp\left[-\frac{1}{2}\varrho^2\right] \sinh(\varrho\varrho_0) \varrho F^2(\varrho) d\varrho.$$

In order to finish the proof of Theorem 3, we need to show that the integral is finite for all $V(r)$ which satisfy the conditions (5.3).

We choose an arbitrary $\varrho_1 > 0$ and C_1 such that

$$\frac{\sinh \varrho\varrho_0}{\varrho\varrho_0} < C_1 \quad \text{for all } \varrho < \varrho_1.$$

On account of the first of conditions (5.3) it follows that

$$\int_0^{\varrho_1} \exp\left[-\frac{1}{2}\varrho^2\right] \sinh(\varrho\varrho_0) \varrho F^2(\varrho) d\varrho < C_1 \varrho_0 \int_0^{\varrho_1} \varrho^2 F^2(\varrho) d\varrho < \infty.$$

Then, because of the inequality

$$\exp\left[-\frac{1}{2}\varrho^2\right] \sinh \varrho\varrho_0 \leq \exp\left[\frac{1}{2}\varrho_0^2\right] (\exp\left[-\frac{1}{2}(\varrho - \varrho_0)^2\right] + \exp\left[-\frac{1}{2}(\varrho + \varrho_0)^2\right])$$

and the second of conditions (5.3) we can choose a ϱ_2 and a number C_2 such

that

$$\int_{\varrho_2}^{\infty} \exp \left[-\frac{1}{2} \varrho^2 \right] \sinh (\varrho \varrho_0) \varrho F^2(\varrho) d\varrho < C_2 \int_{\varrho_2}^{\infty} \exp [-\varrho^2] \varrho F^2(\varrho) d\varrho < \infty.$$

Finally the integral from ϱ_1 to ϱ_2 is always finite. Thus the result:

$$\|V U_t \varphi_{k_0}\|^2 < \infty \quad \text{for all } k_0 \text{ and all } t.$$

We have now established that every function of the form $U_t \varphi_{k_0}$ with arbitrary k_0 and t is in D_{H_0} as well as in D_V . This is also true for every finite linear combination of such functions. By Wiener's theorem such linear combinations generate the dense linear manifold \mathcal{L} . Therefore we have with $\mathcal{L} = D'_V$ obtained a linear manifold which satisfies all the conditions stated in Theorem 3.

This completes the proof of Theorem 3.

We shall now further specialize the potential to be of the form $V(r) = 1/r^{\beta}$ with $1 < \beta < \frac{3}{2}$. For these values of β conditions (5.3) are satisfied.

Since

$$\begin{aligned} \left\| \int_{t_1}^{t_2} V_t V U_t \varphi_{k_0} dt \right\| &\leq \int_{t_1}^{t_2} \|V U_t \varphi_{k_0}\| dt \leq \\ &\leq \int_{t_1}^{t_2} dt \frac{\sqrt{\pi}}{\sqrt{2} \varrho_0^{\frac{1}{2}}} \frac{a^{\beta-\frac{3}{2}}}{\alpha^{\beta}} \left\{ \left| \int_0^{\infty} \exp \left[-\frac{1}{2} \varrho^2 \right] \sinh (\varrho \varrho_0)^{1-2\beta} d\varrho \right| \right\}^{\frac{1}{2}}, \end{aligned}$$

and $\varrho_0 = (a/\alpha)r_0 \rightarrow 2ak_0$ with $t \rightarrow \infty$, and $1 < \beta < \frac{3}{2}$, the integral remains uniformly bounded for $t \rightarrow \infty$, and

$$\left\| \int_{t_1}^{t_2} V_t^* V U_t \varphi_{k_0} dt \right\| \leq \text{const} \int_{t_1}^{t_2} \frac{1}{t^{\beta}} dt = \text{const} \left(\frac{1}{t_1^{\beta-1}} - \frac{1}{t^{\beta-1}} \right).$$

Thus the asymptotic condition is satisfied for such potentials.

This example shows that it is possible to weaken the sufficient condition on $V(r)$ which was previously obtained by COOK⁽⁴⁾. His condition is

$$\int_0^{\infty} V^2(r) r^2 dr < \infty,$$

and it excludes the cases: $1 < \beta < \frac{3}{2}$.

⁽⁴⁾ J. M. COOK: *Journ. Math. and Phys.*, **26**, 82 (1957).

It is regrettable on the other hand that the Coulomb potential ($\beta=1$) cannot be shown to admit a scattering operator with the methods employed.

RIASSUNTO (*)

Si danno le condizioni necessarie e sufficienti perchè un operatore d'interazione di un sistema semplice di scattering ammetta un operatore di scattering. Si applica il risultato allo studio di potenziali radiali scalari.

(*) *Traduzione a cura della Redazione.*

Weak and Electromagnetic Interactions.

ABDUS SALAM

Imperial College - London

J. C. WARD

University of Miami - Miami, Flo. ()*

(ricevuto il 3 Dicembre 1958)

Summary. — The postulate of a « local connection » in a [3] charge space leads to the introduction of three spin one fields. One of these can be identified with the electro-magnetic field and the other two can be shown to mediate all known weak interactions, thus unifying these interactions with electro-magnetism. The theory takes account of the fact that weak interactions violate parity and strangeness conservation while electro-magnetic interactions do not do so.

1. — D'ESPAGNAT, PRENTKI and SALAM ⁽¹⁾ have recently advanced the hypothesis that a three-dimensional [3] charge space Q exists and that all elementary particles correspond to its scalar or vector representations.

These authors show that possibly weak interactions exhibit full rotational symmetry in Q space. Electro-magnetic and strong interactions violate the full symmetry; however these interactions are invariant for rotations around one particular axis in this space (the « charge-axis ») so that Q_z is always conserved.

In this paper we wish to make a fresh approach with the idea of a [3] charge space. Following some ideas first advanced by SCHWINGER ⁽²⁾, we show

(*) Visiting Professor at the University of Maryland, present address, Free University, of Brussels.

(1) B. D'ESPAGNAT, J. PRENTKI and A. SALAM: *Nucl. Phys.*, **5**, 447 (1958). This paper will here be referred to as ESP. Similar ideas have been suggested by G. TAKEDA: to be published. In ESP the Q space is designated as M space.

(2) J. SCHWINGER: *Ann. of Phys.*, **2**, 407 (1957).

that parity-conserving weak and electromagnetic interactions taken together form a unit which exhibits full rotational symmetry in Q space. This full symmetry is broken on the one hand by parity-violating weak interactions (γ_5 -invariance) and on the other hand by strong interactions. We go further in respect of the rotational invariance of electro-magnetic and (parity conserving) weak interactions in Q space; we wish to make the hypothesis that the orientation of all three charge axes can be chosen arbitrarily at all space time points.

Just as it is necessary to introduce the electro magnetic field if it is assumed that the orientation of axes in the conventional [2] ⁽³⁾ space spanned by fields Φ and Φ^* (or alternatively by the fields Φ_1 and Φ_2 , where $\Phi = \Phi_1 + i\Phi_2$) is arbitrary at all space time points, our « three-dimensional gauge invariance » makes it necessary to introduce in Q space a triplet of fields consisting of two charged vector bose fields in addition to the electro-magnetic field ⁽⁴⁾. It will be shown that the form of the interaction of the charged fields is such that they can mediate weak interactions.

2. – Let us first consider the problem of the generalized gauge transformation ⁽⁵⁾. Let ψ represent a vector in charge-space, ($\psi = \psi_1, \psi_2, \psi_3$ where, ψ_1, ψ_2, ψ_3 are 3 Fermi fields), which transforms as

$$(1) \quad \psi' = S\psi.$$

If S is a function of x, y, z, t it is necessary for invariance, that all derivatives of ψ appear in the combination

$$(2) \quad (\partial_\mu - i\varepsilon B_\mu)\psi,$$

where B_μ are 3×3 matrices, and transform as

$$B'_\mu = S^{-1}B_\mu S + \frac{i}{\varepsilon} S^{-1} \frac{\partial S}{\partial x_\mu}.$$

⁽³⁾ A priori, it is more attractive to associate charge with a [3] group structure, rather than with a [2] structure as in conventional theory. This is because infinitesimal matrices describing rotations in three dimensions possess three eigenvalues $\pm 1, 0$ (rather than just ± 1), so that the same formulation can give charge values of *all* charged and neutral particles. We are indebted for this remark to Prof. M. FIERZ.

⁽⁴⁾ This was first done by SCHWINGER (ref. ⁽¹⁾). The difference between our work and Schwinger's is that here the charged Bose fields arise naturally from the 3-dimensional charge-gauge and there is little arbitrariness in writing down the interaction Lagrangian.

⁽⁵⁾ Mathematically the work in this Section is completely analogous with that of YANG and MILLS (*Phys. Rev.*, **96**, 191 (1954)); and R. SHAW (Cambridge dissertation, unpublished (1954)).

YANG and MILLS were considering the possibility of a generalized gauge transformation in three-dimensional isotopic rather than charge-space.

If Q_i are the set of three rotation matrices in Q space, one may write

$$B_\mu = A_\mu(x) \cdot Q$$

and define

$$(3) \quad f_{\mu\nu} = e_{\mu\nu} - S_{\mu\nu},$$

where

$$(4) \quad e_{\mu\nu} = \frac{\partial A_\mu}{\partial x_\nu} - \frac{\partial A_\nu}{\partial x_\mu},$$

$$(5) \quad S_{\mu\nu} = \varepsilon(A_\mu \times A_\nu).$$

Here \times is the symbol for vector-product.

It is easy to verify that

$$F_{\mu\nu} = f_{\mu\nu} \cdot Q$$

transforms as

$$(6) \quad F'_{\mu\nu} = S^{-1} F_{\mu\nu} S.$$

The A field (or alternatively $f_{\mu\nu}$ field) has arisen as a direct consequence of our demand that S depends on x, y, z, t .

A charge-gauge invariant Lagrangian for A field is

$$(7) \quad -\frac{1}{4} f_{\mu\nu} f_{\mu\nu}.$$

The $S_{\mu\nu}$ terms are necessary for the invariance. Analogously to ref. (5), the total lagrangian density is

$$(8) \quad -\frac{1}{4} f_{\mu\nu} f_{\mu\nu} - \bar{\Psi} \gamma (\gamma - i\varepsilon Q A) \Psi - m \bar{\Psi} \Psi.$$

Notice that

$$J = \bar{\Psi} Q \Psi = -i(\bar{\Psi} \times \Psi)$$

so that the interaction term in (8) is

$$J \cdot A = \varepsilon \bar{\Psi}_\Lambda \gamma_\mu \Psi \cdot A.$$

It is easy to verify that the subsidiary condition

$$(9) \quad \frac{\partial A_\mu}{\partial x_\mu} = 0,$$

is compatible with the equations of motion derived from the Lagrangian; also that the «current»

$$(10) \quad \mathcal{F}_\mu = \mathbf{J}_\mu + \varepsilon \mathbf{A}_\nu \times \mathbf{f}_{\mu\nu}$$

satisfies the equation of continuity

$$(11) \quad \frac{\partial \mathcal{F}_\mu}{\partial x_\mu} = 0.$$

Thus

$$\mathbf{Q} = \int \mathcal{F}_4 d^3x,$$

is independent of time.

One can verify that components of \mathbf{A} field carry charge $+\varepsilon, 0, -\varepsilon$. Picking out an arbitrary charge axis and defining

$$(12) \quad A^\pm = \frac{1}{\sqrt{2}} (A_1 \mp iA_2), \quad A^0 = A_3,$$

and similarly for ψ^\pm, ψ^0 we note that

$$\begin{aligned} \frac{1}{2} (f_{\mu\nu}^1 f_{\mu\nu}^1 + f_{\mu\nu}^2 f_{\mu\nu}^2) &= (e_{\mu\nu}^+ - S_{\mu\nu}^+) (e_{\mu\nu}^- - S_{\mu\nu}^-) = \\ &= \left[\left(\frac{\partial}{\partial x_\nu} - i\varepsilon A_\nu^0 \right) A_\mu^+ - \left(\frac{\partial}{\partial x_\mu} - i\varepsilon A_\mu^0 \right) A_\nu^+ \right] \left[\left(\frac{\partial}{\partial x_\nu} + i\varepsilon A_\nu^0 \right) A_\mu^- - \left(\frac{\partial}{\partial x_\mu} + i\varepsilon A_\mu^0 \right) A_\nu^- \right], \end{aligned}$$

while

$$-\frac{1}{4} f_{\mu\nu}^3 f_{\mu\nu}^3 = -\frac{1}{4} e_{\mu\nu}^0 e_{\mu\nu}^0 + \frac{1}{2} S_{\mu\nu}^0 e_{\mu\nu}^0 - \frac{1}{4} S_{\mu\nu}^0 S_{\mu\nu}^0.$$

Identifying A_μ^0 and $e_{\mu\nu}^0$ with the electro-magnetic field, the lagrangian $-\frac{1}{4} \mathbf{f}_{\mu\nu} \mathbf{f}_{\mu\nu}$ is a sum of terms which represent

- 1) the free Maxwell Lagrangian $(-\frac{1}{4} e_{\mu\nu}^0 e_{\mu\nu}^0)$;
- 2) the terms: $-\frac{1}{2} (\partial_\nu^+ A_\mu^+ - \partial_\mu^+ A_\nu^+) (\partial_\nu^- A_\mu^- - \partial_\mu^- A_\nu^-)$,

where

$$\partial^\pm = \left(\frac{\partial}{\partial x} \mp i\varepsilon A^0 \right).$$

These terms describe the conventional electro-magnetic interaction of charged fields A^+, A^- .

3) Terms $-\frac{1}{4}S_{\mu\nu}^0 S_{\mu\nu}^0 = \frac{1}{4}\varepsilon^2((A_\mu^+ A_\nu^- - A_\mu^- A_\nu^+)^2$ which are in a sense « mass » terms for the charged fields A^+ , A^- .

$$4) \text{ A term } \frac{1}{2}S_{\mu\nu}^0 e_{\mu\nu}^0 = -(i/2)(A_\mu^+ A_\nu^- - A_\nu^+ A_\mu^-)e_{\mu\nu}^0.$$

This term would represent a (Pauli) anomalous magnetic moment for A^+ , A^- fields, if these fields had mass.

The A field by itself is then a most remarkable field. One of its components can be identified with the Maxwell field, the other two represent charged particles, carrying « anomalous magnetic moment » while in place of the conventional mass term $-\mu^2 A^+ A^-$, there is a more complicated (quartic) term

$$\frac{\varepsilon^2}{2}[(A_\mu^+ A_\mu^-)^2 - (A_\mu^+)^2 (A_\mu^-)^2].$$

Even in the presence of interactions with other particles the supplementary condition has the transparent form

$$\frac{\partial A_\mu}{\partial x_\mu} = 0.$$

The theory is renormalizable; it is perhaps the only theory of charged vector mesons which can be renormalized. Finally note that

$$-\bar{\Psi} \times \Psi \cdot A = (\bar{\psi}^+ \psi^+ - \bar{\psi}^- \psi^-)A^0 + (\bar{\psi}_0 \psi^- - \bar{\psi}^+ \psi_0)A^+ + \text{h. c.}$$

3. - Let us assume that $L_1 = (e^+, \nu, e^-)$ form a vector in charge-space. With

$$e^\pm = \frac{1}{\sqrt{2}}(\psi_1 \mp i\psi_2), \quad \psi_3 = \nu,$$

(where the three ψ are Majorana fields), the derivative term in the free Lagrangian is

$$\bar{\Psi} \gamma \partial \Psi,$$

which leads to an interaction with A field of the type $\bar{\Psi} \times \Psi \cdot A$. Writing this in full

$$(14) \quad [\bar{e}^+ \gamma_\mu \nu - \bar{\nu} \gamma_\mu e^-]A_\mu^+ + \text{h. c.} + [\bar{e}^+ \gamma_\mu e^+ - \bar{e}^- \gamma_\mu e^-]A_\mu^0.$$

The last term represents electromagnetic interaction while the first two

terms could give the weak interactions of (e, ν) pair. However so far there is nothing in the theory to pick out any one axis in charge-space.

We wish now to do precisely this, by requiring that the neutrino Lagrangian remain invariant for

$$(15) \quad \nu \rightarrow \gamma_5 \nu.$$

in so far as the neutrino mass must be zero. One result of this is that the first term in \bar{L}_{int} reads

$$\frac{1}{2}[\bar{e}^+ \gamma_\mu (1 + \gamma_5) \nu - \bar{\nu} \gamma_\mu (1 + \gamma_5) e^-] A_\mu^+.$$

Thus the neutrino-gauge, conflicting as it does with the [3] charge-gauge, picks an axis in charge-space, and (incidentally) leads to parity violation of interactions of the A_μ^+ , A_μ^- fields. The possibility of gauging the neutrino ($\nu \rightarrow \gamma_5 \nu$) arises from the fact that neutrino has zero mass while the electron does not. In a sense then the existence of mass is incompatible with full rotational symmetry in [3] charge-space; the fact that all known charged particles have mass is the expression of the fact that one particular axis is preferentially chosen in [3] charge-space.

One can consider a second lepton vector $L_2 = (\mu^+, \nu', \mu^-)$, where ν' is gauged as $\nu' \rightarrow -\gamma_5 \nu'$ (*). The interaction Lagrangian for L_2 fields is $-\epsilon \bar{L}_2 \times L_2 \cdot A$. Through the intermediacy of the A^+ , A^- fields, one then has a possibility of $\mu \rightarrow e + \nu + \nu'$, all helicities given by our interaction Lagrangian being precisely the ones which are observed.

The major problem that remains is the problem of the mass of A^\pm fields. Before the introduction of the parity violating term in (14), there was nothing in the theory to differentiate A^\pm from A^0 . The charged A fields would (in spite of the term

$$-\frac{\epsilon^2}{2} [(A_\mu^+ A_\mu^-)^2 - (A_\mu^+)^2 (A_\mu^-)^2],$$

acquire no self-mass from its interactions (**). The parity violating terms give the possibility that self-mass for A^+ , A^- no longer vanishes. Also the charge-renormalization for A^+ , A^- interactions is different than for the A^0 interactions.

(*) In a sense ν and ν' are twin neutrinos.

(**) This has actually been checked to the lowest order by S. KAMEFUCHI. We are indebted for a private communication. He has also checked that an effective mass will appear for the A^\pm fields if parity-violating terms are added.

We propose to come back to this problem in a subsequent paper. Here we simply note that if $\varepsilon^2/4\pi = 1/137$, A^+ , A^- fields would need to have an effective mass $\approx \sqrt{\varepsilon^2/g}$, *i.e.* about $30 m_p$. Note that a (quadratic) self-mass is $\alpha\varepsilon^2\Lambda^2$, where Λ is the cut-off mass. Thus $\varepsilon^2\Lambda^2 \approx \varepsilon^2/g$ gives $\Lambda \approx 350 m_p$. This does not appear too excessive a value for the cut-off.

4. - Baryons and mesons.

For π and K mesons, define the charge space vectors $\boldsymbol{\pi}$ and \mathbf{K} composed from (π^+, π^0, π^-) and (K^+, K_1^0, K^-) particles. (More precisely $\boldsymbol{\pi} = (\pi_1, \pi_2, \pi_3)$)

$$\pi^0 = \pi^3, \quad \pi^\pm = \frac{1}{\sqrt{2}} (\pi^1 \mp i\pi^2), \quad K_1^0 = \frac{1}{\sqrt{2}} (K^0 + \bar{K}^0).$$

The interaction with the A field is

$$- \varepsilon (\partial \boldsymbol{\pi} \times \boldsymbol{\pi} \cdot \mathbf{A}) - \varepsilon^2 [A^2 \boldsymbol{\pi}^2 - (\mathbf{A} \cdot \boldsymbol{\pi})^2]$$

and similarly for the K mesons.

For baryons, we make the fundamental assumption that all bare baryon masses are equal. Defining

$$Y_1 = \frac{1}{\sqrt{2}} (A^0 + \Sigma), \quad Y_2 = \frac{1}{\sqrt{2}} (A^0 - \Sigma^0),$$

we write two baryon vectors

$$\mathbf{B}_1 = \frac{1}{\sqrt{2}} \begin{pmatrix} p + \Sigma^- \\ i(p - \Sigma^-) \\ n + Y_1 \end{pmatrix}, \quad \mathbf{B}_2 = \frac{1}{\sqrt{2}} \begin{pmatrix} \Sigma^+ + \Xi^- \\ i(\Sigma^+ - \Xi^-) \\ Y_2 + \Xi^0 \end{pmatrix}.$$

The free baryon Lagrangian can be written as

$$[\bar{\mathbf{B}}_1 D \mathbf{B}_1 + \bar{\mathbf{B}}_2 D \mathbf{B}_2 + \bar{B}_{s1} D B_{s1} + \bar{B}_{s2} D B_{s2}] + \\ + [\bar{\mathbf{B}}_1^c D \mathbf{B}_1^c + \bar{\mathbf{B}}_2^c D \mathbf{B}_2^c + \bar{B}_{s1}^c D B_{s1}^c + \bar{B}_{s2}^c D B_{s2}^c].$$

Here

$$B_{1s} = \frac{1}{\sqrt{2}} [n - Y_1], \quad B_{2s} = \frac{1}{\sqrt{2}} [Y_2 - \Xi^0],$$

D is the Dirac operator and \mathbf{B}^c is the charge-conjugate vector. (Using Majorana representation of Dirac matrices if $\psi = \psi_1 + i\psi_2$ the charge conjugate spinor is $\psi^c = \psi_1 - i\psi_2$).

We note here an essential difference from the case of leptons. Each one

of our vectors \mathbf{B}_1 , \mathbf{B}_2 , etc., contains complex fields as components. For leptons ($\mathbf{L}_1, \mathbf{L}_2$) as well as for π and K mesons, the corresponding charge-space vectors were real. The reason why $\mathbf{B}_1, \mathbf{B}_2$ are complex lies in baryon-conservation. Thus one can adopt two completely different attitudes for baryons; one can consider that there are essentially four independent charge-space vectors $\mathbf{B}_1, \mathbf{B}_2, \mathbf{B}_1^c$ and \mathbf{B}_2^c and baryon-conservation demands that $\mathbf{B}_1, \mathbf{B}_2$ (for example) should occur symmetrically. Alternatively one may split each of the vectors $\mathbf{B}_1, \mathbf{B}_2$ into real and imaginary parts and work with the resulting four vectors. It is crucial that there are four baryons which are charged ($P, \Sigma^-, (\Sigma^+, \Xi^-)$). One could never arrive at the ideas of charge-space vectors before the discovery of new particles.

A charge space rotation will produce the interaction Lagrangian.

$$(12) \quad \varepsilon[\overline{\mathbf{B}}_1 \mathbf{B}_1 \cdot \mathbf{A} + \overline{\mathbf{B}}_2 \mathbf{B}_2 \cdot \mathbf{A}] - \varepsilon[\overline{\mathbf{B}}_1^c \mathbf{B}_1^c + \overline{\mathbf{B}}_2^c \mathbf{B}_2^c] \cdot \mathbf{A}.$$

The Lagrangian combines formally electro-magnetic interactions, as well as interaction terms which could be responsible (through A^+, A^- fields) for β decays as well as for hyperon decays. However at this stage only parity conserving weak decays are included.

On the other hand we know from our work with leptons, that the postulated γ_5 -invariance of neutrino interactions picks out a direction in charge-space and also symmetrizes the weak lepton interactions for parity-conserving and parity-violating terms. It thus appears that neutrino γ_5 -invariant Lagrangian is also γ_5 -symmetrized in the sense used earlier by SALAM (*).

A term in a Lagrangian is « γ_5 -symmetrized» if the transformation $\psi \rightarrow \gamma_5 \psi$, $m \rightarrow -m$ are made *independently* for all fields concerned (**) and the result summed. Since the lepton and A field interaction Lagrangian happens to be « γ_5 -symmetrized» in the above generalized sense, it seems necessary to « γ_5 -symmetrize» the baryon-Lagrangian as well. Thus

$$(13) \quad p, Y_1, \Sigma^- \rightarrow \gamma_5(p, Y_1, \Sigma^-).$$

A priori (Σ^+, Y_2, Ξ^-) could transform as $+\gamma_5$ or $-\gamma_5$ but Y_1 and Y_2 are related and thus it appears likely that $(\Sigma^+, Y_2, \Xi^-) \rightarrow \gamma_5(\Sigma^+, Y, \Sigma^-)$. After this symmetrization the electro-magnetic interaction remains unchanged, (e.g. $\overline{p}\gamma_\mu p \rightarrow \frac{1}{2}(\overline{p}\gamma_\mu p - \overline{p}\gamma_5\gamma_\mu\gamma_5 p) = \overline{p}\gamma_\mu p$, while $\overline{p}\gamma_\mu n \rightarrow \frac{1}{2}(\overline{p}(1 - \gamma_5)n)$).

(*) A. SALAM: *Phys. Rev. Letters* (to be published). « γ_5 -symmetrization» is not synonymous with « γ_5 -invariance» of a Lagrangian though these may be equivalent in some special cases.

(**) If spin zero Bose fields are present $\varphi \rightarrow -\varphi$ simultaneously with $\psi \rightarrow \gamma_5 \psi$. All currently accepted strong and weak Lagrangians appear to be γ_5 -symmetrized.

It is now necessary to introduce strong interactions of baryons and mesons and to insure that these conserve charge in the conventional sense. This is an important point, for we do not wish to use the vector combinations \mathbf{B}_1 and \mathbf{B}_2 (and singlets B_{s1}, B_{s2}) etc., for writing strong interactions. If we did so, and if strong interactions were rotation invariant in the [3] Q space, there would be no distinction between these interactions and weak and e.m. interactions so far as conventional strangeness, isotopic-spin etc., are concerned. In other words it is necessary to state some criterion which guarantees that even if strong interactions are not rotation-invariant in charge-space these conserve charge in the conventional sense.

Such a criterion is easily stated. Among the \mathbf{A} fields, γ_5 symmetry has picked out the component A^0 . The divergence of the current $\mathcal{F}_\mu^{(1)}$ vanishes.

Here $\mathcal{F}_\mu^{(0)}$ equals the third component of

$$\varepsilon(\bar{\mathbf{L}}_1 \mathbf{L}_1 + \bar{\mathbf{L}}_2 \mathbf{L}_2 + \bar{\mathbf{B}}_1 \mathbf{B}_1 + \bar{\mathbf{B}}_2 \mathbf{B}_2 - \bar{\mathbf{B}}_1^c \mathbf{B}_1^c - \bar{\mathbf{B}}_2^c \mathbf{B}_2^c) + \\ + \text{terms from } \pi, K \text{ and } A \text{ fields. (See Equ. (10)).}$$

Thus charge operator

$$Q = \int \mathcal{F}_4^0 d^3x,$$

can be defined in the usual manner. If we now demand that the hamiltonian for all strong interactions H_s must commute with Q (and must satisfy baryon conservation) charge in the conventional sense is conserved even if H_s is not rotation-invariant in Q -space. Thus the usual isotopic rotation invariant Lagrangian with 8 different coupling constants

$$g_1 \bar{N} N \pi + g_2 \bar{A} \Sigma \pi + g_3 \bar{\Sigma} \Sigma \pi + \dots \quad g_5 \bar{N} K \Lambda + g_6 \bar{N} K \Sigma + \dots$$

is fully acceptable. The mass degeneracy of baryons in the free Lagrangian will be removed by these strong interactions.

5. - The simple interaction Lagrangian written symbolically as

$$(\bar{\mathbf{L}}\mathbf{L} + \bar{\mathbf{B}}\mathbf{B} + \pi\pi + \mathbf{K}\mathbf{K} + \mathbf{A}\mathbf{A}) \cdot \mathbf{A}$$

combines electro-magnetic interactions, as well as weak interactions. For weak interactions γ_5 -symmetrization gives parity-violating terms while electro-magnetic interaction terms still conserve parity. The weak interactions appropriately violate strangeness conservation while electromagnetic interactions do not.

There are also a number of conservation (eq. (10)) laws for the weak inter-

action currents. These are similar to the conservation laws previously discovered by GELL-MANN (*) and ZELDOVICH and GERŠTEJN.

The idea that weak interactions and electromagnetic interactions should be combined, originating as it did with SCHWINGER ⁽²⁾, has been often discussed privately, as has also the possibility that the resulting A -fields should be associated with a Yang-Mills type of gauge transformation. In this connection we are unable to disentangle the extent to which we are indebted to others. Particularly we would like to mention Dr. S. L. GLASHOW who has expressed similar ideas to us privately and a recent preprint (H. MAYER, Dubno) where a future paper on this subject is promised.

* * *

The work of one of the authors (J.C.W.) was supported by the U.S. Air Force through the Office of the Scientific Research of the Air Research and Development Command.

(*) M. GELL-MANN: *Phys. Rev.*, to be published. S. S. GERŠTEJN and ZELDOVICH: *Žurn. Éksper. Teor. Fiz.*, **29**, 698, (1958).

RIASSUNTO (*)

Il postulato di una «connessione locale» in un [3] spazio della carica conduce all'introduzione di tre campi di spin uno. Uno di questi può identificarsi col campo elettromagnetico e si può dimostrare che gli altri due sono il veicolo di tutte le interazioni deboli note, unificando così tali interazioni coll'elettromagnetismo. La teoria tien conto del fatto che, a differenza delle interazioni elettromagnetiche, le interazioni deboli violano la conservazione della parità e della stranezza.

(*) Traduzione a cura della Redazione.

Nuclear Matrix Elements for Some 1st-Forbidden Unique β Transitions.

B. OQUIDAM and B. JANCOVICI

Laboratoire de Physique, Ecole Normale Supérieure - Paris

(ricevuto il 6 Dicembre 1958)

Résumé. — On étudie dans le cadre du modèle des couches les éléments de matrice nucléaires pour les transitions β interdites du premier ordre uniques, autour du nombre de masse $A=40$. L'analyse des résultats expérimentaux permet d'obtenir des éléments de matrice expérimentaux. Puis on calcule ces éléments de matrice, d'abord avec le modèle simple dans lequel les moments angulaires du groupe des protons et du groupe des neutrons sont séparément de bons nombres quantiques; ensuite avec un modèle plus compliqué. Les résultats du deuxième modèle sont en assez bon accord avec l'expérience en ce qui concerne les valeurs relatives des éléments de matrice; un écart systématique est obtenu pour les valeurs absolues. L'étude de transitions γ analogues permet d'attribuer l'écart, au moins pour sa plus grande part, à des effets de structure nucléaire.

1. — Introduction.

It has been established by the work of I. TALMI and his collaborators (¹⁻³) that the shell model with j - j coupling is quantitatively able to account in a very precise way for the energies of the nuclei, at least in certain regions of the mass number. This for a long time unsuspected agreement could be obtained by avoiding the introduction of poorly known numerical values for the radial wave functions or the two-body forces; the energy matrix elements for

(¹) R. THIEBERGER and I. TALMI: *Phys. Rev.*, **102**, 589 (1956).

(²) I. TALMI and R. THIEBERGER: *Phys. Rev.*, **103**, 718 (1956).

(³) S. GOLDSTEIN and I. TALMI: *Phys. Rev.*, **105**, 995 (1957).

simple configurations were instead treated as free parameters, and the energies for more complicated configurations then followed.

Other properties than energies are not expected to be in such a good an agreement with experiment, since the energy is exceptionally favoured by its stationary character. For instance, the nuclear matrix elements for allowed β transitions (⁴) show marked deviations from the j - j coupling shell model values. These deviations however are strongly reduced if some configuration mixing is introduced (⁵).

In the present paper, we study the nuclear matrix elements for 1st-forbidden unique β transitions in the mass number region around $A = 40$. The $d_{3/2}$ shell closes at N or $Z = 20$, and is followed by the $f_{7/2}$ shell. These β^- radioactive nuclei with a proton number $Z < 20$ and a neutron number $N > 20$ undergo transitions in which a $f_{7/2}$ neutron turns into a $d_{3/2}$ proton. All these transitions (with the exception of the ⁴⁰K decay) occur with a spin change of 2 units and with a change of parity: they are unique 1st-forbidden (⁶).

We shall first determine the experimental values of the nuclear matrix elements, through an analysis of the experimental information. We shall then proceed to the calculation of these matrix elements with simple wave functions, and also with more refined wave functions. These results will be discussed. The relation with some γ matrix elements will also be studied.

2. - Experimental β nuclear matrix elements.

In the notation of (⁶), the nuclear matrix element for a 1st-forbidden unique transition is:

$$(1) \quad |M|^2 = \sum |\mathcal{Q}_{2m}(\sigma)|^2,$$

where the summation is on m and on the spin states of the final nucleus. \mathcal{Q}_{2m} is a second-order tensor, bilinear in σ and r , defined by:

$$(2) \quad \mathcal{Q}_{lm}(\sigma) = \frac{1}{l} \sigma \cdot \text{grad } \mathcal{Q}_{lm}(r),$$

where $\mathcal{Q}_{lm}(r)$ is the usual solid spherical harmonic.

(⁴) W. C. GRAYSON JR. and L. W. NORDHEIM: *Phys. Rev.*, **102**, 1093 (1956).

(⁵) R. J. BLIN-STOYLE and C. A. CAINE: *Phys. Rev.*, **105**, 1810 (1957).

(⁶) For a review of the theory of forbidden β decay, see e.g. E. KONOPINSKI, in *Beta- and Gamma-Ray Spectroscopy*, edited by K. SIEGBAHN (Amsterdam, 1955), p. 292. We here follow the notations of this paper.

This matrix element is related to the comparative half-life $f_1 t$ by:

$$(3) \quad f_1 t = \frac{2\pi^3 \ln 2/g^2}{(32\pi/15) |M|^2},$$

where g is the Gamow-Teller coupling constant. We adopt the value which results from the most recent measurements of the half-lives of ^{14}O ⁽⁷⁾ and of the neutron ⁽⁸⁾ which yield $2\pi^3 \ln 2/g^2 = 4366 \text{ s}$, when M in (3) is expressed in units of electron Compton wave length \hbar/mc . f_1 is defined by DAVIDSON ⁽⁹⁾,

TABLE I.

	$\log ft$	$\log f_1 t$	$10^6 M _{\text{exp}}^2 = 651/f_1 t \cdot 10^6$	Simple wave functions		Detailed wave functions	
				Q	$10^6 M _{\text{SP.off}}^2$	Q	$10^6 M _{\text{SP.off}}^2$
(a, b) $^{37}\text{S} \rightarrow ^{37}\text{Cl}$	7.23	7.93	7.7	1	7.7	1	7.7
(c, 19) $^{38}\text{Cl} \rightarrow ^{38}\text{A}$	7.42	8.19	4.20	4/5	5.2	0.80	5.2
(d) $^{39}\text{Cl} \rightarrow ^{39}\text{A}$	7.8	8.3	3.26	1/4	13.0	0.9	3.6
(e, f) $^{39}\text{A} \rightarrow ^{39}\text{K}$	9.91	9.01	0.64	1/2	1.3	0.11	5.8
(g) $^{41}\text{A} \rightarrow ^{41}\text{K}$	8.34	8.50	2.15	3/8	5.7	3/8(*)	5.7 (*)
(h, 19) $^{42}\text{K} \rightarrow ^{42}\text{Ca}$	7.95	8.42	2.48	6/5	2.1	0.66	3.8
(i) $^{43}\text{K} \rightarrow ^{43}\text{Ca}$	8.70	8.62	1.56	1	1.6	0.24	6.5

$|M|^2$ is in units $\hbar = m = c = 1$

(*) These values come from a very rough estimate of the « detailed wave function ».

(a) E. BLEULER and W. ZÜNTI: *Helv. Phys. Acta*, **19**, 137 (1946).

(b) D. STROMINGER, J. M. HOLLANDER and G. T. SEABORG: *Rev. Mod. Phys.*, **30**, 585 (1958).

(c) J. W. COBBLE and R. W. ATTEBERRY: *Phys. Rev.*, **80**, 917 (1950).

(d) J. R. PENNING, H. R. MALTRUD, J. C. HOPKINS and F. H. SCHMIDT: *Phys. Rev.*, **104**, 740 (1956).

(e) A. R. BROSI, H. ZELDES and B. H. KETELLE: *Phys. Rev.*, **79**, 902 (1950).

(f) H. ZELDES, B. H. KETELLE, A. R. BROSI, C. R. FULTZ and R. F. HIBBS: *Phys. Rev.*, **86**, 811 (1952).

(g) A. SCHWARTZSCHILD, B. M. RUSTAD and C. S. WU: *Phys. Rev.*, **103**, 1796 (1956).

(h) P. R. J. BURCH: *Nature*, **172**, 361 (1953).

(i) T. LINDQVIST and A. C. G. MITCHELL: *Phys. Rev.*, **95**, 444 (1954).

(7) J. B. GERHART: *Phys. Rev.*, **109**, 897 (1958).

(8) A. N. SOSNOVSKIJ, P. E. SPIVAK, P. E. PROKOFIEV, A. YU, I. E. KUTIKOV and YU. P. DOBRYNIN: *Contribution to the 1958 Annual International Conference on High Energy Physics at CERN*.

(9) J. P. DAVIDSON JR.: *Phys. Rev.*, **82**, 48 (1951). This reference is inaccurate in its presentation: if the factor

$$|Q_{n+1}(\sigma, \mathbf{r})|^2 = (32 \pi/15) |M|^2$$

is removed from the definition of C_n in eq. (9), the definition (8) of f_1 is then the actual one used by DAVIDSON in his computations, and also by us.

who gives an approximate procedure for computing it. We also computed f_1 by numerical integration of the theoretical spectrum, and checked that the approximation of DAVIDSON is accurate within a few percent. f_1 depends on the Q -value for the β transition. Using the experimental values of Q and of the half-life t , we list the experimental values of $f_1 t$, for the transitions of interest, in Table I. The value of ft , where f is that quantity which is currently used for allowed transitions is also listed for the sake of comparison. We then use (3) to determine an « experimental » value for the squared matrix element, $|M|_{\text{exp}}^2$, which is given in Table I.

3. — Calculated β nuclear matrix elements with simple wave functions.

The matrix element for a single particle transition is easily obtained using the definition (2) of $\mathcal{Q}_{2m}(\sigma)$. One has for this single particle case ⁽¹⁰⁾:

$$(4) \quad |M|_{\text{s.p.}}^2 = (9/7\pi) \left(\int_0^\infty R_f(r) r R_d(r) dr \right)^2,$$

where $R_f(r)/r$ and $R_d(r)/r$ are the radial wave functions for the f and d states. The integral in (4) cannot be computed without somewhat arbitrary assumptions on these wave functions. However, an estimate of this integral can be easily obtained from some model, for instance oscillator well wave functions. The parameter ν of the well can be adjusted to fit the Coulomb energy differences between mirror nuclei ⁽¹¹⁾ in this region of A). In this way we obtain:

$$(5) \quad |M|_{\text{s.p.}}^2 = 9/4\pi\nu \approx 37 \cdot 10^{-6} (\hbar/mc)^2.$$

A numerical integration with wave functions for an infinite square well of radius $R = 1.6 \cdot 10^{-13} (40)^{\frac{1}{3}} \text{ cm}$ ⁽¹²⁾ leads to the value:

$$(5') \quad |M|_{\text{s.p.}}^2 = (9/7\pi) 0.44 R^2 \approx 36 \cdot 10^{-6} (\hbar/mc)^2.$$

We see that the value of $|M|_{\text{s.p.}}^2$ does not depend too much on the model.

⁽¹⁰⁾ Cf. R. NATAF: *Journ. Phys. Rad.*, **14**, 72 (1953). There is a misprint in eq. (5) of this reference, which should be read

$$|a_1|^2 = 12 \frac{L(L-1)}{4L^2-1} \quad \text{if } J > J'.$$

⁽¹¹⁾ B. C. CARLSON and I. TALMI: *Phys. Rev.*, **96**, 436 (1954).

⁽¹²⁾ The radius of the infinite well has to be taken somewhat bigger than the radius of the charge distribution. This value of R leads to a mean square radius of $(3/5)^{\frac{1}{2}} 1.3 \cdot A^{\frac{1}{3}} \cdot 10^{-13} \text{ cm}$, which is suggested by Coulomb energies in this region (see ref. ⁽¹¹⁾).

But the nuclear radius enters by its square, and the uncertainty on this radius would be reflected in $|M|_{\text{S.P.}}^2$.

This single-particle value should be appropriate to the transition $^{37}_{16}\text{Cl}_{17} \rightarrow ^{37}_{17}\text{S}_{16}$. For the other cases, we consider the following «simple» wave functions: the protons (neutrons) in the $d_{3/2}$ ($f_{7/2}$) shell are coupled together to a definite angular momentum J_1 (J_2), equal to 0 if the proton (neutron) is even, to $\frac{3}{2}$ ($\frac{7}{2}$) if the proton (neutron) is odd; J_1 and J_2 are coupled together to give the total angular momentum J . These configurations are given in Table II. The neutrons in the closed $d_{3/2}$ neutron shell play no role in β transitions and can be neglected⁽¹³⁾. The transitions we consider are therefore of the type:

$$(j)_{J_1}^m (j')_{J_2}^{n'} J' \rightarrow (j)_{J_1}^{m+1} (j')_{J_2}^{n-1} J.$$

Table II. — Detailed wave functions.

$^{37}_{16}\text{S}_{21}$	$ f_{7/2}, \frac{7}{2}\rangle$
$^{37}_{17}\text{Cl}_{20}$	$ d_{3/2}, \frac{3}{2}\rangle$
$^{38}_{17}\text{Cl}_{21}$	$ d_{3/2}, f_{7/2}, 2\rangle$
$^{39}_{17}\text{Cl}_{22}$	$0.92 d_{3/2}, (f_{7/2}^2)_0, \frac{3}{2}\rangle + 0.39 d_{3/2}, (f_{7/2}^2)_2, \frac{3}{2}\rangle$
$^{38}_{18}\text{A}_{20}$	$ d_{3/2}^2, 0\rangle$
$^{39}_{18}\text{A}_{21}$	$0.95 (d_{3/2}^2)_0, f_{7/2}, \frac{7}{2}\rangle + 0.31 (d_{3/2}^2)_2, f_{7/2}, \frac{7}{2}\rangle$
$^{41}_{18}\text{A}_{23}$	$\dots (d_{3/2}^2)_0, (f_{7/2}^3)_{\frac{7}{2}}, \frac{7}{2}\rangle + \dots$
$^{39}_{19}\text{K}_{20}$	$ d_{3/2}^3, \frac{3}{2}\rangle$
$^{41}_{19}\text{K}_{22}$	$0.92 (d_{3/2}^3)_{\frac{3}{2}}, (f_{7/2}^2)_0, \frac{3}{2}\rangle - 0.38 (d_{3/2}^3)_{\frac{3}{2}}, (f_{7/2}^2)_2, \frac{3}{2}\rangle$
$^{42}_{19}\text{K}_{23}$	$0.74 (d_{3/2}^3)_{\frac{3}{2}}, (f_{7/2}^3)_2, 2\rangle + 0.65 (d_{3/2}^3)_{\frac{3}{2}}, (f_{7/2}^3)_2, 2\rangle + 0.17 (d_{3/2}^3)_{\frac{3}{2}}, (f_{7/2}^3)_2, 2\rangle$
$^{43}_{19}\text{K}_{24}$	$0.88 (d_{3/2}^3)_{\frac{3}{2}}, (f_{7/2}^4)_0, \frac{3}{2}\rangle - 0.47 (d_{3/2}^3)_{\frac{3}{2}}, (f_{7/2}^4)_2, \frac{3}{2}\rangle + \dots$
$^{42}_{20}\text{Ca}_{22}$	$ d_{3/2}^4, (f_{7/2}^2)_0, 0\rangle$
$^{43}_{20}\text{Ca}_{23}$	$ d_{3/2}^4, (f_{7/2}^3)_{\frac{7}{2}}, \frac{7}{2}\rangle$

The simple wave function is the first term of the detailed wave functions.

The matrix elements for such a transition can be related to the single particle value (4) by the straightforward use of tensor algebra⁽¹⁴⁾ and of coefficients of fractional parentage⁽¹⁵⁾:

$$(6) \quad M/M_{\text{S.P.}} = (-1)^{j+j_2-j'_2} \sqrt{(m+1)n(2J+1)(2j'+1)(2J_1+1)(2J'_2+1)} \cdot$$

$$\cdot \langle j^{m+1} J_1 \{ j^m(J_1) j J_1 \rangle \langle j'^n J'_2 \{ j'^{n-1}(J_2) j' J'_2 \rangle \cdot \begin{Bmatrix} J_1 & J_2 & J \\ J'_1 & J'_2 & J' \\ j & j' & 2 \end{Bmatrix}.$$

⁽¹³⁾ As a check, we also performed the calculations with the $d_{3/2}$ neutrons taken into account, and obtained the same results.

⁽¹⁴⁾ G. RACAH: *Phys. Rev.*, **62**, 438 (1942).

⁽¹⁵⁾ G. RACAH: *Phys. Rev.*, **63**, 367 (1943). See eq. (28) of this reference.

The coefficients of fractional parentage for identical particles, $\langle \{ \} \rangle$, are available ^(16,17). The $9-j$ coefficients $\{ \}$ ⁽¹⁸⁾ can also be computed; incidentally, they reduce to Racah coefficients in the cases where one of the j is zero. The resulting value of the ratio:

$$(7) \quad \rho = |M|^2 / |M|_{\text{S.P.}}^2$$

is listed in Table I.

In order to compare the results to experiment, we define an effective single particle matrix element by the relation:

$$(8) \quad |M|_{\text{S.P. eff}}^2 = |M|_{\text{exp}}^2 / \rho.$$

This procedure allows us to eliminate the uncertain value (5) or (5'). The theory will be satisfactory if $|M|_{\text{S.P. eff}}^2$ is a constant for the different transitions. The values listed in Table I are actually far from constant. Furthermore, the absolute value of $|M|_{\text{S.P. eff}}^2$ is smaller than the estimate (5) or (5').

4. - Calculated β nuclear matrix elements with more detailed wave functions.

The simple wave functions of the last section gave a poor agreement with experiment, both for the relative and for the absolute values of the matrix elements. It is possible to improve these wave functions by using the freedom on the values of J_1 and J_2 . We now choose wave functions of the form:

$$(9) \quad \sum_{J_1 J_2} \alpha_{J_1 J_2} |(d_{\frac{3}{2}})_{J_1}^m (f_{\frac{7}{2}})_{J_2}^n J \rangle,$$

where the summation runs over all possible values of J_1 and J_2 . The coefficients $\alpha_{J_1 J_2}$ should be determined by the diagonalization of an energy matrix.

In the cases where the proton (neutron) number is even, it was argued ⁽³⁾ that the excitation of the proton (neutron) configuration requires much energy, and the admixture of such excited states should be negligible. This argument, however, was made for the calculation of binding energies. The calculation of β transitions requires better wave functions, and we now take into account the admixtures of excited states of the even configurations. Of course, admixtures occur more easily for odd configurations, and these will be also considered.

⁽¹⁶⁾ A. R. EDMONDS and B. H. FLOWERS: *Proc. Roy. Soc. (London)*, A **214**, 515 (1952).

⁽¹⁷⁾ W. C. GRAYSON JR. and L. W. NORDHEIM: *Phys. Rev.*, **102**, 1084 (1956).

⁽¹⁸⁾ G. RACAH and U. FANO: *Irreducible Tensorial Sets* (New York, to be published).

The calculation of the energy matrices closely follows in all cases the techniques which were previously used ⁽³⁾ in the odd-odd case of ⁴²K and this calculation will not be described in detail here ⁽¹⁹⁾. It must however be noted that we do not compute the energy contribution of the forces between identical particles; we rather use the experimental information ⁽²⁰⁾ from neighbouring nuclei. For instance, in the case of ³⁹A, the wave function is of the form:

$$(10) \quad \alpha_0 |(d_{\frac{3}{2}})_0^2 f_{\frac{7}{2}} 7/2\rangle + \alpha_2 |(d_{\frac{3}{2}})_2^2 f_{\frac{7}{2}} 7/2\rangle.$$

The proton-proton energy difference between $(d_{\frac{3}{2}})_2^2$ and $(d_{\frac{3}{2}})_0^2$ is then taken as the experimental excitation energy of the first level $(d_{\frac{3}{2}})_2^2$ of ³⁸A relative to its ground state $(d_{\frac{3}{2}})_0^2$. The neutron-proton forces are treated as in ⁽³⁾ and expressed in terms of the same parameters V_j . The binding energies which are computed by this procedure are excellent ⁽²¹⁾. The wave functions so obtained are listed in Table II. The energy matrices of interest are given in the Appendix.

Some remarks are necessary: in the case of ⁴³K, there are two possible states with $J_2 = 2$ for the neutron configuration $(f_{\frac{7}{2}})^4$. These states have seniorities 2 and 4. The seniority 4 state is expected to have a higher energy but it cannot be identified in a unique way with a given level of ⁴⁴Ca; furthermore, there is no element in the energy matrix directly connecting the corresponding unperturbed state of ⁴³K to the unperturbed ground state of ⁴³K. The admixture of this state is thus expected to be small. On the other hand, it can be shown that this seniority 4 component would not directly contribute to the β matrix element: this component therefore does not interfere with the other ones, and would only cause a slight second order modification of the coefficients of the other components. For all these reasons, we neglect the possible admixture of the seniority 4 state.

We have omitted the energy matrix and the detailed wave function for ⁴¹A. This is because the energy matrix would be too big, and the various states of the $(f_{\frac{7}{2}})^3$ neutron configuration of ⁴¹A cannot be uniquely identified with the levels of ⁴³Ca. Some preliminary calculations however show that ⁴¹A is fairly well represented by the simple wave function $|(d_{\frac{3}{2}})_0^2, (f_{\frac{7}{2}})_2^3, 7/2\rangle$.

It is now possible to compute the β decay matrix elements with the more detailed wave functions (9). Denoting by $M(J_1 J_2 J'_1 J'_2)$ the value computed for M from (6), one immediately sees that:

$$(11) \quad \varrho = |M|^2 / |M|_{\text{S.P.}}^2 = \left| \sum_{J_1 J_2 J'_1 J'_2} \alpha_{J'_1 J'_2} \alpha_{J_1 J_2} M(J_1 J_2 J'_1 J'_2) / M_{\text{S.P.}} \right|^2$$

⁽¹⁹⁾ B. OQUIDAM: *Thesis* (Doctorat de Spécialité de Physique Théorique - Paris), to be published.

⁽²⁰⁾ P. M. ENDT and C. M. BRAAMS: *Rev. Mod. Phys.*, **29**, 683 (1957).

⁽²¹⁾ I. TALMI: private communication.

where $\alpha_{J_1'J_2'}$ and $\alpha_{J_1J_2}$ are the coefficients of the wave function (9) for the initial and final states. The values obtained from (11) are listed in Table I. With the value (11) for Q , (8) gives new values for $|M|_{\text{S.P. eff}}^2$ which are listed in Table I.

It can be seen that the constancy of $|M|_{\text{S.P. eff}}^2$ is improved by the use of the more detailed wave functions. The progress appears when the last column of Table I is compared with the much more dispersed experimental values $|M|_{\text{exp}}^2$. It must also be remembered that the experimental values are sometimes rather imprecise, and on the other hand that the β matrix elements are sensitive to small changes in the wave function.

5. - Discussion.

The approximate consistency of the values for $|M|_{\text{S.P. eff}}^2$ obtained with the detailed wave functions, shows that the shell model, with the refinements of Section 4, provides a fair account for the relative values of the β matrix elements. Comparison with the results obtained in Section 3 shows that the agreement with experiment is always improved by the use of the wave functions of Section 4. It is hoped that the small irregularities which subsist would be removed by further complication of the wave functions, for instance by taking into account the possible admixtures of $f_{\frac{5}{2}}$ orbitals. It must also be remembered that the experimental half-lives and Q values are often uncertain.

On the other hand, the absolute value of $|M|_{\text{S.P. eff}}^2$ shows a marked departure from the estimates (5) or (5'). It does not seem possible to get entirely rid of this discrepancy by a simple change in the radial wave functions. Everything occurs as if the single particle matrix element was consistently smaller by a factor of about 4 than its estimates (5), (5'). The possible reasons for this apparent «renormalization» could be more easily discussed after a study of some γ transitions.

6. - Comparison with γ transitions.

For all the β transitions which were considered here, the daughter nucleus should have an excited state which is in close correspondence with the initial nucleus in its ground state. The γ transition of this excited state to the ground state is closely related to the corresponding β transition, and it is possible to compare their rates in the few cases when the γ lifetime has been measured, *i.e.* for the decays of the 1.52 MeV level of ³⁹A and of the 1.29 MeV of ⁴¹K. The (partial) half-lives are listed in Table III.

TABLE III.

	γ partial half-life	$ M _{\text{exp}}^2$ from γ	Corresponding β transition	$ M _{\text{exp}}^2$ from β
^{39}A (1.52 MeV)	$2.1 \cdot 10^{-9}$ s	$5.2 \cdot 10^{-6}$	$^{39}\text{Cl} \rightarrow ^{39}\text{A}$	$3.3 \cdot 10^{-6}$
^{41}K (1.29 MeV)	$6.6 \cdot 10^{-9}$ s	$3.7 \cdot 10^{-6}$	$^{41}\text{A} \rightarrow ^{41}\text{K}$	$2.2 \cdot 10^{-6}$

These γ transitions with a spin change of 2 and a change of parity should be predominantly of M2 character. We assume that the possible E3 contribution is negligible, as indicated by simple estimates ⁽²²⁾. The γ transition results from the jump of a proton between the $f_{\frac{3}{2}}$ and $d_{\frac{3}{2}}$ orbits. We can take into account some rearrangement of the other particles, using the same model as in Section 3. The important point however is that within this model, *i.e.* with definite orbitals $f_{\frac{3}{2}}$ and $d_{\frac{3}{2}}$ for the proton states, the M2 γ matrix element reduces to the β matrix element ⁽²³⁾. The γ transition probability per second is then:

$$(12) \quad T = \frac{4\pi}{75} \frac{e^2 E^5}{\hbar^4 m_p^2 c^7} \left(\mu_p - \frac{1}{3} \right)^2 \sum |\mathcal{Q}_{2m}(\sigma)|^2,$$

where m_p is the proton mass, μ_p the proton magnetic moment in nuclear magneton units, E the γ -ray energy. $\mathcal{Q}_{2m}(\sigma)$ is here in cm. This formula is used to compute an experimental squared matrix element $|M|_{\text{exp}}^2$, as defined in (1), from the observed γ -transition probability. The value of $|M|_{\text{exp}}^2$ which is listed in Table III can be compared with the experimental value for the corresponding β transition matrix element, which is also repeated in Table III. It is seen that the two γ and β determinations are not in bad disagreement.

It thus appears that the γ matrix element is damped by a factor which is roughly the same as for the β matrix element. This fact would tend to prove that most of the «renormalization» of the matrix elements cannot be connected with the field-theoretical nature of the interaction (β or γ) under consideration, since the effect is the same for both interactions, although they are so different in their nature. The «renormalization» should thus mostly be a nuclear structure effect. For instance, if the $d_{\frac{3}{2}}$ and $f_{\frac{3}{2}}$ particles are weakly coupled to collective motions of the core, we expect such «renormalization» effects to occur, although many characters of the spherical shell-model will subsist. This aspect of the question is now being studied in our group.

The difference which subsists between the β and the γ matrix elements could reasonably result from the nuclear model imperfections. For instance, with an admixture of $f_{\frac{3}{2}}$ orbitals, (12) would no longer be valid.

⁽²²⁾ V. F. WEISSKOPF: *Phys. Rev.*, **83**, 1073 (1951).

⁽²³⁾ S. A. MOSZKOWSKI: p. 390 of ref. ⁽⁶⁾.

To summarize this work, the conclusion of our study is that the relative values of the β decay matrix elements are fairly accounted for by the shell model. The absolute values are consistently too small by a «renormalization» factor of about 4.

Finally, we see that it cannot be shown here that the effective operator which is responsible for 1st-forbidden unique β transitions is significantly different from $\mathcal{Q}_{2m}(\sigma)$. We very tentatively suggest that this is perhaps not a trivial statement, since it has been proposed that the axial β interaction could, like the vector one, be of a more complicated nature than the conventional one. It is indicated by our results that the effective β -decay coupling constant that appears for 1st-forbidden unique transitions does not seem to be actually different by more than 50% from the coupling constant for allowed transitions (which was introduced in (3)). It would be interesting to see, by a more careful knowledge of the nuclear structure, if it is possible to establish more precisely the equality of these constants, or if, conversely, they appear as being definitely different.

* * *

We are indebted to Professor I. TALMI for a stimulating discussion, for his kind interest, and for communication of results that he calculated independently. Thanks are due to Mrs. OQUIDAM who checked some of the calculations. The Centre d'Etudes Nucleaire de Saclay kindly made available 9- j coefficients which were calculated on their electronic computer.

APPENDIX

The energy matrices which do not reduce to a number are the following:

³⁹ Cl	J_2	0	2
	0	2.03	0.77
	2	0.77	0.56

³⁹ A	J_1	0	2
	0	2.03	0.77
	2	0.77	— 0.07

^{41}K	J_2	0	2
	0	6.08	-0.71
	2	-0.71	4.61

^{43}K	J_2	0	2
	0	12.17	-0.82
	2	-0.82	11.06

The energies which are taken into account here are the neutron proton interaction between $d_{\frac{3}{2}}$ and $f_{\frac{7}{2}}$ shells, and the excitation energy of the even group. Minus the energies are given.

The matrix for ^{42}K is given in ⁽³⁾. The matrix for ^{41}A is not given here.

RIASSUNTO (*)

Si studiano nel quadro del modello a shell gli elementi di matrice nucleare per le transizioni β proibite del primo ordine, uniche, intorno al numero di massa $A = 40$. L'analisi dei risultati sperimentali permette d'ottenere degli elementi di matrice sperimentali. Poi si calcolano questi elementi di matrice, prima col modello semplice in cui i momenti angolari del gruppo dei protoni e del gruppo dei neutroni sono separatamente buoni numeri quantici; poi con un modello più complicato. I risultati del secondo modello sono in sufficiente buon accordo con l'esperienza per quanto riguarda i valori relativi degli elementi di matrice; pei valori assoluti si ottiene uno scarto sistematico. Lo studio delle analoghe transizioni γ permette di attribuire lo scarto, almeno per la maggior parte, ad effetti della struttura nucleare.

(*) Traduzione a cura della Redazione.

NOTE TECNICHE

A Device for Dynamical Measurements of Pressure.

P. BASSI

Istituto di Fisica dell'Università - Padova
Istituto Nazionale di Fisica Nucleare - Sezione di Padova

R. CANO

Istituto di Fisica dell'Università - Trieste
Istituto Nazionale di Fisica Nucleare - Sezione di Trieste

S. FOCARDI and C. RUBBIA (*)

Istituto di Fisica dell'Università - Pisa
Istituto Nazionale di Fisica Nucleare - Sezione di Pisa

A. MICHELINI

Istituto di Fisica dell'Università - Roma
Istituto Nazionale di Fisica Nucleare - Sezione di Roma

F. SAPORETTI

Istituto di Fisica dell'Università - Bologna
Istituto Nazionale di Fisica Nucleare - Sezione di Bologna

(ricevuto il 24 Novembre 1958)

Summary. — A device for fast measurements of pressure variations to be used in liquid hydrogen bubble chamber technique, is described. Its characteristic features are speedy and linear response, output signal independence of cable capacity variations, possibility of adjustment at a distance and simplicity of the detecting circuit.

There are several methods in use to transform a fast variation of pressure into an electric signal through capacity variation as well as through resistance variation, piezoelectric effect or e.m. induction.

(*) Now at Columbia University.

The pressure gage which will be described is supposed to work at liquid hydrogen temperature in a bubble chamber. The apparatus should, therefore, have the following characteristics.

- a) Work correctly in a magnetic field of the order of 15 000 G.
- b) Allow steady pressure calibration and further adjustment at a distance.

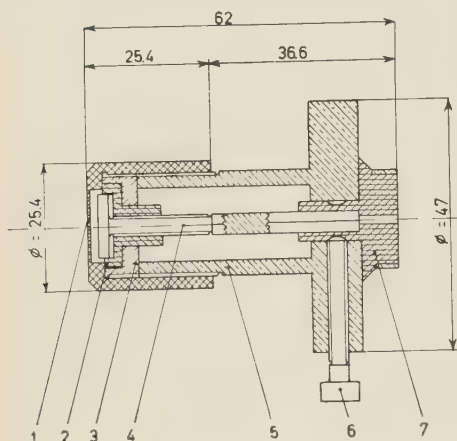


Fig. 1. - Pressure cell. During the present measurements the spacing between diaphragm A and the internal electrode was 0.03 mm (at pressure 0 atm) equivalent to an electric capacity of 35 pF.

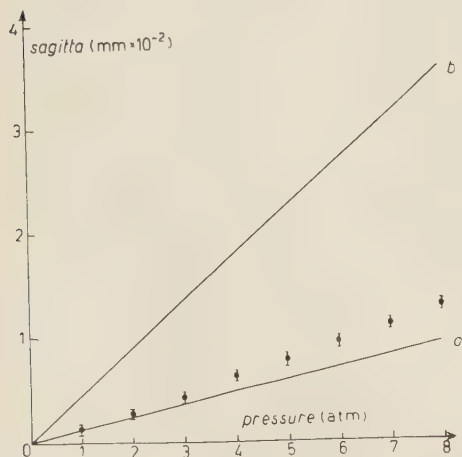


Fig. 2. - Diaphragm A sagittae vs. pressure.

c) Have an output signal as independent as possible of capacity variations (due, f.i. to temperature variations) in the coaxial cable connecting the pressure cell to the detecting circuit.

d) Have a response time less than 10^{-4} s to ensure reproduction of pressure transients to a few tenths of a millisecond.

To meet these requirements we have decided to use a system capable of transforming mechanical deformations into electric signals through the capacity variations of a condenser ⁽¹⁻³⁾.

The pressure cell is shown in Fig. 1: diaphragm A is made of stainless steel 0.63 mm thick; the distance of the inner electrode from diaphragm A can be adjusted by means of a screw. The accuracy in the machining of the condenser was 0.01 mm; the two electrodes are parallel within a few hundredths mm. The spacing between the electrodes can be adjusted within 1/360 mm by means of the screw. Fig. 2 shows the measured sagitta diaphragm A as a function of the applied pressure; straight lines c and t are the sagittae evaluated in the two limiting cases of a circular diaphragm clamped, and simply supported at the edges.

As was already pointed out the electric circuit was designed to be insensitive to the capacity variations of the cable. The scheme of the circuit is shown in Fig. 3.

(1) T. WRATHALL: *Instrument*, **26**, 736 (1955).

(2) W. I. LINLOR and Q. A. KERN: UCRL-3173.

(3) W. I. LINLOR, Q. A. KERN and J. W. MARK: *Rev. Sci. Instr.*, **28**, 535 (1957).

A 1.5 mH inductance (not critical) is connected in series with the pressure cell; the LC circuit thus forms the impedance load of a 75 Ω coaxial cable matched on its characteristic impedance.

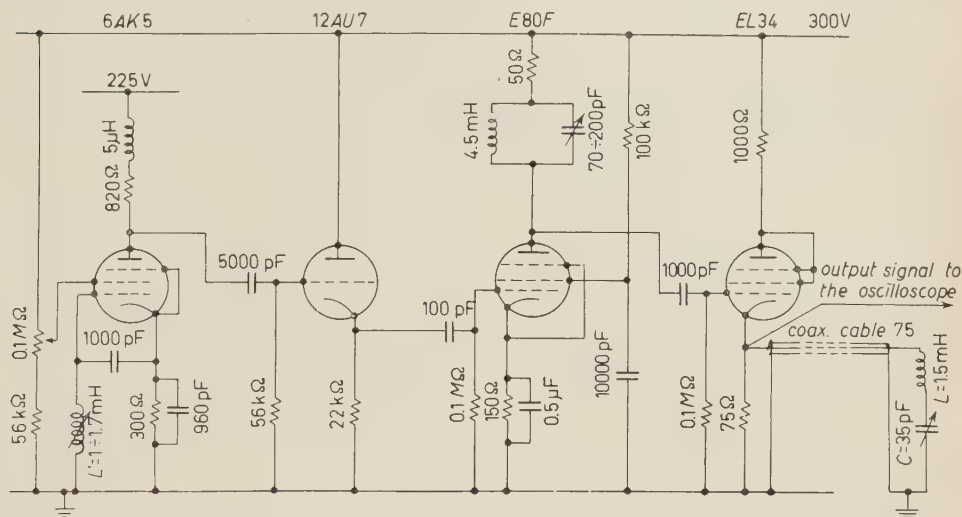


Fig. 3. — *Electric circuit.* The frequency of the 6AK5 oscillator can be modified by varying L' between 630 and 745 MHz.

The first stage consists of an oscillator whose frequency can be adjusted by changing L' . A decoupling and an amplifying stage follow. The EL34 is a low impedance adapter which easily gives an output signal up to 8 V (peak to peak) on 75 Ω .

The cathodic impedance of the EL34 is.

$$(1) \quad Z_k = \frac{R\sqrt{r^2 + (L\omega - 1/\omega c)^2}}{\sqrt{r^2 + (L\omega - 1/\omega c)^2 + R}}$$

For the case of resonance, Z_k is clearly minimum and is the resultant of the two impedances R ($= 75 \Omega$) and r (resistive component of the LC circuit) in parallel.

Variations of C around the resonance may cause an increase in the cathodic impedance.

In Fig. 4 we have plotted the difference between the peak to peak output signal (V) and the signal at resonance (M), measured on the oscilloscopes *vs.* pressure. This was a steady pressure calibration at room temperature.

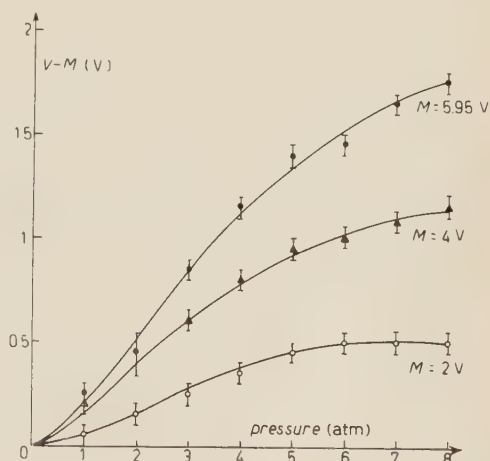


Fig. 4. — *Calibration curves.* The difference between the peak to peak output signal (V) and the signal at resonance (M) *vs.* pressure. Resonance corresponds to 0 atm, the working frequency was 715 MHz.

The frequency of the oscillator was adjusted to coincide with the resonance frequency of the LC circuit at 0 atm.

Fig. 5 shows that, as expected, there is a linear dependence between the modulation and the carrying wave amplitude.

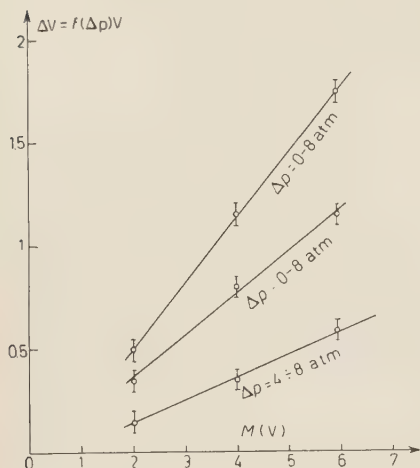


Fig. 5. — Peak to peak modulated signal vs. carrying wave amplitude, at resonance (M).

We have investigated the dependence of the instrument characteristics on some parameters with the following results:

— The instrument's sensitivity obviously increases with the decrease of the distance between the two electrodes of the pressure cell. Such an increase in the sensitivity of the system reduces the linearity of the output signal since, with a high value of ΔP , the circuit is working near the saturation of the resonance curve.

— The sensitivity improves with the decrease of r (see (1)). It is then necessary to work with high Q -factor.

— We have found that, by putting 1000 pF in parallel to the cable (10 m cable-70 pF/m), the amplitude of the modulated signal was not modified.

— By varying the working frequency by 15%, the modulated signal proved to be constant within the precision of our measurements (2%).

Furthermore it is possible to perform a readjustment of the frequency up to 15%, if the resonance frequency changes because of thermal effects, without a recalibration of the amplitude.

RIASSUNTO

Viene descritto uno strumento per la misura di variazioni rapide di pressione da usarsi nella tecnica delle camere a bolle a idrogeno liquido. Le sue caratteristiche sono risposta rapida e lineare, indipendenza del segnale d'uscita dalle variazioni di capacità del cavo, possibilità di regolazione a distanza e semplicità nel circuito di rivelazione.

On a 200 keV Radiofrequency Deuteron Accelerator of the Cockcroft and Walton Type.

F. DEMANINS and G. POIANI

Istituto di Fisica dell'Università - Trieste
Istituto Nazionale di Fisica Nucleare - Sottosezione di Trieste

(ricevuto il 24 Novembre 1958)

Summary. — A description is given of a deuteron accelerator of 200 keV for the production of neutrons through the d-d and d-t reactions. It is pointed out that its principal characteristic is that high tension is obtained by means of a radiofrequency voltage multiplying circuit.

1. — Introduction.

Recently the improvement of the technique for accelerating deuterons has made it frequently possible to use fast monoenergetical neutron beams obtained from the exothermic reactions $^2\text{H}(\text{d}, \text{n})^3\text{He}$ and $^3\text{H}(\text{d}, \text{n})^4\text{He}$.

The accelerators commonly used for this purposes are of the voltage multiplying type which, as is well known, are based on the original Greinacher circuit ⁽¹⁾, successively improved by Cockcroft and Walton ⁽²⁾.

Because of the use to which they are expected to be employed, a strict definition in the energy of the ions and a very small value in the ripple is not important. Therefore they may be constructed with generators of alternating current at industrial frequency.

However, as shown by LORRAIN ⁽³⁾, the use of high frequencies to feed the multiplier presents many advantages. First of all a sensible economy can be achieved in the project of the capacitors, then the size can be reduced and furthermore it makes it possible to increase considerably the number

⁽¹⁾ H. GREINACHER: *Zeits. f. Phys.*, **4**, 195 (1921).

⁽²⁾ J. D. COCKCROFT and E. T. S. WALTON: *Proc. Roy. Soc.*, A **136**, 619 (1932).

⁽³⁾ P. LORRAIN: *Rev. Sci. Instr.*, **20**, 216 (1949).

of stages in the cascade. Another advantage, which has not a negligible practical importance, arises from the fact that the filaments of the rectifying diodes can be fed directly with the radiofrequency itself.

Of course the increase of the working frequency, brings about some disadvantages such as, for instance, the requirement of a somewhat more elaborated generator with respect to the one used in the low frequency set up, but nevertheless similar to the electronic feedings used at low frequency, also because of their easy regulation.

Another disadvantage is the increased influence of stray capacitances among the parts of the multiplier and the consequent occurrence of stray currents along the cascade columns of the multiplier. It has to be remarked that this circumstance practically prevents the use of the conventional multiplying scheme when the number of stages is very large.

However, since it is possible to use parts easily obtained on the ordinary market at a comparatively low price, the use of high frequency becomes advisable for constructing a tube accelerating the ions up to the energy of some hundred keV. Apart from economical reasons, this is indeed possible because a perfect stabilization is obtained with rather simple circuits.

With the aim in view of using a source of monoenergetic neutrons either for research or for teaching purposes, a cheap, small deuteron accelerator has been constructed in this Institute.

2. - The voltage generator.

The usual layout of the voltage multiplying circuit is not very suitable when the feeding frequency is high. This, as already pointed out, is in particular due to the existence of stray currents which bring about a voltage decrease even when one has no load current.

The Everhart and Lorrain theory ⁽⁴⁾ leads to the following formula for the voltage efficiency F :

$$(1) \quad F = \frac{b}{N} \operatorname{tgh} \frac{N}{b},$$

where N is the number of stages in the multiplying circuit and b^2 is the ratio between the real capacitance for the stage C_s and the stray capacitance for the stage C , so that the output voltage effectively obtainable is the ideal voltage multiplied by F .

Several methods have been suggested for increasing the factor F . Particularly interesting is the method consisting in load inductances put at the low and high voltage terminals of the multiplying circuit ⁽⁵⁾. The one at low voltage is nothing but the secondary winding of the input transformer earthed in the middle. Correspondingly the utilizing current is derived from the middle of the high voltage inductance.

⁽⁴⁾ E. EVERHART and P. LORRAIN: *Rev. Sci. Instr.*, **24**, 221 (1953).

⁽⁵⁾ See ref. ⁽⁴⁾.

Such a symmetric method gives two evident advantages: it halves the voltage in the circuit of the input transformer and eliminates the ripple due to stray currents. The ripple due the load can also be reduced by tentatively shifting the high voltage connections to the corresponding inductance. In this case, the voltage efficiency improves and its expression, as calculated by Everhart and Lorrain, is formally equal to eq. (1), provided that b/N is replaced by $2b/N$. In this case the optimum value of the load inductance Q_{opt} is equal to:

$$(2) \quad Q_{opt} = \frac{1}{\omega^2 b C} \coth \frac{N}{2b},$$

where ω represents the angular frequency of the current used.

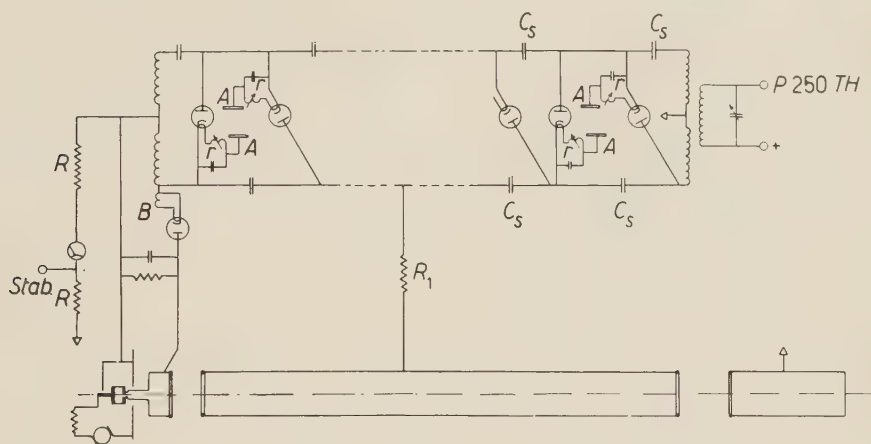


Fig. 1. — Electric scheme of the voltage generator.

The multiplying circuit of our generator, previously discussed, is of the symmetric type. Its layout is given in Fig. 1 and its electrical characteristics are listed in Table I.

TABLE I. — *Electrical characteristics of the multiplier used for the 200 KeV deuteron accelerator.*

Number of stages	20
Frequency	480 kHz
Capacitance of stage C_s	500 pF
Capacitance at the base of columns . .	1000 pF
Stray-capacitance for stage	1 pF
Peak input voltage	10 KV
Output voltage	200 KV
b	22.4
Voltage efficiency, F	0.94

The value chosen for the capacitances allows one to employ the normal capacitors used in television, while diodes EY 51 were chosen as rectifiers.

The use of these components gives, at the output, a working current of 0.5 mA, which is sufficient for the requirements of a normal accelerating tube.

The feeding of the multiplying circuit is supplied by a three-stage oscillator, using a 250 TH as output power tube, having the primary winding of the transformer in its anodic circuit.

The use of high frequency allows one to solve in a simple way the problem of feeding the diode filaments. As shown in Fig. 1, each filament is connected to a small resonance circuit (r), having a variable inductance connected to an antenna (A), crudely obtained from an equipotential ring of the multiplier column.

The variation of the inductance enables one to find out the most suitable intensity of the current for the required heating of the filaments.

A coil of a few turns, placed alongside the load inductance, heats an EY 51 diode which rectifies the e.m.f. obtained from suitable connections on the inductance. The rectified e.m.f. is then used for the extraction of the beam from the ion source.

To obtain a greater stability in the working of the multiplier a current of 100 μ A is continuously derived by means of an ohmic resistor (R), made up by 200 resistances of 10 Mohm each, and placed in a column of paraffin oil.

Using the decrease of voltage brought about by this resistor, a signal is derived for stabilizing the high voltage of the circuit. A stabilization of the output voltage of the order of 1% is possible provided this circuit is carefully constructed.

The feeding voltage for the lenses of the accelerating tube is derived, by means of a 20 Mohm resistance, from a link placed on one of the pulsating columns, in such a way as to give the best focusing of the beam. The RC system consisting of the resistance and the capacitance of the electrode is sufficient to equalize the radiofrequency on the electrode.

3. — The ion source and the accelerating tube.

Several types of ion sources have been carefully examined. The one which offers suitable characteristics as far as simplicity of construction and minimum of power is concerned, is the well known ⁽⁶⁾ Penning cold cathode type. The source used in the 200 keV deuteron accelerator is shown in Fig. 2. This source possesses aluminium cathodes (c), and a cylindrical anode (a), of graphite. The magnetic field is supplied by a permanent magnet (M), of alnico. The flux of deuterium comes from an electrolytic cell with automatic pressure regulation. The electric voltage for the discharge is supplied by a small converter with $(12 \div 800)$ V d.c., fed by a battery. This battery is used also for the various requirements concerned with a satisfactory working of

⁽⁶⁾ D. KAMKE: *Handb. d. Phys.*, Vol. XXXIII (Berlin, Göttingen, Heidelberg, 1956).

the accelerator. The only detail of this source which is somewhat unusual concerns the extraction of the beam which is transversal instead of axial and is performed through a hole in the cylindrical anode.

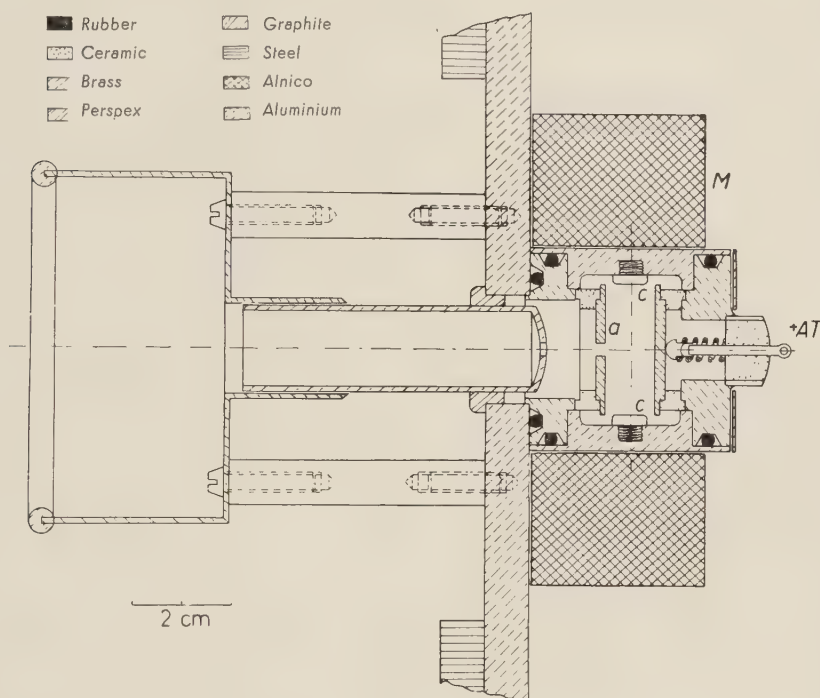


Fig. 2. — Penning ion source. Section parallel to the magnetic field.

The magnetic analysis of the beam, obtained with deuterium containing 0.5% of hydrogen has shown the following percentages for the most abundant components:

H_1^+	0.1%
D_1^+ and H_2^+	18 %
D_2^+ and H_2D^+	12 %
D_3^+	15 %
remainder	54.9%

The extraction was carried out by means of a cylindrical electrode fed with the voltage obtained by rectifying the H.V. existing on the load inductance as previously mentioned. This allows the introduction in the accelerating tube of a thin, cylindrical, slightly divergent beam of ions. The focusing and acceleration of the beam is obtained using two electrostatic and cylindrical

lenses (see Fig. 3) of the same diameter. The distance between the borders is 35 mm for the first lens and 70 mm for the second one. The beam is concentrated on the target having passed through a valve, placed in the accelerating tube in order to interrupt, when needed, the vacuum line, and through a shutter with an electromagnetic remote control.

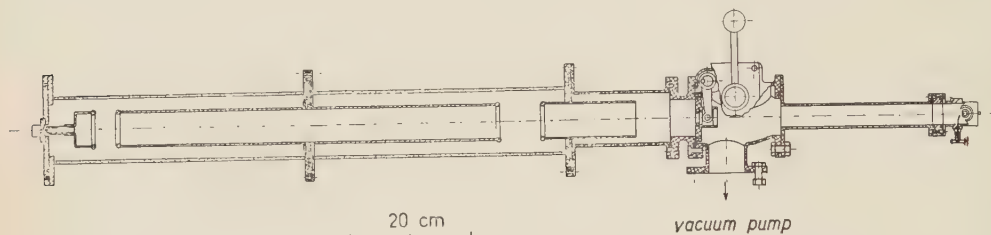


Fig. 3. - Accelerating tube.

The central cylinder of the two lenses is connected to its staff by means of regulating screws. In this way it is possible by subsequent adjustment to obtain the exact alignment of the lenses and the focusing of the beam on the target.

4. - General arrangement and accessories.

Since no sufficient room was available in height, the tube of the accelerator has been placed horizontally. The plan of this arrangement is shown in Fig. 4. The insulating staff columns of the accelerating tube and of the high voltage

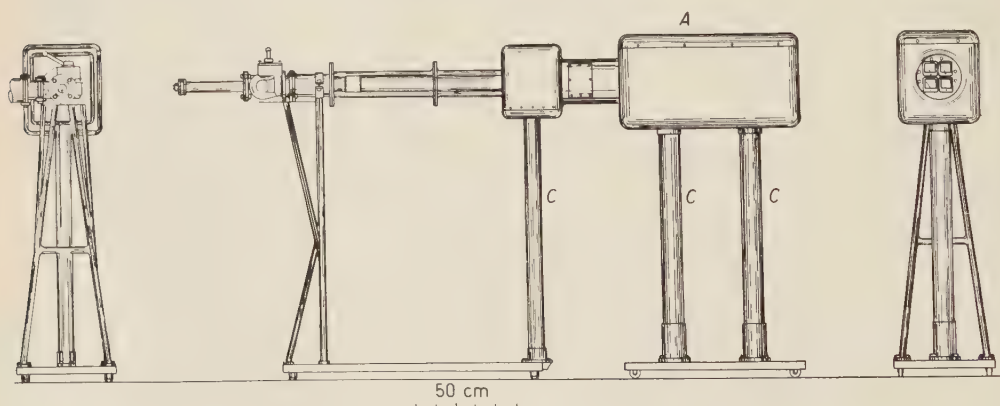


Fig. 4. - General layout of the accelerator.

screen (C) are made of perspex. Controls are carried out by means of perspex bars situated at the rear of the high voltage screen (A). On the same wall, in a suitable board mounted on the plate, are placed the control instruments concerning the source.

The vacuum plant consists in a 900 l oil diffusion pump, with a backing rotary pump. The pumping speed is sufficiently large in order to create within the tube, when the beam is on, a vacuum of $8 \cdot 10^{-6}$ mm Hg.

5. — Operational performances.

Satisfactory performance of the accelerator has been achieved during six months of continuous operation. It has been used essentially as a neutron generator by producing only d-d reactions. For this purpose, various kinds of targets have been examined, namely self targets constructed with different metals, a target of heavy ice and also a target with deuterium absorbed in zirconium. The best yield was found using the last kind of target. The neutron yield as a function of the deuteron accelerating voltage is represented in Fig. 5 (curve B). The absolute value of the yield has been derived by a comparison of a Ra-Be source, and measurements of neutron intensity have been performed with the long counter method.

In the same figure is reported the yield curve obtained by LADENBURG *et al.* ⁽⁷⁾ with a heavy ice target. Normalization has been carried out for a current of 10^{13} deuterons per second.

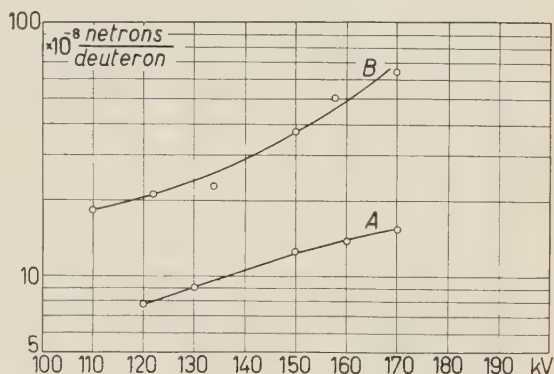


Fig. 5. — Neutron per deuteron yield as a function of the deuteron accelerating voltage. Curve B: our accelerator, deuterium in zirconium target. Curve A: yield of LADENBURG *et al.* ⁽⁷⁾ with a heavy ice target. Normalization is obtained for a current of 10^{13} deuterons s^{-1} .

⁽⁷⁾ R. LADENBURG and M. H. KANNER: *Phys. Rev.*, **52**, 911 (1937).

RIASSUNTO

Viene illustrato un acceleratore di deutoni da 200 keV, impiegato per la produzione di deutoni mediante la reazione d-d e d-t. Si sottolinea la caratteristica principale dell'acceleratore di avere l'alta tensione realizzata con un sistema a moltiplicazione di tensione a radiofrequenza.

A Wave-Length Shifter for Čerenkov Radiation in Water and Aqueous Lead Salt Solution.

K. SAITO and K. SUGA

Institute for Nuclear Study, University of Tokio - Tanashi, Tokio

(ricevuto il 3 Dicembre 1958)

Summary. — An increase factor of 4.4 in photomultiplier pulse-height was obtained by the use of pure amino G acid as a wave-length shifter for Čerenkov radiation in water. Further attempts were made to use this compound in an concentrated lead salt solution (1 M), and an increase factor of 1.8 was recorded, with the lead ion in the form of its ethylenediamine tetra-acetate (EDTA) complex.

1. — Introduction.

Only little information is available concerning wave-length shifters for Čerenkov radiation emitted in water. HEIBERG and MARSHAL⁽¹⁾ suggested the use of amino G salt (sodium 2-amino-6.8-naphthalenedisulphonate) and recorded a photomultiplier pulse-height increase by a factor 1.3. PORTER studied the use of β -methylumbelliferone and recorded an increase factor of 2.0⁽²⁾.

The present authors were of the opinion that an improvement of the increase factor would be expected by a closer study with reference to the purity of amino G acid, the optical properties of this solution in water, the pH and the concentration. Therefore, after examination of the optical properties of the solution under various conditions, a test for increase in pulse-height was made with a photomultiplier and an increase factor of 4.4 was obtained under the optimum condition.

Attempts were further made to utilise this compound in a concentrated lead salt solution which is used for a total-absorption Čerenkov detector⁽³⁾.

⁽¹⁾ E. HEIBERG and J. MARSHAL: *Rev. Sci. Instr.*, **27**, 618 (1956).

⁽²⁾ N. A. PORTER: *Nuovo Cimento*, **5**, 526 (1957).

⁽³⁾ T. MATANO, I. MIURA, M. ODA, K. SUGA, G. TANAHASHI and Y. TANAKA: *I.N.S.J.*, **9** (1958) (Institute for Nuclear Study, University of Tokyo).

Although the presence of heavy metal ions decreases the intensity of fluorescence, the effect of the lead ion will be masked to a certain extent by conversion into a suitable complex compound, such as ethylenediaminetetraacetate (EDTA). In this case an increase factor of 1.8 was recorded in a 1 M lead salt solution.

2. - Experimental methods.

2.1. *Materials.* - Commercial amino G acid was recrystallized from an aqueous solution in the presence of activated charcoal. The absorption maximum and the molar extinction coefficient were in good agreement with those in the literature. Further purification did not result in an increase of the intensity of fluorescence (see Fig. 1).

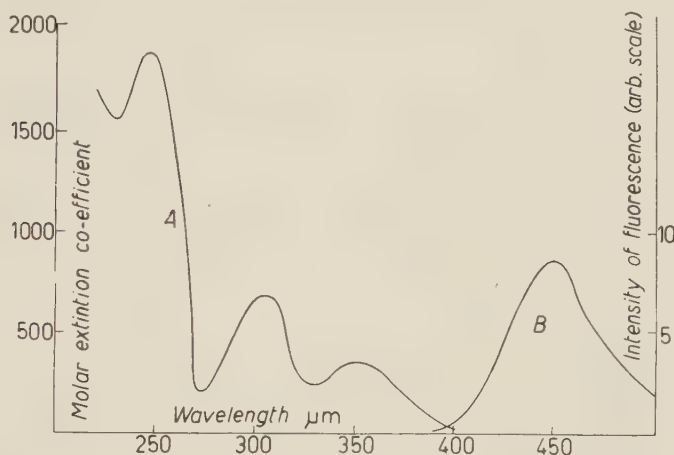


Fig. 1. - Absorption (curve A) and fluorescence (curve B) spectrum of amino G acid in water.

Lead EDTA complex was prepared from known equivalent amounts of lead hydroxide and disodium salt of EDTA. The acid-form complex (H_2PbY , $Y = \text{EDTA radical } C_{10}H_{12}O_8N_4$) was precipitated with perchloric acid and acetone, washed with a mixture of acetone and water and then with acetone, and filtered off. The product was dissolved in sodium hydroxide or aqueous ammonia solution to produce the 1 M solution (*e.g.* 250 ml) of its disodium or diammonium salt. It was essential to prepare as pure a compound as possible for a good result to be obtained.

For the fundamental test of optical properties of the amino G acid solution, the pH value was adjusted with an acetate buffer (0.2 M) and the ionic strength with sodium nitrate.

2.2. *Measurements.* - The pH value was measured with a glass-electrode pH-meter. The absorption and the fluorescence spectra were measured with

a Beckmann-type spectrophotometer (made by Hitachi Co.) with appropriate accessories.

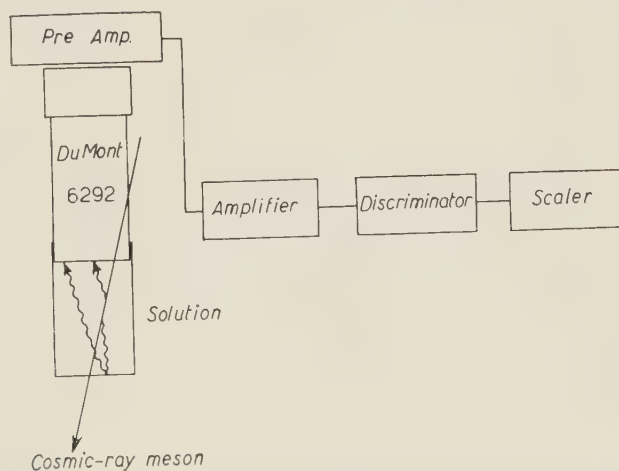


Fig. 2. - Arrangement for the measurement of the photomultiplier pulse-height.

The increase factor of the light output was measured with the aid of cosmic-ray mesons, by the use of an arrangement shown in Fig. 2. The aqueous solution of amino G acid with or without lead EDTA complex was placed in cylinder

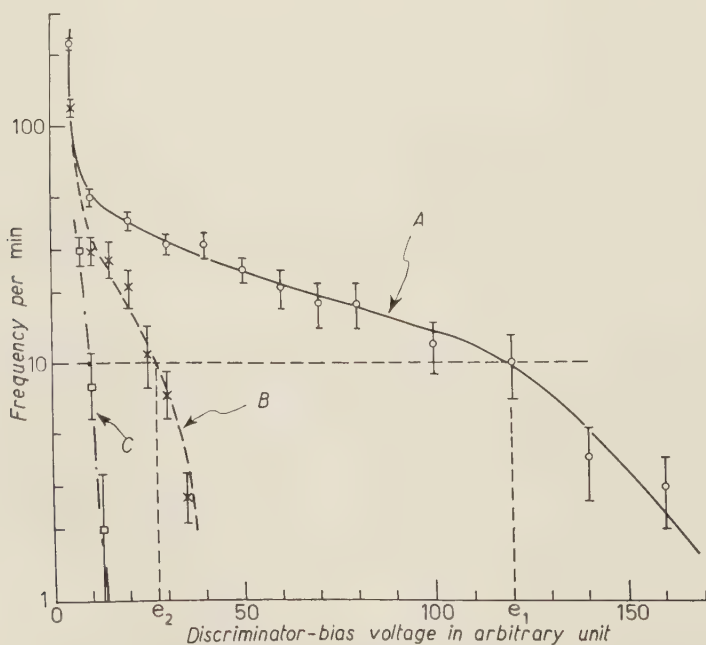


Fig. 3. - Frequency vs. discriminator-bias diagram. Curve A for aqueous solution of pure amino G acid; B for distilled water; C, noise of the photomultiplier.

(diameter 5.5 cm, length 7.5 cm) lined with titanium-white reflective paint, to optically couple with the photomultiplier (DuMont 6292). The photomultiplier output voltage pulse, with a time constant of $10\ \mu\text{s}$, was amplified by a conventional amplifier, and the pulse-height was analysed with a discriminator. Fig. 3 shows the frequency *vs.* discriminator-bias diagram. Curve *A* was obtained with aqueous solution of amino-G-acid and curve *B* with pure water, the increase factor being represented by the ratio e_1/e_2 .

3. - Results and discussion.

3.1. Use of amino-G-acid in water. - The intensity of fluorescence of this acid markedly decreases at a pH more than nine and less than unity, the shape of the spectrum remaining unchanged. The intensity also decreases with increasing ionic strength, as shown in Fig. 4. The intensity depends on the concentration of this acid, the optimum concentration varying with the ionic strength as shown in Fig. 5.

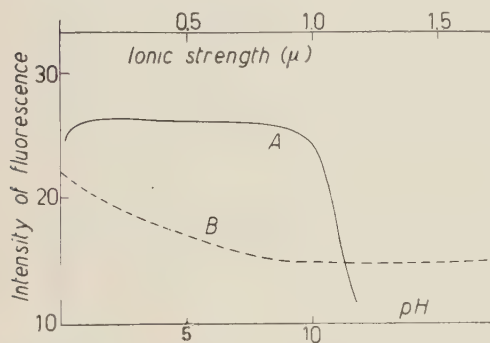


Fig. 4. - Change in intensity (arbitrary scale) of fluorescence with the pH (curve *A*) and the ionic strength (curve *B*) of the aqueous solution.

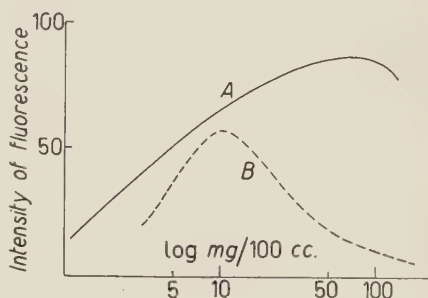


Fig. 5. - Change in intensity (arbitrary scale) of the fluorescence with the concentration of amino G acid in water (curve *A*) and in an aqueous solution of $\mu = 1$ (curve *B*).

Aqueous solution of amino-G-acid (a few hundred milligrams per litre) has a pH value near 3 and can be used as wave-length shifter without buffer. The maximum increase factor amounts to 4.4 in the absence of dissolved oxygen; the extent to which the pulse-height increases is largely affected by oxygen. The results are summarized in Table I. The pulse-height decreases on prolonged storage, presumably owing to dissolution of atmospheric oxygen; the deteriorated solution does not recover the initial activity even after the removal of dissolved oxygen. When kept sealed, however, the solution maintains its activity for months.

3.2. Use of amino-G-acid in the presence of a large amount of lead. - For the aqueous amino-G-acid solution to be used as a total-absorption Čerenkov detector, a large amount of lead should be present in water to increase the

radiation length of the material. Although the lead ion quenches the fluorescence of this acid to a marked extent, this action is suppressed by converting the lead ion into stable lead EDTA complex. Since the degree of dissociation of the complex decreases with increasing pH, the aqueous solution is made at pH 8 (with aqueous ammonia or sodium hydroxide), where amino-

TABLE I. - *Increase factor under various conditions.*

Solution	Increase factor	Condition
water + amino G acid	4.4	with nitrogen bubbling
water + amino G acid	1.7	after 3 months' storage
water + amino G acid	2.3	without nitrogen bubbling
water + amino G acid + $(\text{NH}_4)_2\text{PbY}$	1.8	with nitrogen bubbling
water + amino G acid + Na_2PbY	1.5	with nitrogen bubbling
water + amino G acid + Na_2PbY	1.2	without nitrogen bubbling
water (standard)	1.0	distilled water
Concentration of amino G acid, 200 mg per litre; concentration of the lead salt, ca. 1 M; Y stands for ethylenediaminetetraacetate radical.		

G-acid still exhibits an intense fluorescence (see Fig. 4). The results shown in Table I indicate that the increase factor (1.8 with ammonium salt and 1.5 with sodium salt) is not so great as in the absence of lead, but it is quite significant and very useful for practical purposes.

3.3. *The verification of the role of amino-G-acid as a wave-length shifter and the decay time.* - Although the amount of the direct fluorescence is expected to be very small from the slight amount of this acid in water, its participation was measured in the following procedure. A very intense source of ^{210}Po , free from its parent activity (*), was added to the solution and the light emitted by this solution was similarly measured. It was found that the amount of direct scintillation light is less than a few percent of the total light from the

(*) Carrier-free ^{210}Po was distilled from 0.1 N nitric acid solution of RaD in the presence of diphenylcarbazide (4), into 1 N hydrochloric acid, which was, after distillation, evaporated with a small amount of hydrogen peroxide,

(4) K. KIMURA and H. MABUCHI: *Bull. Chem. Soc. Japan*, **28**, 535 (1955).

solution. Therefore, though the detector involving the use of amino-G-acid loses the directional property, it preserves the role of a velocity discriminator.

Further examination was made to find whether such a detector is suitable for fast detection of particles. The current pulse of the photomultiplier which received the light from the solution was displayed on a Tektronics 545 synchroscope. The decay time was estimated to be less than $2 \cdot 10^{-8}$ s. The real value of the decay time was not determined from the above procedure, but the solution is suitable for fast detection of particles.

RIASSUNTO (*)

Usando G-aminoacido puro per spostare la lunghezza d'onda si è ottenuto l'aumento per un fattore di 4.4 della radiazione Čerenkov nell'acqua. In ulteriori tentativi di usare detto composto sotto forma di una soluzione concentrata del suo sale di piombo (I M) si è registrato un aumento per un fattore 1.8, collo ione piombo in forma del suo complesso etilendiamminatetracetato (EDTA).

(*) Traduzione a cura della Redazione.

LETTERE ALLA REDAZIONE

(La responsabilità scientifica degli scritti inseriti in questa rubrica è completamente lasciata dalla Direzione del periodico ai singoli autori)

Associated Production by Non-Local Interaction.

S. N. BISWAS (*)

*Department of Theoretical Physics,
Indian Association for the Cultivation of Science - Calcutta*

(ricevuto il 14 Luglio 1958)

The observed associated production of the K-mesons and Λ -hyperons from the meson-nucleon interaction in $T=\frac{1}{2}$ state may be obtained from the following two Feynman diagrams.

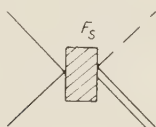


Fig. 1

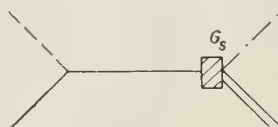


Fig. 2

—— nucleon line. -·-·- K-meson line.
····· meson line. === hyperon line.

In the above diagrams the shaded area G_s in Fig. 1 denotes the 3-body non-local (N-K- Λ) interaction and F_s in Fig. 2 indicates a direct 4-body non-local (π -N-K- Λ) interaction.

One way of introducing the above 3 and 4-body non-local interaction is to assume a compound hypothesis for K-mesons and Λ -hyperons and accordingly suggest that the K-meson may be an excited bound state of two pions and the Λ -hyperon is composed of a nucleon and a pion. In a recent paper ⁽¹⁾ the present author has introduced such a composite model for K-mesons and on the basis of the solution all the observed phenomena including that of associated production could well be explained. Similar conclusions were also obtained from the meson-nucleon compound system for the hyperon introduced first by FERMI, FEYNMAN, GREEN and from detailed

(*) Now at Tata Institute for Fundamental Research, Bombay.

(1) S. N. BISWAS: *Nuovo Cimento*, **7**, 577 (1958).

calculations by MACCARTHY⁽²⁾. The nature of the wave function for the composite model suggests that one may also assume the particle as elementary, having a structural co-ordinate as suggested by YUKAWA⁽³⁾ for other elementary particles. It should be mentioned that the model suggested here is not the only one of its kind; one can also use Sakata's interesting compound model⁽⁴⁾.

Assuming pure pseudoscalar meson-nucleon interaction we will find the nature of the interaction G_s and F_s and it turns out that G_s and F_s are non-local but covariant depending upon the four-momenta of the interacting particles and are also spin dependent. The existence of a spin-dependent term shows that the K-particle may be produced in parity-mixture states. In the extreme relativistic region, however, the spin-dependent term disappears but the interaction still remains non-local.

In the following we will calculate G_s from the following simplest Feynman diagram assuming strangeness conservation as well as charge conservation.

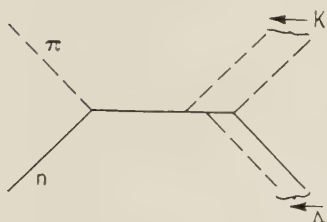


Fig. 3

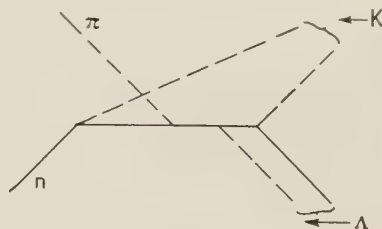


Fig. 4

It should be pointed out that the explicit determination of G_s requires a knowledge of the internal structure of both the K and Λ -particle. As a trial function we introduce the momentum distribution of the form

$$N\theta(l) = N'\Lambda(l) = \{l^4 - \mu^4\}^{-1},$$

for θ - and Λ -particles; l is the variable four-momentum of the particle concerned, μ is the meson mass, and N, N' are the normalization constants. Following Feynman we have from Fig. 3 for G_s ,

$$(1) \quad G_s = G^3 \{ (2\pi)^4 i \}^{-2} \iint \tau_3 \gamma_5 S(2p - q - p_1) \tau_k \gamma_5 S(p - p_1 - r) \tau_1 \gamma_5 \theta(2p_1) \Lambda(2r) d^4 p_1 d^4 r,$$

where G is the ordinary pion-nucleon coupling constant, τ 's are as usual the isotopic spin-matrices and $S(p)$ stands for the nucleon propagator $2p - k, 2p - 2q, k$ and $2q$ are the four-momenta of the nucleon, hyperon, pion and K-meson respectively.

The determination of the normalization constants N and N' can be effected by noting that the equation satisfied by (1) has the form

$$\varphi(k) = \lambda' \int K(k, l) \varphi(l) d^4 l,$$

(2) I. E. MACCARTHY: *Ph. D. Thesis* (Adelaide University, 1955; unpublished).

(3) H. YUKAWA: *Phys. Rev.*, **77**, 219 (1956).

(4) S. SAKATA: *Progr. Theor. Phys.*, **16**, 686 (1950).

with

$$K(k, l) = (k^4 - \mu^4)^{-1}(l^4 - \mu^4)^{-1} \quad \text{and} \quad \frac{i\lambda'}{(2\pi)^4} \int (l^4 - \mu^4)^{-2} d^4l = 1,$$

and using the normalization condition ⁽¹⁾ for the wave equation, we have from (1)

$$(2) \quad G_s \rightarrow f\gamma_5(A + Bp_\mu\gamma^\mu),$$

with

$$f = \tau_f \tau_k \tau_l (2M_\theta M_\Lambda G^3) / (2\pi)(r_1 r_2)^2; \quad r_1 = M_\theta/\mu, \quad r_2 = M_\Lambda/\mu,$$

M_θ and M_Λ are the K-meson and Λ -hyperon mass respectively.

$$A = \{p \cdot q - 5p^2/4\}/(2p)^4 + \frac{1}{4}m(M_\Lambda - m)/(2p)^4, \quad \text{and} \quad B = \frac{1}{4}M_\Lambda(2p)^{-4}.$$

The result (2) shows that the interaction G_s is non-local depending on the momentum of the interacting particles. The interaction is thus in general a mixture of (ps) scalar and (pv) vector-type fields. If, however, we make an extreme relativistic approximation by neglecting the masses of the nucleon and hyperon compared to the high incident energy of the meson the interaction is purely pseudoscalar but non-local. The appearance of the scalar and the spin-dependent terms shows that the K-meson may be produced with even or odd integer spin. That is to say that the K-meson is produced in a parity-mixture state. The same may be true of the Λ -particle. We have at the extreme relativistic energy the production cross section of the θ -particle using the diagram of Fig. 1 having a pure pseudoscalar interaction of the type $fA\gamma_5$:

$$(3) \quad \sigma = \frac{2r_0^2 G^8}{\pi\omega_1^2} \left\{ \frac{4}{3} \left(\frac{\omega_2}{\omega_1} \right)^4 - \frac{5}{2} \left(\frac{\omega_2}{\omega_1} \right)^3 + \frac{25}{16} \left(\frac{\omega_2}{\omega_1} \right)^2 \right\},$$

where $r_0 = (M_\theta M_\Lambda) / (\omega_1^2 r_1^2 r_2^2)$.

ω_1 and ω_2 are the incident pion and final K-meson energies respectively. For a 1.4 GeV incident pion and using the pseudoscalar pion-nucleon coupling constant $G^2 \approx 12$ we have the total production cross section,

$$\sigma = .7264 \cdot 10^{-27} \text{ cm}^2,$$

the experimentally determined value being ≈ 1 mb.

A similar calculation can be made for F_s from the Feynman diagram Fig. 4: the conclusions are on similar lines. A detailed calculation involving all possible Feynman diagrams for the associated production of the strange particles will soon be reported.

* * *

The author is grateful to Prof. BASU for giving him the opportunity to work in his department and for discussion from time to time. He is also grateful to Prof. H. S. GREEN for a stimulating discussion on strange particles while the author was a Research Fellow of the Adelaide University during 1956-57.

Neutron Capture Gamma-Rays of Iodine, Iridium and Cerium.

R. BALZER, H. KNOEPFEL, J. LANG, R. MÜLLER and P. STOLL

Federal Institute of Technology - Zürich

(ricevuto il 10 Novembre 1958)

We have investigated (n, γ) -spectra of several elements at the Swimmingpool-Reactor «Saphir» in Würenlingen ⁽¹⁾. For the energy range above 3 MeV a pair-spectrometer of high intensity was used ⁽²⁾. The γ -rays below 3 MeV were determined by a gray wedge spectrometer ⁽³⁾.

1. — Measurements with the pair-spectrometer.

1.1. *Iodine*. — The upper part of the measured spectrum (deduced background and random coincidences) of the reaction $^{127}\text{I}(n, \gamma)^{128}\text{I}$ is shown in Fig. 1. The

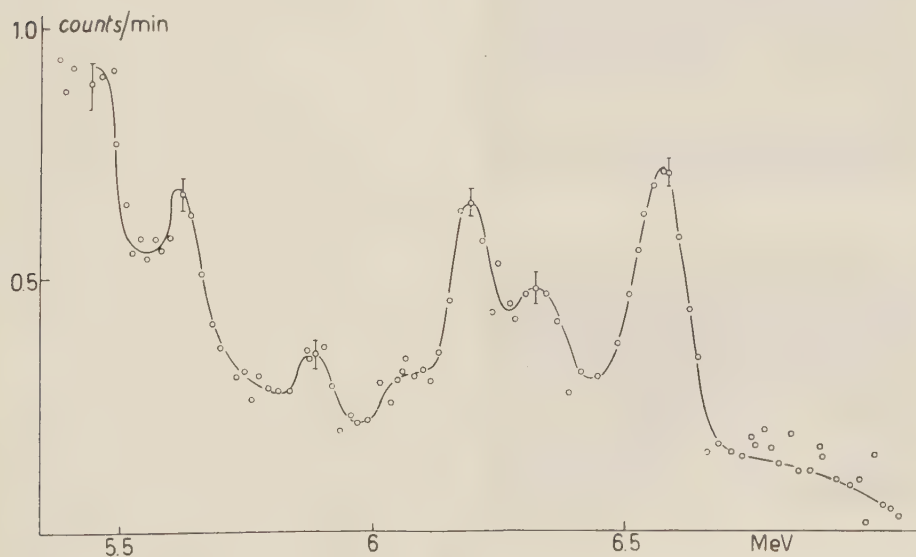


Fig. 1.

⁽¹⁾ H. KNOEPFEL, CH. MENOUD and P. STOLL: *Helv. Phys. Acta*, **31**, 339 (1958).

⁽²⁾ R. BALZER, H. KNOEPFEL, P. STOLL and W. WÜLFELI: *Helv. Phys. Acta*, **31**, 328 (1958).

⁽³⁾ D. MAEDER: *Nucl. Instr.*, **2**, 299 (1958).

ordinates are reduced to « weight one », that means, that depending on the counting channel, we actually have measured 5 to 9 times more counts per minutes as given in the figure. The target consisted of 1.5 kg of pure Iodine enclosed in a polyethylene container. The spectrum was evaluated by resolving it to single lines ⁽⁴⁾, the shape of which has been determined experimentally with Fe, Ti and Ni-lines. We found γ -rays with following energies:

- | | |
|--|---------------------------|
| a) (6.71 ± 0.02) MeV (neutron binding energy); | |
| b) (6.45 ± 0.03) MeV; | e) (6.29 ± 0.03) MeV; |
| d) (6.16 ± 0.04) MeV (?); | e) (5.99 ± 0.03) MeV; |
| f) (5.75 ± 0.03) MeV; | g) (5.57 ± 0.03) MeV. |

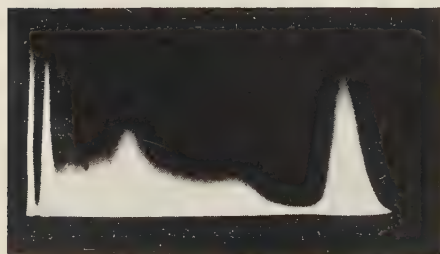
1'2. *Iridium*. — The measurement was performed with 40 g of pure Iridium (Isotopes: ¹⁹¹Ir and ¹⁹³Ir). The counting rate was higher than for the Iodine probe and therefore the statistic better. The mean width of the lines is 110 keV. For the natural isotope mixture we have measured the following γ -ray energies of ¹⁹²Ir and ¹⁹¹Ir:

- | | | |
|-------------------------------|---------------------------|-------------------------------|
| a) (6.085 ± 0.015) MeV; | b) (5.98 ± 0.02) MeV; | c) (5.92 ± 0.03) MeV; |
| d) (5.77 ± 0.03) MeV; | e) (5.67 ± 0.03) MeV; | f) (5.59 ± 0.04) MeV (?); |
| g) (5.48 ± 0.04) MeV (?); | h) (5.34 ± 0.03) MeV. | |

Cerium



Cs (calibration)



0 200 400 600 800
 +-----+-----+-----+-----+
 Energy in keV

Fig. 2.

2. — Measurements with the gray wedge spectrometer.

2'1. *Cerium*. — Fig. 2 shows a photograph of the Ce(n, γ)-spectrum, as it was taken with our crystal-spectrometer. For comparison and calibration the Cesium spectrum is also shown. Our results are:

- (1170 ± 20) keV,
- (940 ± 20) keV,
- (671 ± 10) keV,
- (504 ± 10) keV (annihilation),
- (344 ± 8) keV,
- (277 ± 8) keV,
- (217 ± 6) keV,
- (88 ± 6) keV,
- (72 ± 4) keV (Pb + Bi, X-ray?),
- (38 ± 3) keV (Ce, X-ray?).

⁽⁴⁾ B. B. KINSEY, and G. A. BARTHOLOMEV: *Can. Journ. of Phys.*, **31**, 537 (1953).

2.2. *Iodine*. — This element has been measured for low energies by other authors ^(5,6), but their results are contradictory. We found the following γ -rays:

(652 ± 20) keV,	(501 ± 10) keV (annihilation),
(435 ± 15) keV,	(260 ± 15) keV,
(130 ± 10) keV,	(75 ± 8) keV (Pb+Bi, X-rays).

We confirm the 130 keV line, but concerning the intensity, this line is not stronger as the one of 260 keV, in contradiction with ⁽⁶⁾. We can not find the 85 keV γ -ray ⁽⁵⁾, because it is covered by the X-ray of Pb and Bi (from the collimator). The new lines at 435 keV and 652 keV are probably due to inelastic neutron scattering, as measured by ⁽⁷⁾, because of the still high epithermal neutron flux in the target region (cfr. ⁽¹⁾).

The discussion about the measured spectra and the absolute intensities of the different lines follows together with the description of the γ pair-spectrometer in a later publication.

⁽⁵⁾ M. REIER and M. G. SHAMOS: *Phys. Rev.*, **100**, 1302 (1955).

⁽⁶⁾ I. V. ESTULIN, L. F. KALINKIN and A. S. MELIORANSKY: *Nucl. Phys.*, **4**, 91 (1957), *Soviet Phys. Journ. Exp. Theor. Phys.*, **4**, 752 (1957).

⁽⁷⁾ D. A. LIND, R. B. DAY and R. M. KLOEPPER: *Bull. Am. Phys. Soc.*, **2**, no. 6, 309, H 5.

A Possible Parity Assignment for Strange Particles and a New Kind of Heavy Meson.

H. KATSUMORI

Department of Physics, Osaka Gakuhei University - Osaka

(ricevuto il 14 Gennaio 1959)

The possibility was suggested, in our previous report ⁽¹⁾, that the observed level ordering of baryon masses can be explained in the lowest order approximation, assigning the opposite parities between N and Ξ (case (a)), or the opposite parities between Λ and Σ as well as between N and Ξ (case (b)). It was assumed that the baryons are Dirac particles and the K -meson is a spinless particle, and the interaction Lagrangian is given by D'ESPAGNAT and PRENTKI's charge independent interaction ⁽²⁾ with common coupling constants g_K and g_π for K - and π -couplings respectively.

It goes without saying that there is another possibility to explain the baryon mass levels apart from such a parity assignment, assuming different coupling constants for the different interaction terms instead of the common g_K and the common g_π . Since only the first approximation starting with an hypothetical world, where the strong interactions are absent, has been considered in our previous and the present reports, all the K - and π -coupling constants are assumed to be equal to the unrenormalized g_K and g_π respectively, and moreover the masses of all baryons appearing in the real and virtual states are assumed to equal the unrenormalized (degenerate) baryon mass.

It has been further shown ⁽³⁾ that the numerical estimate, of the baryon mass levels according to our proposal, is not inconsistent with the observation, when the reasonable magnitudes of coupling constant g_K and of cut-off momentum are used. It should be noted that the correct direction of level splittings $\Xi - (\Sigma, \Lambda) - N$ and the approximately correct interval ratio $[M(\Xi) - M(\Sigma, \Lambda)]/[M(\Sigma, \Lambda) - M(N)] = 1$ are obtained from only the K -coupling assuming the above parity assignment (a) or (b), and these features are independent of the magnitude of cut-off momentum. However, as to the numerical estimate of the Σ - Λ mass difference for case (b), the consistency is not so good and therefore it is difficult to know whether the Σ - Λ mass

⁽¹⁾ H. KATSUMORI: *Memoirs of the Osaka Gakuhei Univ.*, B, no. 6, 48 (1957); *Progr. Theor. Phys. (Japan)*, **19**, 342 (1958).

⁽²⁾ B. D'ESPAGNAT and J. PRENTKI: *Nucl. Phys.*, **1**, 33 (1956).

⁽³⁾ H. KATSUMORI and K. SHIMOURA: *Progr. Theor. Phys. (Japan)*, **20**, 578 (1958).

difference comes mainly from the lowest order effect of π -coupling or from the higher order effect of K-coupling or from both. In spite of such ambiguousness, the assignment (b) seems to be favorable, because the lowest order self energies for the case (b) give the level splittings $M(\Sigma) - M(\Lambda)$ as well as $M(\Xi) - M(N)$ with the correct directions. This calculation has been carried out using the d'Espagnat and Prentki interactions for the case (b),

$$(1) \quad L_K = g_K [\bar{N} \boldsymbol{\tau} \cdot \boldsymbol{\Sigma} K + \bar{N} (i\gamma_5) \Lambda K + \bar{\Xi} (i\gamma_5) \tau_2 \boldsymbol{\tau} \cdot \boldsymbol{\Sigma} K^* + \bar{\Xi} \tau_2 \Lambda K^*] + \text{H. C.},$$

$$(2) \quad L_\pi = g_\pi [\bar{N} (i\gamma_5) \boldsymbol{\tau} \cdot \boldsymbol{\pi} N + \bar{\Xi} (i\gamma_5) \boldsymbol{\tau} \cdot \boldsymbol{\pi} \Xi + (i \boldsymbol{\Sigma} (i\gamma_5) \times \boldsymbol{\Sigma}) \cdot \boldsymbol{\pi} + (\bar{\Lambda} \boldsymbol{\Sigma} \cdot \boldsymbol{\pi} + \text{H. C.})].$$

The validity of this type of interactions, especially L_K , ought to be experimentally tested in the future by the baryon-K scattering or the hyperon production (*).

Now it should be interesting to conjecture why both the relative parity between N and Ξ and that between Λ and Σ happen to be odd. As has been pointed out by TIOMNO and YANG (4), there are four kinds of spinor transformation under space reflection,

$$(3) \quad \psi \rightarrow \eta_R \gamma_4 \psi, \quad \eta_R = \pm i, \quad \pm 1.$$

Then it seems tempting to speculate that each type of the spinor fields should have an equal right for existence in the natural world and that the four kinds η_R 's ($\pm i, \pm 1$) just correspond to the «four» kinds of existing baryons which would degenerate in the limit of vanishing strong interaction. According to this conjecture, the following is the desired parity assignment,

$$(4) \quad \begin{cases} \eta_R = \pm i & \text{for } (N, \Xi), & \pm i & \text{for } (N^c, \Xi^c) \\ \eta_R = \pm 1 & \text{for } (\Lambda, \Sigma), & \mp 1 & \text{for } (\Lambda^c, \Sigma^c) \end{cases}$$

or

$$(4') \quad \begin{cases} \eta_R = \pm 1 & \text{for } (N, \Xi), & \mp 1 & \text{for } (N^c, \Xi^c) \\ \eta_R = \pm i & \text{for } (\Lambda, \Sigma), & \pm i & \text{for } (\Lambda^c, \Sigma^c) \end{cases}$$

where a superscript C indicates the charge conjugate of the corresponding baryon. In the interaction Lagrangian L_K , (1), it was assumed that all the baryon fields have either $\eta_R = \pm 1$ or $\pm i$, and therefore the K-meson field transforms as $K \rightarrow \pm K$ under space reflection. On the contrary, if the parity assignment (4) or (4') is taken, the transformation $K \rightarrow \pm iK$ under space reflection must be assumed. When this parity assignment is used, one has to introduce a new kind of heavy meson field, which is called as K' hereafter, in order that our previous argument on the mass level splitting similarly applies. The K' field is introduced as a second kind isospinor and couples with Ξ (but not with N), while the K field is a first kind isospinor and couples with N (but not with Ξ). The assumption is made that $K'^{(-,0)}$ and $K^{C(-,0)}$ (therefore $K'^{C(+,0)}$ and $K^{(+,0)}$) are not the same particles but have opposite parities.

(4) C. N. YANG and J. TIOMNO: *Phys. Rev.*, **79**, 495 (1950).

(*) After this report has been written, S. BARSHAY's recent article [*Phys. Rev. Lett.*, **1**, 97 (1958)] has reached us. He points out that the analysis of hyperon production and K-N scattering experiments may give an indirect support not only for the opposite parities between Λ and Σ but also for the coupling types of (ΛNK) , (ΣNK) and $(\Sigma \Lambda \pi)$ interactions in our equations (1) and (2).

In the following the assignment (4) is chosen instead of (4'), since (4') leads to the same space parity (η_R) and the same isospace parity (η_I)⁽⁵⁾ for N and Ξ^c (therefore also for N^c and Ξ). As it is a matter of convention whether $\eta_R = \pm 1$ or ∓ 1 is chosen for Σ and Λ (therefore $\eta_R = \pm i$ or $\mp i$ for K, K' and K^c , K'^c), the former one is chosen here. η_R for bosons is defined by the transformation $\varphi \rightarrow \eta_R \varphi$ under space reflection. The thus specified parities for all the baryons and all the mesons are listed in Table I (*). For the sake of comparison, the isoparity η_I which is defined by the transformations $\psi \rightarrow \eta_I \psi$ and $\varphi \rightarrow \eta_I \varphi$ under isospace reflection is also added in the table. This table seems to suggest a close connection between ordinary space parity and isoparity. Furthermore the charge singlet pion field (π') is included in the table, which was never detected experimentally but its existence was proposed by several authors^(c-s). It seems interesting to note that, if a scalar π' is introduced, the four kinds of mesons π , π' , K and K'^c correspond to the four possible η_R 's (± 1 , $\pm i$) for the bosons just like for the baryons.

TABLE I.

	η_R	η_I		η_R	η_I
$N^{(+,0)}$	i	i	$N^{c(-,0)}$	i	$-i$
$\Xi^{(-,0)}$	$-i$	$-i$	$\Xi^{c(+,0)}$	$-i$	i
$\Sigma^{(+,0,-)}$	1	1	$\Xi^{c(-,0,+)}$	-1	1
$\Lambda^{(0)}$	-1	1	$\Lambda^{c(0)}$	1	1
$\pi^{(+,0,-)}$	-1	1	$\pi^{c(-,0,+)}$	-1	1
$(\pi'^{(0)})$	(1)	(1)	$(\pi'^{c(0)})$	(1)	(1)
$K^{(+,0)}$	i	i	$K^{c(-,0)}$	$-i$	$-i$
$K'^{(-,0)}$	i	$-i$	$K'^{c(+,0)}$	$-i$	i

Now the parity conserving interaction Lagrangian L_K is written as

$$(5) \quad L_K = g_K [\bar{N} \boldsymbol{\tau} \cdot \boldsymbol{\Sigma} K + \bar{N} (i\gamma_5) \Lambda K + \bar{\Xi} (i\gamma_5) \boldsymbol{\tau} \cdot \boldsymbol{\Sigma} K' + \bar{\Xi} \Lambda K'] + \text{H. C.},$$

which also gives us a similar mass splitting as before. Within the Yukawa type baryon-meson direct interaction, the charge independence and parity conservation would lead to additional interaction terms like

$$g_K [\bar{N} \tau_2 \Lambda K'^* + \bar{N} (i\gamma_5) \tau_2 \boldsymbol{\tau} \cdot \boldsymbol{\Sigma} K'^* + \bar{\Xi} (i\gamma_5) \tau_2 \Lambda K^* + \bar{\Xi} \tau_2 \boldsymbol{\tau} \cdot \boldsymbol{\Sigma} K^*] + \text{H. C.}.$$

(5) G. RACAH: *Nucl. Phys.*, **1**, 302 (1956).

(*) After this report has been written, F. GÜRSEY's recent article [*Phys. Rev. Lett.*, **1**, 98 (1958)] has reached us. He has discussed a connection between strangeness and parity, assuming a parity assignment similar to that we have used here. The coupling type of his Lagrangian L_K is, however, different from ours at the $(\Xi \Sigma K)$ and $(\Xi \Lambda K)$ terms, and it does not lead to the N- Ξ mass splitting as far as the common g_K is used and unless the K' field is introduced.

(6) M. GELL-MANN: *Phys. Rev.*, **106**, 1296 (1957).

(7) Y. NAMBU: *Phys. Rev.*, **103**, 1366 (1957).

(8) J. SCHWINGER: *Ann. of Phys.*, **2**, 407 (1957).

These terms, however, contradict the foregoing assumption that N does not couple with K' , and Ξ does not couple with K . The above description may be written as a symmetrical form of a 4-dimensional isospace. If 4-isospinors and 4-isovectors are defined by

$$(6) \quad \Psi = \begin{pmatrix} N^+ \\ N^0 \\ i\gamma_5 \Xi^0 \\ i\gamma_5 \Xi^- \end{pmatrix}, \quad \mathcal{K} = \begin{pmatrix} K^+ \\ K^0 \\ K'^0 \\ K'^- \end{pmatrix},$$

and

$$\Sigma_\mu = (\mathbf{\Sigma}, i\gamma_5 \Lambda), \quad T_\mu = (\mathbf{\tau}, 1),$$

the K -interaction Lagrangian L_K , which is invariant with respect to rotations in a 4-isospace, is given below:

$$(7) \quad L_K = g_K \bar{\Psi} T_\mu \Sigma_\mu \mathcal{K} + \text{H. C. .}$$

Similarly the π -interaction Lagrangian L_π may be written in a 4-isospace invariant form, if a 4-isovector Π_μ and a tensor $\Pi_{\mu\nu}$ which consist of π (and π' if necessary) are introduced. These Lagrangians are essentially equivalent to those of (5) and (2), and lead to the same self energies. It is clear that L_K , (7), is invariant for the simultaneous substitution, $N \leftrightarrow i\gamma_5 \Xi$ and $K \leftrightarrow K'$, but has no symmetry either between N and Ξ or between K and K' , so it gives not only the N - Ξ mass splitting but also the K - K' mass splitting. The K - K' mass difference will be discussed below. L_K is also invariant for the substitution $i\gamma_5 \Lambda \leftrightarrow \mathbf{\tau} \cdot \mathbf{\Sigma}$, but has no symmetry between Λ and $\mathbf{\tau} \cdot \mathbf{\Sigma}$, and then it gives the Λ - Σ mass splitting to the higher orders, although the lowest order splitting turns out to vanish. On the other hand, L_π is invariant for the substitution $N \leftrightarrow i\gamma_5 \Xi$ and also has a symmetry between N and Ξ , so the L_π gives no mass splitting between them even to the higher orders. This L_π has no symmetry between $\delta_{\alpha\beta} \Lambda$ and $(\mathbf{\tau} \cdot \mathbf{\Sigma})_{\alpha\beta}$, and gives the Λ - Σ mass splitting even to the lowest order. As a matter of fact, the contributions arising from the cross terms of L_K and L_π might have a complicated effect on the mass splitting in the higher order approximation.

It seems that at present there is no experimental objection against the introduction of the K' field, since so far most of the experimental evidence has been concerned with K and K^0 (but not with K' and K'^0). If a Ξ -production experiment, such as

$$N + \pi \rightarrow (\Lambda \text{ or } \Sigma) + K \rightarrow \Xi + K + K',$$

is done with better statistics in the future, it will be possible to test the existence of the K' meson. Using the above L_K , the lowest order self energies of K and K' can be calculated as has been done for the baryons,

$$(8) \quad \begin{cases} \Delta M(K) = g_K^2 (F_{ps} + 3F_s), \\ \Delta M(K') = g_K^2 (F_s + 3F_{ps}), \end{cases}$$

where F_{ps} and F_s stand for the contributions from the pseudoscalar and scalar couplings respectively. Then the mass difference of K and K' , which would dege-

nerate in the limit of vanishing K-baryon interaction, becomes

$$(9) \quad M(K) - M(K') = 2g_K^2 (F_s - F_{ps}) = \\ = \left(\frac{g_K^2}{4\pi} \right) \frac{M}{\lambda} \frac{2}{\pi} \int_0^1 du [1 - (1-u)\lambda] \left\{ \log \frac{\kappa + \sqrt{\kappa^2 + 1 - u(1-u)\lambda^2}}{\sqrt{1 - u(1-u)\lambda^2}} - \frac{\kappa}{\sqrt{\kappa^2 + 1 - u(1-u)\lambda^2}} \right\},$$

where the straight cut-off technique has been adopted, and M is the degenerate baryon mass, $\lambda = (\text{the degenerate heavy meson mass } m_K)/M$, and $\kappa = (\text{the cut-off momentum})/M$. Although both F_s and F_{ps} are quadratically divergent, the difference $F_s - F_{ps}$ is only logarithmically divergent, because coefficients of the quadratically divergent terms for both expressions are equal. Moreover, as $F_s - F_{ps}$ is always positive irrespective of the cut-off momentum, the K' meson happens to be lighter than the K meson as far as the lowest order is concerned. Table II shows how the mass difference $M(K) - M(K')$ depends on the magnitude of the cut-off parameter κ , assuming $M = 2000 m_e$, $m_K = 1000 m_e$ and $g_K^2/4\pi = 1$. If $M(K')$ is smaller than $\sim 810 m_e$, K' cannot decay into three pions. Besides the mass difference, the K and K' mesons would show different behaviors for the scattering by nucleons and for the absorption by nuclei, etc. According to our assumption, K and K' do not strongly couple either directly with each other or indirectly through baryons, and so γ -decay of K into K' through strong interactions cannot take place.

TABLE II.

Cut-off parameter κ	0.5	0.75	1.0
Mass difference: $M(K) - M(K')$	$67 m_e$	$188 m_e$	$346 m_e$
Mass of K' meson: $M(K')$	$900 m_e$	$779 m_e$	$621 m_e$

* * *

The author wishes to thank Dr. T. NAKANO (Osaka City University) for valuable discussions.

PROPRIETÀ LETTERARIA RISERVATA

Direttore responsabile: G. POLVANI

Tipografia Compositori - Bologna

Questo Fascicolo è stato licenziato dai torchi il 28-III-1959